

APPENDIX

Appendix A	Survey Documents, Data Forms & Flow Accumulation Model	4
A.1	Local municipalities survey items	4
A.1.1	Letter to Communities	5
A.1.2	Example of a color topographic map	9
A.2	Road-Stream Crossing Inventory Field Data Form.....	10
A.3	Culvert Condition Assessment Field Data Form.....	15
A.4	TU Culvert and Bridge Assessment Field Form	18
A.5	Crossing Flow Accumulation Assignment.....	22
Appendix B	Fluvial Geomorphological Scoring System.....	26
B.1	Introduction	26
B.2	Stream Power Analysis.....	26
B.2.1	Components of Stream Power	26
B.2.2	Calculation of Stream Power.....	29
B.3	Crossing Vulnerability Screen and Scoring System Development	30
B.3.1	Vulnerability Screen	30
B.3.2	Slope Analysis	37
B.3.3	Vulnerability Screen Sensitivity Analysis	41
B.3.4	Scoring System Development.....	44
B.4	Quality Control Check	50
B.5	References	53
Appendix C	Regional Climate Model Data Set Comparison	54
Appendix D	NARCCAP Data Bias Correction.....	57
D.1	Overview	57
D.2	Climate Model Data Bias Adjustment Procedure.....	57
D.3	Summary of Results	57
D.4	References	64
Appendix E	Malone & MacBroom Report.....	65
Appendix F	Jacobs Overview	191
F.1	Considered Basins and Characteristics	191
F.2	Regression Equations.....	191
F.3	References	192
Appendix G	Specific Stream Power Map	193

Appendix H	Culvert Flow Capacity	194
H.1	Method Theoretical Details	194
H.1.1	Bentley's CulvertMaster	194
H.1.2	Manning's Equation	195
H.2	Culvert Master Interface	196
H.3	Culvert Master Performance Curve	196
H.4	Estimating Entrance Coefficients and Manning's Roughness	198
H.5	Effects of Tailwater Elevation Variation on Critical Discharge	198
H.6	Flow Sensitivity to Manning's Roughness Coefficient.....	201
H.7	Flow Sensitivity to Varying Entrance Coefficients	203
Appendix I	USGS RPF E Overview	204
I.1	Overview of Methodology	204
I.2	MA RPF E s	204
I.3	NH RPF E s	205
I.4	VT RPF E s	206
I.5	References	207
Appendix J	TU Model Protocol	209
J.1	Introduction	209
J.2	Hydrology	209
J.2.1	SCS Method	209
J.2.2	Regional Regression Equations for New Hampshire	210
J.2.3	Discussion	211
J.3	Hydraulics	211
J.3.1	Existing Culvert Hydraulics.....	211
J.3.2	Proposed Culvert Hydraulics	212
J.4	Instructions for Using the Excel Model.....	213
J.4.1	Instructions	213
J.4.2	GIS Input	213
J.4.3	User Input	214
J.4.4	Results	214
J.5	References	215
Appendix K	HBV and HSPF Overview	216
K.1	Model Overviews.....	216
K.1.1	Hydrologiska Byråns Vattenbalansavdelning (HBV) Model	216
K.1.2	Hydrologic Simulation Program Fortran (HSPF) Model	216

K.2	Regionalization	219
K.3	Climate Data	220
K.4	Flow Data Utilized for Calibration.....	220
K.5	Catchment Characteristics	221
K.6	Model Application Details	222
K.7	Calibration and Validation.....	223
K.8	Results	226
K.9	Acknowledgements	231
K.10	References	231
Appendix L	WRFH Overview.....	235
L.1	Model Summary.....	235
L.2	Implementation for Deerfield River Watershed.....	236
L.3	Application.....	238
L.4	References	239
L.5	Acknowledgments	240
Appendix M	Cornell’s Culvert Capacity Calculations	241
Appendix N	Hydraulic Risk Methodology Comparison	242
N.1	Overview	242
N.2	Summary of Other Project Methods	242
N.2.1	Cornell	242
N.2.2	Trout Unlimited.....	242
N.3	Risk Assessment Comparison Approach.....	242
N.4	Comparison of Results.....	243
Appendix O	Digital Repository	246
O.1	GIS Layers	246
O.2	Access Database	246
O.2.1	Raw Data	246
O.2.2	Derived Data.....	247
O.3	Stream Crossing Explorer Data	247
O.4	Additional Data	248

Appendix A SURVEY DOCUMENTS, DATA FORMS & FLOW ACCUMULATION MODEL

A.1 Local municipalities survey items

See following pages:

- Letter that was sent to municipalities
- Example of companion topographic map

A.1.1 Letter to Communities



WATER RESOURCES RESEARCH CENTER

University of Massachusetts
Blaisdell House, 113 Grinnell Way
Amherst, MA 01003-0820
Phone: (413) 545-5531 or
(413) 545-5528

February 23, 2015

Dear Town Representative:

MassDOT and UMass Amherst are working to identify potential vulnerabilities in the transportation system within the Deerfield River watershed. We are interested in the impacts of extreme weather on both local and state roads. While our primary focus is on culverts and bridges, we are also interested in roadway washouts.

One goal of the project is to collect as much information as possible on the history of flooding and related failures in the transportation network. As a town within the watershed, addressing the attached questions will help the project team identify potential problem areas within local communities not readily detected from existing data sets. This information will help MassDOT prioritize road-stream crossings for repair/replacement.

One of our team members, Beckie Finn, will follow up with a call and will be happy to schedule a time to meet in person. If anyone would like further details regarding the project or this data collection effort, please feel free to contact Beckie at the Massachusetts Water Resources Research Center at (413) 545.5579 or email her at esfynn@cns.umass.edu.

Thank you for considering this request. We would appreciate your response before April 1, 2015.

Best,

Dr. Paula L. Sturdevant Rees
Director, Massachusetts Water Resources Research Center
University of Massachusetts Amherst
rees@ecs.umass.edu

Project Data Collection Team:

Paula Rees
Massachusetts WRRC, UMass
Email: rees@umass.edu

Beckie Finn
Massachusetts WRRC, UMass
Email: esfinn@cns.umass.edu

Stephen Mabee
Massachusetts State Geologist, UMass
Email: sbmabee@geo.umass.edu

Nicholas Venti
Massachusetts Geological Survey
Email: nventi@geo.umass.edu

Scott Jackson
Environmental Conservation, UMass
Email:

Colin Lawson
Trout Unlimited National
Email: clawson@tu.org

Project MassDOT Team:

Katherin McArthur
Project Manager
Email: katherin.mcarthur@state.ma.us

Amer Raza
Environmental Engineer, District 1
Email: amer.raza@dot.state.ma.us

Tim Meyer
Environmental Engineer, District 2
Email: timothy.meyer@dot.state.ma.us

Tim Dexter
Environmental Analyst
Email: timothy.dexter@state.ma.us

Community Questions

1. In the past 10 years or so, have road-stream crossing failures occurred in your town? We are interested in both local and state roads. If yes, please:

- Circle the location of known failures on the accompanying map
- Indicate to the best of your knowledge how each road-stream crossing failed by indicating beside the location on the map one of the following abbreviations:

O – overtopped

E – embankment failed

B – blocked by debris

S – structural failure

W – washed out

Other – please indicate

- Do any of these locations show a history of repeated failures? If yes, please indicate these locations with an asterisk.

2. Are there any other road locations where flooding has been an issue in the past? If so, please:

- Indicate the locations on the map and denote the location with an “F”

F – roadway flooding, segment other than road-stream crossing

- Do any of these locations show a history of repeated failures? If yes, please indicate these locations with an asterisk.

3. In the past ten years or so, has stream erosion caused side slope failures and/or roadway washouts in your town? If yes, please:

- Circle the location of known failures on the accompanying map and denote the location with an “L”

L – fluvial erosion of roadway

- Do any of these locations show a history of repeated failures? If yes, please indicate these locations with an asterisk.

4. Please let us know about on-going town projects and concerns:
 - Is any road crossing (culvert/bridge) or flood related roadway repair work scheduled? If yes, please note on the accompanying table and indicate the:
 - a) Phase of the work (design, construction ready, construction scheduled or active construction), and
 - b) Approximate time scale for completing the work.
 - Have other (e.g., not described above) specific priority road-stream or roadway restoration projects / locations been identified within your town? If so, please highlight them on the table & briefly describe the reason for concern.
5. Are there any culverts/bridges you are aware of that are not shown on the accompanying map? If so, please add them.
6. We welcome any additional information you can provide on areas of concern and failures. Feel free to add notes to the accompanying table or attach/email comments.

THANK YOU!

Return via post:

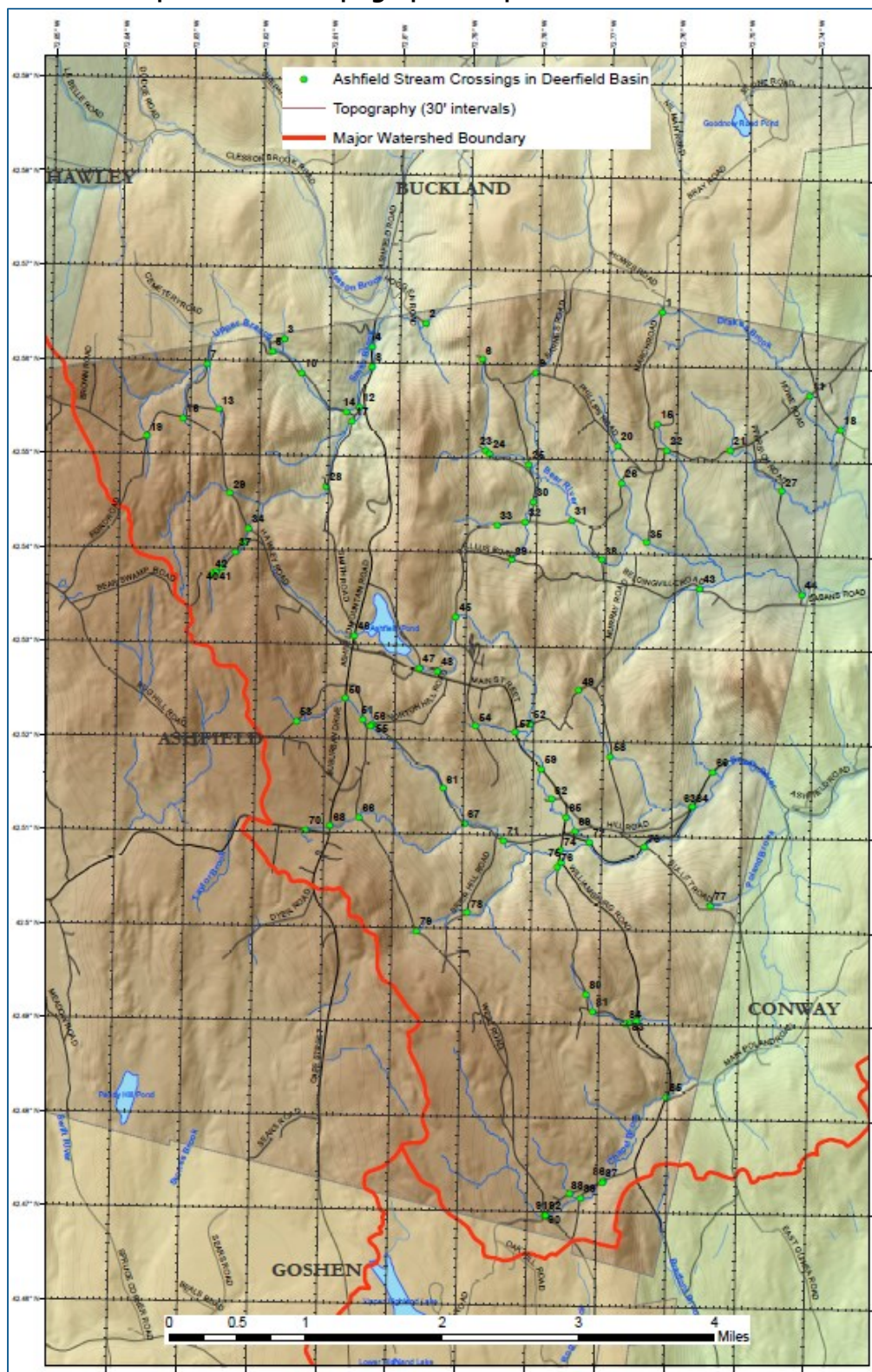
Attn: Beckie Finn (DOT project)
Massachusetts Water Resources Research Center
Blaisdell House
113 Grinnell Way
Amherst, MA 01003

OR

Return via email:

esfinn@cns.umass.edu

A.1.2 Example of a color topographic map

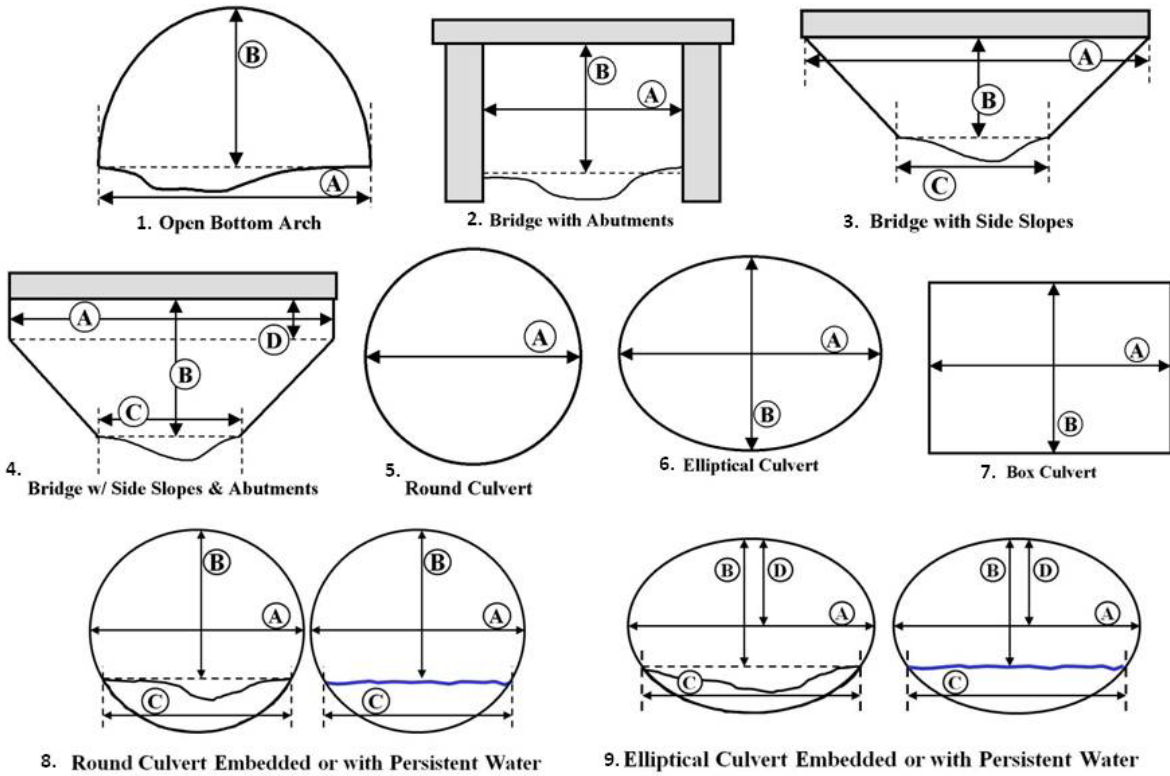


A.2 Road-Stream Crossing Inventory Field Data Form

(see next 3 pages)

For the following questions use as a reference a portion of the natural stream channel that is outside the influence of the crossing structure and not otherwise altered.

- Water depth matches stream?** Yes (comparable) No (deeper) No (shallower) Dry
- Water velocity matches stream?** Yes (comparable) No (slower) No (faster) Dry
- Structure Slope matches stream?** Yes (comparable) No (flatter) No (steeper)



Length of stream through structure: _____ Feet

Inlet Structure Type (from above): 1. 2. 3. 4. 5. 6. 7. 8. 9. Ford Removed

Inlet Dimensions: A) _____ (ft.) B) _____ (ft.) C) _____ (ft.) D) _____ (ft.) Clogged/Collapsed/Submerged

Inlet Water Depth (max depth inside the structure at the inlet): _____ Inches Measured Estimated

Inlet Drop None, or if present _____ Inches Measured Estimated

Outlet Structure Type (from above): 1. 2. 3. 4. 5. 6. 7. 8. 9. Ford Removed

Outlet Dimensions: A) _____ (ft.) B) _____ (ft.) C) _____ (ft.) D) _____ (ft.) Clogged/Collapsed/Submerged

Outlet Water Depth (max depth inside the structure at the outlet): _____ Inches Measured Estimated

Outlet Drop

a. Culvert bottom to water surface None, or if present _____ Inches Measured Estimated

b. Culvert bottom to stream bed None, or if present _____ Inches Measured Estimated

c. With an outlet drop, check one: Cascade Freefall Freefall onto cascade No drop

Armored streambed at outlet? Extensive Not extensive None

Comments _____

STRUCTURE WORKSHEET FOR MULTIPLE CULVERT OR BRIDGE CELL CROSSINGS Crossing ID#

Note: When inventorying multiple culverts or bridge cells, label left culvert/cell #1 and go in increasing order from left to right from downstream end (outlet) looking upstream.

Culvert or Bridge Cell #

Culvert/Bridge Cell Characteristics

Structure embedded? Not embedded Partially embedded Fully embedded No Bottom

Structure substrate: None (smooth) None (rough/corrugated) Inappropriate Contrasting Comparable

Internal features None Slip lined Baffles/Sills Weir(s) Support structures

Physical Barriers to fish and wildlife passage: Severe Moderate Minor None

Describe any barriers: _____

Is there a clear line of sight through the structure? Yes No

Does the structure provide dry passage suitable for use by terrestrial wildlife? Yes No

If yes, what is the maximum structure height in the portion that offers dry passage? _____ Feet

Comments _____

For the following questions use as a reference a portion of the natural stream channel that is outside the influence of the crossing structure and not otherwise altered.

Water depth matches stream? Yes (comparable) No (deeper) No (shallower) Dry

Water velocity matches stream? Yes (comparable) No (slower) No (faster) Dry

Structure Slope matches stream? Yes (comparable) No (flatter) No (steeper)

Length of stream through structure: _____ Feet

Inlet Structure Type: 1. 2. 3. 4. 5. 6. 7. 8. 9. Ford

Inlet Dimensions: A) _____ (ft.) B) _____ (ft.) C) _____ (ft.) D) _____ (ft.) Submerged

Inlet Water Depth (max depth inside the structure at the inlet): _____ Inches Measured Estimated

Inlet Drop None, or if present _____ Inches Measured Estimated

Outlet Structure Type: 1. 2. 3. 4. 5. 6. 7. 8. 9. Ford

Outlet Dimensions: A) _____ (ft.) B) _____ (ft.) C) _____ (ft.) D) _____ (ft.) Submerged

Outlet Water Depth (max depth inside the structure at the outlet): _____ Inches Measured Estimated

Outlet Drop

a. Culvert bottom to water surface None, or if present _____ Inches Measured Estimated

b. Culvert bottom to stream bed None, or if present _____ Inches Measured Estimated

c. With an outlet drop, check one: Cascade Freefall Freefall onto cascade No drop

Armored streambed at outlet? Extensive Not extensive None

A.3 Culvert Condition Assessment Field Data Form

(see next 2 pages)

Field Data Form: Culvert Condition Assessment

INLET

Crossing Code _____

Culvert # _____ of _____

For multiple culvert crossings label left culvert #1 and go in increasing order from left to right from downstream end (outlet) looking upstream.

Culvert material: Concrete Metal (corrugated) Metal (smooth) Metal (lined/smooth)
 Plastic (smooth) Plastic (corrugated) Masonry Other _____

Appurtenance: Projecting Mitered Head wall Head wall/wing walls Flared end section Other

	Poor	Critical
Invert Deterioration <input type="checkbox"/> Not poor or critical <input type="checkbox"/> Unable to observe <input type="checkbox"/> Not applicable	<input type="checkbox"/> Perforations visible and/or connection hardware failing (metal) <input type="checkbox"/> Heavy abrasion and scaling with exposed steel reinforcement (concrete) <input type="checkbox"/> Heavy abrasion or scour damage (plastic) <input type="checkbox"/> Displaced mortar and/or blocks, holes in invert area (masonry)	<input type="checkbox"/> Holes or section loss with extensive voids beneath invert and/or embankment/roadway damage <input type="checkbox"/> Holes and gaps with extensive infiltration of soil, bedding or backfill material (masonry)
Joints and Seams <input type="checkbox"/> Not poor or critical <input type="checkbox"/> Unable to observe <input type="checkbox"/> Not applicable	<input type="checkbox"/> Open or displaced with significant infiltration of soil and/or leakage of water and voids visible <input type="checkbox"/> Missing mortar or displaced blocks (masonry)	<input type="checkbox"/> Open or displaced with significant infiltration of soil and accompanying embankment/roadway damage
Cross-Section Deformation <input type="checkbox"/> Not poor or critical <input type="checkbox"/> Unable to observe	<input type="checkbox"/> Significant perceptible deformation <input type="checkbox"/> Deformation with accompanying longitudinal cracking (concrete)	<input type="checkbox"/> Excessive deformation resulting in significant reduction of available flow area, and/or extensive infiltration of soil, voids, structural failure or embankment/roadway damage
Structural Integrity of barrel <input type="checkbox"/> Not poor or critical <input type="checkbox"/> Unable to observe	<input type="checkbox"/> Open cracks >1/8" wide (concrete) or missing and/or displaced blocks (masonry) with voids and significant infiltration of soil and/or leakage of water <input type="checkbox"/> Several splits, tears and cracks >6" long (plastic) <input type="checkbox"/> Significant deformation of liner or wall buckling (plastic) <input type="checkbox"/> Heavy rust staining and/or exposed steel reinforcement in sides and top of barrel (concrete)	<input type="checkbox"/> Cracks, tears, splits, bulges, holes or section loss have led to extensive infiltration of soil, structural failure, voids and embankment/roadway damage
Longitudinal Alignment <input type="checkbox"/> Not poor or critical <input type="checkbox"/> Unable to observe <input type="checkbox"/> Not applicable	<input type="checkbox"/> Significant horizontal or vertical misalignment of the pipe (Note: do not confuse this with constructed pipe bends)	<input type="checkbox"/> Significant misalignment resulting in deformation of pipe or embankment/roadway damage
Footings <input type="checkbox"/> Not poor or critical <input type="checkbox"/> Unable to observe <input type="checkbox"/> Not applicable	<input type="checkbox"/> Top portion of footing exposed, but no cracking or breaking off of flakes or chips	<input type="checkbox"/> Footing exposed with signs of cracking or breaking off of flakes or chips <input type="checkbox"/> Bottom of footing exposed and/or undercut
Headwall/Wingwalls <input type="checkbox"/> Not poor or critical <input type="checkbox"/> Unable to observe <input type="checkbox"/> Not applicable	<input type="checkbox"/> Cracking or breaking off of flakes or chips affecting >50% of area and/or exposed steel reinforcement <input type="checkbox"/> Gap >4" between barrel and wall <input type="checkbox"/> Footing exposed and undermined	<input type="checkbox"/> Partially or totally collapsed with damage to embankment/roadway
Flared End Section <input type="checkbox"/> Not poor or critical <input type="checkbox"/> Unable to observe <input type="checkbox"/> Not applicable	<input type="checkbox"/> Significant cracks, piping or undermining affects >50% of section <input type="checkbox"/> End crushed or separated from barrel	<input type="checkbox"/> Deterioration is significantly affecting performance and/or causing embankment/roadway damage
Blockage at Inlet <input type="checkbox"/> Not poor or critical <input type="checkbox"/> Unable to observe	<input type="checkbox"/> Debris/sediment/vegetation blocks 1/3 of more of the inlet opening	<input type="checkbox"/> Sediment blocks more than 1/2 the inlet opening (and not designed that way for aquatic organism passage)
Performance Problems <input type="checkbox"/> Not poor or critical <input type="checkbox"/> Unable to observe	<input type="checkbox"/> Buoyancy-related inlet failure: inlet barrel raised above streambed	<input type="checkbox"/> Embankment piping: settlement, deep cracks or holes in roadway or embankment outside of culvert

Field Data Form: Culvert Condition Assessment

OUTLET

Crossing Code _____

Culvert # _____ of _____

For multiple culvert crossings label left culvert #1 and go in increasing order from left to right from downstream end (outlet) looking upstream.

Appurtenance: Projecting Mitered Head wall Head wall/wing walls Flared end section Other

Scour protection: Apron (describe) _____ Armor (describe) _____

	Poor	Critical
Invert Deterioration <input type="checkbox"/> Not poor or critical <input type="checkbox"/> Unable to observe <input type="checkbox"/> Not applicable	<input type="checkbox"/> Perforations visible and/or connection hardware failing (metal) <input type="checkbox"/> Heavy abrasion and scaling with exposed steel reinforcement (concrete) <input type="checkbox"/> Heavy abrasion or scour damage (plastic) <input type="checkbox"/> Displaced mortar and/or blocks, holes in invert area (masonry)	<input type="checkbox"/> Holes or section loss with extensive voids beneath invert and/or embankment/roadway damage <input type="checkbox"/> Holes and gaps with extensive infiltration of soil, bedding or backfill material (masonry)
Joints and Seams <input type="checkbox"/> Not poor or critical <input type="checkbox"/> Unable to observe <input type="checkbox"/> Not applicable	<input type="checkbox"/> Open or displaced with significant infiltration of soil and/or leakage of water and voids visible <input type="checkbox"/> Missing mortar or displaced blocks (masonry)	<input type="checkbox"/> Open or displaced with significant infiltration of soil and accompanying embankment/roadway damage
Cross-Section Deformation <input type="checkbox"/> Not poor or critical <input type="checkbox"/> Unable to observe	<input type="checkbox"/> Significant perceptible deformation <input type="checkbox"/> Deformation with accompanying longitudinal cracking (concrete)	<input type="checkbox"/> Excessive deformation resulting in significant reduction of available flow area, and/or extensive infiltration of soil, voids, structural failure or embankment/roadway damage
Structural Integrity of barrel <input type="checkbox"/> Not poor or critical <input type="checkbox"/> Unable to observe	<input type="checkbox"/> Open cracks >1/8" wide (concrete) or missing and/or displaced blocks (masonry) with voids and significant infiltration of soil and/or leakage of water <input type="checkbox"/> Several splits, tears and cracks >6" long (plastic) <input type="checkbox"/> Significant deformation of inner liner or wall buckling (plastic) <input type="checkbox"/> Heavy rust staining and/or exposed steel reinforcement in sides and top of barrel (concrete)	<input type="checkbox"/> Cracks, tears, splits, bulges, holes or section loss have led to extensive infiltration of soil, structural failure, voids and embankment/roadway damage
Longitudinal Alignment <input type="checkbox"/> Not poor or critical <input type="checkbox"/> Unable to observe <input type="checkbox"/> Not applicable	<input type="checkbox"/> Significant horizontal or vertical misalignment of the pipe (Note: do not confuse this with constructed pipe bends)	<input type="checkbox"/> Significant misalignment resulting in deformation of pipe or embankment/roadway damage
Footings <input type="checkbox"/> Not poor or critical <input type="checkbox"/> Unable to observe <input type="checkbox"/> Not applicable	<input type="checkbox"/> Top portion of footing exposed, but no cracking or breaking off of flakes or chips	<input type="checkbox"/> Footing exposed with signs of cracking or breaking off of flakes or chips <input type="checkbox"/> Bottom of footing exposed and/or undercut
Headwall/Wingwalls <input type="checkbox"/> Not poor or critical <input type="checkbox"/> Unable to observe <input type="checkbox"/> Not applicable	<input type="checkbox"/> Cracking or breaking off of flakes or chips affecting >50% of area and/or exposed steel reinforcement <input type="checkbox"/> Gap >4" between barrel and wall <input type="checkbox"/> Footing exposed and undermined	<input type="checkbox"/> Partially or totally collapsed with damage to embankment/roadway
Flared End Section <input type="checkbox"/> Not poor or critical <input type="checkbox"/> Unable to observe <input type="checkbox"/> Not applicable	<input type="checkbox"/> Significant cracks, piping or undermining affects >50% of section <input type="checkbox"/> End crushed or separated from barrel	<input type="checkbox"/> Deterioration is significantly affecting performance and/or causing embankment/roadway damage
Apron <input type="checkbox"/> Not poor or critical <input type="checkbox"/> Unable to observe <input type="checkbox"/> Not applicable	<input type="checkbox"/> Significant cracking affects >50% of apron <input type="checkbox"/> Significant piping or undermining	<input type="checkbox"/> Partially or totally collapsed, significantly affecting performance and/or causing embankment/roadway damage
Armoring <input type="checkbox"/> Not poor or critical <input type="checkbox"/> Unable to observe <input type="checkbox"/> Not applicable	<input type="checkbox"/> Significant displacements, undermining or deterioration affecting the performance of the culvert structure	<input type="checkbox"/> Partially or totally failed, significantly affecting performance and/or causing embankment/roadway damage or undermining of the culvert barrel or footings

A.4 TU Culvert and Bridge Assessment Field Form

(This page and next 3 pages)

Culvert and Bridge Assessment Field Form Deerfield River Watershed Project

Crossing ID		TGR-21	Date		6-19-15
Observers		DF, SR	Latitude (N/S)		42.61611
Town		Greenfield	Longitude (E/W)		72.59892
Road Name		Golf Course Access Rd.	No. of Structures		1
Nearest Junction or Marker		Flag of Hole #2	Road Type		<input checked="" type="checkbox"/> Paved <input checked="" type="checkbox"/> Gravel <input type="checkbox"/> Trail
Stream Name		Trio Mill Brook	Flow Stage		<input type="checkbox"/> Low <input checked="" type="checkbox"/> Average <input type="checkbox"/> High
Structure Material	<input checked="" type="checkbox"/> Steel Corrugate	Headwall Material	<input type="checkbox"/> Stone	Structure skewed to roadway? :	<input checked="" type="checkbox"/> Yes <input type="checkbox"/> No
	<input type="checkbox"/> Tank/ Smooth Steel		<input type="checkbox"/> Concrete		Angle (approx.) <u>30</u> °
	<input type="checkbox"/> Plastic Corrugate		<input type="checkbox"/> Riprap	Rust line height:	<u>0.4</u> (0.0ft)
	<input type="checkbox"/> Plastic Smooth		<input type="checkbox"/> Wood	Overflow pipes? :	<input type="checkbox"/> Yes <input checked="" type="checkbox"/> No
	<input type="checkbox"/> Aluminum		<input checked="" type="checkbox"/> None		
	<input type="checkbox"/> Stone		<input type="checkbox"/> Other		
	<input type="checkbox"/> Concrete				
	<input type="checkbox"/> Timber				
	<input type="checkbox"/> Other				

Crossing Condition:

Structure Shape:	<input checked="" type="checkbox"/> Round Pipe <input type="checkbox"/> Elliptical Pipe <input type="checkbox"/> Box <input type="checkbox"/> Arch <input type="checkbox"/> Bridge				
Problem Conditions:	<input type="checkbox"/> Fill eroding <input type="checkbox"/> Debris in culvert <input type="checkbox"/> Break inside culvert (location) _____				
	<input type="checkbox"/> Debris blocking culvert <input type="checkbox"/> Bottom rusted through <input type="checkbox"/> Other _____				
Floodplain filled by roadway:	<input checked="" type="checkbox"/> Entirely (> ¾ of floodplain) <input type="checkbox"/> Partially (1/4 - ¾ of floodplain) <input type="checkbox"/> Not significantly				
Break in valley slope?	<input type="checkbox"/> Yes <input checked="" type="checkbox"/> No	Crossing aligned to stream:		<input type="checkbox"/> Yes <input type="checkbox"/> No ?	
Baffles or weirs? :	<input type="checkbox"/> Yes <input checked="" type="checkbox"/> No If yes: material _____ description _____				
Structure embedded?	<input type="checkbox"/> Fully embedded <input checked="" type="checkbox"/> Partially embedded <input type="checkbox"/> Not embedded <input type="checkbox"/> No bottom				
Culvert Slope:	<input type="checkbox"/> Higher than channel <input type="checkbox"/> Lower than channel <input checked="" type="checkbox"/> About the same				
Water depth compared to stream:	<input type="checkbox"/> Higher than channel <input type="checkbox"/> Lower than channel <input checked="" type="checkbox"/> About the same				
Water velocity compared to stream:	<input type="checkbox"/> Higher than channel <input type="checkbox"/> Lower than channel <input checked="" type="checkbox"/> About the same				

Upstream Conditions:

Inlet type:	<input type="checkbox"/> Projecting <input type="checkbox"/> Apron <input type="checkbox"/> Wingwall (10°-30°) <input type="checkbox"/> Wingwall (30°-70°) <input type="checkbox"/> Trashrack <input type="checkbox"/> Mitered <input checked="" type="checkbox"/> None <input type="checkbox"/> Other		
Angle of stream approaching?	<input checked="" type="checkbox"/> Sharp bend (45°-90°) <input type="checkbox"/> Mild bend (5°-45°) <input type="checkbox"/> Naturally straight <input type="checkbox"/> Channelized straight		
Steep riffle present? :	<input type="checkbox"/> Yes <input checked="" type="checkbox"/> No	Upstream streambed:	<input type="checkbox"/> Erosion <input type="checkbox"/> Aggradation <input type="checkbox"/> None
If channel avulses:	<input type="checkbox"/> Cross road <input type="checkbox"/> Follow road <input type="checkbox"/> Unsure	Distance avulsion would follow road? :	<input checked="" type="checkbox"/> _____ (ft)
Dominant substrate:	<input type="checkbox"/> Bedrock <input type="checkbox"/> Boulder <input type="checkbox"/> Cobble <input type="checkbox"/> Gravel <input type="checkbox"/> Sand <input type="checkbox"/> Unknown <input checked="" type="checkbox"/> None		
Sediment deposit type? :	<input type="checkbox"/> None <input type="checkbox"/> Side <input type="checkbox"/> Delta <input type="checkbox"/> Point <input type="checkbox"/> Mid-channel	Deposit ≥ ½ bankfull height? :	<input type="checkbox"/> Yes <input checked="" type="checkbox"/> No
Bank erosion:	<input type="checkbox"/> High <input type="checkbox"/> Low <input checked="" type="checkbox"/> None	Hardbank armoring:	<input type="checkbox"/> Intact <input type="checkbox"/> Failing <input checked="" type="checkbox"/> None
Streambed scour around structure:	<input type="checkbox"/> Culvert <input type="checkbox"/> Footer <input type="checkbox"/> Wingwalls <input type="checkbox"/> None	Bedrock present? :	<input type="checkbox"/> Yes <input checked="" type="checkbox"/> No

Downstream Conditions:

Culvert Outlet:	<input type="checkbox"/> Backwatered <input checked="" type="checkbox"/> At grade <input type="checkbox"/> Cascade <input type="checkbox"/> Freefall		
Tailwater control:	<input type="checkbox"/> Boulder <input type="checkbox"/> Cobble <input type="checkbox"/> Gravel <input type="checkbox"/> Sand <input checked="" type="checkbox"/> Wood <input type="checkbox"/> Other _____		
Outlet apron? :	<input type="checkbox"/> Yes <input checked="" type="checkbox"/> No	Pool present?	<input type="checkbox"/> Yes <input checked="" type="checkbox"/> No
Downstream streambed:	<input type="checkbox"/> Erosion <input type="checkbox"/> Aggradation <input checked="" type="checkbox"/> None	Higher bank heights downstream? :	<input checked="" type="checkbox"/> Yes <input type="checkbox"/> No
Dominant substrate:	<input type="checkbox"/> Bedrock <input type="checkbox"/> Boulder <input type="checkbox"/> Cobble <input checked="" type="checkbox"/> Gravel <input type="checkbox"/> Sand <input type="checkbox"/> Unknown <input type="checkbox"/> None		
Sediment deposit type? :	<input checked="" type="checkbox"/> None <input type="checkbox"/> Side <input type="checkbox"/> Delta <input type="checkbox"/> Point <input type="checkbox"/> Mid-channel	Deposit ≥ ½ bankfull height? :	<input type="checkbox"/> Yes <input checked="" type="checkbox"/> No
Bank erosion:	<input type="checkbox"/> High <input type="checkbox"/> Low <input checked="" type="checkbox"/> None	Streambed armoring:	<input type="checkbox"/> Yes <input checked="" type="checkbox"/> No
Streambed scour around structure:	<input type="checkbox"/> Culvert <input type="checkbox"/> Footer <input type="checkbox"/> Wingwalls <input checked="" type="checkbox"/> None	Hardbank armoring:	<input type="checkbox"/> Yes <input checked="" type="checkbox"/> No
		Bedrock present? :	<input type="checkbox"/> Yes <input checked="" type="checkbox"/> No

Wildlife Corridor: banks determined L/R facing downstream

	Left bank (US)	Right bank (US)	Left bank (DS)	Right bank (DS)
Dominant vegetation type:	H	H	M	M
Riparian buffer 50' wide x 500' long? :	<input checked="" type="checkbox"/> Yes <input type="checkbox"/> No	<input checked="" type="checkbox"/> Yes <input type="checkbox"/> No	<input type="checkbox"/> Yes <input type="checkbox"/> No	<input checked="" type="checkbox"/> Yes <input type="checkbox"/> No
Road-killed wildlife within ¼ mi? :	10			
	Outside Structure		Inside Structure	
Wildlife sign/species observed?				

Veg types: Coniferous, Deciduous, Mixed, Shrub/sapling, Herbaceous, Bare, Road

In structure:

Material throughout? :	<input checked="" type="checkbox"/> Yes <input type="checkbox"/> No		
Dominant substrate:	<input type="checkbox"/> Bedrock <input type="checkbox"/> Boulder <input type="checkbox"/> Cobble <input checked="" type="checkbox"/> Gravel <input type="checkbox"/> Sand <input type="checkbox"/> Unknown <input type="checkbox"/> None		
Sediment deposit type? :	<input checked="" type="checkbox"/> None <input type="checkbox"/> Side <input type="checkbox"/> Delta <input type="checkbox"/> Point <input type="checkbox"/> Mid-channel	Deposit ≥ ½ bankfull height? :	<input type="checkbox"/> Yes <input checked="" type="checkbox"/> No

Lengths and Measurements: all measurements in 0.0ft

Structure Height (US):		Structure Height (DS):	0.7
Structure Width (US):		Structure Width (DS):	0.7
Inlet water depth:		Outlet water depth:	0.5
Upstream control:		Downstream control:	4.5
Length of stream through structure:	137.0ds	Backwater length:	
Outlet drop:		Depth 6" from outlet:	0.3
Range across floodplain:		Max pool depth:	0.4
Upstream bankfull (5)	1) 2) 3) 4) 5)		
Upstream reference (5)	1) 2) 3) 4) 5)		
Downstream bankfull (5)	1) 4.0 2) 4.0 3) 4.5 4) 4.0 5) 4.2		

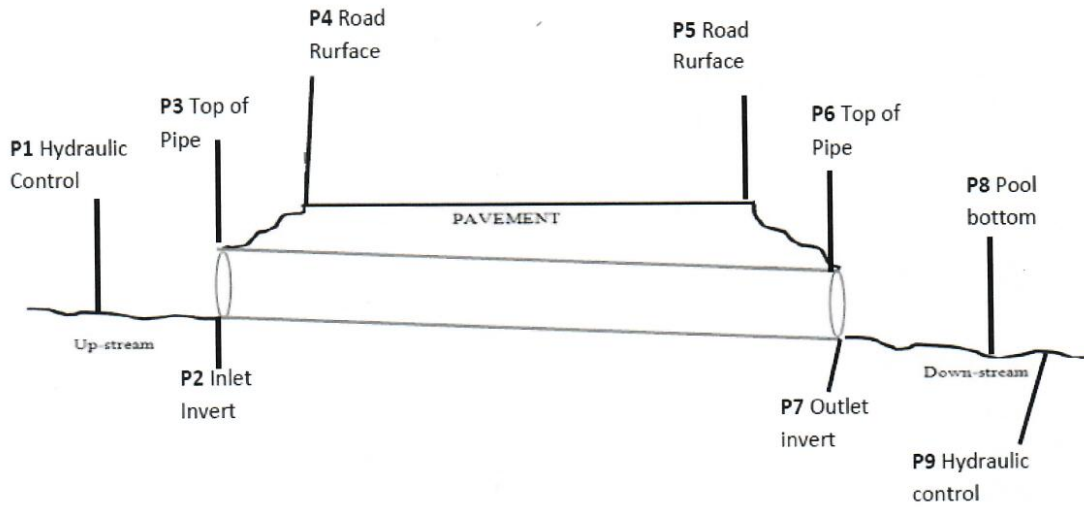
Other information:

Photos:	<input type="checkbox"/> US from road <input type="checkbox"/> US towards structure <input checked="" type="checkbox"/> DS from road <input checked="" type="checkbox"/> DS towards structure <input type="checkbox"/> Above towards US structure <input type="checkbox"/> Above towards DS structure <input type="checkbox"/> Substrate with scale		
<input checked="" type="checkbox"/> GPS point taken above structure	Current weather conditions:		
Date last precip:		Approx amount precip:	

Comments: TGR 20 crosses Country Club Rd and then a golf course Access Rd. ^{Drops into} To the Drainage Box @ GPS Point TGR 21. The Drainage Box is Barred and we are unable to physically access the Outlet/Inlet Drainage.

All -Dashes- are "unable to observe" or "N/A"

Elevations:



Culvert 1 (0.00ft):

P1 _____ P2 _____ P3 _____ P4 _____ P5 _____ P6 _____ P7 _____ P8 _____ P9 _____

Culvert 2 (0.00ft):

P1 _____ P2 _____ P3 _____ P4 _____ P5 _____ P6 _____ P7 _____ P8 _____ P9 _____

Pebble count, 50: measure intermediate axis (mm)

Size categories	Size ranges	Count
Sand (small, grainy)	<2	
Gravel (pea-tennis ball diameter)		
-Fine gravel	2-8	
-Medium gravel	9-16	
-Coarse gravel	17-64	
Cobble (tennis to basketball diameter)		
-Small cobble	65-90	
-Medium cobble	91-128	
-Large cobble	129-256	
Boulder (basketball to car diameter)		
-Small boulder	257-512	
-Medium boulder	513-1024	
-Large boulder	>1024	
Bedrock		

A.5 Crossing Flow Accumulation Assignment

Steps completed: ALR 11-18-2014

Reproject culverts from streamcontinuity.org database

Shapefile of culverts in the Deerfield R basins was downloaded from

http://streamcontinuity.org/cdb2 on 11-18-2014.

1) Define projection/datum

```
Executing: DefineProjection export
GEOGCS['GCS_WGS_1984',DATUM['D_WGS_1984',SPHEROID['WGS_1984',6378137.0,298.257223563]],PRIMEM['Greenwich',0.0],UNIT['Degree',0.0174532925199433]]
```

2) Reproject with geographic transformation

```
Executing: Project export
C:\ALR\Projects\MassDOT\data\culvert_data\cdb2_culverts\culverts_cdb2_11_18_2014
PROJCS['USA_Contiguous_Albers_Equal_Area_Conic_USGS_version',GEOGCS['GCS_North_American_1983',DATUM['D_North_American_1983',SPHEROID['GRS_1980',6378137.0,298.257222101]],PRIMEM['Greenwich',0.0],UNIT['Degree',0.0174532925199433]],PROJECTION['Albers'],PARAMETER['False_Easting',0.0],PARAMETER['False_Northing',0.0],PARAMETER['Central_Meridian',-96.0],PARAMETER['Standard_Parallel_1',29.5],PARAMETER['Standard_Parallel_2',45.5],PARAMETER['Latitude_Of_Origin',23.0],UNIT['Meter',1.0]] NAD_1983_To_WGS_1984_5
GEOGCS['GCS_WGS_1984',DATUM['D_WGS_1984',SPHEROID['WGS_1984',6378137.0,298.257223563]],PRIMEM['Greenwich',0.0],UNIT['Degree',0.0174532925199433]]
```

Prepare points from stream grid (raster) for snapping

3) Create points from stream grid raster

```
Executing: RasterToPoint streams
C:\ALR\Projects\MassDOT\data\culvert_data\cdb2_culverts\flowgrid_point.shp VALUE
```

4) Select and export stream centerline points

```
Executing: SelectLayerByAttribute flowgrid_point NEW_SELECTION ""GRID_CODE" = 1"

Executing: CopyFeatures culverts_stream_grid
C:\ALR\Projects\MassDOT\data\culvert_data\cdb2_culverts\flowgrid_centerline_point.shp # 0 0 0
```

Identify problem culverts to move

5) Extract stream grid values

```
Executing: ExtractValuesToPoints culverts_cdb2_11_18_2014 streams
C:\ALR\Projects\MassDOT\data\culvert_data\cdb2_culverts\culverts_stream_grid.shp NONE VALUE_ONLY
```

6) "Rename" stream grid value field

```
Executing: AddField culverts_stream_grid stream_grd LONG # # # # NON_NULLABLE
NON_REQUIRED #
Adding stream_grd to culverts_stream_grid...

Executing: CalculateField culverts_stream_grid stream_grd [RASTERVALU] VB #

Executing: DeleteField culverts_stream_grid RASTERVALU

Dropping RASTERVALU from culverts_stream_grid...
```

7) Select and export culverts *on* stream grid centerlines

```
Executing: SelectLayerByAttribute culverts_stream_grid NEW_SELECTION ""stream_grd" = 1"

Executing: CopyFeatures culverts_stream_grid
C:\ALR\Projects\MassDOT\data\culvert_data\cdb2_culverts\culverts_on_stream_center.shp # 0 0 0
```

8) Select and export culverts *on* stream grid but *off* stream centerlines
(These are the ones we're going to move with the snap tool)

```

(There are 90 such points in the Deerfield R basin, 61 of which are in Mass)

Executing: SelectLayerByAttribute culverts_stream_grid NEW_SELECTION ""stream_grd" = 2"

Executing: CopyFeatures culverts_stream_grid
C:\ALR\Projects\MassDOT\data\culvert_data\cdb2_culverts\culverts_off_stream_center.shp # 0 0 0

9) Select and export culverts *off* stream grid entirely
(These are *not* going to moved in an automated way, but should be manually checked)
(There are 8 such points in the Deerfield R basin, all in Mass)
Executing: SelectLayerByAttribute culverts_stream_grid NEW_SELECTION ""stream_grd" = -
9999"

Executing: CopyFeatures culverts_stream_grid
C:\ALR\Projects\MassDOT\data\culvert_data\cdb2_culverts\culverts_off_stream_grid.shp # 0 0 0

### Move culverts

10) Create copy of problem culverts for moving
Executing: CopyFeatures culverts_off_stream_center
C:\ALR\Projects\MassDOT\data\culvert_data\cdb2_culverts\culverts_off_center_moved.shp # 0 0 0

11) Snap culvert points to centerline points
Executing: Snap culverts_off_center_moved "flowgrid_centerline_point VERTEX '30 Meters'"

*****

Steps completed: NV 11-21-2014

*****

### Manual check/corrections

15) a) Manually check culvert that *were* on stream grid but off stream center (moved in step
11) ("culverts_off_center_moved");
b) Move again as needed "culverts_off_center_moved_QC"

16) a) Manually check culvert points not on streams grid: "culverts_off_stream_grid"
b) Move again as needed: "culverts_off_stream_gridQC"

*****

Steps completed: ALR 11-25-2014

*****

17) Create duplicates of the 3 gage shapefiles (Create a new version that will have updated
geometry)

Executing: CopyFeatures culverts_off_center_moved_QC "C:\Users\arosner\Dropbox\DOT UMass
Deerfield Culvert Project\GIS culvert and gage data\Culverts points on stream grid\Data
prep\culverts_off_center_QC_geom.shp" # 0 0 0

Executing: CopyFeatures culverts_off_stream_gridQC "C:\Users\arosner\Dropbox\DOT UMass
Deerfield Culvert Project\GIS culvert and gage data\Culverts points on stream grid\Data
prep\culverts_off_stream_QC_geom.shp" # 0 0 0

Executing: CopyFeatures culverts_on_stream_center "C:\Users\arosner\Dropbox\DOT UMass
Deerfield Culvert Project\GIS culvert and gage data\Culverts points on stream grid\Data
prep\culverts_on_stream_center_geom.shp" # 0 0 0

18) Save previous "Latitude" and "Longitude" columns to archived lat_11_18 and long_11_18
columns
Executing: AddField culverts_off_stream_QC_geom lat_11_18 DOUBLE # # # NON_NULLABLE
NON_REQUIRED #

Executing: CalculateField culverts_off_stream_QC_geom lat_11_18 [Latitude] VB #

```

Executing: AddField culverts_off_stream_QC_geom long_11_18 DOUBLE # # # # NON_NULLABLE
NON_REQUIRED #

Executing: CalculateField culverts_off_stream_QC_geom long_11_18 "[Longitud] " VB #

Executing: AddField culverts_off_center_QC_geom lat_11_18 DOUBLE # # # # NON_NULLABLE
NON_REQUIRED #

Executing: CalculateField culverts_off_center_QC_geom lat_11_18 [Latitude] VB #

Executing: AddField culverts_off_center_QC_geom long_11_18 DOUBLE # # # # NON_NULLABLE
NON_REQUIRED #

Executing: CalculateField culverts_off_center_QC_geom long_11_18 "[Longitud] " VB #

Executing: AddField culverts_on_stream_center_geom lat_11_18 DOUBLE # # # # NON_NULLABLE
NON_REQUIRED #

Executing: CalculateField culverts_on_stream_center_geom lat_11_18 [Latitude] VB #

Executing: AddField culverts_on_stream_center_geom long_11_18 DOUBLE # # # # NON_NULLABLE
NON_REQUIRED #

Executing: CalculateField culverts_on_stream_center_geom long_11_18 "[Longitud] " VB #

19) Calculate geometry

Open attribute table

Right click on header of "Latitude" column, select "Calculate Geometry" from dropdown

Options: Property: "Y Coordinate of Point"

Coordinate system: Use coordinate system of data source: USA Cont. Albers Eq
Area Conic USGS

Units: Decimal degrees

Repeat for "Longitud" column, choosing "X Coordinate of Point"

Merge the three sets of culverts

20) Rename Pixel_Aprr/Point_Aprr, and add blank fields so that all three shapefiles have
identical files

Executing: AddField culverts_off_center_QC_geom OffStrmApr TEXT # # # # NON_NULLABLE
NON_REQUIRED #

Executing: AddField culverts_off_stream_QC_geom OffStrmApr TEXT # # # # NON_NULLABLE
NON_REQUIRED #

Executing: AddField culverts_on_stream_center_geom OffStrmApr TEXT # # # # NON_NULLABLE
NON_REQUIRED #

Executing: AddField culverts_off_center_QC_geom OffCtrAprr TEXT # # # # NON_NULLABLE
NON_REQUIRED #

Executing: AddField culverts_off_stream_QC_geom OffCtrAprr TEXT # # # # NON_NULLABLE
NON_REQUIRED #

Executing: AddField culverts_on_stream_center_geom OffCtrAprr TEXT # # # # NON_NULLABLE
NON_REQUIRED #

Executing: CalculateField culverts_off_center_QC_geom OffStrmApr [Pixel_Aprr] VB #

Executing: CalculateField culverts_off_stream_QC_geom OffStrmApr [Place_Aprr] VB #

Executing: DeleteField culverts_off_center_QC_geom Pixel_Aprr

Executing: DeleteField culverts_off_stream_QC_geom Place_Appr

21) Append

(I usually use merge tool, was having problems, using "append" instead

Create copy of culverts_off_center_QC_geom, named culverts_append

Executing: Append culverts_off_stream_QC_geom;culverts_on_stream_center_geom
culverts_append TEST # #

Sample flow accumulation grid

22) Sample flow accumulation grid

ExtractValuesToPoints tool

Executing: ExtractValuesToPoints culverts_all_QC_geom flowaccumkm

C:\ALR\Projects\MassDOT\data\culvert_data\cdb2_culverts\geom_and_merge\culverts_flowacc_11_25.sh
p NONE VALUE_ONLY

24) "Rename" flow acc column name

Executing: AddField culverts_flowacc_11_25 flowacckm FLOAT # # # # NON_NULLABLE
NON_REQUIRED #

Executing: CalculateField culverts_flowacc_11_25 flowacckm [RASTERVALU] VB #

Executing: DeleteField culverts_flowacc_11_25 RASTERVALU

Appendix B FLUVIAL GEOMORPHOLOGICAL SCORING SYSTEM

B.1 Introduction

Milone and MacBroom, Inc. (MMI) was hired as a subcontractor to develop a vulnerability screening tool for bridges and culverts to gauge the potential risk of failure. MMI was charged with three tasks: 1) conduct a watershed-scale stream power analysis that can be used as an indicator of erosion or deposition risk along specific stream reaches, 2) prepare and verify a vulnerability screening tool for bridges and culverts that incorporates stream power and other physical features of the river system on a subset of 200± crossings in the watershed, and 3) check field data acquired by Trout Unlimited (TU) and UMass on a subset of 20 crossings for quality assurance and provide recommendations for method improvements in the future.

The screening tool provided by MMI was then combined with other geomorphic data provided by TU and UMass to produce a fluvial geomorphological scoring system (hereafter, scoring system) for each crossing. The scoring system includes four categories, each expressing a specific geomorphic condition at a crossing that could lead to a crossing failure under extreme flooding conditions. These include the propensity for woody debris accumulation, susceptibility to sedimentation, susceptibility to scour and evidence of blockage.

This appendix provides a summary of how the stream power analysis, screening tool and final scoring system were developed. For details on the stream power analysis and screening tool, refer to the “River and Stream Power Assessment Report Including Culvert and Bridge Vulnerability Analysis” prepared by MMI with a revision date of April 4, 2017 (hereafter, MMI final report). This report is provided in Appendix E. Most of the figures and some of the text were drawn from the MMI final report.

B.2 Stream Power Analysis

Stream power is sometimes used to describe the erosive power of a river because it is easier to compute than other formulas that rely on stream velocity and shear stress. Total stream power (Ω) is the product of the density of water (ρ , kg/m³), acceleration of gravity (g , m/sec²), discharge (Q , m³/sec) and channel slope (S , m/m), expressed as Watts per meter (W/m). It is the work done by a river on a unit length of river at some specific cross section. It is often more convenient to normalize the total stream power per unit area by dividing the total stream power by the active channel width. This is referred to as specific stream power (ω) and is expressed in W/m².

B.2.1 Components of Stream Power

B.2.1.1 Stream Reaches

The entire Massachusetts portion of the Deerfield River watershed was divided up into 1,960 reaches (MMI Final Report). Reach identification follows the Vermont Agency of Natural Resources (2007) protocol and separates distinct reaches of streams based on degree of valley confinement, type of surficial deposits, changes in substrate type (bedrock vs. gravel), abrupt changes in slope and proximity to the confluence of major tributaries (Table B-1).

Table B-1: Number of reaches by stream order¹ for the Massachusetts portion of the Deerfield River watershed

Stream Order	Number of Reaches
1	1,125
2	414
3	183
4	107
5	40
6	91

¹Stream order is a method of classifying streams. First-order streams are small headwater streams. Two first-order streams join to create a second-order stream, two second order streams make a third order stream and so on.

B.2.1.2 Slope

Following Tropical Storm Irene, LiDAR data were collected for the Hudson, Deerfield and Hoosic River watersheds. The area was flown in April 2012 and data were subsequently processed by Northrop Grumman, Advanced GeoINT Solutions Operations Unit, Huntsville, AL. Horizontal resolution is 2 meters and vertical resolution is 0.15 meters. The horizontal datum is NAD83 and vertical datum is NAVD88. Reaches were laid over the bare earth model of the topography in GIS. The difference between the elevation at the start and end of each reach was divided by the length of the reach to determine reach slope. The LiDAR data were used only for the calculation of slope.

B.2.1.3 Discharge

Discharge (Q) was computed using the Jacobs (2010) equation developed for estimating the magnitude of peak flows for steep gradient streams in New England. Comparison of the Jacobs equation and the USGS Regional Regression equations for Massachusetts (Bent and Waite, 2013) with statistical analysis of the 2-year frequency flood at 5 gauging stations in the Deerfield River Basin showed that the USGS equations underestimate significantly the 2-year peak discharge (Table B-2). The USGS regression equations are based on a statewide analysis of Massachusetts gauging stations, whereas the Jacobs equation is derived explicitly from gauging stations in the hillier parts of New England where main channel gradients exceed 0.01. The average gradient of the Deerfield River is 0.004 but most of the tributaries are confined in valleys, have cobble to gravel substrates and have steeper gradients. Exceptions are portions of the East Branch of the North River in Colrain, the southern end of the Green River, and the Charlemont and Deerfield Meadows sections of the Deerfield River. Based on this analysis, Jacobs equation was deemed a better choice for estimating discharge for stream power calculations.

Table B-2: Estimated channel forming discharges comparison, cubic feet per second (cfs)

USGS Gauge Station	USGS Regional Regression EQ (Bent and Waite, 2013)	Listed USGS Bankfull Q at Gauge ⁽²⁾	Statistical Gauge Analysis, 2-Year Frequency Flood ⁽³⁾		Jacobs 2-Year Regression Eq. (2010)
			USGS up to 2009 ⁽²⁾	MMI up to 2013	
Deerfield River at Charlemont ⁽¹⁾	4,121	N/A	N/A	10,943	10,540
Deerfield River at West Deerfield ⁽¹⁾	5,829	N/A	N/A	16,032	14,134
North River	1,345	3,070	4,895	4,718	3,025
South River	471	1,710	1,937	1,906	950
Green River	729	2,110	2,450	2,268	1,469

⁽¹⁾Regulated by upstream dams

⁽²⁾As reported in Bent and Waite (2013)

⁽³⁾Based upon MMI statistical analysis of gauge data

B.2.1.4 Precipitation

The Jacobs equation ($Q_2 = 0.01601A^{0.889}P^{2.12}$, where Q is the 2-year flood frequency in cubic feet per second--also assumed to be the bankfull channel forming flood, A is the drainage area in square miles, and P is mean annual precipitation in inches) requires Area and Precipitation. Mean annual precipitation is obtained from the 1961 to 1990 Parameter-elevation Regressions on Independent Slope Model (PRISM) maps developed by the U.S. Department of Agriculture with Oregon State University. The annual map is produced by summing the 12 monthly maps. This approach accounts for orographic effects by distributing the rainfall totals spatially over the entire watershed.

B.2.1.5 Area

For this project one standard digital elevation model (DEM) was used for area determinations so that hydraulic calculations would be consistent across methods. Though 2-meter LiDAR and 5-meter DEM data are available, it was decided to use the North Atlantic Landscape Conservation Consortium (NALCC) 30-meter DEM. The reason for selecting this lower resolution DEM is that it is consistent with the resolution of DEMs from other parts of New England. Many other regions do not have high resolution DEMs. This will enable other researchers to compare data from the Deerfield River watershed with other parts of New England using the same base maps. In addition, a flow accumulation layer was already developed for this DEM that has been checked for quality assurance. Drainage areas for each reach exit point were determined using the flow accumulation layer. Using the precipitation and area calculations, the two-year discharge (Q_2) was computed in GIS for each reach and tabulated.

B.2.1.6 Bankfull Width

The channel-forming discharge is assumed to occur when the stream is at bankfull and is referred to as the bankfull discharge. It has a return period of approximately 1.67 years. From a practical matter, the 2-year return period is taken as the bankfull discharge. Several regime equations exist that relate bankfull discharge (Q_2) to bankfull width (W). Soar and Thorne (2001) provide a rigorous summary. The USGS has also developed regime equations (also referred to as hydraulic geometry curves) for Massachusetts (Bent and Waite, 2013). MMI conducted a series of explorations by comparing field measured bankfull widths along the Deerfield River and selected tributaries with hydraulic geometry

relations and regime equations (at gauging stations only) (Table B-3). Results show that the use of the Jacobs equation to estimate Q_2 combined with the Soar and Thorne version of the Lacey equation (Lacey, 1930) is a better predictor of bankfull width when compared to field measurements than the Massachusetts statewide hydraulic geometry regression equations developed by the USGS (Bent and Waite, 2013). The primary reasons for this discrepancy are the steeper gradients and gravel/cobble dominated substrates typical of the Deerfield River watershed. The equation used to estimate bankfull width is: $W = 3.68 Q_2^{0.5}$.

Table B-3: Comparison of bankfull widths at USGS gauges

USGS Gauge Site	Bankfull Widths, ft			
	Drainage Area, sm	USGS Measured	Regression EQ (Bent, 2013)	Jacobs Q ₂ and Regime
North River	89.0	106.3	92.1	116
South River	24.1	65.55	54.3	64.7
Green River	41.4	104.75	67.6	80.5
West Branch Westfield	94.0	124.15	94.2	116
Hubbard River	19.9	73.25	50.3	58
Green River Williamstown	42.6	79.0	68.4	81.5
Mill River Northampton	52.6	84.5	64.5	89.5

Residual = $\frac{\text{measured width}}{\text{regression equation}} = \%$

Mean = 28.1%
sm = square miles

Regression EQ Width = $W_b = 15.0418 (DA)^{0.4038}$

B.2.2 Calculation of Stream Power

Slope, precipitation, and drainage area data for each reach were brought into ArcGIS. Bankfull discharge was then computed using the Jacobs equation, which in turn was used in the Lacey equation to compute reach-average bankfull width. Once these additional components were calculated, the specific stream power was estimated for each reach by applying the equation:

$$\omega = (\rho g Q_2 S) / W$$

where ω is specific stream power (W/m^2), ρ is water density (kg/m^3), g is acceleration of gravity (m/sec^2), Q is bankfull discharge (m^3/sec), S is slope (m/m), and W is bankfull width (m). River reaches were then classified, color coded and overlain with crossing locations. The stream power map is provided in Appendix G. The classification system is provided below (Table B-4).

Table B-4: Specific stream power classification on the stream power map

Color	SSP, W/m^2
Green	0 – 30
Light Green	31 – 60
Pale Green	61 – 200
Yellow	201 – 300
Orange	301 – 600
Red	>600

SSP = Specific Stream Power
 W/m^2 = Watts per square meter

Specific stream power was also calculated for the 100-year event (Q_{100}) using the Nature Conservancy valley bottom mapping tool to calculate the valley bottom area. However, the floodplain width determined by this method was considered less reliable than the bankfull width calculations and not used to estimate stream power.

B.3 Crossing Vulnerability Screen and Scoring System Development

The development of the vulnerability screen by MMI described in this Appendix refers to culvert condition, not risk of failure, where a low score <0.4 indicates poor condition (high vulnerability), ≥ 0.4 to <0.6 indicates moderate condition (moderate vulnerability) and ≥ 0.6 to 1.0 indicates good condition (low vulnerability). However, during project development MassDOT decided that risk of failure was a better measure of vulnerability and that a high score should indicate an elevated risk of failure and a low score suggestive of a minimal risk of failure. In other words, risk of failure should be the direct inverse of culvert condition (e.g., a condition score of 0.2 (poor condition) is equivalent to a risk of failure score of 0.8 (considerable risk of failure)). However, MMI had completed their work before the change from condition to risk of failure occurred. Rather than change all MMI's graphs and analyses, we decided that it would be more cost-effective for the purposes of screen development to evaluate all culverts in terms of "condition," then make the conversion to risk of failure as the last step. Accordingly, Appendix B refers to all analyses with respect to culvert condition and Chapter 5 provides the final scoring system in terms of risk of failure.

B.3.1 Vulnerability Screen

MMI selected a subset of 197 bridges and culverts to use in developing and testing a screening tool for identifying structures vulnerable to damage due to geomorphic stressors. Structures were selected for evaluation if they were reported or observed to be damaged according to the municipalities, MassDOT, TU or MMI. Structures were also included in this subset if they could potentially be damaged based on the stream power map.

B.3.1.1 Data Collection and Analysis

MMI developed a field form that included the CAPS ID, xycode, Culvert or Bridge ID, stream name, road name, descriptive location, latitude and longitude, number of culvert cells, culvert shape, width, height, length, culvert slope relative to channel slope, culvert width as a percent of bankfull channel width, culvert alignment with channel, and past observations of any damage. Other data collected were the drainage area above the crossing, channel bankfull width, upstream channel slope, estimated bankfull flow, median grain size (D_{50}), and upstream and downstream substrate type. The specific stream power was determined from the stream power map. Slope measurements were made using a folding rule and level or a TruePulse Model 360 laser rangefinder. D_{50} was determined using pebble counts (Wolman, 1954).

Damaged structures in this subset were assigned a damage letter (Table B-5). A total of 78 structures were assigned a damage letter based on input from the towns and MassDOT. However, upon field review by MMI, only 51 culverts indicated confirmed damage¹. Each damaged culvert was assigned a damage code. Each damage code contains a compilation of all observed types of damage and is

¹ MMI email dated 1/26/2017 details the basis for identifying damaged culverts used in their analysis.

represented by the combination of damage letters. The range of damage codes present in this dataset is shown in Table B-6.

Table B-5: Structure damage letters

O	Overtopping
E	Embankment Failed
B	Blocked by Debris
S	Structural Failure
W	Washed Out
F	Roadway Flooding
L	Fluvial Erosion
*	Repeated Failures

Table B-6: Damage codes assigned to damaged culverts by damage type

Table of Damage Code Options						
1	2	3	4	5	6	7
OEB	EL	B	BSL			L
OW		BF	SL			EL
OE			SL			FL
O			BSL			
OB						
OEW						
OEWL						
OS						
OL						

The vulnerability screen was developed through a trial and error process by selecting geomorphic variables that serve as practical predictors of vulnerability. The selection of these variables was based in part on a review of the literature and previous work in the region by MMI, specifically work in Vermont, New Hampshire, and New York. These variables include:

1. Specific stream power versus bed resistance – It is assumed that more damage will occur as the stream power increases. However, to begin moving particles the stream must overcome the streambed's resistance to shear stress. The bed resistance is a function of particle size. MMI combines stream power and bed resistance as a proxy for initiation of scour or deposition.
2. Structure Width Ratio – This is the ratio of the structure width to the channel width. The lower the ratio (expressed as a %), the more constricted the opening. The assumption is that a smaller opening can promote blockage and/or ponding with subsequent overtopping or other damage.

3. Structure slope – This is the difference between the local channel slope and the slope of the structure (ft/ft). A change in slope, either the structure is flatter or steeper than the channel, can result in erosion or deposition of sediment.
4. Sediment continuity – This is the ability of the structure to transmit sediment and is based on field observations of either scour or deposition at the down or upgradient ends of the structure.
5. Structure alignment – This is the alignment of the structure to flow in the channel. Skewed alignments are assumed to produce greater erosion of embankments, which can compromise structural integrity or produce large woody debris capable of blocking structure openings.

Success or failure of the vulnerability screen was determined by comparing the number of damaged structures (n=51) with undamaged structures (n=146). These comparisons are made with respect to each variable and to the combined, single condition score. In other words, if high stream power equates to greater damage, a higher percentage of damaged culverts should occur at culverts associated with high stream power. Similarly, if skewed structures produce a greater vulnerability to failure, then a higher percentage of damaged culverts should fall in the skewed category.

The vulnerability screen that MMI developed is shown in Figure B-1. Note that in the MMI vulnerability screen specific stream power vs. bed resistance, structure width ratio and change in slope are scored from 0 to 4, whereas sediment continuity and alignment are scored from 1 to 3, indicating that the latter parameters have less influence on the final scores than other variables. This is because sediment continuity and alignment are based on qualitative observations rather than quantitative data. Also note that structure width has five categories and the change in slope has 6 categories.

To compute the combined condition score for each culvert, the assigned scores for each category 0-4 or 1-3 are summed then divided by the maximum score (in this case, 18) to obtain a normalized (between 0 and 1) overall condition score.

Vulnerability Score							
< 0.4	>=0.4 to 0.6	>=0.6 to 1					
High	Medium	Low					
Specific Stream Power versus Bed Resistance							
		Dominant Particle Size (Bed Resistance)					
		Silt	Sand	Gravel	Cobble	Boulder	Bedrock
Specific Stream Power (W/m ²)	0-60	3	3	2	3	4	4
	60-100	3	3	0	1	3	3
	100-300	3	2	0	0	2	2
	300+	2	1	0	0	1	2
Structure Width Ratio							
Structure Width / Channel Bankfull Width (%)							
< 50%	50 - 75%	>75 - 100%	>100 - 125%	>125%			
0	1	2	3	4			
Change in Slope							
Local Channel Slope - Structure Slope (feet / feet)							
<= -0.03	>-0.03 and <=-0.02	>-0.02 and <=0	>0 and <=0.02	>0.02 and <=0.03	>0.03		
1	2	4	4	3	1		
Sediment Continuity							
		Downstream Bed					
		Erosion	None	Aggradation			
Upstream Bed	Aggradation	1	2	3			
	None	2	3	3			
	Erosion	3	3	3			
Structure Alignment							
Skewed	Aligned						
1	3						

Figure B-1: Original vulnerability screen developed by MMI.

B.3.1.2 Analysis Results

Examination of the overall condition score (all five variables combined as a composite score) shows an increase in the number of damaged structures as the vulnerability level increases (Figure B-2). 41% of the structures indicating high vulnerability also had observed damage. In contrast, 14% of structures in the low vulnerability category were observed to have damage.

B.3.1.3 Stream Power and Bed Resistance

Most of the damage to structures occurred with specific stream power between 60 and 300 W/m². 41 of the 51 damaged culverts occurred on streams with specific stream power within this range. 7 culverts experienced damage between 300 and 600 W/m², only one culvert was damaged above 600 W/m² and 3 showed damage below 60 W/m² (Figure B-3).

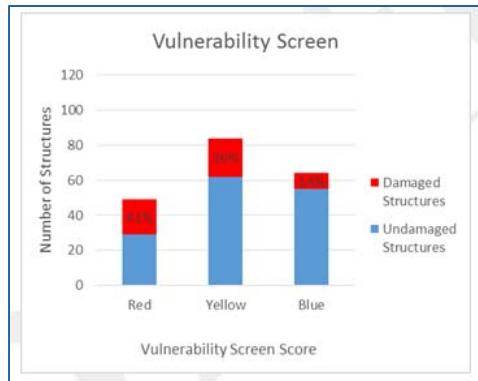


Figure B-2: Overall condition score from MMI data.

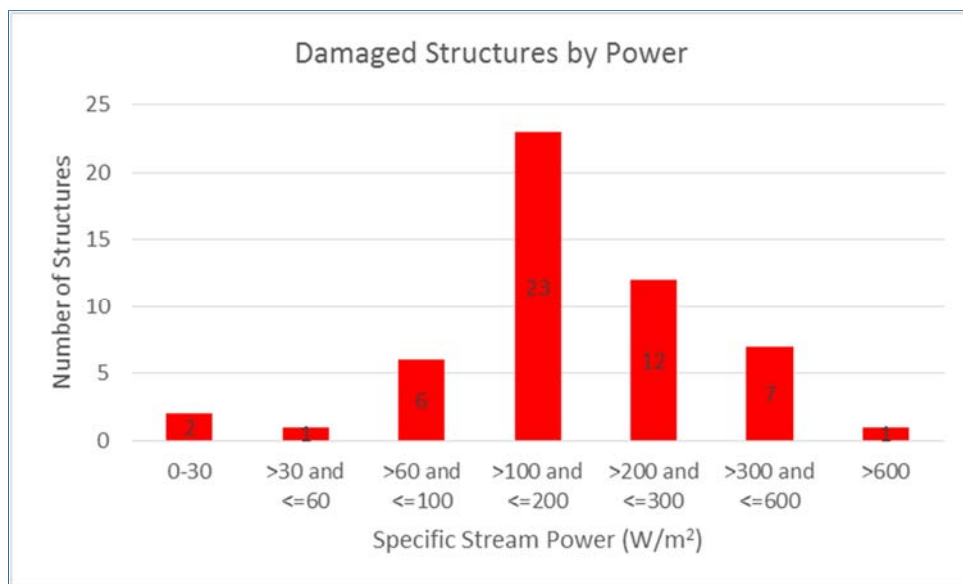


Figure B-3: Number of damaged structures by specific stream power.

The highest percentage of damaged structures occurs in streams where the bed material is dominated by gravel and cobble (Figure B-2). Stream power does increase as the dominant grain size increases, as expected, and most of the damage is concentrated in streams that have gravel and cobble substrates (Figure B-3). One explanation for this distribution is that bedrock and boulder substrates, while experiencing high stream power, are not as mobile or as easily eroded, and sand, silt and clay substrates in the Deerfield River watershed are not as common (an exception is the lower Deerfield River near the confluence with the Connecticut River) or have already been eroded. Damage is concentrated in gravel and cobble substrates and is more common in the mid-stream power ranges (i.e., 100 to 300 W/m²). This is a key finding of the study. This pattern of damage occurring in the intermediate stream power range has been observed in Vermont by MMI and in other studies (Knighton, 1999).

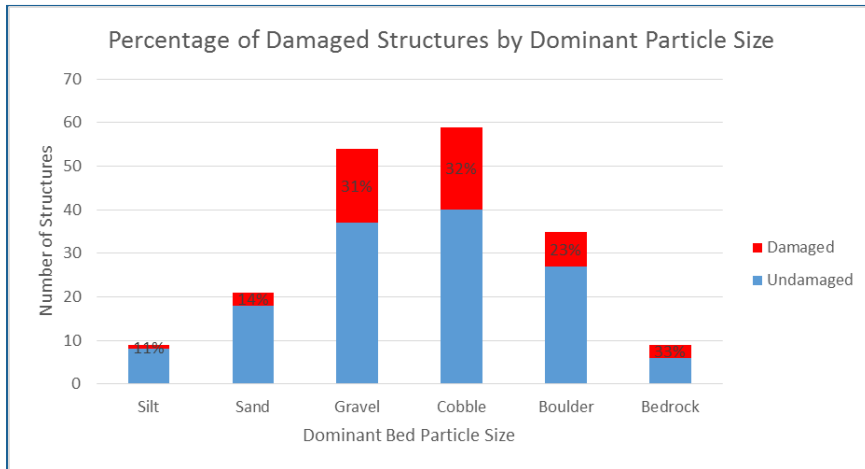


Figure B-4: Percent of damaged structures as a function of dominant bed particle size.

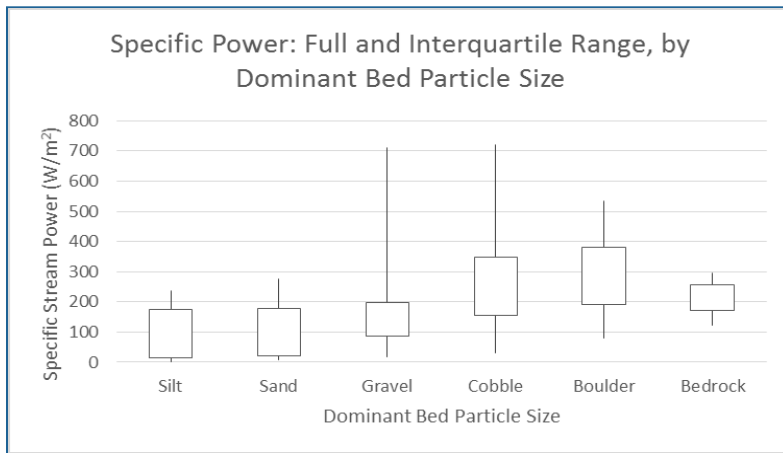


Figure B-5: Box plot of specific stream power as a function of dominant bed particle size. Boxes represent the interquartile range and the whiskers the full data range.

B.3.1.4 Structure Width Ratio

The greatest number of structures had structure width to channel width ratios between 25% and 50%. This group also had a high failure rate (Figure B-6). Overall, a higher percentage of structures experienced damage when the structure spanned less than 75% of the bankfull channel width. These results support the notion that damage is more common on undersized structures.

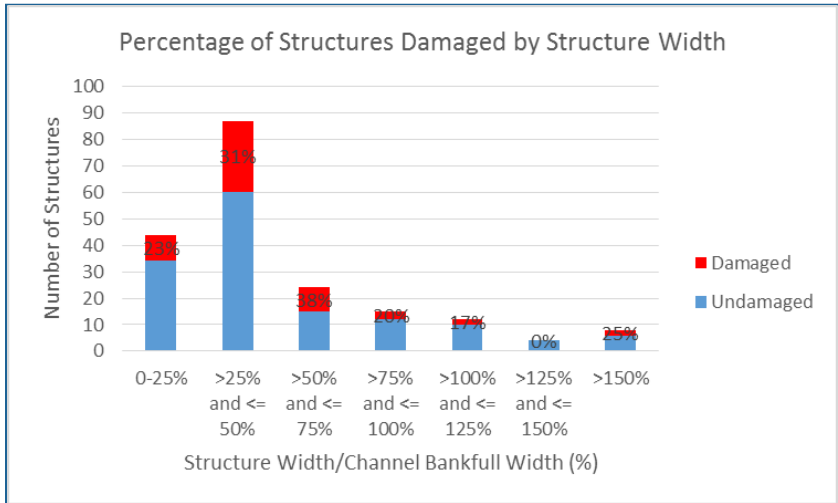


Figure B-6: Percentage of damaged structures by structure width to channel bankfull width ratio.

B.3.1.5 Structure Slope

Structures that were either flatter or steeper than the channel slope indicated a higher percentage of damaged structures (Figure B-7). Overtopping and blockage by debris occurred most frequently in structures that were flatter than the local channel slope.

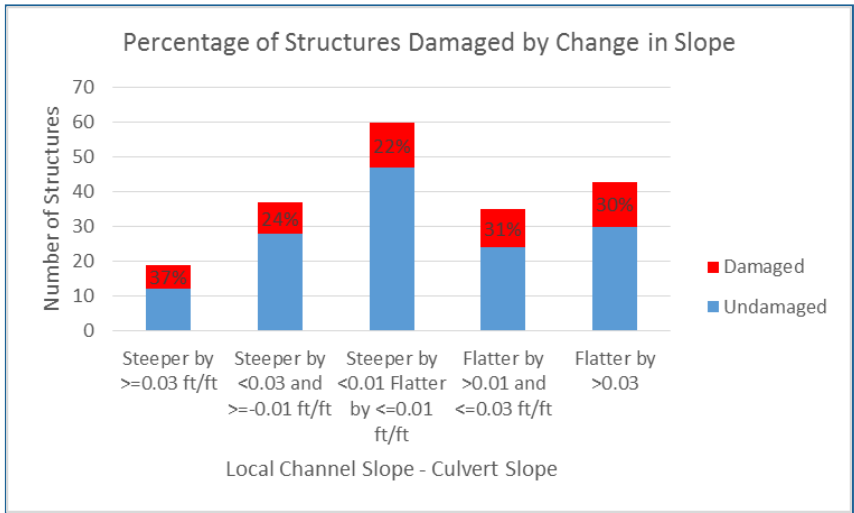


Figure B-7: Percent damaged structures as a function of difference between the local channel slope and the structure slope.

B.3.1.6 Structure Alignment

A higher percentage of structures are damaged if the structure is not aligned with the channel, as expected (Figure B-8). Overtopping was the most common type of damage observed in culverts that were skewed.

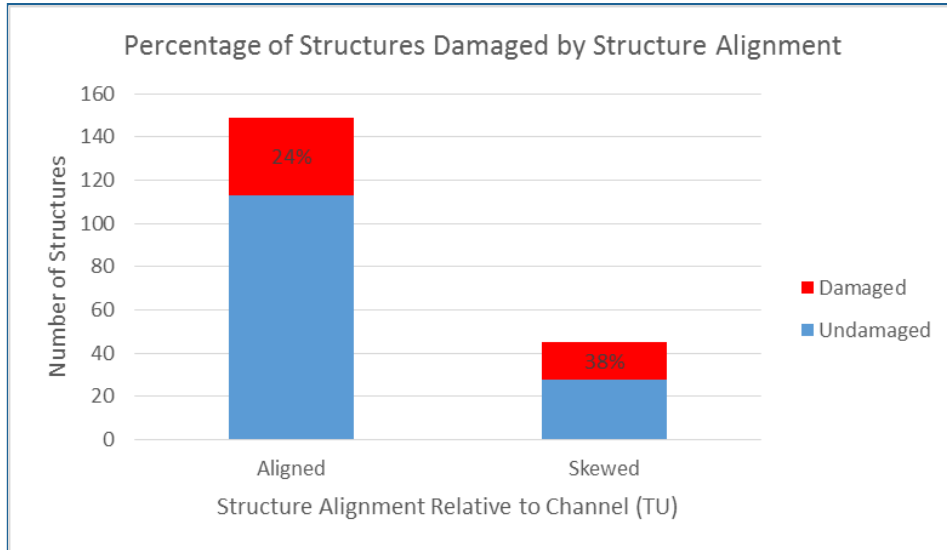


Figure B-8: Percent of damaged structures as a function of structure alignment relative to the channel.

B.3.1.7 Sediment Continuity

Structures were considered vulnerable if they disrupted the stream's ability to transport sediment, causing aggradation or erosion at the upstream or downstream end of the structure. Structures that showed aggradation on the upstream side and erosion on the downstream end of the structure were considered the most vulnerable.

B.3.1.8 Summary of Vulnerability Screen

The results above indicate that all five described variables, are related to whether damage occurs. Accordingly, the scores in the vulnerability screen (see Figure B-2) reflect the trends observed in the data.

B.3.2 Slope Analysis

The development of the vulnerability screen by MMI used slope as a criterion for geomorphic vulnerability. However, local channel slope was not measured as a matter of course at all locations. Accordingly, the slope criterion presented by MMI cannot be applied to all structures in the watershed. The following evaluates the effect of removing slope from the vulnerability screen.

Other than the removal of slope, the modified vulnerability screen operates under the same conditions. Vulnerability is computed for the subset of 197 culverts by summing the assigned scores for each category, minus the slope category, and dividing by the maximum score (14 in this case) to obtain a normalized (between 0 and 1) overall condition score. Results, again, refer to culvert condition, not risk of failure, where a low score <0.4 indicates poor condition (high vulnerability), ≥ 0.4 to <0.6 indicates moderate condition and ≥ 0.6 to 1.0 indicates good condition (low vulnerability).

Removal of the slope category from the vulnerability screen produced results like those observed when slope was included (see Figure B-2 for comparison). 30% of the culverts in the moderate and poor condition categories (red and yellow in Figure B-9) were damaged whereas 12% of culverts in the poor condition category (blue in Figure B-9) were damaged (Figure B-9). Excluding slope increased the number of culverts that fell in the moderate condition category (increase from 84 culverts to 108

culverts). Most of the culverts moved from the good condition category (a drop from 64 to 43 when slope is removed) and only 3 culverts moved from poor condition to moderate condition. The removal of slope tended to move the culverts in the direction of poorer condition (i.e., more conservative direction) (Figure B-10).

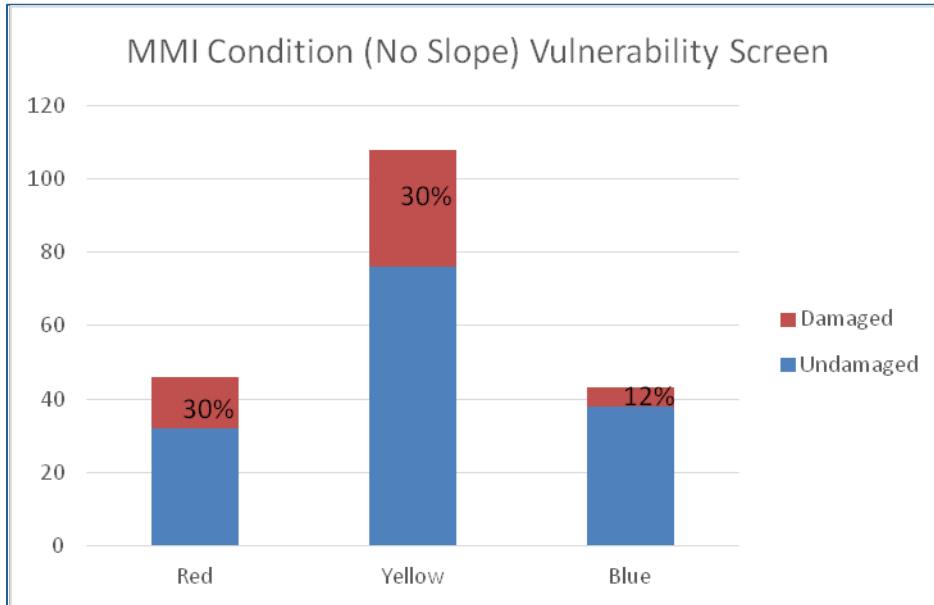


Figure B-9: Condition score with slope excluded from the 197 structures analyzed by MMI

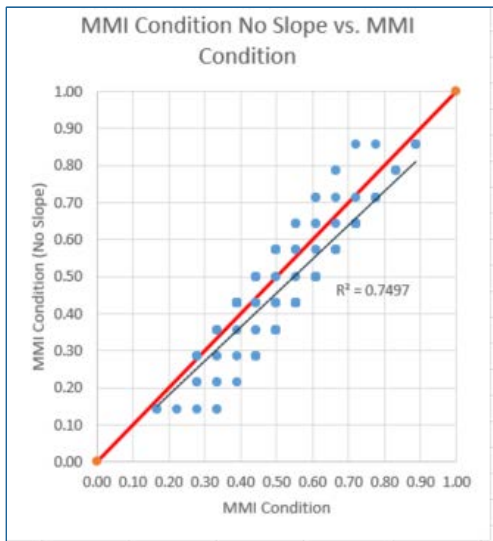


Figure B-10: Regression comparing MMI condition score with slope versus no slope. Black line is the regression and red line is the one to one line. $R^2=0.75$, $n=197$

Overall, it appears that excluding slope does tend to assign more conservative overall condition scores, but there remains a significant difference in the percentage of damaged culverts occurring in the good condition category from the percentage of damaged culverts occurring in the moderate and poor condition categories. Results suggest slope can be eliminated without shifting damaged culverts into better condition categories.

Obtaining slope data in the field, especially high-accuracy slope data, is time consuming. It can be done using a folding rule and level, laser rangefinder or total station. For this study, MMI used a rangefinder and folding rule. Slope was evaluated by determining the slope on the upstream side of the culvert and the slope on the downstream side of the culvert (typical distance from the culvert of ~100 feet), combining those two measurements to obtain an average slope, and subtracting the structure slope from the average channel slope. One consideration in measuring slope is, at what horizontal distance should the measurement be taken? How far upstream or downstream from the culvert one goes before making a measurement affects the final measurement. Should the distance be 50 feet from the culvert or 100 feet, and what about sight lines? In addition, it matters where in the river the measurement is made. Should it be the river bottom in the thalweg, at the river's edge, water surface at the edge of a cobble? The ranges used by MMI to distinguish slope score categories are quite small, in some cases only 0.01 ft/ft (Figure B-1). It could be argued that this is comparable to the range of measurement uncertainty associated with the decision-making described above. Accordingly, if slope measurements are instituted in the protocol, a consistent, repeatable field procedure needs to be developed. The data obtained so far does not appear to justify the labor needed to collect the data, in that it does not affect the overall condition score significantly.

B.3.2.1 Substitution of Reach-Scale Slope

Given the potential uncertainty associated with local channel slope determination, an analysis was performed where reach-scale slope was substituted for local slope. Reach scale slope was determined by MMI during the stream power analysis using GIS. The Deerfield River watershed was divided into 1,960 reaches based on significant changes in slope, degree of valley confinement, material changes, or confluence with tributaries. Slope was determined from Lidar data by taking the maximum Z value at the upstream end of the reach and the minimum Z value at the downstream end of the reach along a flow line, finding the difference between these two values and dividing by the reach length. Reach lengths in the entire data set range from a few tens of feet to 16,000 feet (but ranged typically between 2000 to 5000 feet).

Results show the number of culverts in each condition category is evenly distributed with 62 culverts in the poorest condition category (red), 72 in the moderate condition category (yellow) and 63 in the best condition category (blue) (Figure B-11). 32% of the culverts in the poorest and moderate condition categories are damaged whereas 13% of the culverts in the best condition category are damaged. Again, there is a clear separation between the best condition category and other categories. There are always significantly fewer damaged culverts observed in the good condition category.

The effect of substituting reach scale slope is to decrease the condition score in the higher ranges (>0.6) and increase slightly condition scores in the low ranges (<0.3) (Figure B-12). This may be the result of steeper gradients at the reach scale compared to local scale slopes.

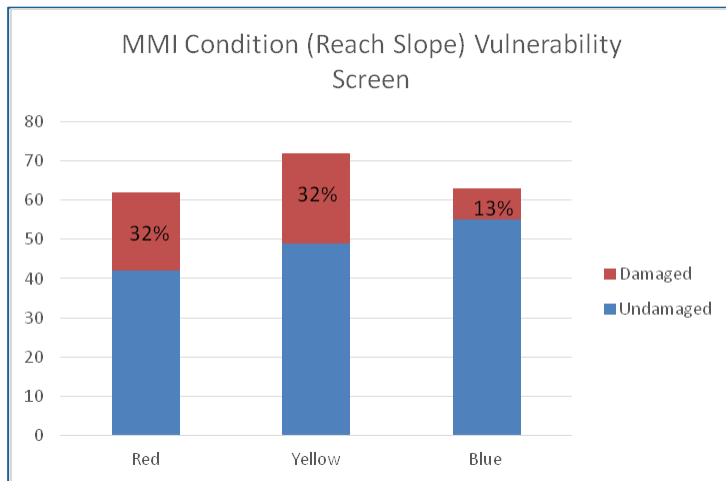


Figure B-11: Percentage of damaged culverts occurring in the three condition categories when reach-scale slope is substituted in the data set instead of local slope.

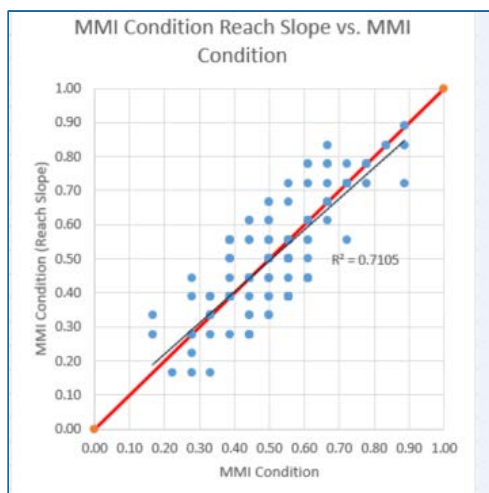


Figure B-12: Regression comparing condition scores using reach scale slope vs. local slope. Red is the 1 to 1 line, black line is the best fit regression. $R^2 = 0.71$, $n=197$.

Comparison of vulnerability scores incorporating reach scale slopes with scores that don't incorporate slope confirms that removal of reach scale or local scale slope from the vulnerability screen produces lower scores (Figure B-13). In other words, removal of slope provides more conservative results by assigning generally poorer condition scores. Based on these results it appears reasonable to omit slope from the calculation of overall vulnerability. The uncertainty associated with the local channel slope measurement does not warrant the additional labor cost to acquire the information from the field. If slope is desired, reach scale slope can be substituted.

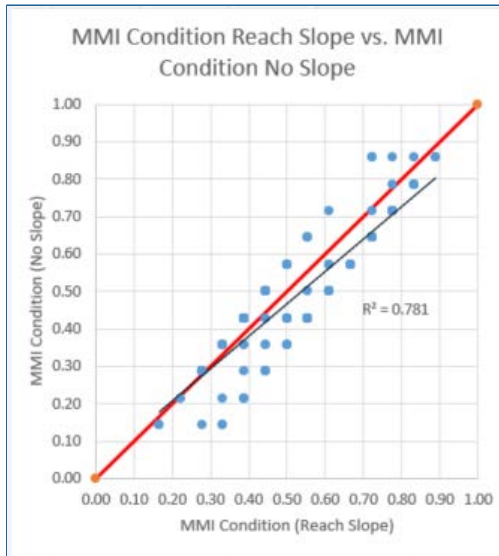


Figure B-13: Regression comparing condition scores using reach scale slope vs. no slope. Red is the 1 to 1 line, black line is the best fit regression. $R^2 = 0.78$, $n=197$

B.3.3 Vulnerability Screen Sensitivity Analysis

Condition is calculated by combining the stream power, structure width ratio, sediment continuity and alignment scores and dividing the sum by the maximum possible score to come up with a final vulnerability score between 0 and 1. A score <0.4 indicates a poor condition and is colored red, ≥ 0.4 to <0.6 a moderate condition (yellow) and scores ≥ 0.6 represent good condition and are designated as blue.

In this analysis, the overall vulnerability score was recalculated using each individual geomorphic parameter in different combinations to determine which combination showed the highest percentage of damaged culverts in the red category and the lowest percentage of damaged culverts in the blue category. In other words, which combination of parameters does the best job of explaining the occurrence of damaged vs. undamaged culverts in the dataset. The combinations that were tested are shown in Table B-7.

Results show that the combination of stream power and stream alignment (AD in Table B-7) is a good predictor of damage (Figure B-14). 42% of the culverts in the poorest condition category (red) are damaged whereas 12% of the culverts in the lowest category are damaged. Stream power (A) alone is also a good predictor of damage. We define a good predictor as one that gives maximum range in the percent damaged between red and blue categories. Other promising combinations include ABD, ABC, and ACD.

Table B-7: Geomorphic Combinations Used in the Vulnerability Sensitivity Analysis

Parameter	Symbol	Combinations
Stream Power/Resistance	A	A
Structure Width Ratio	B	AB
Stream Continuity	C	AC
Alignment	D	AD
		ABC
		ABD
		ACD
		ABCD
		B
		BC
		BD
		BCD
		C
		CD
		D

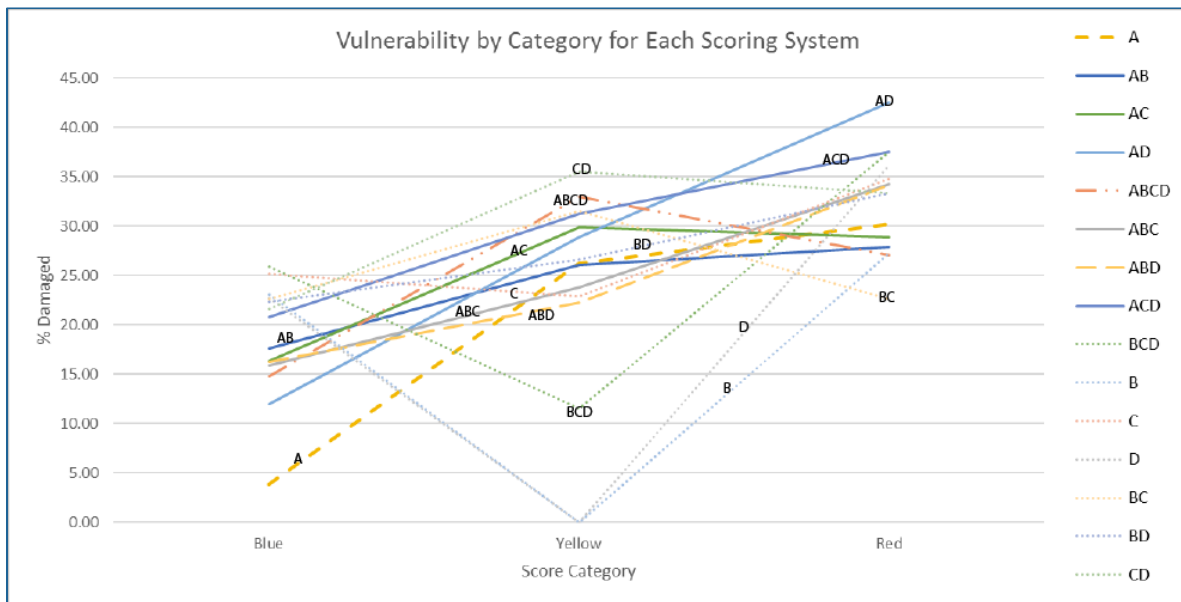


Figure B-14: Condition scores recalculated for different geomorphic parameter combinations

Figure B-14 shows only the percentage of culverts that are damaged within each category. For example, in the stream power scoring system (A in Figure B-14), 4% of the culverts in the blue category (best condition) are damaged. How does this plot change if the percentage of damaged culverts is recalculated based on the total number of damaged culverts (51) in the dataset?

Figure B-15 plots the percentage of all damaged culverts as a function of condition (blue, yellow, or red) for each scoring system. Stream power (scoring system A) appears most robust. For stream power, 74% of all the culverts that are damaged occur in the poorest condition category as expected. 2% of all damaged culverts fall in the best condition category. Other combinations that provide reasonable results include AB, ABD and ABC.

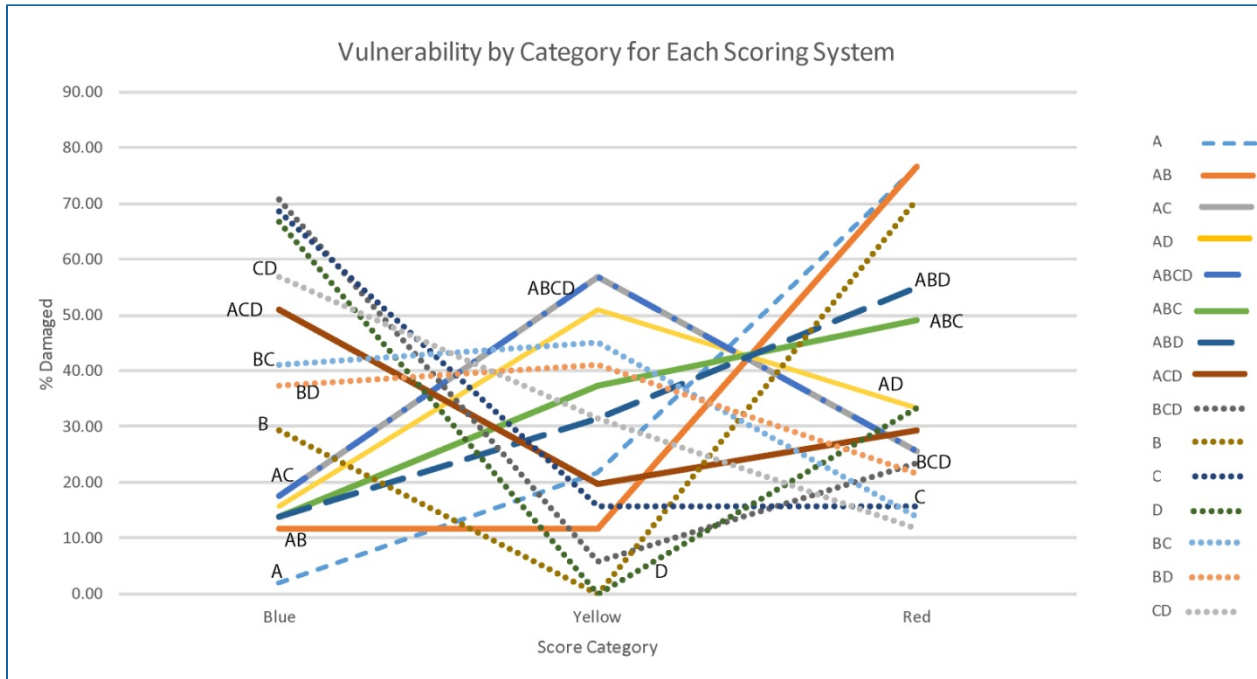


Figure B-15: Condition scores recalculated for different geomorphic parameter combinations plotted as a percent of all damaged culverts

Figure B-16 compares the results of several vulnerability screens: A, AB, AD, ABD and ABCD. Each histogram represents the number of undamaged (blue section) and damaged (orange) culverts that fall in each condition category. The number posted on the histogram is the relative percentage of culverts in that category that showed damage. The line on the plot shows the total percentage of damaged culverts occurring in each condition category. Blue represents good condition, yellow moderate condition and red poor condition. Ideally, a decrease in the total number of damaged culverts is desired along with a relatively even distribution in the number of culverts that occur in each category. The ABD vulnerability screen best meets these criteria. However, intuition suggests that stream continuity should also be included in the scoring system because it is based on direct observation of sedimentation and scour.

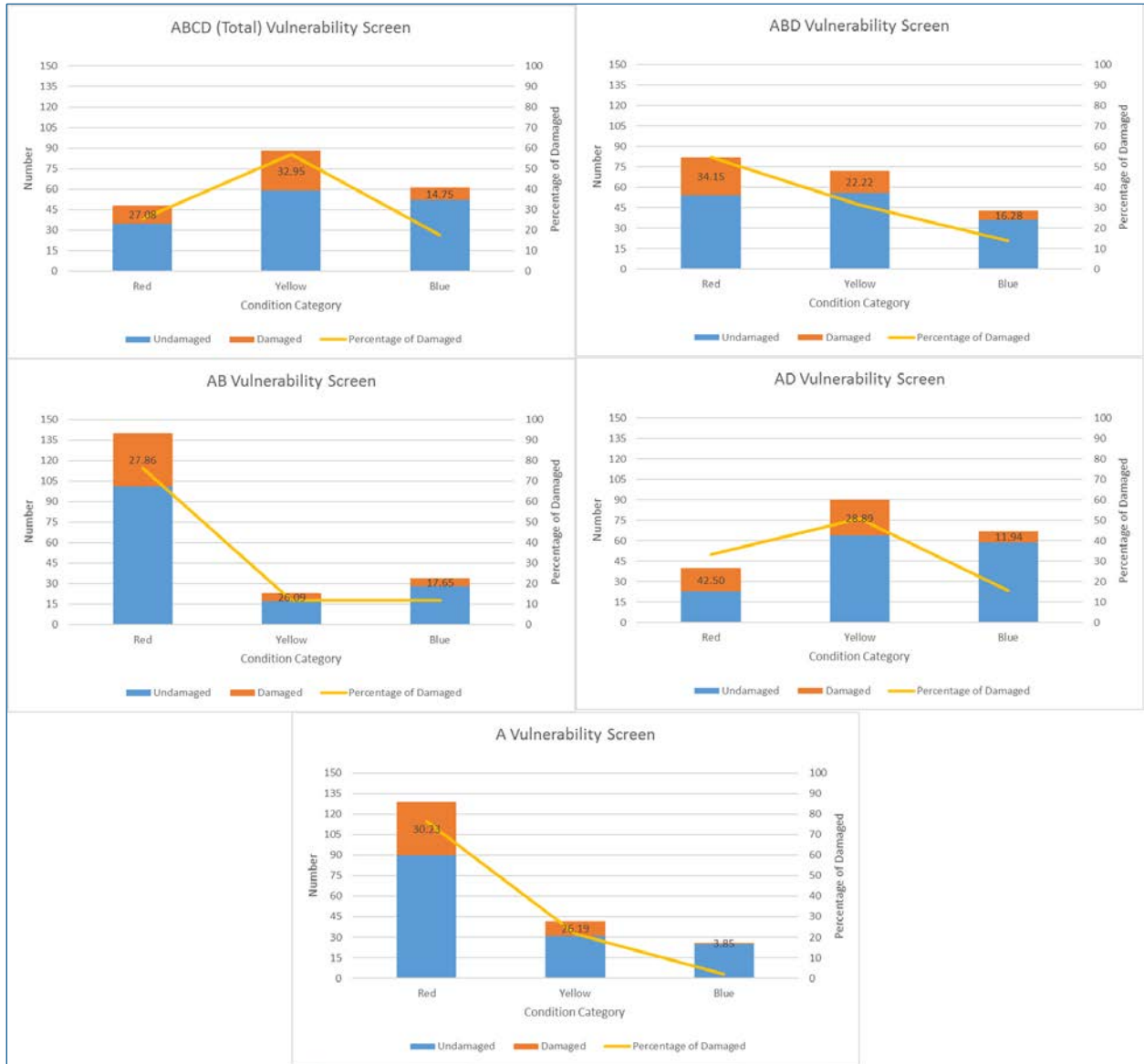


Figure B-16: Comparison of selected vulnerability screens. See text above for explanation of figure.

B.3.4 Scoring System Development

Based on these results and discussions with team members and MassDOT, a scoring system was devised using the components of the vulnerability screen and other condition data. Four categories, each expressing a specific geomorphic condition at a crossing that could lead to failure, were selected (Table B-8). These categories include propensity for woody debris accumulation, susceptibility to sedimentation, susceptibility to scour, and evidence of blockage.

Table B-8: Scoring system organizing the geomorphic parameters into four scoring categories: Woody debris, sedimentation, scour and blockage.

Category	Parameter
Woody Debris	Structure Alignment, Absolute Structure Width
Sedimentation	Stream Power ≤ 100 W/m ² , Structure Width Ratio, Sediment Continuity (Aggradation)
Scour	Stream Power, Sediment Continuity (Erosion), Footing Score, Downstream Scour Pool Score
Blockage	Blockage reported on the condition survey

Individual parameters from the vulnerability screen and condition surveys were then selected and placed in one of the four geomorphic categories (Figure B-17). For example, structure alignment and absolute structure width were considered to have the greatest influence on causing blockage by woody debris, thus these variables were combined to create a woody debris category.

Stream power, structure width ratio and sediment continuity were considered key factors affecting the propensity for blockage via sedimentation. Literature review conducted by MMI showed that low stream power or a sudden drop in stream power causes sedimentation. Degree of deposition is a function of stream power, but not erodibility of the bed. Therefore, only the specific stream power, not bed resistance, was considered when assigning values. Accordingly, we flag crossings with stream power ≤ 100 W/m², low structure width ratio or field evidence for aggradation of sediment as being at high risk of sedimentation.

High stream power, evidence of erosion in the field, and evidence of footing scour or a large downstream scour pool suggest a susceptibility to scour. For the scour score, a footing labeled as critical was given a score of zero. A footing with a score of poor was assigned a value of 2. Similarly, if there is a large downstream scour pool it is considered critical and could undermine the culvert or embankment. It is given a score of zero. If the downstream scour pool is considered small it is given a value of 2. Footings and downstream scour pools were given a score of 4 if they were "not poor or critical." Note: if either the footing or downstream scour pool was determined to be "not poor or critical" their scores were not factored into the overall scour score. If these are included, it skews the scores toward the good condition classification.

Blockage is provided as a separate category based on field evidence. If during the field visit the blockage was considered critical, it is given a score of 0. This score trumps all other scores and means the crossing is in poor condition. If it is poor the score is 0.5, otherwise 1. Blockage can mean blockage by woody debris or sediment, it is not specified in the condition field sheet.

The overall geomorphic score is determined by taking the lowest score determined in each of the four categories. The average score is not valid because a poor scour score will be cancelled out by a good sedimentation score and vice versa.

Woody Debris Score						
Structure Alignment		Absolute Structure Width (ft)				
Skewed	Aligned	<1	1-2	2-3	3-5	5-10
1	4	0	0.5	1	2	3
		>10	4			

Sedimentation Score						
Structure Width Ratio				Sediment Continuity		
Structure Width/Channel Width (%)				Downstream		
< 50%	50 - <100%	100 - <125%	≥125%	Aggradation	None	Erosion
0	1	2	4	1	1	1
Severe	Mild	Spans Bank to Bank	Spans Channel and Bank	Upstream Aggradation	2	3
				Upstream None	2	3
				Upstream Erosion	2	3

Specific Stream Power versus Bed Resistance							
		Dominant Particle Size (Bed Resistance)					
		Silt	Sand	Gravel	Cobble	Boulder	Bedrock
Specific Stream Power (W/m ²)	0-60	0	0	0	0	0	0
	60-100	1	1	1	1	1	1
	100-300	4	4	4	4	4	4
	300+	4	4	4	4	4	4

Scour							
Specific Stream Power versus Bed Resistance							
		Dominant Particle Size (Bed Resistance)					
		Silt	Sand	Gravel	Cobble	Boulder	Bedrock
Specific Stream Power (W/m ²)	0-60	3	3	3	3	4	4
	60-100	3	3	1	2	3	3
	100-300	3	2	0	1	2	2
	300+	3	2	0	0	2	2

Sediment Continuity				
		Downstream		
		Aggradation	None	Erosion
Upstream	Aggradation	3	3	3
	None	1	3	1
	Erosion	0	1	0

Footing Score			
Not Poor/Critical	Poor	Critical	If footing score is not poor or critical or there is no downstream scour pool then they were not included in the scour score.
4	1	0	
Downstream Scour Pool			
None	Small	Large	
4	1	0	

Blockage			
Not Poor/Critical	Poor	Critical	Blockage only included if its score is lower than the woody debris, sedimentation or scour score
1	0.5	0	

Figure B-17: Scoring system with initial scoring values.

Other modifications needed to develop the initial scoring system include:

1. Structure width score was reduced from five categories to four and rescaled as follows:
 - a. Structure width/channel bankfull width (%) <50% is equivalent to culverts described as a severe constriction
 - b. Structure width/channel bankfull width (%) between 50 and <100% is equivalent to culverts described as a mild constriction
 - c. Structure width/channel bankfull width (%) between 100 and <125% is equivalent to culverts described as spanning bank to bank
 - d. Structure width/channel bankfull width (%) >125% is equivalent to culverts described as spanning channel and banks.
2. Slope was removed from the analysis.
3. The woody debris category uses the absolute structure width rather than the structure width ratio, as structure width is considered a more realistic measure of the propensity of a structure to be blocked by woody debris.
4. Structure width ratio, absolute structure width, stream power/bed resistance, footing score, and downstream scour pool scores were scaled from 0 to 4.
5. Alignment was scaled from 1 to 4.
6. Sediment continuity in the Sedimentation category was rescaled between 1 and 3 and rescaled from 0 to 3 in the Scour category. Greater weight is given to the scour category because scour is expected to be a dominant process in the Deerfield River watershed due to the steeper gradients in the watershed.

Figure B-18 shows the distribution of the minimum geomorphology scores. The x axis is the scoring bins. A zero represents culverts with a minimum score of between 0 and <0.1. A 1 represents culverts with a score between 0.1 and <0.2, and so on. A value of 10 means the crossing scored a 1.0. The y axis is the number of culverts falling in each category. The values in the gray boxes are percent of culverts damaged in each category.

Results show that many of the culverts (61%) have scores <0.4. Forty-seven culverts (24%) have scores between 0.4 and <0.6 and 29 culverts (15%) have scores greater than 0.6. In addition, 73% of all damaged culverts have scores <0.4, 20% of all damaged culverts have scores between 0.4 and <0.6 and 7% of damaged culverts have scores \geq 0.6. While these results indicate most damaged crossings have poorer overall condition scores, it also indicates the majority of the culverts are classified as highly vulnerable and less useful as a screening tool requiring the additional adjustments (see below).

The last step in developing the scoring system was to invert the condition score to a risk of failure score and make final adjustments. Under the risk of failure assumption, a high score indicates an elevated risk of failure whereas a low score indicates a minimal risk of failure.

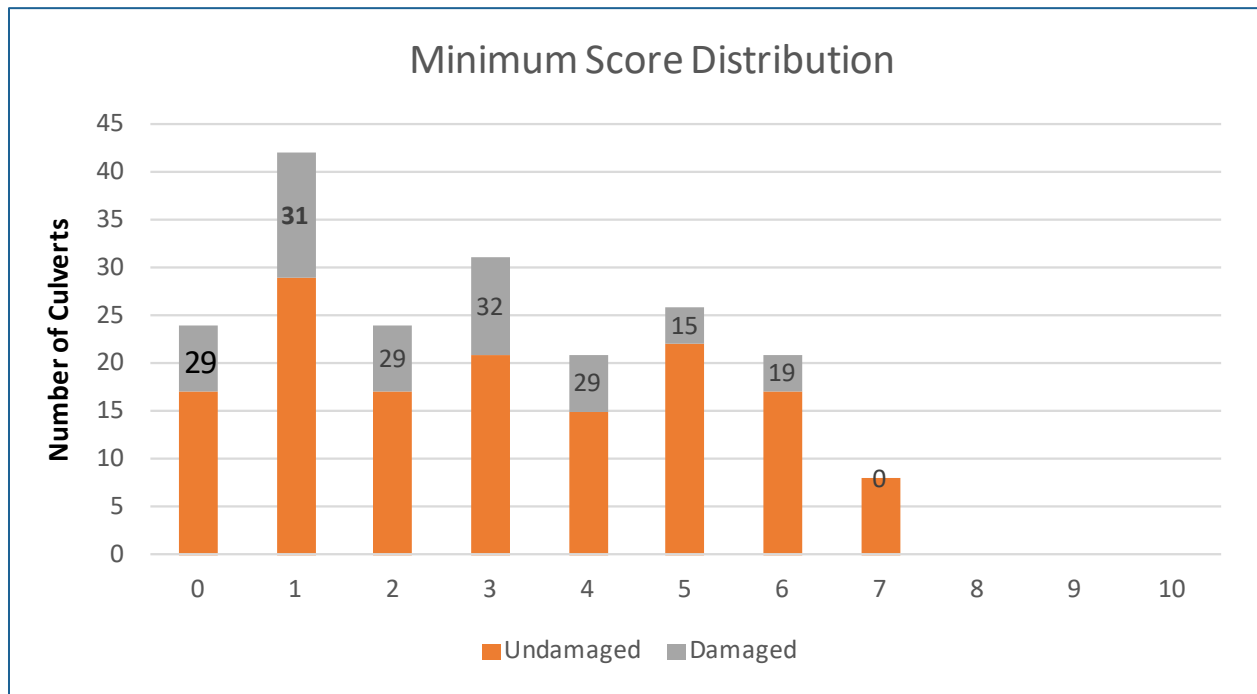


Figure B-18: Distribution of geomorphology minimum scores using the initial scoring system. See text for details.

Comparison of geomorphic, structural and hydraulic risk of failure scores indicates the geomorphic risk score is the maximum score for >68% of all crossings. In addition, the distribution of the overall risk of failure (taken as the maximum value of the three scores) is heavily skewed on the high side. 26% of the crossings have an overall risk score >0.9 and >43% have scores >0.8 (Figure B-19). Most of the skew is produced by the geomorphic scoring indicating the scoring system requires revision. Furthermore, evidence of scour was responsible for much of the elevated geomorphic scores.

Accordingly, the following revisions were made:

- For the scour score, footings that were labeled “not poor or critical” were given a score of 0 but were not included in the calculation of the score because it was thought that would skew the scores too low. In fact, not including the “0” score skewed the scores too high. The zero scores have now been included in the calculation of the scour score.

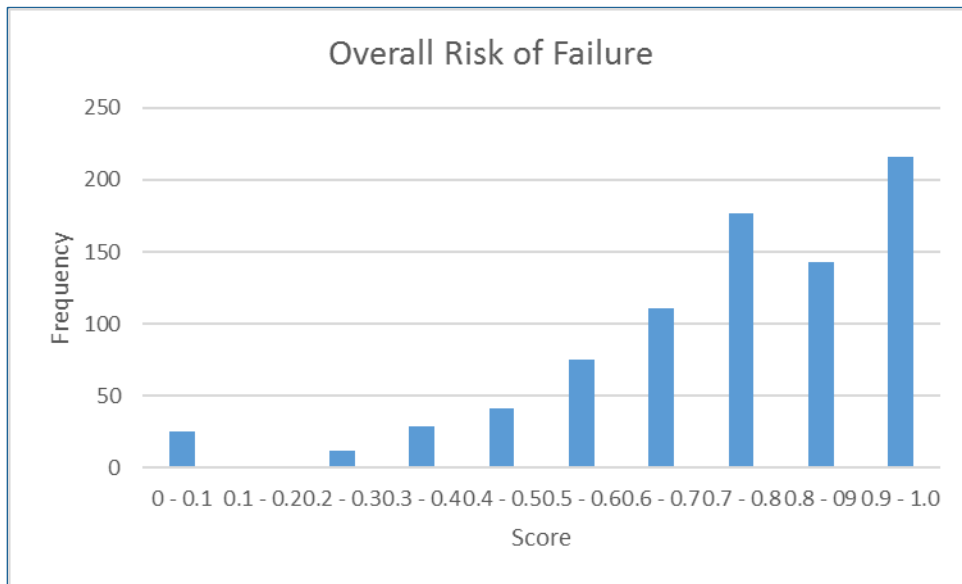


Figure B-19: Distribution of overall risk of failure (maximum of structural, hydraulic and geomorphic scores)

- For the downstream scour pool score, downstream scour pools that were labeled “not poor or critical” were assigned a “0” score but not included in the overall scour score. They are now included. In addition, the downstream scour pool score was rescaled from 0 to 4 to 0 to 2 because many crossings are armored and the scour pool may not be as much of a concern for the structure.
- A series of photographs of culverts were examined by two geologists and scored independently for each category. Values in the matrix were modified systematically until the computed scores were comparable to the scores estimated by the two geologists. Values modified in this process include changing the structure alignment from 1 to 4 to 0 to 3 and structure width ratio from 0 to 4 to 0 to 3.
- Analysis of the 197 culverts also indicated that bridges (widths >20 feet) were biased toward being in the higher risk category. However, bridges are designed to a higher standard than culverts and they are often inspected and maintained with greater frequency. Accordingly, a value of 0.1 was subtracted from all bridge scores as a final adjustment.

The final geomorphic risk of failure score is shown in Figure B-20

Woody Debris Score						
Structure Alignment		Absolute Structure Width (ft)				
Skewed	Aligned	<1	1-2	2-3	3-5	5-10
3	0	4	3.5	3	2	1
Sedimentation Score						
Structure Width Ratio				Sediment Continuity		
Structure Width/Channel Width (%)				Downstream		
< 50%	50 - <100%	100 - <125%	≥125%	Aggradation	None	Erosion
3	2	1	0	3	3	3
Severe	Mild	Spans Bank to Bank	Spans Channel and Bank	Upstream Aggradation	2	1
				Upstream None	2	1
				Upstream Erosion	2	1
Specific Stream Power versus Bed Resistance						
		Dominant Particle Size (Bed Resistance)				
		Silt	Sand	Gravel	Cobble	Boulder
Specific Stream Power (W/m ²)	0-60	3	3	3	3	3
	60-100	2	2	2	2	2
	100-300	0	0	0	0	0
	300+	0	0	0	0	0
Scour						
Specific Stream Power versus Bed Resistance						
		Dominant Particle Size (Bed Resistance)				
		Silt	Sand	Gravel	Cobble	Boulder
Specific Stream Power (W/m ²)	0-60	1	1	1	1	0
	60-100	1	1	3	2	1
	100-300	1	2	4	3	2
	300+	1	2	4	4	2
				Sediment Continuity		
				Downstream		
				Aggradation	None	Erosion
				1	1	1
				Upstream Aggradation	3	3
				Upstream None	4	4
				Upstream Erosion	3	3
Footing Score						
Not Poor/Critical		Poor	Critical			
0		3	4			
Downstream Scour Pool						
None		Small	Large			
0		1	2			
Blockage						
Not Poor/Critical		Poor	Critical			
0		0.5	1			

Figure B-20: Final risk of failure scoring system.

B.4 Quality Control Check

A subset of 20 structures was selected by MMI as a quality control check on data collected by TU and UMass. MMI collected field data using the Stream Continuity, TU Culvert and Bridge Assessment and MassDOT Culvert Condition Assessment field forms. These field data were then compared to prior assessments performed by TU and UMass using the same field forms.

Most data discrepancies between assessments occurred for qualitative data (e.g., UMass “Crossing Condition” and TU “Substrate Particle Size”). Some of the differences may result from changing field

conditions as MMI data were collected a year apart. The MMI assessment reported "None" more frequently for the "Streambed: Erosion/Aggradation/None" and Deposit Type fields.

Some significant differences in collected data did exist. For example, width measurement for larger bridges varied between the TU and MMI data. TU appeared to be measuring the road span of the bridge while MMI measured the width of the hydraulic opening between the abutments. Larger differences also existed for the "Floodplain filled by roadway" variable. TU consistently indicated more floodplain fill than MMI. MMI observed the amount of floodplain covered by the road embankment. Perhaps TU noted the amount of floodplain disconnected from the channel by a road embankment.

Pebble counts were conducted to identify the substrate characteristics (e.g., median grain size D_{50}) that could represent bed resistance to erosion. Out of the 197 structures assessed by MMI, UMass provided pebble counts for 34, with particle sizes placed into 11 size bins (<2 mm, 2-8 mm, 9-16 mm, 17-64 mm, 65-90 mm, 91-128 mm, 129-256 mm, 257-512 mm, 513-1,024 mm, >1,024 mm, and bedrock). MMI used this bin system for pebble counts performed on the remaining 166 structures. When D_{50} was calculated from the pebble count data, it became evident that these bins were too wide. As a result, most of the D_{50} calculations landed in the same size grouping.

A qualitative observation of dominant bed particle size was substituted for D_{50} when developing the "specific stream power and bed resistance" vulnerability screen. The qualitative observation seemed to do a better job of describing bed particle size and resolving damages. It is recommended that standard gravelometer-sized bins be used in future work if pebble counts are used to obtain quantitative data on bed resistance.

The vulnerability screen uses data obtained during MMI field assessments whenever possible. Qualitative data from prior fieldwork conducted by project team members is available for the dominant particle size and structure slope relative to local channel slope. These qualitative data may be substituted for missing field data if necessary but will likely result in a loss of detail. An initial trial was conducted to replace the variable indicating the difference in the slope of the local channel and structure with a qualitative observation of a "steeper" or "flatter" culvert. The loss of detail limited the use of the slope variable to help identify when structure damages are more likely. It may be best to eliminate a variable with missing data rather than substitute qualitative information. More work is needed to determine the best data substitution method.

Specific stream power derived from the GIS analysis was compared with specific stream power calculated using bankfull width and local slope measured in the field. It was assumed that these would indicate a good correlation (Figure B-21). The results do not match well ($R^2=0.23$) and show considerable variability. Due to the uncertainty inherent in local channel slope measurements, the GIS-derived specific stream power was considered more appropriate.

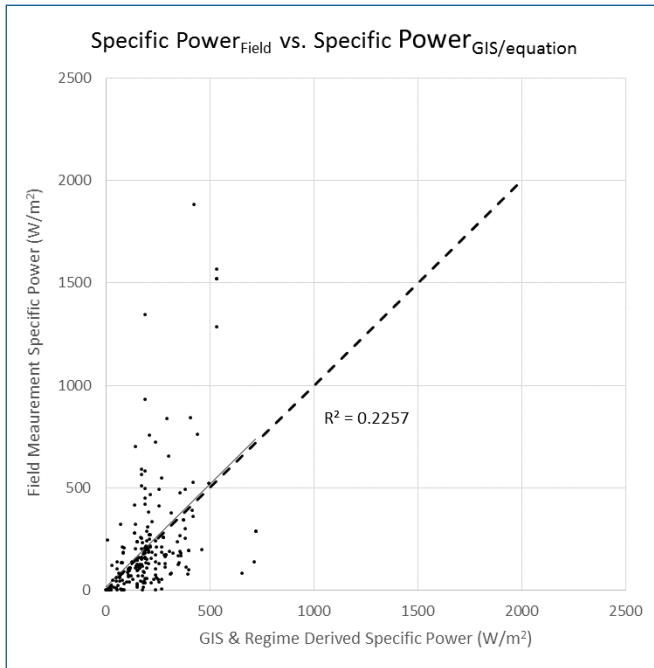


Figure B-21: Comparison of specific stream power derived from GIS data with specific stream power calculated from field measurements.

Bankfull width measurements measured by TU were very similar to bankfull widths measured by MMI; they matched very well. In addition, bankfull widths obtained from field measurements by TU and MMI were averaged and compared with the bankfull widths derived from the Soar and Thorne regime equations (Figure B-22). There is a strong correlation ($R^2=0.85$) between the field measured and regime equation-derived bankfull widths suggesting that the regime equation is a good representation of field measured values.

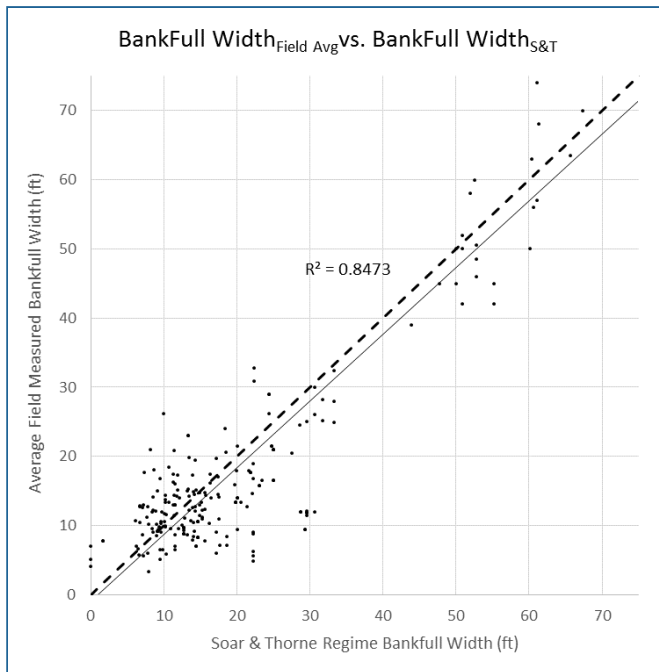


Figure B-22: Comparison of bankfull width from field measurements with bankfull width derived from the Soar and Thorne regime equation.

B.5 References

- Bent, G.C. and A.M. Waite. 2013. *Equations for estimating bankfull channel geometry and discharge for streams in Massachusetts*. U.S. Geological Survey Scientific Investigations Report 2013-5155, 61p.
- Jacobs, J. 2010. *Estimating the magnitude of peak flows for steep gradient streams in New England*. New England Transportation Consortium, Project No. NETC 04-3, 49 p.
- Knighton, A. D. 1999. Downstream Variation in Stream Power. *Geomorphology* v.29, nos. 3-4, pp. 293-306.
- Lacey, G. 1930. *Stable channels in alluvium*. Minutes of the Proceedings of the Institute of Civil Engineers, London, v.229, pp.259-292.
- Soar, P. and C. Thorne. 2001. *Channel restoration design for meandering channels*. U.S. Army Corp of Engineers, Vicksburg, MS, Engineer Research and Development Center, ERDC CR-01-1, 454p.
- Wolman, M. G. 1954. A Method of sampling coarse river-bed material. *Transactions of American Geophysical Union* 35, pp.951-956.

Appendix C REGIONAL CLIMATE MODEL DATA SET COMPARISON

Two sets of dynamically downscaled projections were originally considered for this project, data from the North American Regional Climate Change Assessment Program (NARCCAP) and data from the NASA Earth Exchange Global Daily Downscaled Projections (NEX-GDDP) project. NARCCAP data are based on CMIP3, and daily precipitation and air temperature data are available for two 30-year periods, 1971-2000 (present) and 2041-2070 (future). In contrast, NEX-GDDP data are based on CMIP5, and data are available for the period from 1950 – 2100.

As a first step, the NARCCAP and NEX-GDDP model outputs for the Deerfield River watershed under current conditions, defined for this purpose as 1971 – 2000, were compared against observed station data. Several precipitation values were considered, but focus was placed on the average number of days predicted by each model to have a precipitation accumulation of 1-inch or greater. There are two main reasons behind interest in this statistic: 1) the importance of such events on rainfall – runoff processes and high streamflow conditions, and 2) observed changes in extreme precipitation and predictions that rainfall intensity in the Northeast U.S. will continue to increase. Data are compared both on an annual (Figure C-1) and monthly basis (Figure C-2).

A wide range of predictions in terms of the number of 1-inch precipitation days is observed across the models. In general, the NEX-GDDP projections are bias low compared to observed data at both the annual and monthly time scales. These differences were determined to be too large to effectively bias-correct the data, and as such the NEX-GDDP ensemble results were not utilized for hydrologic-hydraulic prediction. In addition, two of the NARCCAP models – HADCM3_mm5 and HADCM3_HRM3 – were omitted from further analysis as they were deemed to be biased too low and high, respectively.

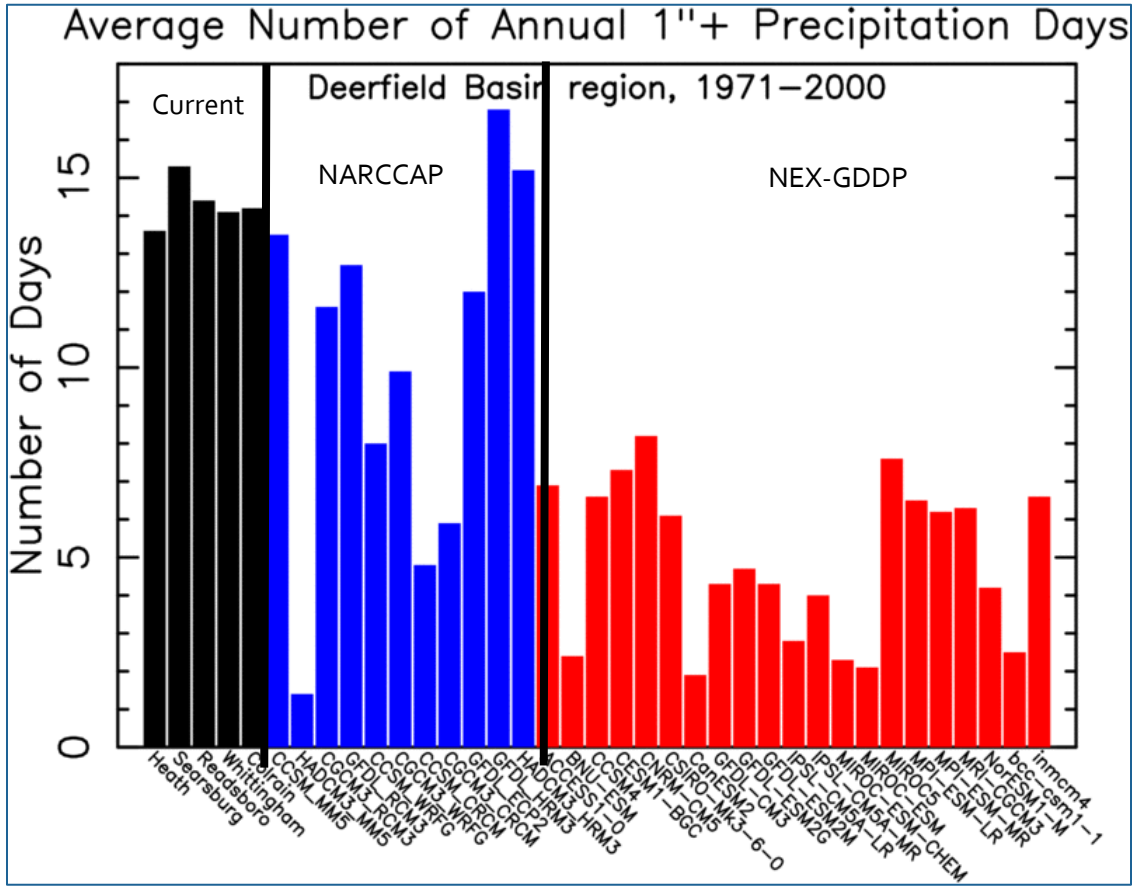


Figure C-1: Comparison of NARCCAP (blue bars) and NEX-GDDP (red bars) model projections against observed current conditions (black bars) on an annual basis

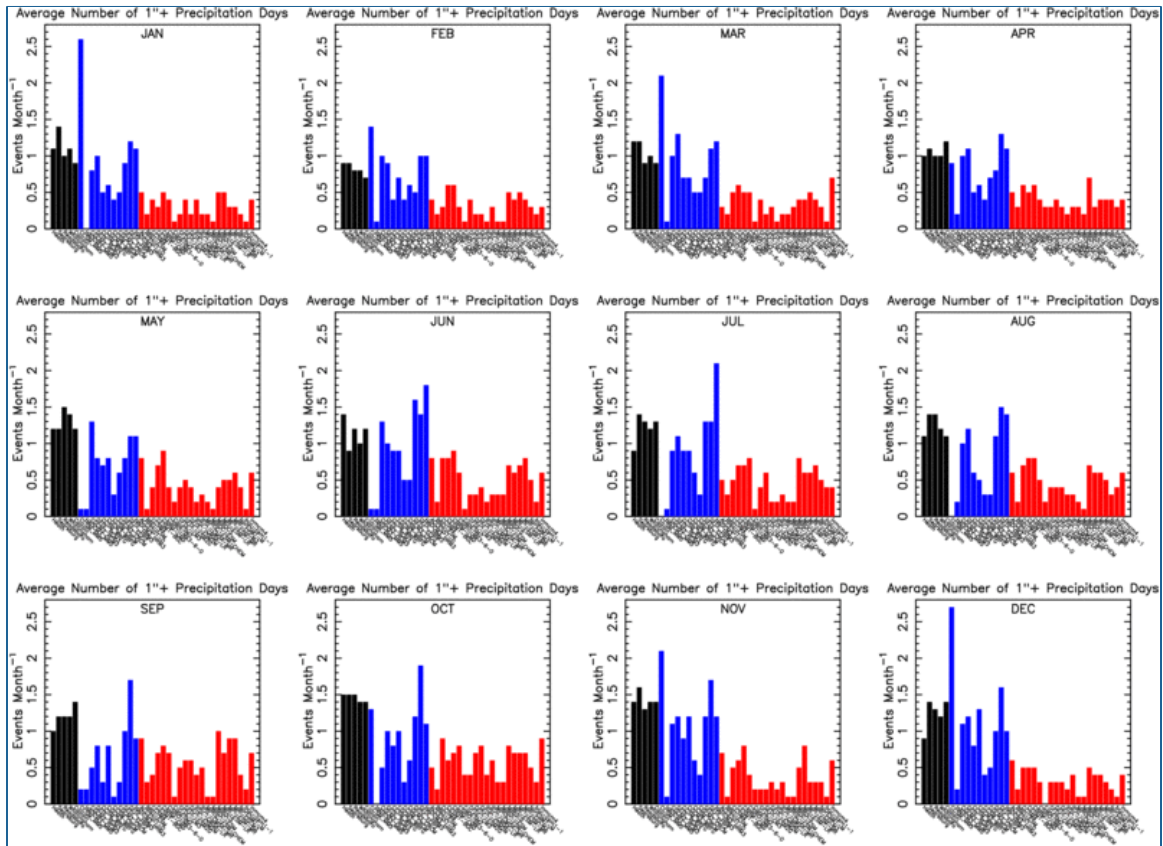


Figure C-2: Comparison of NARCCAP (blue bars) and NEX-GDDP (red bars) model projections against observed current conditions (black bars) on a monthly basis

Appendix D NARCCAP DATA BIAS CORRECTION

D.1 Overview

This appendix briefly describes the bias correction procedure applied to the nine NARCCAP GCM-RCM climate projections utilized as input to the physically based models. Climate projections are compared against observed data from 1971 – 1999, collected at four co-op stations nearby and within the Deerfield River watershed, and are appropriate with respect to the grid cells of the NARCCAP data: Readsboro, Searsburg, Amherst, and Ball Mountain. Data from these Co-op stations were also used as the basis of the bias-correction.

D.2 Climate Model Data Bias Adjustment Procedure

NARCCAP data were first downloaded for the grid cells closest to each co-op station. Because all NARCCAP datasets have different projections, the exact coordinates of the grid cell centers varied slightly for each GCM-RCM data set and are not presented. One co-op station, Searsburg, was utilized for bias adjustment following a monthly bias correction method described in Rätty et al. (2014). Specifically quantile mapping, methodology M8, was used. The monthly bias correction was applied to each day of a given month.

D.3 Summary of Results

The mean daily current and future 30-year annual norms for temperature and precipitation, as predicted by the nine NARCCAP GCM-RCM projections, are summarized on Figure D-1 and Figure D-2 **Error! Reference source not found.**, respectively, prior to and after bias correction. Unadjusted data are shown by the solid, colored symbols (blue triangles for current, and red squares for mid-century), while the bias adjusted data are shown as open symbols (triangles for current, squares for mid-century). The horizontal dashed line indicates either the mean daily average temperature (°C) or precipitation (mm) based on observed data in the watershed during current conditions (1971 – 1999). After bias correction, the mean daily norms for the 9 NARCCAP projections (open triangles) correspond well with the observed conditions (dashed line), increasing confidence in the applicability of the adjusted future climate projections.

Additional figures summarize the impact of the bias adjustment on precipitation projections as follows:

- Figure D-1 summarizes the mean daily precipitation by month for each NARCCAP projection (blue bars) prior (top panel) and after bias-adjustment (bottom panel). In both panels, data observed at the four co-op stations are also shown (black bars on left). Months are as numbered on the top of the individual graphs, starting with January (top left) and ending with December (bottom right). This figure shows that the bias-adjustment procedure utilized in the project was also effective at the monthly time-scale.
- Figure D-4 summarizes the average number on annual 1-inch precipitation days, as predicted by the nine NARCCAP models (blue bars) prior to bias-adjustment (top panel) and after bias adjustment (bottom panel). In both panels, data observed at the four co-op stations are also shown (black bars on left). This figure shows that the bias-adjustment procedure used in the project is also effective for heavy rainfall at the annual time-scale.

- Figure D-5 summarizes the average number on annual 1-inch precipitation days, as predicted by the nine NARCCAP models (blue bars) prior to bias-adjustment (top panel) and after bias adjustment (bottom panel). In both panels, data observed at the four co-op stations are also shown (black bars on left). Months are as numbered on the top of the individual graphs, starting with January (top left) and ending with December (bottom right). This figure shows that the bias-adjustment procedure used in the project is also effective for heavy rainfall at the monthly time-scale.

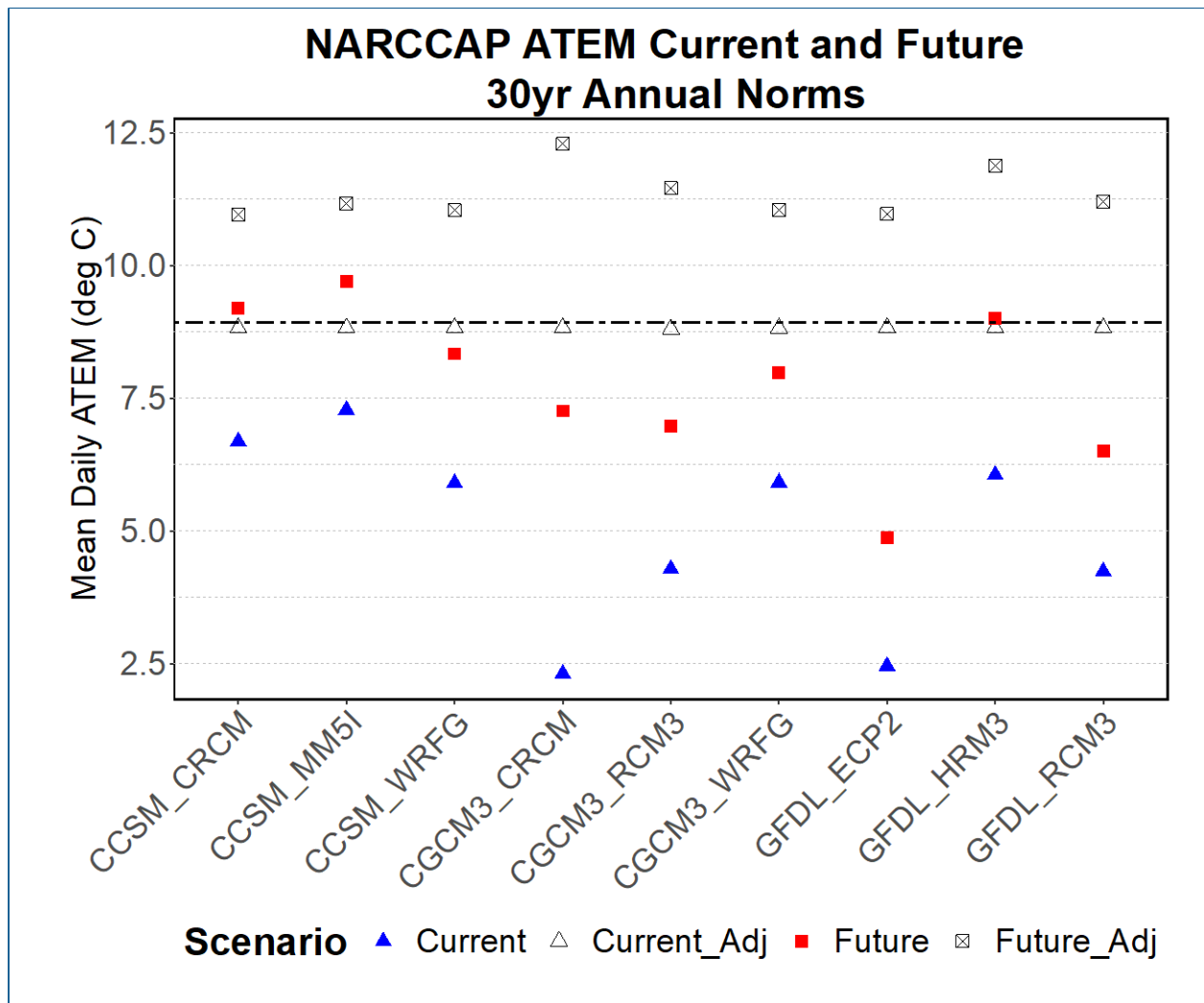


Figure D-1: Comparison of mean daily temperature (°C) across the Deerfield River watershed from 1971 – 1999 based on observed data (dashed horizontal line) and NARCCAP model unadjusted (closed symbols) and adjusted (open symbols) current and future climate predictions

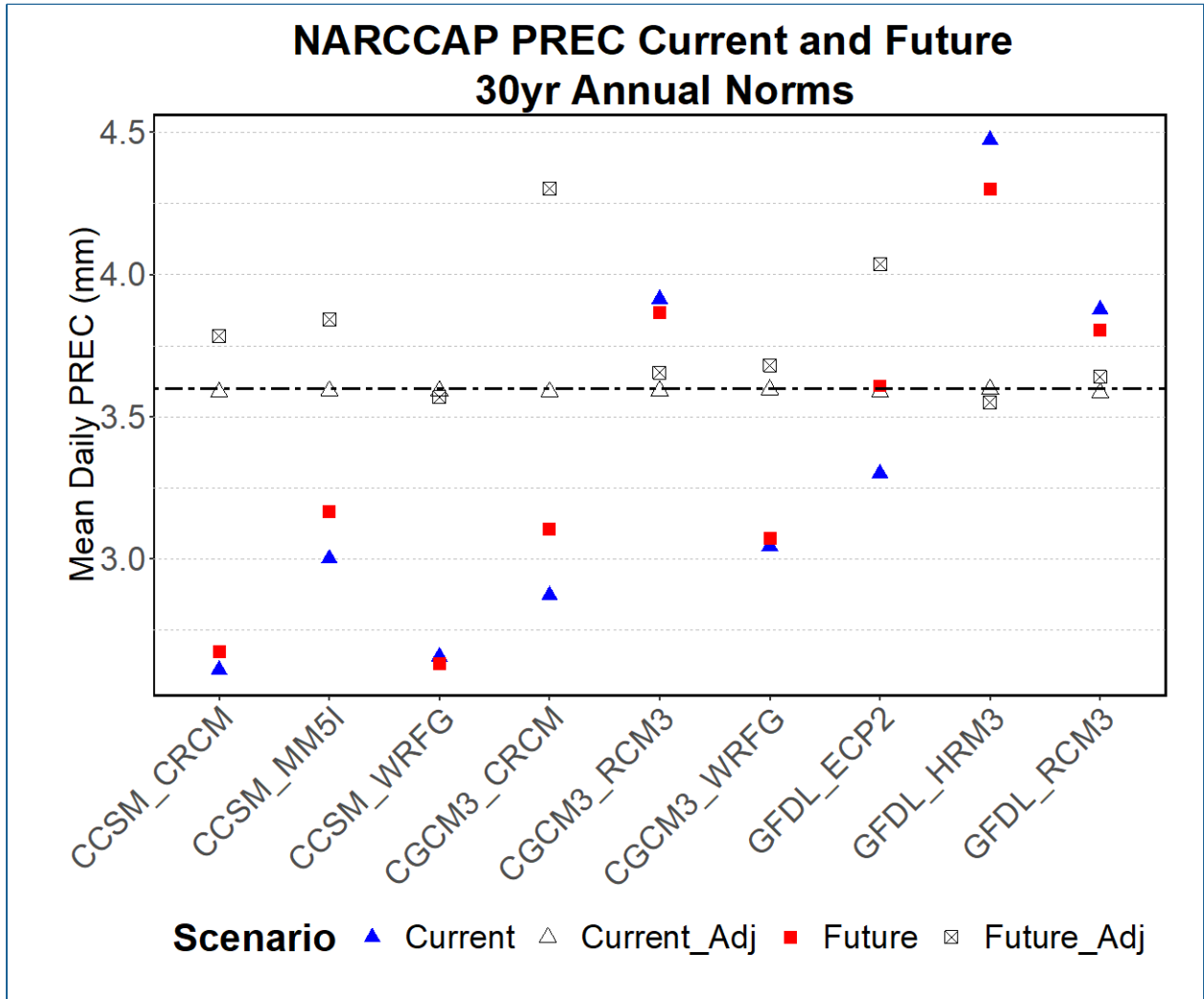


Figure D-2: Comparison of mean daily precipitation (mm) across the Deerfield watershed from 1971 – 1999 based on observed data (dashed horizontal line) and NARCCAP model unadjusted (closed symbols) and adjusted (open symbols) current and future climate predictions

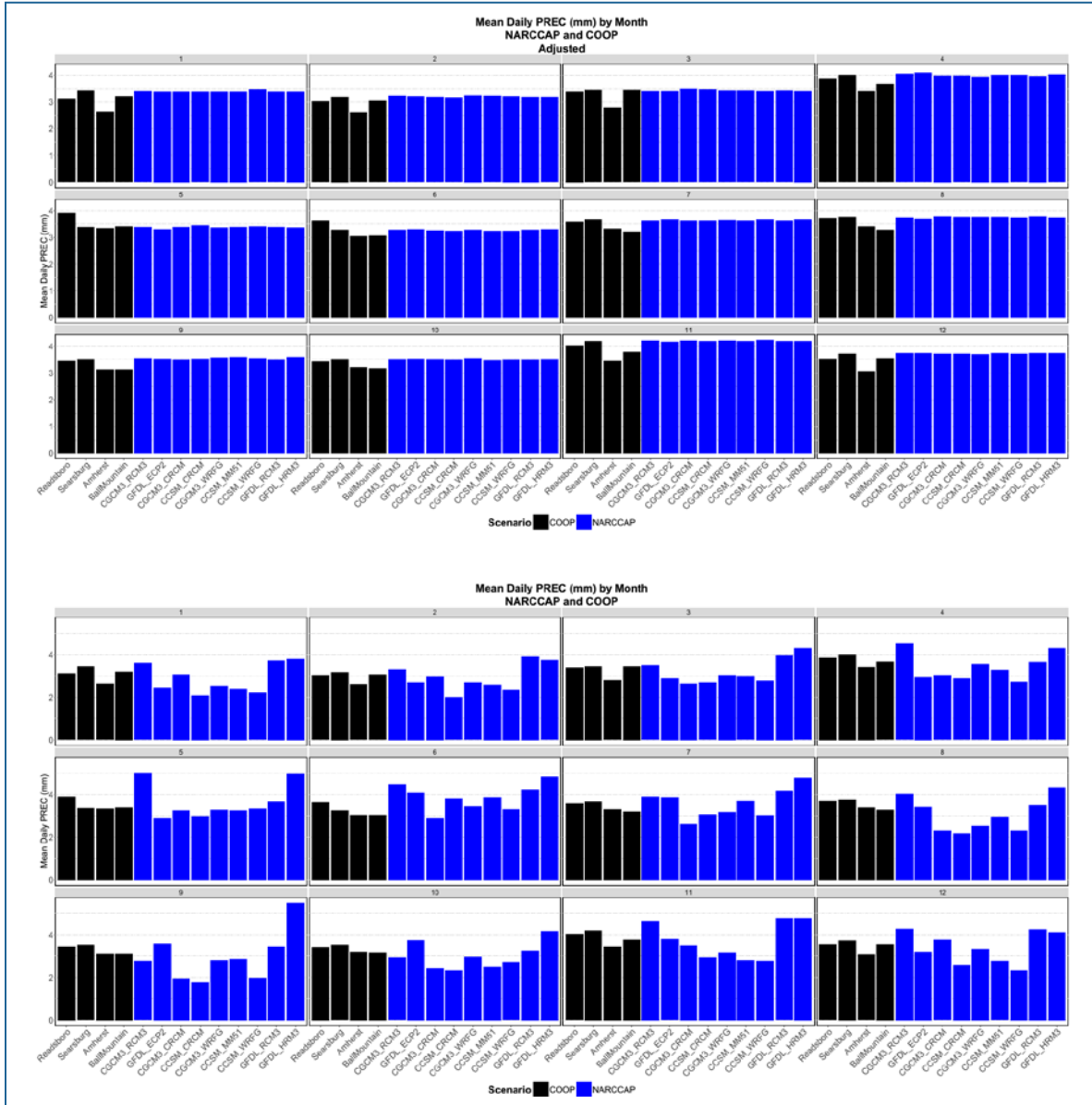


Figure D-3: Mean daily precipitation by month, as predicted by the nine NARCCAP models, compared to observed data prior to bias-adjustment (top panel) and after bias adjustment (bottom panel)

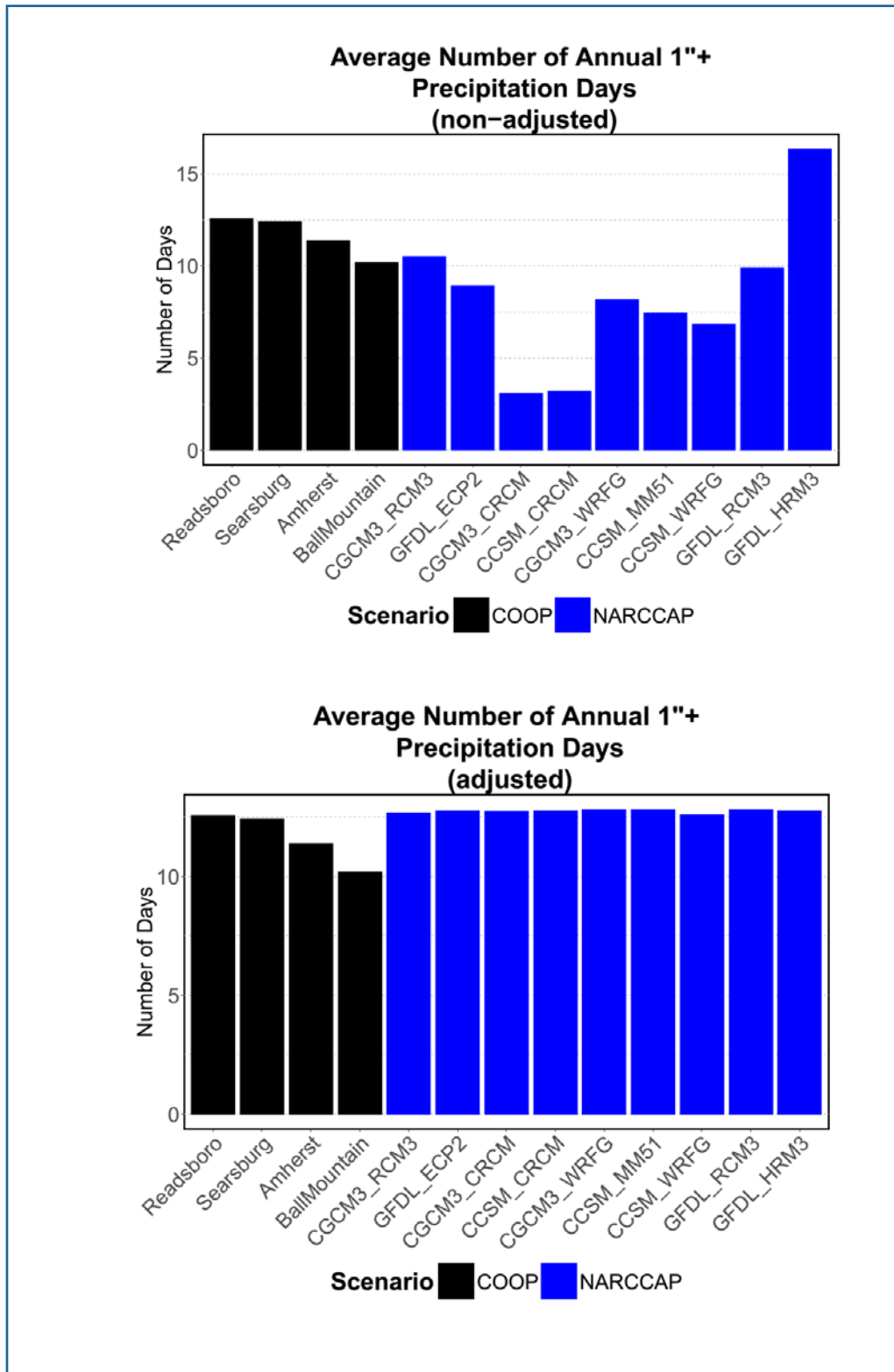


Figure D-4: Average number on annual 1-inch precipitation days, as predicted by the nine NARCCAP models, compared to observed data prior to bias-adjustment (top panel) and after bias adjustment (bottom panel)

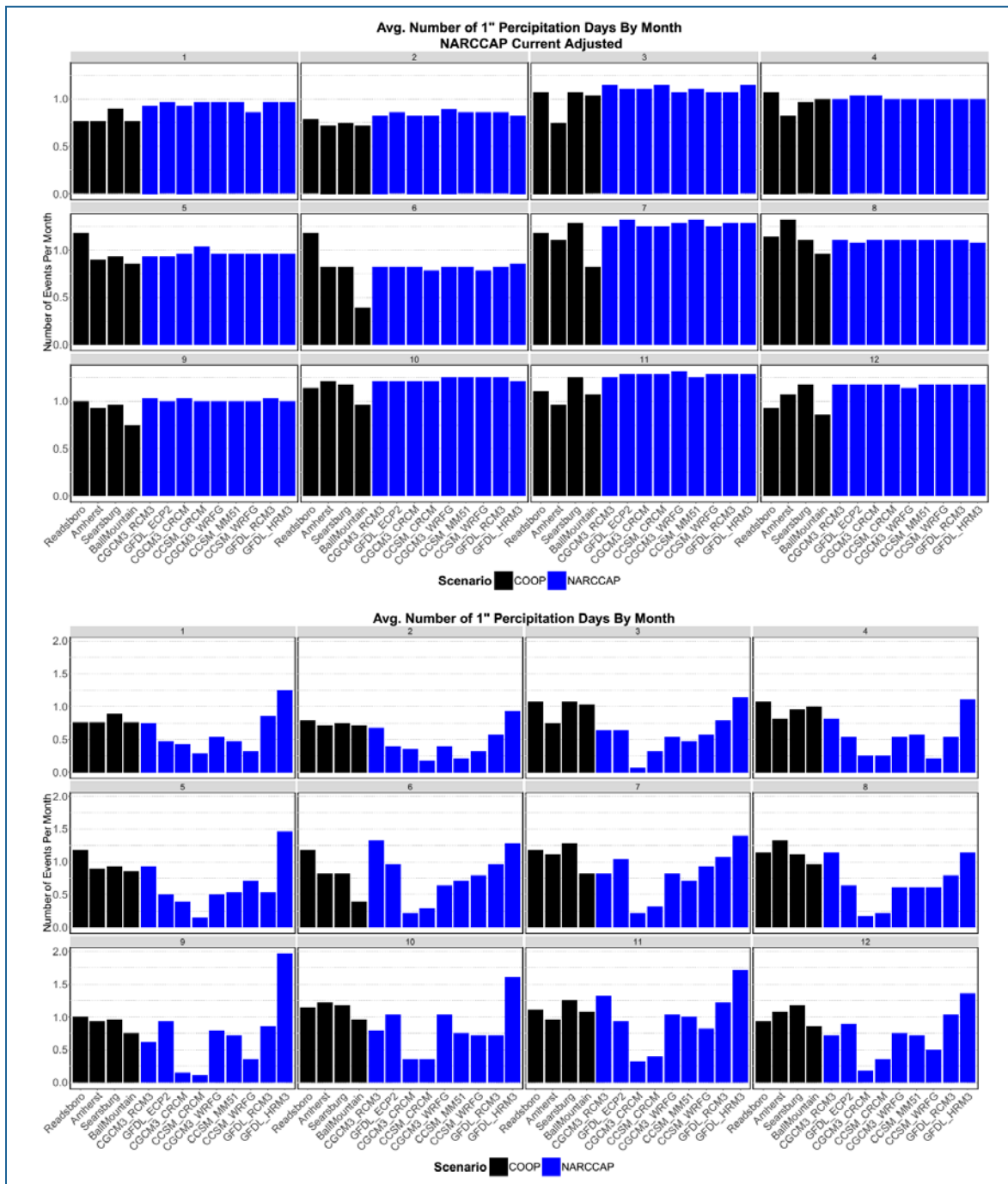


Figure D-5: Average number on annual 1-inch precipitation days by month, as predicted by the nine NARCCAP models, compared to observed data prior to bias-adjustment (top panel) and after bias adjustment (bottom panel)

The range of change in average daily temperature by month (x-axis) on a degree C basis from current (1971 – 1999) to mid-century (2041 – 2070), as predicted by the nine NARCCAP models after bias adjustment, is summarized on Figure D-6. The range of change in average daily precipitation by month (x-axis) on a percent basis from current (1971 – 1999) to mid-century (2041 – 2070), as predicted by the NARCCAP models after bias adjustment, is summarized on Figure D-7.

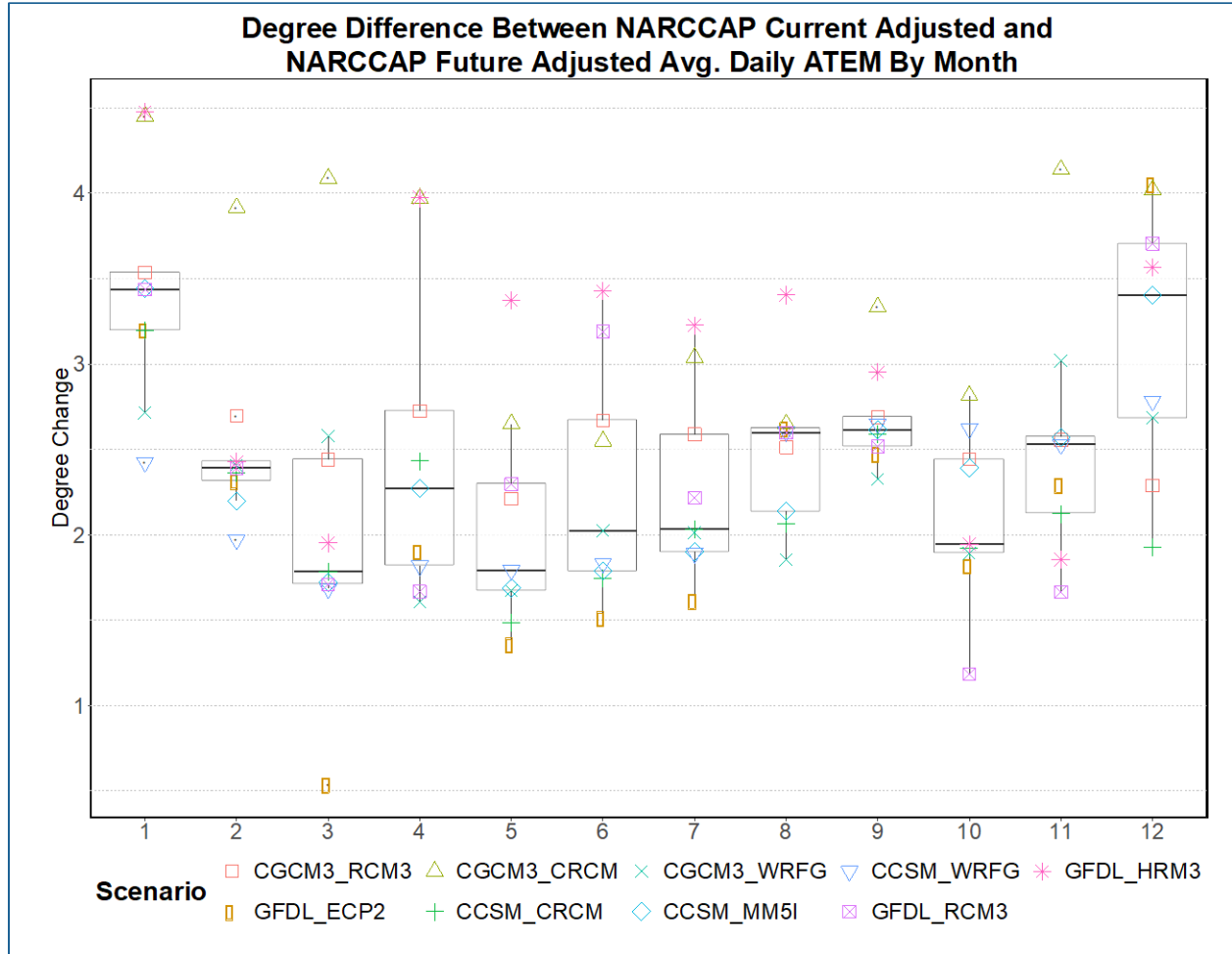


Figure D-6: Range of change in average daily temperature by month (x-axis) on a degree C basis from current (1971 – 1999) to mid-century (2041 – 2070), as predicted by the NARCCAP models after bias adjustment

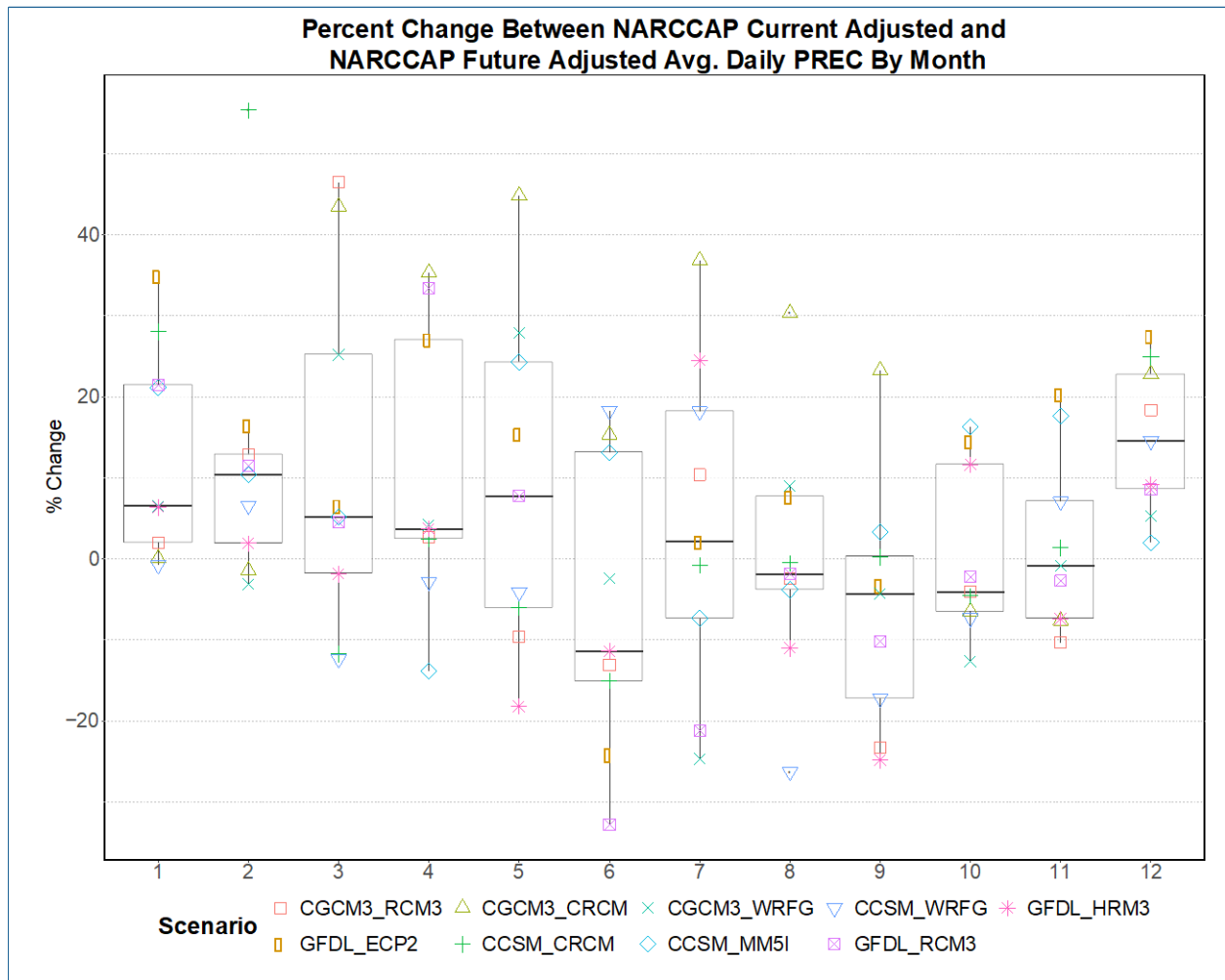


Figure D-7: Range of change in average daily precipitation by month (x-axis) on a percent basis from current (1971 – 1999) to mid-century (2041 – 2070), as predicted by the NARCCAP models after bias adjustment

D.4 References

Räty, O., J. Räisänen, and J.S. Ylhäisi. 2014. Evaluation of delta change and bias correction methods for future daily precipitation: intermodel cross-validation using ENSEMBLES simulations. *Climate Dynamics*, 42(9–10), pp. 2287–2303. <https://doi.org/10.1007/s00382-014-2130-8>

Appendix E MALONE & MACBROOM REPORT

See next page

RIVER AND STREAM POWER ASSESSMENT REPORT
INCLUDING CULVERT AND BRIDGE
VULNERABILITY ANALYSIS

DEERFIELD RIVER BASIN
MASSACHUSETTS AND VERMONT
HUC 01080203

December 30, 2014
(Revised April 4, 2017)

MMI #4297-03

Prepared for:

University of Massachusetts
Amherst, Massachusetts
and
Massachusetts Department of Transportation

Prepared by:

MILONE & MACBROOM, INC.
99 Realty Drive
Cheshire, Connecticut 06410
(203) 271-1773
www.miloneandmacbroom.com

TABLE OF CONTENTS

	<u>Page</u>
Preface	
1.0 River Assessment.....	1
1.1 Introduction.....	1
1.2 River Assessment Methodology	1
1.3 Fluvial Assessments.....	2
1.4 Equilibrium and Adjustments	3
2.0 Deerfield Watershed	5
2.1 Bedrock Geology	8
2.2 Surficial Geology	8
2.3 Deerfield River.....	9
2.4 Flood Insurance Studies.....	16
3.0 Hydrology	17
3.1 Introduction.....	17
3.2 Long-Term USGS Gauging Stations	18
3.3 Channel Forming Discharges.....	19
3.4 Flood Frequency Analysis	20
3.5 Hurricane Irene	21
3.6 FEMA Hydrology	22
3.7 Annual Peak Flood Flow Trends	23
3.8 Sediment Yield.....	24
4.0 Fluvial Assessment	25
4.1 Channel Classification	25
4.2 Channel Slope	26
4.3 Channel Alignment and Pattern	27
4.4 Bankfull Width Channel Dimensions	30
4.5 Stream Power	32
4.6 Geomorphic Changes.....	42
4.7 Geomorphic Assessment Conclusion	43
5.0 Floodplains.....	45
5.1 Introduction.....	45
5.2 Flood Inundation Mapping	47
5.3 High Water Marks and Historic Floods	49
5.4 National Flood Insurance Program Floodplain Maps.....	49
5.5 Surficial Geology Maps	50
5.6 Soil Survey Data for Floodplain Mapping.....	52

5.7	River Corridor Floodplain Mapping	54
5.8	Floodplain Vegetation Mapping	55
5.9	Floodplain Stream Power Classification.....	55
5.10	Floodplain Adjustments.....	59
5.11	Floodplain Summary.....	60
6.0	Management Issues.....	62
6.1	Introduction.....	62
6.2	Regulated Flows.....	63
6.3	Bypass Segments	63
6.4	Fish Passage	63
6.5	Recreation	64
6.6	Floodplain Mapping.....	65
6.7	Conclusion	65
7.0	Culvert and Bridge Vulnerability Analysis.....	66
7.1	Introduction.....	66
7.2	Methods.....	66
7.3	Results.....	70
7.4	Discussion	81
Appendix A - Geomorphic Segmentation and Descriptions.....		85
References.....		117

TABLES

2-1	Hydrologic Unit Codes (HUC).....	7
3-1	Long-term Gauging Stations	18
3-2	Mean Monthly Flow	18
3-3	Estimated Channel Forming Discharges Comparison.....	20
3-4	Peak Flood Flows	21
3-5	Hurricane Irene Peak Flows	22
3-6	100-Year Flood Flows.....	23
4-1	Segment Classification	26
4-2	Mean Channel Slope Calculations (Alluvial Segments)	27
4-3	Deerfield River Bankfull Widths.....	31
4-4	Comparison of Bankfull Widths at USGS Gauges.....	32
4-5	Summary of Selected Geomorphic Activity as a Result of Hurricane Irene, August 2011 ..	43
7-1	Vulnerability Analysis Project Team	66
7-2	Structure Damage Codes	67

FIGURES

1-1	Deerfield River Watershed Map*	6
2-1	Deerfield River Profile	12
2-2	Major Dams and USGS Gauges*	13
5-1	Surficial Geology*	46
7-1	Vulnerability Screen Variable Scoring	69
7-2	Overall Vulnerability Screen Results	70
7-3	Specific Stream Power vs. Resistance Results	71
7-4	Structure Width Results	71
7-5	Change in Slope Results	71
7-6	Sediment Continuity Results	71
7-7	Structure Alignment Results	71
7-8	Specific Stream Power Comparison	72
7-9	Number of Damaged Structures by Specific Stream Power	73
7-10	Percentage of Damaged Structures by Specific Stream Power	73
7-11	Percent of Damaged Structures by Dominant Bed Particle Size	74
7-12	Specific Stream Power Full and Interquartile Range by Dominant Bed Particle Size	74
7-13	Specific Stream Power vs. Dominant Bed Particle Size, Data Colored by Damage	75
7-14	Specific Stream Power Full and Interquartile Range by Dominant Bed Particle Size, Damaged Structures Only	76
7-15	Number of Structures by Structure Width/Channel Bankfull Width	76
7-16	Percentage of Damaged Structures by Structure Width/Channel Bankfull Width	77
7-17	Specific Stream Power vs. Damage Code, Data Colored by Structure Width/Channel Bankfull Width (%)	77
7-18	Percent of Damaged Structures by Difference Between Local Channel Slope and Structure Slope	78
7-19	Specific Stream Power vs. Damage Code, Data Colored by Structure Width/Channel Bankfull Width	78
7-20	Percent of Damage Structures by Structure Alignment Relative to Channel	79
7-21	Specific Stream Power vs. Damage Code, Data Colored by Structure Alignment Relative to Channel	79
7-22	Bankfull Width Comparison	80
7-23	Slope Comparison	81
7-24	Slope and Stream Order Comparison	81
A	Culvert and Bridge Vulnerability	Rear Pocket

* Figures 1-1, 2-2, and 5-1 are reproduced from the Deerfield River Assessment, 2004-2008, prepared by Massachusetts Office of Executive Affairs.

PREFACE

The authors would like to thank the entire project team for their generous help in conducting this study including collecting field data, developing the extensive data base, discussing means and methods, and helping to assess the findings. Special thanks go to the following people:

Christine Hatch, Benjamin P. Werner, Marie-Francous Hatte, Noah Slovin, Nicole Gillett, Steve Mabee, Paula Sturdevant Rees, Scott Jackson, Katie McArthur, Erin Rodgers, Colin Lawson, Eve Vogel, Jerry Schoen, and John Gartner

Submitted by James G. MacBroom, Roy Schiff, and Jessica Louisos

1.0 RIVER ASSESSMENT

1.1 Introduction

This geomorphic assessment of Deerfield River in western Massachusetts and southern Vermont has been prepared by Milone & MacBroom, Inc. (MMI) on behalf of the University of Massachusetts as part of its "Farms, Floods, and FGM" project, funded by the United States Department of Agriculture – National Institute of Food and Agriculture National Integrated Water Quality Program (USDA – NIFA NIWQP) program. This project is a broad-based geomorphic assessment of the Deerfield River and its adjacent riparian corridor to define its characteristics, processes, and management issues. The river channel is used extensively for hydroelectric power generation and recreation, with agricultural land uses on the floodplains.

This river assessment focuses upon temporal river processes and resulting features rather than the more common assessment of local cross section forms and characteristics that change after annual floods. The Deerfield River has been found to be remarkably stable with moderate specific stream power (SSP) except in highly contracted segments, and the few large floodplains are more prone to sediment deposition rather than dynamic migratory channels or avulsions. In contrast, several larger tributaries have steep gradients and narrow confined valleys that lead to high stream power and dramatic geomorphic changes during floods. Consequently, the anticipated hydrologic effects of climate change will be more acute along the tributaries than the main stem.

The second part of this project included developing a Geographic Information System (GIS)-based model to compute specific stream power and using the results to help predict culvert and bridge vulnerability of failure. This vulnerability screening tool uses remote sensing data and a regression equation to predict hydrology and channel reach slope and a prediction of channel and structure condition that is compared to a field inventory of culverts. The purpose of the vulnerability screen analysis is to help identify the potential for channel and structural risk at culverts due to erosion, sedimentation, debris, and flooding. Vulnerable structures can then be ranked by priority for subsequent on-site investigation.

1.2 River Assessment Methodology

Conventional stream assessments focus upon use of remote sensing data and a visual inspection of existing channel conditions, with qualitative comments on channel defects and adjustments, with little or no quantitative evaluation of hydrology, floodplains, or river mechanics. In contrast, for this project, MMI uses a "hydro-morphology" approach, similar to European and the River Styles procedures that evaluate a series of nested spatial scales that include the watershed hydrology, valley form and confinement, floodplain, and then the actual main river channel and its major tributaries. Watersheds are complicated places with many variables to be considered. The hydro-morphology system assessment includes the role of independent variables such as runoff patterns, peak flows, and geologic conditions, plus valley slope and confinement, followed by the resulting dependent elements of geomorphic change including channel pattern,

bankfull width, slope, and bank conditions. By evaluating watershed scale geomorphic processes as well as stream power and climate trends, one can begin to anticipate future geomorphic landscape adjustments.

The culvert vulnerability risk screening assessment included field inspection of approximately 200 culverts and the completion of an *Excel* spreadsheet database. Remote sensing data and GIS was then used to compute stream power and to evaluate risk.

1.3 Fluvial Assessments

Fluvial assessments include inspecting and inventorying existing river corridor and channel conditions in order to evaluate river processes and adverse conditions that affect ecological health or human activities. The inventory includes classifying the type of channel plus large-scale past and present natural channel adjustments such as bed scour, bank erosion, channel widening, and sediment deposition. Anthropogenic concerns include the role of bridges and culverts, dams and weirs, levees, channelization, fill material, dredging, flood channels, and diversions.

Prior to the actual channel inventory, it is essential to understand the watershed characteristics that produce and influence the key watershed processes that affect river processes including runoff rates, sediment loads, and sediment type. These watershed processes are then influenced by additional independent conditions, including the valley confinement, valley slope, and geologic materials. Watersheds and fluvial systems are complex and dynamic, with irregular adjustments. Some adjustments are slow and barely noticeable; others are rapid and dramatic during floods (see Section 4.5).

<u>Selected Watershed Characteristics</u>	<u>Independent Watershed Products</u>	<u>Selected Valley Characteristics</u>	<u>River Channel Dependent Variables</u>
Size	Stream runoff	Confinement	Channel pattern
Shape	Sediment loads	Slope	Channel slope
Elevation	Sediment size	Glacial deposits	Bankfull width
Geology	Organic debris	Aquifers	Bankfull depth
Climate		Vegetation	Roughness
Land use		Valley wall slides	Bank slopes
		Floodplains	Local incision
			Sediment bars

Nonalluvial channels have bed and bank perimeters of stable non-erosive materials such as bedrock, boulders, and colluvium. In contrast, alluvial channels are bounded sediments that may be prone to erosion, transport, and deposition. Ideally, the width, depth, slope, and pattern of alluvial channels are proportional to bankfull discharges and sediment loads and over long periods have mean equilibrium conditions. However, it is increasingly accepted that the 19th Century concept of equilibrium seldom occurs and that climate change and its more frequent floods are creating a new paradigm.

Changes in discharges, sediment loads, sediment sizes, and tectonic factors can lead to adjustments in channel and corridor characteristics, the most common driving force being rare flood flows and human activities. Some channels are more sensitive to change than others due to their confinement, slope, or boundary materials.

The Active River Area

This report focuses upon just two elements of the Active River Area – the channel and its floodplain. The Active River Area that influences river form and processes is larger than just the channel and floodplain. It has been described by The Nature Conservancy as including those places where river-related processes occur (Smith et al., 2008). The specific components of the Active River Area include:

- 1) Material contribution areas – are sources of river inputs, including headwater streams and near bank overland flow areas
- 2) Meander belt zones – areas where channels migrate over time
- 3) Floodplains – sedimentary areas subject to periodic inundation and composed of modern sediment
- 4) Terraces – former floodplains formed by rivers and created by past events and which may still be inundated by rare flood events and still support floodplain species
- 5) Riparian wetlands – low gradient areas with hydric or alluvial soils related to adjacent streams and supporting riparian water-tolerant vegetation

1.4 Equilibrium and Adjustments

Alluvial rivers that are formed in modern sediments are able to adjust their channel width, depth, and slope in proportion to their flood flows and sediment loads. Undersized channels with high velocities are prone to scour, and oversized channels have low velocities and tend to fill due to sediment deposition. River channels subject to steady conditions tend to approach equilibrium dimensions that are in balance with their peak flows and loads. In contrast, steep mountain rivers that are still adjusting their grade and valleys are less likely to be in equilibrium. During the 20th Century, the equilibrium concept was used in reference to channels' short-term cycles; today, we consider "equilibrium" to have spatial and temporal aspects such as annual cycles for alluvial sand channels and decadal/century cycles for gravel bed channels and floodplains.

River channels respond slowly to external stress, and reported floods or watershed changes may prevent equilibrium from occurring. There is growing concern that the current cycle of increasing precipitation and runoff will deter equilibrium conditions and void those river management strategies that assume equilibrium. For example, there may not be enough time

lapse between floods for rivers to adjust back toward equilibrium, and great floods can cause landslides, mass failures, and boulder transport that is irreversible.

Rivers and their floodplains adjust their geometry in response to changes in watershed hydrology or sediment load. Channel adjustments may include scour and erosion that alter width or depth, sediment deposition, changes in bed gradient, and modified alignment and pattern. Floodplain adjustments also occur, including aggradation or scour from channel migration or avulsion. Sediment deposition frequently occurs during large floods, burying the previous floodplain surface.

Specific human activities that may lead to channel or floodplain adjustments include forest clearing, drainage, filling wetlands, channel realignment, and undersized bridges and culverts. Drastic adjustments are associated with channelization, dams, and use of levees.

Classic river adjustments include both horizontal and vertical channel modifications and, in extreme cases, may alter floodplain and valley form.

Fluvial Adjustments

<u>Horizontal</u>	<u>Vertical</u>	<u>Floodplain</u>
Channel width	Channel slope	Topography
Meander migration	Channel incision	Side channels
Avulsions	Aggradation	Oxbows
Floodplain linkages	Degradation	Vegetation
Braiding	Bank height	Riparian wetlands
Bank failures	Local scour	Natural levees

2.0 DEERFIELD WATERSHED

The Deerfield River watershed (see Figure 1-1) is located in the Berkshire highlands region (Franklin County) of northwestern Massachusetts and in the southern part of Vermont. It is tributary to the Connecticut River, the largest river in New England. It is the drainage area from which water and sediment is supplied to the main stem river channel. It is largely a rural forested area with small farms and villages with moderate development in downstream areas near the Connecticut River Valley. It has a total area of 665 square miles divided between 318 square miles in Vermont and 347 square miles in Massachusetts.

Water quality is a critical part of ecological evaluations. The watershed's water quality is discussed in detail in separate Vermont and Massachusetts "Deerfield River Watershed Assessment Reports" by state agencies and is not repeated here in detail. The river has a class B water quality designation in most sections indicating that it is suitable for human contact recreation (swimming, boating, wading) as well as habitat for fish and wildlife. There are a few local concerns about fecal coliform and metals and the influence of solid waste landfills. Portions of the Green River are impaired.

The national system of hydrologic unit codes (HUC) was established by the U.S. Geological Survey (USGS) in order to map and identify the nation's watersheds. The HUC serves as the equivalent of a postal "zip" code that provides a unique identification for each watershed. Massachusetts has 183 of the 12-digit subwatershed scale basins. The Deerfield River basin HUC is 01080203, at the 8-digit accounting unit scale, which is also the state planning basin number. It is further designated with 5 of the 12-long digit cataloging units and many 16-digit tributary codes. The watershed is contiguous with the Hoosic River basin on the west, Westfield River basin to the south, and Connecticut River basin to the east. In Vermont, the north side of the Deerfield River basin abuts the West River basin. The full HUC designations are in Table 2-1.

Figure 1-1: Deerfield River Watershed Map

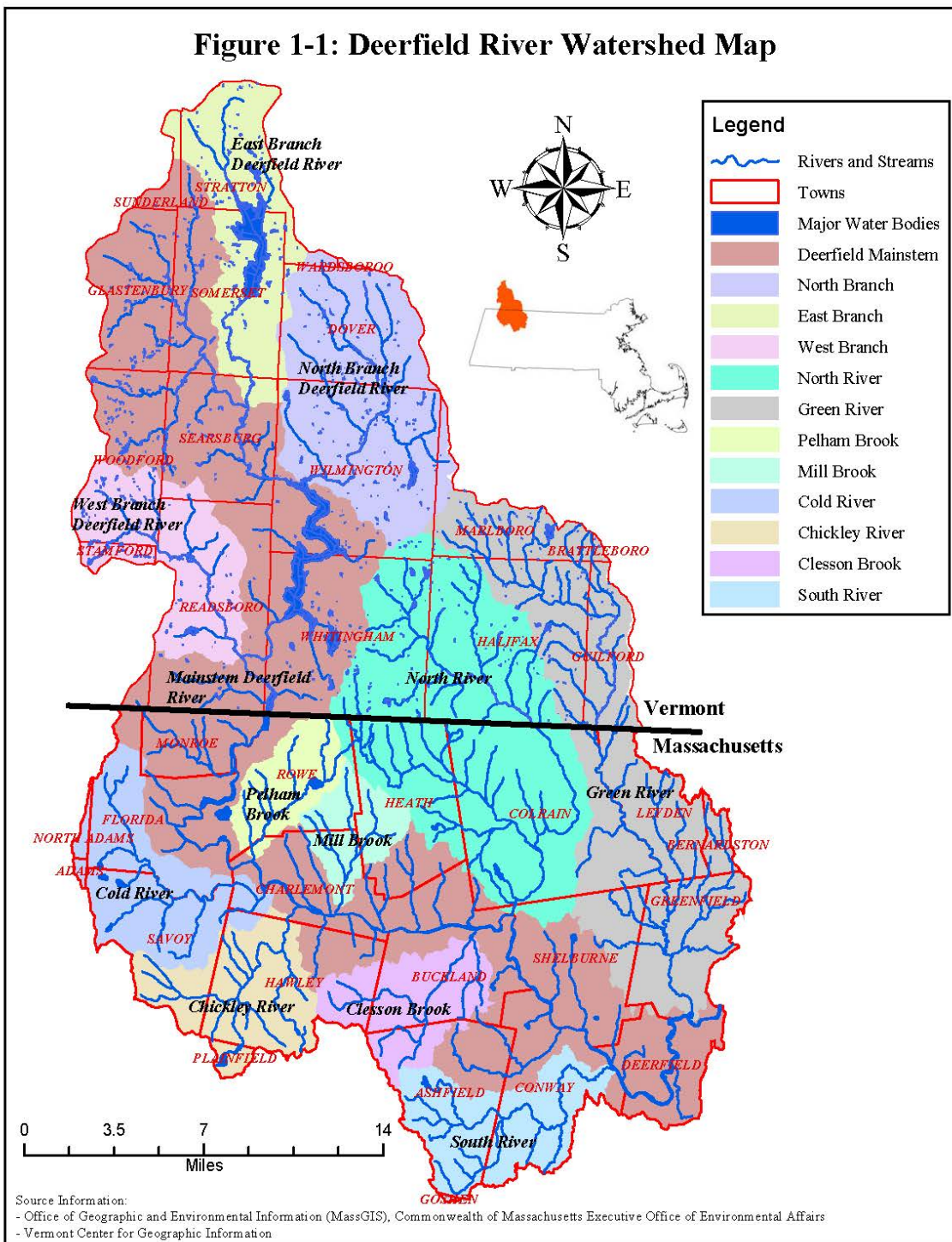


**TABLE 2-1
Hydrologic Unit Codes (HUC)**

Catalog Unit 8 Digit	Watershed 10 Digit	Subwatershed 12 Digit	No. Tributaries 16 Digit	Location
01080203				
	01			Deerfield River, Vermont
	02			Mid Deerfield
		01	10	Dunbar, Pelham
		02	9	Cold River
		03	8	Chickley
		04	7	Clesson
		05	8	Charlemont (Rice, Mill)
	03			
		01	4	East Branch North River
		02	8	West Branch North River
	04			Green River
		01	2	Upper Green
		02	17	Lower Green
	05			Lower Deerfield
		01	8	South River
		02	6	Main Channel
Total	5	11	87	

The northern half of the watershed is in Vermont and characterized by upland areas that are generally above elevation 2,000 feet (NGVD) with several mountain peaks at over elevation 3,500 feet NGVD. The headwaters are west of the Stratton Mountain Ski Resort. The East Branch, West Branch, and main branch are within the Green Mountain National Forest. The North Branch parallels the well-known Route 100, past the base of the Mount Snow Ski Resort.

The Deerfield River basin has a humid temperate climate zone with a New England mixed forest composed of glaciated mountains underlain largely by granite and metamorphic rocks of schist and gneiss. Vegetation reflects a mixture of deciduous hardwood forests dominated by maple, birch, and beech, with some hemlock and pine (Bailey, 1995). The uplands are covered with glacial till soils and have short growing seasons, impairing agricultural activity. In contrast, the flat, fertile floodplain in the Connecticut River Valley was settled prior to 1700 due to its rich soils. Massachusetts Route 2 is a major highway through the watershed and is known as the Mohawk Trail, named after the precolonial Native American foot path over the mountains to the Hoosic River Valley to the west.

The base level elevation, below which the Deerfield River cannot erode, is controlled by the Connecticut River. The Connecticut River may adjust its elevation due to glacial rebound, degradation, or aggradation, and the Deerfield River will follow. Local base levels are present in several areas where bedrock is exposed and controls the river's elevation and/or alignment, and artificial local elevation controls are located at the series of dams.

Throughout this report, there are references to locations based on "river mile," (RM) which refers to the distance upstream of the Connecticut River. The existing RM system is already used on hydropower Federal Energy Regulatory Commission (FERC) maps and Federal Emergency Management Agency (FEMA) flood studies. Features along the valley or banks are described as being on the left or right side, always while facing downstream.

2.1 Bedrock Geology

The Deerfield River basin and the larger region have a very complex bedrock geology that influences the topography, river valleys, and surficial soils. The region was once the continental edge and was subject to plate tectonics as ancient continents collided along north-south shorelines followed by rifts as continents pulled apart. As a result, ancient sediments were metamorphosed into harder gneiss and schist with a band of marble and limestone in the Hoosic Valley. Multiple continental collisions created thrust belts along the north-south axis with the rock layers stacked sideways like books on a shelf. The ancient mountains have eroded down to a relatively piedmont plain that was later incised into valleys by the rivers. When in the deep valleys, the valley sides appear to be steep mountains but, when in the highlands, one can observe the broad summits and moderate upland gradients, and the valleys appear as cracks in the plateau surface.

A new bedrock geology map of Vermont (Ratcliff et al., 2011) describes the southern Green Mountains as a giant antisyncline composed of fault-bounded slices of rock placed by tectonic plate movement.

The oldest basement rocks on the west side of the Deerfield River basin are the Granville gneiss, which are in a syncline overlaid with schists of various ages. The west end of this syncline daylights along the crest of the Hoosic Range. The ridges and valleys of the Deerfield River basin east of the Hoosic Range are mainly schist. A description of the famous Hoosic Railroad tunnel between the Deerfield and Hoosic valleys describes the bedrock layers (from east to west) as Rowe schist, Stamford granite gneiss, metamorphic conglomerate, Hoosic schist, and Stockbridge limestone. The eastern end of the Deerfield River basin slopes rapidly down into the Connecticut River rift valley, which is filled with erosion-prone reddish shale and sandstone sedimentary rock.

2.2 Surficial Geology

The region is dominated by the Hoosic Mountain Range, which extends from north to south, and by incised bedrock controlled valleys. The watershed is underlain by tough metamorphic rocks of folded schist and gneiss, plus a limited area of reddish brown Triassic sandstone and shale rock in the Connecticut River Valley. During the ice ages, the rift valley was covered by glacial Lake Hitchcock. Immediately west of the Deerfield River basin lies the limestone valley of the Hoosic River. The primary ridge lines have a north to south orientation parallel to the rift valley.

Much of the Deerfield River's channel is incised into narrow bedrock valleys surrounded by steep hillsides, leaving little space for bottom lands. As a result, the Deerfield River, and especially its undammed tributaries, can have rapid runoff and flash floods with limited wetlands and natural water retention. The combination of shallow bedrock, steep slopes, and glacial till soils also influences agricultural activities, much of which is limited to floodplain and terrace area soils.

The entire Deerfield River basin was covered by glaciers several times, scraping soil off hilltops and leaving a mantle of glacial till. The till has a random mixture of sand and gravel mixed with silt, clay, and rocks, creating a dense nutrient-poor soil. Many valley bottoms received fluvial sediments from upland areas that formed stratified drift and level floodplains along the large rivers.

Holocene and Pleistocene sediments with large rounded boulders and cobbles are found in old terraces. The stratified drift outwash deposits of sand and gravel lie in the valley bottoms and form the outer limits of modern floodplains. Portions of the original postglacial drift have eroded, leaving high and low terraces along the valley edges that often correspond to active agricultural land uses. Rivers flowing across the stratified drift may further incise channels and have lateral meander movement that reworks the old sediment, plus modern alluvium will be deposited. The younger geologic floodplains may be used to approximate flood hazard areas and supplement FEMA floodplain maps that are based upon hydraulic engineering analysis (see Section 5.0 of this report).

Vermont and Massachusetts surficial geology maps depicting stratified drift were compiled from individual USGS topographic quadrangle maps, then digitized and combined. Surficial geology maps depict little stratified drift in Vermont where the Deerfield River is largely confined in narrow valleys or impounded. A narrow band of stratified drift is mapped along the Deerfield River downstream of the Hoosic tunnel area becoming a little wider in Charlemont and Buckland and narrowing in Conway. The most significant stratified drift deposit is along the Green River in Greenfield and along the town of Deerfield floodplain, which also has mapped modern alluvium.

Narrow bands of stratified drift extend to the North River in Colrain, the South River in Conway, Clesson Brook in Buckland, and Chickley River in Hawley. The USGS has explored several of the stratified drift deposits in terms of groundwater sources and hydrogeology characteristics (Friesz, 1996). The North River and South River deposits were reworked by Hurricane Irene while the Cold River and Chickley River fine-grain bed deposits were removed.

2.3 Deerfield River

2.3.1 Introduction

The main channel flows in a southerly direction through narrow, confined valleys in its Vermont sector and then generally flows southeasterly through Franklin County, Massachusetts, as a

slightly entrenched gravel and cobble bed river to the Connecticut River at Greenfield. The river length is 76 miles with a fall of 1,700 feet. Major tributaries include the North River, Green River, Cold River, Pelham Brook, Mill Brook, Chickley River, Clesson Brook, and South River. For most of its length, the Deerfield River is incised with steep-sided bedrock valleys that likely follow ancient fault zones. The 1846 *Gazetteer of Massachusetts* by John Haywood describes the river as "a beautiful and important Indian Stream" that is rapid with precipitous banks. The surrounding piedmont-like uplands have mild gradients and a rolling surface with broad summits. Streams generally drain along northwest and southeast axes.

The area of subwatersheds is available in Wandle (1984) and digital GIS files.

Key Subwatersheds

	Basin Area, Square Miles	Comments
East Branch (VT)	36.9	Rural, GMNF, Somerset Reservoir
North Branch (VT)	55.9	Rural, GMNF
West Branch (VT)	31.8	Short, steep, whitewater sports
North River	92.9	Cold-water fishery, agricultural land
Green River	89.8	Class A watershed, then urban area, downstream region
Cold River	31.7	Steep, clean, provides recreation, gorge
Pelham Brook	13.7	Narrow step valley
Mill Brook	15	Acid mine drainage, nonsupport status
Chickley River	27.4	State forest, recent channelization and restoration
Clesson Brook	21.2	Landfill, aquatic life alert
South River	26.3	303(d) list, agricultural, downstream gorge

GMNF = Green Mountain National Forest

The two largest tributaries, North River and Green River, are near the downstream end of the basin and have limited influence. The latter is located near the Deerfield River confluence with the Connecticut River and shares the same gap through a basalt ridge. Several tributaries are semiconfined to fully confined with limited floodplains.

2.3.2 River Gradient

Rivers receive their energy for transporting water and sediment from gravitational forces, which are reflected in the river gradient. The river's longitudinal profile is a graphical plot of the river bed elevation versus distance and is a critical tool in understanding river hydraulics, sediment transport, and stream power (see Figure 2-1). The classic river channel gradient usually declines from its narrow, rocky headwaters to a broad, meandering, low-gradient channel at its mouth.

The Deerfield River main channel has an elevation drop of approximately 1,700 feet in 75 miles with an average gradient of 23 feet per mile (see Figure 2-2). Its longitudinal profile generally has the classic "concave up" shape with steep headwaters and an increased gradient near the downstream quarter point from Clesson Brook to South River where the Deerfield River cuts down into the side of the Connecticut River rift valley. However, bedrock grade controls and

dams create a somewhat irregular profile. The final 7 miles of the Deerfield River lie across the flat Connecticut River lowlands. This profile type is very similar to the nearby Westfield and Farmington Rivers, which also have headwaters in the western highlands with hydroelectric plants located where they down cut through basalt dikes into the rift valley.

For most of its length, the Deerfield River is bedrock controlled. Even the main valley with its alluvial channel from dam #4 near Shelburne Falls to the Route 2 bridge west of Shelburne has a few bedrock outcrops that provide vertical and horizontal confinements.

The river slope and waterfalls led to its early development with water-powered industries and 20th Century hydroelectric power generation. The river profile includes waterfalls, many whitewater rapids, long runs with pools and riffles, and several reaches with a low-gradient meandering channel.

Figure 2. Profile showing altitude of the Deerfield River and locations of hydroelectric developments, streamflow-gaging stations, and major tributaries, northwestern Massachusetts. (Modified from Gay and others, 1974.)

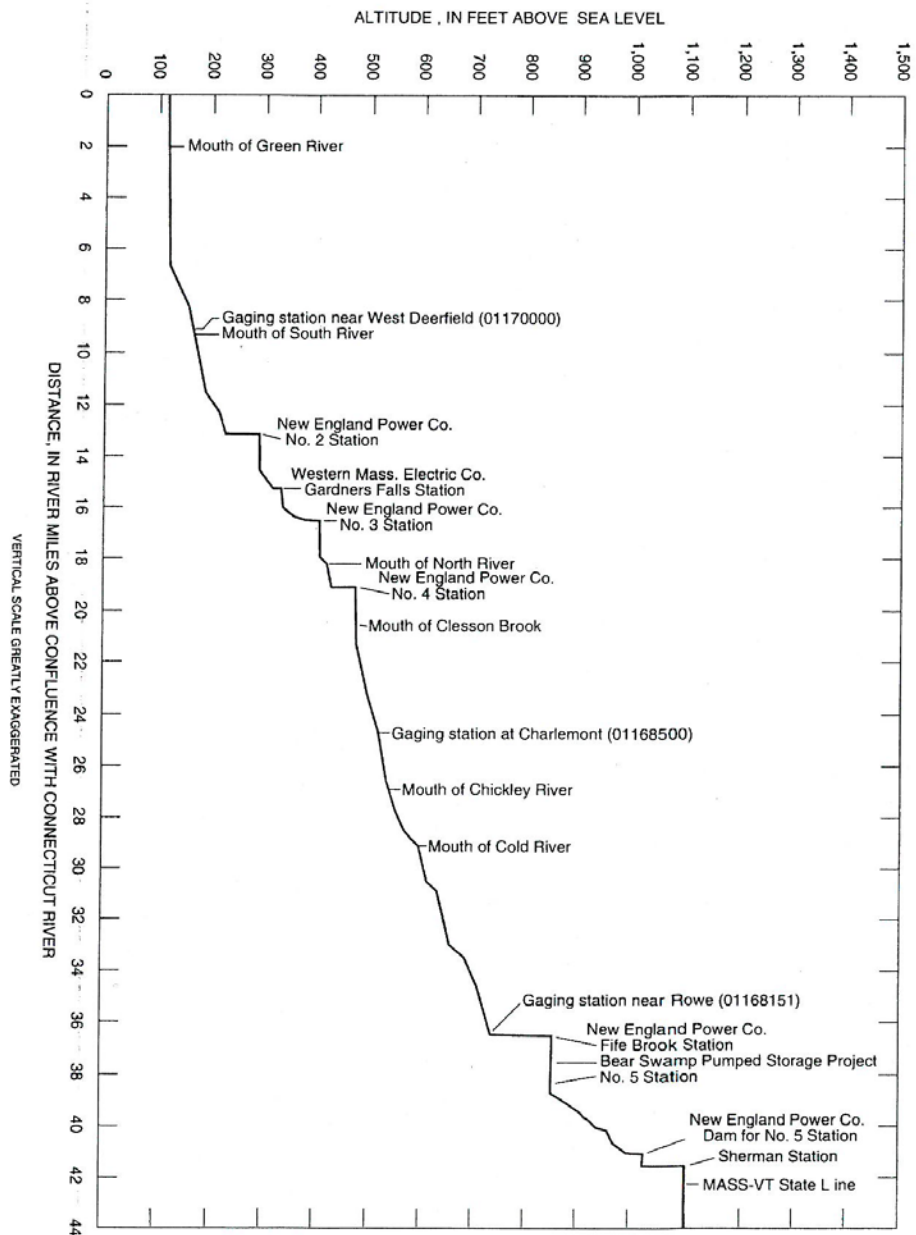
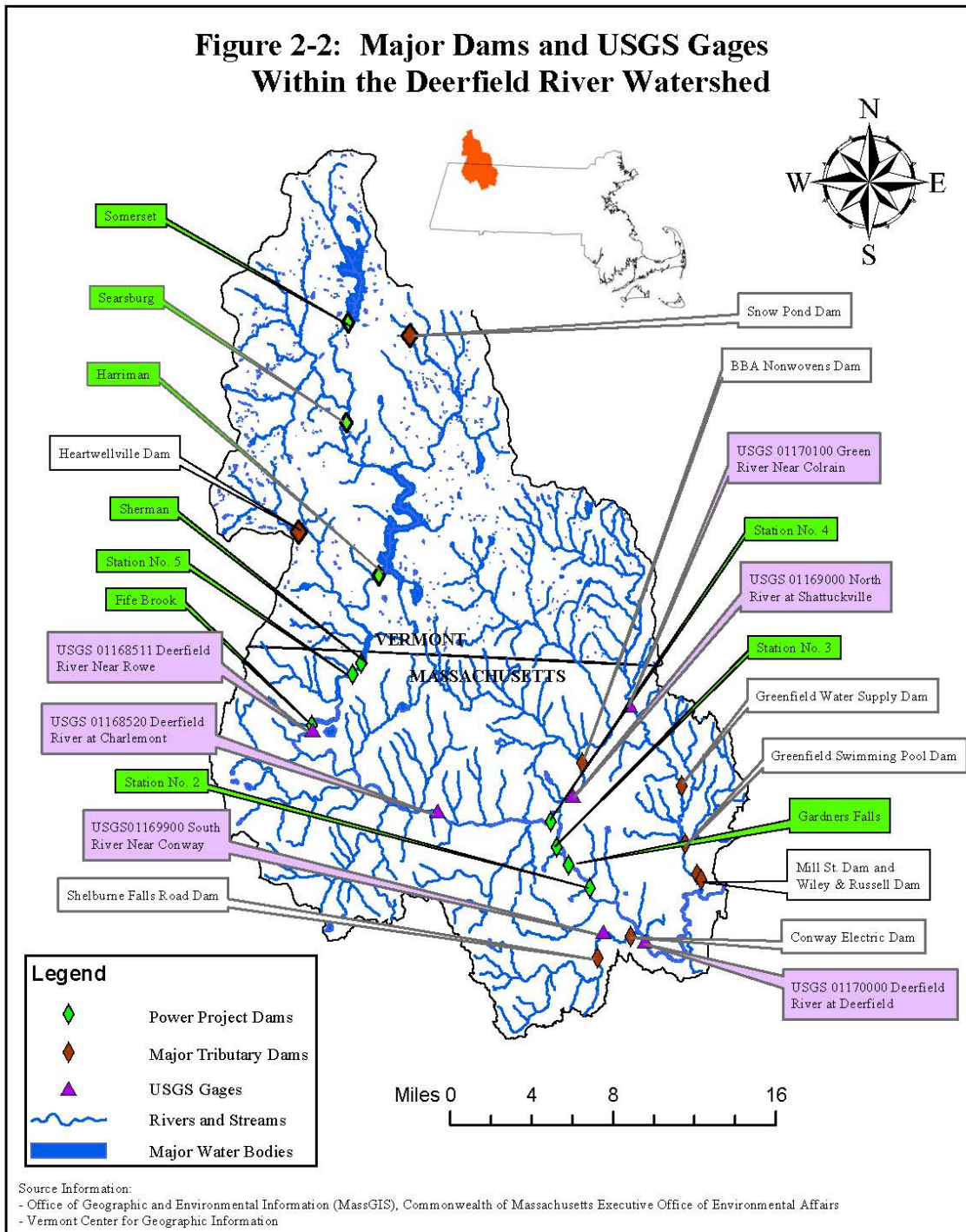


Figure 2-1: Deerfield River Profile

Figure 2-2: Major Dams and USGS Gages Within the Deerfield River Watershed



Deerfield River Dams*

Name and Comments	River Mile	Construction Date	Pool Area, Ac.	Dam Size	Pool Length, Miles	Bypass, Miles**
Somerset Reservoir, VT (East Branch) (U.S. Gen.)	66	1912	1,514	110' x 2,100'	5.6	N/A
Searsburg Reservoir, VT (Confluence) (U.S. Gen.)	60.3	1922	30	50' x 475'	0.9	3.5
Harriman Reservoir, VT (U.S. Gen.)	48.5	1925	2,039	215' x 1,250'	9	4.4
Sherman, VT/MA (Former Yankee Power) (U.S. Gen.)	42.0	1927	218	110' x 810'	2	N/A
No. 5 Monroe, MA (Head of dryway bypass) (U.S. Gen.)	41.2	1974	38	35' x 90'	0.75	2.7
Fife Brook, MA (Bear Swamp Pump Storage) (Brookfield Renewable Power)	39.0	1974	132 Lower 118 Upper	130' x 900'	1.6	N/A
No. 4, Shelburne, MA (U.S. Gen.)	20.0	1913	75	50' x 400'	2	1.5
No. 3, Shelburne Falls (U.S. Gen.)	17.0	1912	42	15' x 475'	1.3	0.2
Gardners Falls, MA (Consolidated Edison)	15.8	1904	21	30' x 337'	0.6	
No. 2 (first fish block) (U.S. Gen.)	13.2	1913	63	70' x 447'	1.5	N/A

* Compiled from A) Slater, Mass DFW, 1/28/10 B) LIHI Certificate No. 90

**River bypasses are located where dams divert a portion of the flow to downstream powerhouses that are separate from the dam.

2.3.3 Habitat

The Deerfield River and its major tributaries have outstanding habitat and support a wide range of aquatic species. The river is particularly known for its trout populations and is popular for recreational fishing despite flow modifications. The hydropower releases actually enhance fishing due to summer flow augmentation with cold reservoir water. Wild rainbow, brook, and brown trout plus stocked fish provide year-round opportunities.

The river corridor is listed as a "Priority Habitat" for state-listed endangered species including oscillated darter, 12-spotted tiger beetle, Stygian shadow dragon, and longnose sucker plus several rare plants.

The river is popular for whitewater rafting and canoeing in the 17-mile reach below Fife dam and from Charlemont to Shelburne Falls. Whitewater kayaking is also found in the area of Zoar Gap and in the Cold River. Class I waters are found in the Deerfield Meadows reach approaching the Connecticut River confluence.

The Massachusetts portion of the Deerfield River has a Class B water quality designation. It is suitable for supporting fish and other aquatic species and for water contact recreation such as swimming and whitewater boating. Historically, the river has had high dissolved oxygen levels but low alkalinity. Locally, sanitary landfills may affect water quality during low flows along Pelham Brook, Clesson Brook, and North River. Mill Brook has had reports of high acidity from old sulfur mines in Rowe.

2.3.4 Hydroelectric Facilities

The river gradient, shallow water, and Salmon Falls in the village of Shelburne Falls preclude commercial navigation on the Deerfield River but enables extensive hydroelectric power generation and regulated flows for whitewater recreational boating. The river has 10 hydroelectric dams and generating stations along its length plus the Bear Swamp pump storage facility connected to the Fife Brook dam.

Three large dams and their reservoirs are located in Vermont and serve as seasonal storage systems to generate power plus regulate flow to seven downstream hydroelectric dams. The storage reservoirs are at Somerset, Searsburg, and Harriman. The hydroelectric dams were relicensed based upon a 1994 FERC agreement with coordinated water management, including minimum flow releases, providing 84 megawatts (MW) of electricity. The former Yankee Rowe Nuclear Power Station was the third commercial unit in the United States and was located along the Deerfield River next to the Sherman dam at the Vermont/Massachusetts border. The plant was in use from 1960 to 1992 and has been fully decommissioned and removed.

Some of the hydroelectric facilities include long "bypass" river segments where most flow is diverted from the river and into power station canal and/or pipe headraces that convey water from the dams to power stations. Minimum flows are maintained in the bypass segments for

fisheries and recreation, but the dam release rates may rapidly change based on operational conditions. The improved water quality, scheduled flow releases, and rural character make the Deerfield River a popular recreation area. It is well known for whitewater boating, fishing, and public parks and forests. The nine power facilities operated by TransCanada are licensed by the FERC as project No. 2323, and the separate Gardners Falls site is FERC No. 2334.

The last dam constructed was the Fife Brook dam associated with the Bear Swamp pump storage facility. The lower dam has pumps that force water to the hilltop storage reservoir for later release during peak hours, generating up to 600 MW.

Each of the dams poses a potential flood risk and is inspected under FERC guidance. They have Emergency Action Plans that are referred to in the *Town of Deerfield 2011 Multihazard Mitigation Plan*.

2.4 Flood Insurance Studies

FEMA Flood Insurance Studies (FIS) prepared as part of the National Flood Insurance Program (NFIP) are an invaluable source of information on the nation's rivers and are available for some of the towns in the Deerfield River basin. The reports contain important information on the rivers' hydrology, flood history, floodprone areas, and longitudinal profiles of selected rivers. They also contain information on computed floodwater elevations, cross section velocities, and floodway data.

The flood insurance maps that accompany the FIS define the boundaries of floodprone areas and regulated floodway areas that are essential to convey floodwaters (see Section 5.3). Fill material encroachments are banned from designated floodways. The Flood Insurance Rate Maps (FIRMs) are used to establish insurance rates and building elevations.

FIS are available for the selected rivers in the following communities:

<u>Town</u>	<u>Date</u>
Buckland	1979
Charlemont	1980
Colrain	1980
Conway	1979
Deerfield	1980
Greenfield	1980
Shelburne	1980

As part of this project, the designated floodplain boundaries have been digitized into a combined GIS layer map (see Section 5.4).

3.0 HYDROLOGY

3.1 Introduction

Watershed hydrology, in particular the peak flood flows, is the primary factor influencing river processes. Understanding watershed hydrology and its trends is an essential part of river assessments.

The Deerfield River basin has a pleasant four-season climate with mild summers and cold winters. Annual precipitation ranges from 53 inches in the upper watershed at Searsburg, Vermont, to 45 inches in Greenfield, with a fairly uniform annual distribution. Precipitation events range from summer thunderstorms to continental frontal systems, with rare coastal tropical storms such as the 1938 hurricane and 2011 remnants of Hurricane Irene.

Surface water hydrology refers to the movement of runoff through the watershed including its spatial and temporal distribution over time. Runoff includes the dry weather "base flow" from groundwater discharges at seeps and springs plus reservoir release and snowmelt, and runoff from excess precipitation. Long-term National Oceanic and Atmospheric Administration (NOAA) data on regional climate demonstrates a steady rise in mean annual precipitation, consistent with other Northeastern states. The long-term mean annual precipitation in the Deerfield River watershed is 45 inches, but some recent years have had up to 60 inches.

Flow rates in the main stem of the Deerfield River are regulated by the large upstream storage reservoirs in Vermont plus the smaller pools at the downstream hydroelectric dams. The storage reservoirs are used to capture and retain excess runoff from the wet winter and spring months and later release it to generate electricity during the drier summer season. The smaller pools at the individual generator stations appear to be drawn upon to meet daily and weekly peak-hour electrical needs. As a result, flow rates and water levels may rapidly change on an hourly basis.

The FERC License for the Fife Brook dam near the Massachusetts border requires a minimum flow release of 125 cubic feet per second (cfs) for the protection of fisheries, plus timed supplemental flows for whitewater boating. During the summer recreation season, daytime flow releases are often between 800 and 1,000 cfs, with off-peak flows of 125 to 200 cfs. The 125 cfs release is insufficient for boating over most riffles. Recreational activities are timed to match flow releases.

In Massachusetts, the USGS operates two active stream gauging stations on the Deerfield River plus along three tributaries measuring daily flow rates as well as peak flows. There are no active USGS gauges in the Vermont portion of the watershed. The stations provide an invaluable record of the watershed hydrology. Additional partial duration stations are also located in the watershed with shorter records.

3.2 Long-Term USGS Gauging Stations

The watershed has five long-term USGS gauging stations that measure stream flow (shown in Figure 1-3) plus numerous partial record stations. The five active long-term gauging stations are listed below:

**TABLE 3-1
Long-term Gauging Stations**

ID Number	River	Location	Watershed Area, SM	Period of Record
01168500	Deerfield	Charlemont	361	1913 – present
01170000	Deerfield	West Deerfield	557	1940 – present
01169000	North	Shattuckville	89.0	1939 – present
01170100	Green	Colrain	41.4	1967 – present
01169900	South	Conway	24.1	1966 – present

SM = square miles

The main stem Deerfield River gauges have been influenced by the giant Somerset and Harriman Reservoirs since 1924, plus the power plants. The latter have daily store and release patterns that result in very irregular daily discharges in downstream segments. The mean monthly flows at the centrally located Charlemont gauge and the unregulated North River gauge are tabulated below through 2012 for comparison.

**TABLE 3-2
Mean Monthly Flow, cfs**

	Deerfield at Charlemont*		North River at Shattuckville	
	Mean Monthly, cfs	CFSM	Mean monthly, cfs	CFSM
January	1,030	2.85	157	1.76
February	1,000	2.77	157	1.76
March	1,390	3.85	344	3.86
April	1,850	5.12	558	6.27
May	1,110	3.07	269	3.02
June	689	1.91	152	1.71
July	469	1.30	75	0.84
August	494	1.37	63	0.71
September	500	1.38	69	0.78
October	646	1.79	126	1.42
November	858	2.38	183	2.06
December	1,040	2.88	198	2.22

* Regulated by reservoirs and dams

cfs = cubic feet per second

cfs/m = cubic feet per second, per square mile of watershed area

A comparison of the unit discharges, cfs per square mile, confirms the regulated Deerfield River has lower flows in the winter and spring and higher flows in the summer and fall seasons

compared to the unregulated North River. Local whitewater boaters and fishermen have adapted to this schedule as well as to sub daily release patterns.

There have also been a series of short-term USGS gauging stations along the tributaries, primarily used in the 1960s drought and for water quality tests.

3.3 Channel Forming Discharges

It is generally accepted that the width, depth, and slope of active alluvial river channels is proportional to an equivalent channel-forming flood discharge. The latter is variously described as being similar in magnitude to the bankfull discharge, which fills the channel up to the elevation of the alluvial nonincised floodplain. The average return frequency of the bankfull discharge is usually 1 to 2 years, with the 2-year frequency flood often used as a surrogate.

Channel-forming discharges in the Deerfield River basin have been estimated based upon the regional regression equations for bankfull discharges developed by the USGS (Bent and Waite, 2013). The report uses long-term annual peak flow rates at gauging stations to develop regression equations for bankfull discharges based upon actual bankfull discharge rating curves at the gauges. Peak flows have also been predicted by MMI statistical Log Pearson analysis of peak annual flood flows at the five long-term USGS stream gauges in the basin, which should be the best data (see Table 3-3).

The right column in the table below represents the predicted 2-year frequency peak flood flows, determined with the Jacobs (2010) regression equation for the steep channels. This series of regression equations is for channels with mean gradients over 50 feet per mile (1 percent) and includes the 2-, 5-, 10-, 25-, 50-, and 100-year events. It was prepared for the New England Transportation Consortium using USGS gauge data. The resulting peak-flow predictions fall in between the Bent (2013) and actual gauge statistics. For steep ungauged stream locations, the Jacobs (2010) regression equations appear to be a valid choice.

TABLE 3-3
Estimated Channel Forming Discharges Comparison, cfs

USGS Gauge Station	USGS Regional Regression EQ (Bent, 2013)	Listed USGS Bankfull Q at Gauge ⁽²⁾	Statistical Gauge Analysis, 2-Year Frequency Flood ⁽³⁾		Jacobs 2-Year Regression Eq. (2010)
			USGS up to 2009 ⁽²⁾	MMI up to 2013	
Deerfield River at Charlemont ⁽¹⁾	4,121	N/A	N/A	10,943	10,540
Deerfield River at West Deerfield ⁽¹⁾	5,829	N/A	N/A	16,032	14,134
North River	1,345	3,070	4,895	4,718	3,025
South River	471	1,710	1,937	1,906	950
Green River	729	2,110	2,450	2,268	1,469

(1) Regulated by upstream dams

(2) As reported in Bent, 2013

(3) Based upon MMI statistical analysis of gauge data

The above channel-forming discharge data reveals a surprisingly wide spread between the peak flood flows determined by regional regression equations and the statistical analysis of gauge data. Even a simple visual observation of the plotted annual peak flows at the gauges indicates they are much higher than the values predicted by the USGS regional regression equation. However, the statistical 2-year frequency peak flows are more similar to the actual individual bankfull discharges reported by USGS at the gauges. The statewide regression equations may yield lower estimates because the Berkshires are a mountainous area with high precipitation. The USGS Bent (2013) report indicates the Berkshires do have above-average runoff but that there were insufficient gauges to break it out as a separate region. The USGS did do a multiple regression analysis in search of physical parameters without finding the source of residuals. However, we note that the Berkshire basins have high elevations and slopes plus shallow bedrock.

The actual bankfull discharges measured at the gauge rating curves are also substantially higher than the regional data at the three unregulated stations (North, South, and Green Rivers). It appears that the use of the Massachusetts regression equations (Bent, 2013) for design of culverts, bridges, or channels in the Deerfield River basin could lead to underperformance. Similarly, the use of bankfull discharges based on long-term field indicators in reference segments may also lead to erroneous results. MMI has found similar conditions with the use of bankfull regression equations and indicators in the Catskill Mountain region of New York compared to actual gauge data.

3.4 Flood Frequency Analysis

The current USGS stream gauge annual peak-flow data was accessed via the internet and imported to the U.S. Army Corps of Engineers (USACE) Hydrologic Engineering Center's Statistical Software Package (HEC-SSP) computer model to evaluate peak flood discharge

versus frequencies. The statistical analysis was conducted at the long-term stations using the standard Log Pearson procedures as per interagency Bulletin 17B.

TABLE 3-4
Peak Flood Flows, cfs
Statistical Analysis of Gauge Data

Gauge	Return Frequency, Years					Ratio Q ₁₀₀ /Q ₂
	2	10	50	100	500	
Deerfield at Charlemont*	10,943	25,096	44,371	54,965	86,573	5.0
Deerfield at West Deerfield*	16,032	33,900	60,918	76,853	128,301	4.79
North River	4,718	11,523	23,005	30,232	55,137	6.41
Green River	2,268	4,943	9,561	12,519	22,948	5.52
South River	1,906	4,684	9,475	12,531	23,225	6.57

*Regulated by upstream dams

The ratio between the 100-year frequency flood and the 2-year flood is shown in the right column of Table 3-4. The representative ratio in the Northeast is typically about 5 and is a useful "rule of thumb" for estimating the 100-year flood when only the bankfull or 2-year flood is known. This ratio also supports use of river corridor conservation areas that are four to six times wider than the bankfull channel width.

3.5 Hurricane Irene

Hurricane Irene struck the Northeast on August 28, 2011, and caused extensive damage in New York and Vermont and moderate to severe damage in western Massachusetts but spared the eastern part of the state. Irene dropped 4 to 9 inches of rain in the Berkshires and led to the flood of record at some Deerfield River basin gauges. Floods along the Cold River in Florida created havoc, washing out sections of Route 2 and creating landslides and mudslides that blocked the river and delivered huge sediment quantities downstream, and portions of Zoar Road were washed out along the Deerfield River. Floodplains along the middle segments of the Deerfield River were then inundated and were left covered with a layer of white sandy sediment, and local farmers lost crops of corn and potato. Route 112 had to be closed due to washouts in both Colrain and Buckland, and sections of Charlemont and Buckland were evacuated as the Deerfield River rose in the lower basin behind the Shelburne Falls dam.

There was extensive flooding in the town of Deerfield including damage at the Deerfield Academy, Route 5, the Upper Road Stillwater Bridge, I-91, which was closed for inspection and scour repairs, and widespread crop loss on the north and south meadows floodplain.

The Chickley River washed out a section of Route 8A in Hawley, Massachusetts, and eroded its channel, resulting in 5 miles of channelization as work crews sought to repair damages. The latter work included dredging, realignment, stone bank lining, and berms that then had to be mitigated due to damages to this former cold-water fishery.

Information on peak flood flow rates is available from both the above USGS gauging stations and from the NFIP. The gauging stations reflect major regional floods plus the annual peak flows. At the Charlemont and South River gauges, Hurricane Irene had an average return frequency of approximately 100 years (1% chance of occurring each year) while the same event had an average return frequency of 200 years at the West Deerfield and Green River gauges. The USGS revised peak flows for Hurricane Irene were posted as of March 26, 2015. The USGS gauge data was revised between the draft and final versions of this report and have been updated.

**TABLE 3-5
Hurricane Irene Peak Flows, cfs**

Gauge Location	2011 Hurricane Irene, cfs (Revised)	Approximate Average Return Frequency, Years	Typical Annual Peak Flow Range	Previous Maximum Flow, cfs
Deerfield at Charlemont*	54,000	100	5,000 – 20,000	56,300
Deerfield at West Deerfield*	89,800	200	5,000 – 30,000	61,700
North River	30,300	500	3,000 – 12,000	18,800
Green River	13,200	200	2,000 – 5,000	6,540
South River	9,300	100 – 200	1,000 – 4,000	12,700

*Regulated by dams

Hurricane Irene caused even more peak-flow records and damages in Vermont, New Hampshire, and New York. In southern Vermont, downtown Brattleboro and Wilmington were both flooded, and many roads and bridges washed out, which resulted in recommendations to include Fluvial Erosion Hazard Corridors into regional plans. The Windham Regional Commission in Vermont has mapped Hurricane Irene damages.

3.6 FEMA Hydrology

FEMA sponsors the NFIP, a federal program created by Congress beginning in 1968 and which has been periodically updated. The intent is to minimize flood hazards and flood losses and provide federally backed insurance to help cover flood losses. The program includes FIRMs of hazard areas to guide land use planning and to set insurance rates plus locally managed land use and building regulations.

The key maps of floodprone areas are based upon engineering studies that compute floodwater elevations for the regulatory base flood. They are based upon the magnitude of the 100-year frequency base flood flow rate in cfs. A review of the FIS for the Deerfield River basin reveals they are quite old, generally adopted in 1979 and 1980. The FEMA FIS base flood flows are compared to the new MMI-computed 100-year flood flows at the USGS stream gauges in the following table.

**TABLE 3-6
100-Year Flood Flows**

Location	FEMA Base Flood, Q₁₀₀, cfs	Gauge Statistics Q₁₀₀*, cfs
Deerfield River at Charlemont	53,700	54,700
Deerfield River at West Deerfield	68,280	76,853
North River	16,370	30,232
Green River	7,360	12,519
South River	4,330	12,531

*Computed by MMI with HEC-SSP software

The above data indicates that in all cases the 35-year-old FEMA FIS underestimate the 100-year frequency peak flood flows when compared to current USGS gauge data. Consequently, the elevation, size, and width of the FEMA 100-year regulatory floodplains are underestimated, particularly on the tributaries.

3.7 Annual Peak Flood Flow Trends

The annual peak-flow plots published on the USGS website for the five gauged sites were reviewed to ascertain if there are any visible trends in long-term peak flow rates.

Gauge Location	Flood Trend Comments
Deerfield River at Charlemont*	Trend toward decreasing mid-size floods since 1950, possibly due to dam operations
Deerfield River at West Deerfield*	No visible trend
North River	Slight trend toward larger floods
Green River	No visible trend
South River	Trend toward larger floods; the three largest floods are within the past decade

*Regulated by dams

The USGS gauge on the North River has peak-flow data since 1940 with the two largest floods occurring in the past decade. On the South River, the three largest floods were also in the past decade. At the Green River USGS gauge, the annual peak flows have been quite uniform since 1967, never exceeding 5,000 cfs, except for the two highest flows that were in the past decade. Consequently, recent bank erosion and channel enlargement are to be expected due to recent flood flows. Peak flows at Deerfield gauges are regulated by dams and are not rising. In comparison, coastal areas of the Northeast are finding increased peak flows with an expectation of higher peak flows (Walter and Vogel, 2010; Collins, 2011).

3.8 Sediment Yield

Most of the Deerfield River basin (upstream of I-91) is in a hard bedrock region underlain by tough glacial till soils and currently covered by mixed hardwood and softwood forests. There are no known long-term sediment measurement stations, and the numerous dams along the main stem interrupt sediment transport. Based on regional data for similar watersheds, the mean annual natural sediment yield would be expected to be in the range of 30 to 100 tons per square mile per year (MacBroom, 2014).

Except for wash loads of fine silt and clay, little coarse sediment would be expected to pass the Fife dam and upstream structures. Thus, the bedload yield from 263 of the total 665-square-mile watershed is minimal except during great floods.

Yellen et al. (2014) have estimated the Deerfield River basin's suspended sediment yield during Hurricane Irene to have been 875 tons per square mile, extremely high due to the mobilization of hill slope soils during this rare flood. The bedload sediments that create channel bars and contribute to the channel form are usually a small portion of the total sediment load, in the range of 10 to 20 percent.

The dams along the Deerfield River in Vermont are expected to trap and retain most bedload sediment that approaches them plus a fraction of the bed material size suspended load. Portions of South River are incised, and the channel is currently degrading and removing old impounded sediment from mill dam sites (Field, 2013). The Cold River and Chickley River are both degrading and were observed to be major sediment sources, and from that area downstream, the Deerfield River has large attached lateral bars, confluence bars, and a delta going into Reservoir 4. This sediment-rich segment does not have bank erosion and is not degrading, confirming its sediment load is from the tributaries.

Limited sand and fine sediment is found along the Deerfield River except in Charlemont and along Deerfield Meadows. The moderate to high flows flush fines through the system and are still removing terrace deposits in the tributaries. The Deerfield River bed is generally armored, and the rounded cobbles tend to form loose clusters on riffles without imbrication. The bed is coarser than the banks. The steep coarse riffles downstream of Zoar Gap and in the Cold River include larger rounded boulders over 2 feet in diameter that will be stable except in another catastrophic flood. The many mass bank failures and landslides along Cold River and Pelham Brook provide a source for this coarse material.

4.0 FLUVIAL ASSESSMENT

A Phase I-Level Fluvial Assessment has been performed along the Deerfield River and portions of major tributaries. The tributaries generally have steep-sided confined valleys and serve as a collection area for surface runoff and sediment, conveying material to the mid-watershed transport segments of the Deerfield River, with discontinuous lateral floodplains in the less confined valleys. The final downstream region in Deerfield has a broad alluvial unconfined floodplain due to sediment deposition and the backwater from the Connecticut River. This river assessment includes the normal stream classification process plus a preliminary evaluation of the channel's "river mechanics," which quantifies and links river form and process. It addresses channel classification, channel slope, alignment and pattern, and bankfull channel dimensions.

A separate Phase II-Level Fluvial Assessment of the South River has been prepared by John Field including a detailed on-the-ground site inventory.

4.1 Channel Classification

Geomorphic classifications are used herein to describe the current condition of the Deerfield River using several standard methods. The river is divided into relatively homogenous segments with uniform hydrology between major tributaries and land features and inspected. The segments are classified using the Rosgen classification system Table 4-1 (Rosgen, 2006; Rosgen, 1994), Montgomery and Buffington (M&B) (1993), and River Styles (Brierley and Friars, 2005) and described in Appendix A. The Rosgen classification identifies channel form via visual inspection and basic measurements of sinuosity, slope, entrenchment ratio, width to depth ratio, and bed substrate size. This simple empirical system is widely used and is a preferred method used by the Vermont Agency of Natural Resources (VTANR) and the New York Department of Environmental Protection (NYDEP) as well as for Natural Channel Design (NCD). It is heavily influenced by 1950s through 1960s USGS (Leopold, Wolman) literature and predates modern hydrology and hydraulic techniques. NCD is best used for natural equilibrium alluvial systems, so application is limited along the Deerfield River by the high percentage of channel confinement and current impounded conditions. It does not address the impact of major flood events, floodplain types, or stability.

The M&B classification (1993, 1997) system was developed in and for mountainous areas based upon a qualitative assessment of sediment processes. The primary metrics are channel slope and sediment bed forms that create profile elements. The M&B classification does not address floodplain or low-gradient meandering channel types.

The River Styles classification and river assessment system by Australians Gary Brierley and Kirstie Fryirs is noted for its spatial hierarchy from watersheds to microhabitats and its linkage to modern stream power quantitative analysis. River Styles is related to the Nanson floodplain classification system and is being used by MMI to assess floodplain dynamics with stream power. It can be used to predict the geomorphic effect of temporal changes in hydrology. A modified version has been adopted by the European Commission.

The channel segment classifications in Table 4-1 are based on a combination of remote sensing and field measurements along with pebble counts and visual inspections to identify substrate type and bed forms.

**TABLE 4-1
Segment Classification**

Segment	Slope, %	Rosgen Classification	Montgomery & Buffington Channel Form	River Styles		
				Valley Setting	Channel Character	Floodplain
1	0.92	F	Runs and rapids	Confined	Steep headwater	None
2	1.2	F	Runs and rapids	Confined	Steep headwater	Trace
3	---	---	Ponded	Confined	Reservoir	Ponded
4	0.71	B	Plane bed	Semiconfined	Low sinuosity	Trace
5	0.89	F	Plane bed	Confined	Low sinuosity	None
6	---	---	Ponded	Confined	Reservoir	Ponded
7	0.95	G	Runs and rapids	Confined	Low sinuosity	None
8	0.47	F	Plane bed	Semiconfined	Floodplain pockets	Discontinuous pockets
9	0.34	F	Runs and rapids	Confined	Low sinuosity	None
10	6.0*	G	Rapids	Confined	Straight gorge	None
11	0.32	C	Plain bed run	Unconfined	Low sinuosity	Yes
12	0.17	B/C	Plain bed, run	Semiconfined	Straight	Discontinuous
13	---	F	Rapids, ponded	Semiconfined	Sinuosity	None
14	---	---	Ponded	Confined	Reservoir #3	Ponded
15	---	---	Ponded	Confined	Reservoir #2	Ponded
16	0.275	G	Run and rapids	Confined	Gorge	None
17	0.10	C	Meander, gravel bed	Unconfined	Floodplain/terrace	Major floodplain
18	0	G	Straight, gravel bed	Confined	Gorge	None

*Very short rapids at Zoar Gap

The valley settings and channel characteristics listed under River Styles provide a large scale picture of the Deerfield River and how it varies along its length. It has irregular variation in its valley slope and width that dictate the channel and floodplain form.

4.2 Channel Slope

Classic discussions on channel slope and profile types describe the bed slope as declining in the downstream direction (M&B, 1997). However, specific situations such as variable bedrock and glaciated terrain lead to many exceptions. In most segments, the main channel of the Deerfield River does have declining slope in the downstream direction as shown in Table 4-1, declining from a segment mean slope of 1 percent to just 0.1 percent.

A river channel's slope provides the only source of significant energy (gravity) to convey water and sediment. Slope is not only closely related to water and sediment transport but also to channel alignment, bed form, sediment size, and channel dimensions. The slope of the Deerfield

River was compared to an estimation of equilibrium slope calculations, first using an appropriate method (Shield's resistance to motion), and then using sediment transport analysis. The objective of the analysis is to see if the channel should be steeper or shallower to establish an equilibrium balance for the current flow and sediment (Lane, 1955). Channel slope for key individual segments was determined from topographic maps and bed substrate size measurements. Table 4-2 presents mean channel slope (Shields equation) calculations for the key unconfined segment locations.

TABLE 4-2
Mean Channel Slope Calculations (Alluvial Segments)

Location	Segment	Topographic Slope	D ₅₀ , mm	Equilibrium Slope
To Charlemont (Route 8)	11	0.0032	100	0.0044
To Shelburne Dam #3	12	0.0017	57	0.0016
Deerfield Meadows	17	0.001	25	0.0006

The static stability calculations illustrate that the channel may be understeepened upstream of the current tributary erosion sites or conversely that the sediment supplied from upstream is too large for the modern channel slope. Data suggest that the channel slope is similar to expected equilibrium slope in the long Charlemont to Shelburne segment.

Sediment Transport and Slope Example

The overall equilibrium slope was also computed for a dynamic equilibrium condition that assumes a live bed with sediment transport using the USACE Sediment Analysis Model (SAM). The analysis first estimated the sediment concentration from upstream, and then routed it through the representative Segment #12. Based upon the estimated channel forming discharge ($Q = 10,943$ cfs, see Table 3-3) and the measured substrate size ($D_{50} = 57$ mm), the resulting equilibrium slope is 0.016 feet per foot versus the measured overall slope of 0.0017 feet per foot. Based upon this, it is concluded that the alluvial segment is in equilibrium and has an appropriate slope, so it is stable and unlikely to degrade.

4.3 Channel Alignment and Pattern

Evaluating a channel's existing alignment and pattern helps to identify whether it is fundamentally stable or whether there may be a tendency toward lateral migration that can lead to bank erosion. The influence of the river valley and valley sides can lead to confined, semiconfined, or unconfined channels with or without connected floodplains. Rivers can further be described as straight or sinuous, with single, multiple, or numerous channels (often referred to as a braided channel). Over long geologic time spans of many thousands of years, river channels widen their valleys by lateral erosion and create depositional floodplains in low energy segments. They also adjust their longitudinal slope by scour and fill toward equilibrium conditions

influenced by flood discharge rates, valley slope, substrate size and type, roughness, and sediment loads.

The Deerfield River is fully confined in many segments (1, 2, 3, 5, 6, 7, 9, 10, 14, 15, and 16 due to bedrock incision and gorges). Some segments are impounded by dams and are no longer a free-flowing channel. Segments 4, 8, 11, and 12 are semiconfined with limited narrow floodplains or on only one side. There are only two unconfined segments (17, 18), thus there are very limited areas with the potential for free meanders primarily near Old Deerfield Village.

Confined and semiconfined channels are typical of geologically young landscapes with mountainous terrain where rivers and valley width have not segmented long-term equilibrium. Permanent human infrastructure in these confined river corridors is hydropower and impoundments. During floods, the Deerfield River is unable to modify its valley bottom and side walls, either laterally and longitudinally, in the confined segments due to bedrock and lack of alluvium. However, road fill at Zoar Gap can and does erode in floods due to artificial confinement. Portions of Cold River, North River, and Chickley River have high specific stream power and had extensive erosion during Hurricane Irene with local valley widening.

Deerfield Meadows (Stillwater Segment)

The only fully unconfined alluvial channel segments along the main stem channel are at the Deerfield Meadows downstream of the I-91 bridge. Segments 17 and 18 have a large radius meandering channel with an active floodplain backed up by terraces (Rosgen Type C).

Predicting equilibrium and potential channel planform patterns is not a mature science; and the various methods are not always reliable, so we use a series of procedures. To address the essential question about whether this meandering segment is stable, potential channel patterns have been predicted using five methods, all assuming there is no channel confinement and that the river is free to adjust in its valley bottom. The two empirical methods employed, Church (2002) and Ferguson (1984), are based on field observations that updated and expanded earlier work by Leopold and Wolman (1957) that differentiated between meandering and braided channels as a function of the mean annual flood and slope. The third method is a deterministic sediment transport model by Chang (1988) that differentiates stream pattern as a function of slope, sediment size, and bankfull discharge. The fourth approach to predicting channel pattern was Kleinhans' (2010) analysis of channel pattern and slope as a function of stream power. The analyses were based on an estimated channel-forming discharge of 16,032 cfs (the 2-year flood as derived from West Deerfield stream gauge data, see Table 4-4) and a representative D_{50} sediment size of 50 millimeters (mm) for the active bedload.

The results of the two older empirical methods (Church, Ferguson) both inaccurately forecast a braided channel, which is usually straight when considered at the segment and valley scale. However, upstream dams reduce this river's sediment load, so braided channels at this location are most unlikely. Chang's sediment transport method correctly forecasts a meandering point bar

channel. The stream power-based Kleinhans' specific stream power method also predicts a moderately active meandering channel with scrolls.

The newer River Styles channel pattern data focuses on the combination of confinement and stream power concepts. For Deerfield Meadows, the mean specific stream power for the 0.1 percent valley slope is a stream power of 68 watts/square meter. This is a relatively low value consistent with low-gradient sandy, stable meandering channels that are unlikely to have avulsions, consistent with research publications by Kleinhans and Chang.

In summary, the stream power methods of predicting the channel pattern forecast that the natural channel form would tend toward moderately active meandering if not confined, and this matches the existing condition. However, the specific stream power is quite modest, so one would not expect rapid or dramatic channel adjustments even with increases in flow. This is confirmed by the river's mild response to Hurricane Irene, which caused little geomorphic change in the floodplain segments.

Historic Channel Alignment Analysis

It is common practice for geomorphic assessment to include a review of historic documents to help identify past river and land use trends, particularly for alluvial segments subject to migration. Historical meander patterns of the alluvial Deerfield Meadows segments were observed using aerial photographs and USGS topographic mapping. The USGS mapping at five time periods was reviewed including 1892, 1936, 1941, 1954, and the present series of maps.

The 1892 USGS map has a contour interval of 20 feet using a mean sea level datum and a map scale of 1:62,500 (1 inch equals 1 mile). This map predates the current Route 5 and I-91, of course, but does depict early roads, buildings, and land features. The alignment of the Deerfield River across the Deerfield Meadows is very similar to the current conditions, except at the first big bend where an additional side channel (or canal) is present. Floodplain features are not shown.

The 1936 USGS map is at a larger scale with 10-foot contour intervals. The channel alignment is similar to the present, with point bar chutes and islands. The floodplain features its oxbows and scroll lines. The subsequent USGS maps up to 1954 are essentially the same as the 1992 Google Earth aerial photograph.

The September 2011 aerial photograph was taken shortly after Hurricane Irene and shows fresh, light-colored sediment deposits over the lower floodplain areas and reflected inundated accretion areas. Minor changes in the meander geometry are present but no avulsions or mass migration despite the huge flood flows.

Similarly, the above documents show minor evolution of the big bars at the mouth of Cold River, Chickley River, below the Route 8 bridge, and the Dam #4 delta. No drastic geomorphic changes are evident at these points.

The historic photographs and maps provide valuable data but are not perfect due to challenges in comparative image overlaps and indexing. As a result, field observations that verify past channel or floodplain evidence are invaluable.

4.4 Bankfull Width Channel Dimensions

The width of an alluvial channel measured at the elevation of the bankfull discharge provides guidance on the preferred size of regional self-formed channels that are in equilibrium. It is expected that undersized channels will tend to widen and that oversized channels (usually due to flood scour) will tend to narrow via deposition if excess coarse sediment is supplied.

Semiconfined and confined channels that adjust their width via eroding into a terrace or valley wall can cause mass bank failures and will generate new sediment. Bankfull channel analysis was used to help assess whether the Deerfield River channel has an appropriate size for its channel-forming discharge. Bankfull width data is also used for planning the size of riparian buffer zones and conservation corridors for existing or future hydrologic conditions.

The concept of having equilibrium bankfull channel dimensions such as regime relations (later called hydraulic geometry bankfull channel widths) was developed in India in the later 19th Century for unconfined canals and later applied to rivers in the United States and in Europe. Several methods are available to predict equilibrium dimensions including regime relations based on discharge rates and substrate, regional hydraulic geometry relations based on watershed area, multiparameter regression equations, and sediment transport relations.

The theoretical approach to predicting the dimensions of a channel in equilibrium is to first estimate (or measure) the incoming sediment load from an upstream channel segment, then find the size of the downstream design segment channel that will convey both the sediment load and the discharge. The solution is accomplished by iteration or simultaneous equations, with the best solution being the one that conveys water and sediment most efficiently (with the least energy). For example, based upon the upstream segment geometry and bed material for Segment #12, the SAM solution has a bottom width of 87 feet and a depth of 14.1 feet. Assuming 2:1 side slopes similar to existing boulder edges, the width at bankfull is 143 feet for an unconfined segment. This is narrower than field conditions, suggesting that this example river reach has ample width.

The bankfull channel widths along selected reaches of the Deerfield River and key tributaries were measured in the field with a handheld laser distance meter. Cross sections were selected at the free-flowing riffles or runs, preferably in less confined areas. Table 4-3 summarizes the measured bankfull channel widths and compares them with regional hydraulic geometry relations and regime equations (only at gauges). The regime equation is the Soar & Thorne (2001) calibrated version of the Lacey equation, using the channel forming discharge (bankfull or Q_2) as its predictor.

**TABLE 4-3
Deerfield River Bankfull Widths**

Segment	Drainage Area, sm ⁽¹⁾	Mean Slope Ft/Ft ⁽²⁾	Bankfull Width, Ft		
			Measured ⁽⁴⁾	Regional HGR ⁽³⁾	Regime EQ ⁽⁵⁾
1	50.9	0.0092	75	74	
2	99.3	0.012	80	99	
3	184	Searsburg Reservoir	--		
4	191	0.0071	100	132*	
5	224	0.0089	120	142*	
6	236	Sherman Reservoir	--		
7	253	0.0095	125 (dryway)	140	
8	263	0.0047	170	143	
9	279	0.0034	175	146	
10	279	0.06	75 (Zoar Gap)	146	
11	340	0.0032	195	158*	
12	403	0.0017	230	169*	212
13	498	Dam #3 Reservoir	--	*	
14	498	Dam #3	--	*	
15	507	Reservoir #2	--	*	
16	562	0.00275	252	194*	
17	662	0.0010	170 – 250	207*	257
18	665	0			

Comments:

- * Watershed area exceeds hydraulic geometry relationship (HGR) data and curves
- 1. Based on USGS *StreamStats* Website
- 2. Based on USGS *StreamStats*, Google and FEMA
- 3. Based on USGS SIR-2013-5155 and Vermont Department of Environmental Conservation (VTDEC), 2006
- 4. Rounded figures
- 5. Based upon Q₂ at gauging stations

Channel segments in Vermont were compared with the Vermont DEC (2006) data; channels in Massachusetts were compared with USGS data by Gardner Bent (2013). In general, the mean existing bankfull channel dimensions are greater than regional hydraulic geometry relations, which do not account for regulated flows. The results are consistent with the observation that the gauged 1.1- to 2-year frequency floods are substantially larger than the regional data for both the regulated main stem gauges and the tributaries. In contrast, based upon gravel bed rivers, the Lacey-type regime equations developed for the USACE (Soar and Thorne, 2001) have a better fit at the two gauges where peak flows are actually known.

Berkshire Regional Bankfull Width Regression Equations

The USGS has developed a simple, one-parameter regression equation to predict bankfull channel dimensions in Massachusetts (Bent, 2013). They have also published their actual measured bankfull channel widths based on field indicators at the gauging stations that were used

for the regression equations. The report mentions that predicted bankfull dimensions for the Berkshire region tend to deviate from the measured results (page 8).

In order to explore this, MMI solved the regression equation for bankfull widths at seven Berkshire region gauges using the Bent (2013) regional regression equation and compared the results to the USGS field measurements as shown below. MMI then tested several alternatives including the combination of using the Jacobs (2010) equation to predict the 2-year frequency (Q2) peak flows combined with the Soar and Thorne version of the Lacey regime equation as published by Copeland (2001).

**TABLE 4-4
Comparison of Bankfull Widths at USGS Gauges**

USGS Gauge Site	Bankfull Widths, ft.			
	Drainage Area, sm	USGS Measured	Regression EQ (Bent, 2013)	Jacobs Q2 and Regime
North River	89.0	106.3	92.1	116
South River	24.1	65.55	54.3	64.7
Green River	41.4	104.75	67.6	80.5
West Branch Westfield	94.0	124.15	94.2	116
Hubbard River	19.9	73.25	50.3	58
Green River Williamstown	42.6	79.0	68.4	81.5
Mill River Northampton	52.6	84.5	64.5	89.5

Residual = $\frac{\text{measured width}}{\text{regression equation}} = \%$ Mean = 28.1%

Regression EQ Width = $W_b = 15.0418 (DA)^{0.4038}$

In the critical Deerfield Meadows segment, the hybrid regime method predicts a bankfull channel width of 255 feet versus a measured width of 250 feet.

The above table indicates that the Bent (2013) regression equation significantly underestimates the measured bankfull channel widths at the seven gauging stations checked in the Berkshire region. However, the Jacobs equation is a good alternate for bankfull discharges, and the Soar and Thorne regime equation predicts the bankfull width for threshold gravel bed channels in the Berkshire region well. The subsequent GIS-based culvert vulnerability analysis (see Chapter 7.0) used the regime equations to predict bankfull width after comparison with field data (see Section 7.3.8).

4.5 Stream Power

4.5.1 Introduction to Stream Power

The erosive impact of flowing water is usually described in terms of water velocity or shear stress and less commonly as a function of stream power. Stream power is an important metric that influences sediment transport and deposition plus many related stream and floodplain patterns and processes. In addition to the discussion below on stream power as an erosive

force, it is discussed in Section 4.0 of this report with regard to predicting channel patterns and profiles types, in Section 5.0 in regard to floodplain classification, and in Section 7.0 concerning culvert vulnerability. Modern stream power channel classification systems include River Styles (2005) and Nanson and Croke (1994) for floodplains and the EU REFORM (2014) program.

Our interest in stream power is stimulated by "observations that floods of similar magnitude and frequency sometimes produce surprisingly dissimilar geomorphic results" (Costa and O'Conner, 1995). MMI witnessed these same phenomena during Hurricane Irene in August 2011 where some Schoharie Creek (New York) and Deerfield River (Massachusetts) reaches conveyed huge flood flows with a frequency of 100 to 500 years with extensive inundation but limited damage while nearby confined reaches of Cold River that concentrated the flow suffered tremendous geomorphic adjustments and community damage. Despite over 50 years of periodic research, there is uncertainty in the scientific community to apply stream power for predicting future flood responses and for design of river channels and flood mitigation programs. This report attempts to advance stream power applications by compiling previous literature data plus new observations.

Stream power is a function of just channel slope and discharge, so it is easy to determine, requiring less data than predicting velocity or shear stress.

Bruce Rhoads (1987) commented on the confusing stream power terminology then in use and the need for consistent definitions. This report seeks to adhere to his recommended nomenclature. The general term "stream power" refers to the broad concept of work performed by flowing water moving down slope, in a qualitative sense.

Total stream power is the rate of energy expenditure per unit length of channel at a cross section location. It is the amount of potential geomorphic work done by the weight of the water times the channel's vertical drop, defined using the metric power units of watts.

TP= YQS Y = unit weight of water
 Q = discharge rate
 S = Channel slope

The total stream power is the amount of work done per unit of time. It is the product of the fluid density, energy grade line slope, gravity acceleration, and water discharge rate. It may also be expressed as shear stress times velocity. In English units, the total stream power equation is the weight of flowing water per second: $P = 62.4 QS$, compared to the specific stream power per square foot, which is also the product of shear stress times velocity ($T \times vel$), with the units of power per unit bed area. Stream power increases as the discharge rate or slope increases. Although discharges increase in the downstream direction, the total stream power may decrease because channel and valley slopes decrease downstream.

The specific or mean stream power (SSP) is the total stream power at a cross section divided by the active channel (or flood) flow width, with the metric units of watts per square meter. It is usually computed for the bankfull or 1.5-year frequency flood (Petit, 2005) for the median

annual maximum flood (Barker, 2008) or the 2-year frequency flood (Bizzi, 2013), all of which are intended to approximate the channel-forming discharge. For large floods, the total stream power is divided by the flood flow width, often the floodplain width. The unit stream power is the power per unit weight of water.

Bagnold (1960, 1966) introduced stream power in relation to the physics of sediment transport. His 1960 paper published by the USGS as *Circular #421* provides the development of the stream power concept theory, claiming that sediment transport under steady state conditions requires continuous work, which equates to the rate of power expenditure supported by sediment transport tests and use of the famous Gilbert (1914) flume data in USGS paper 86. Bagnold also showed that transport rates matched stream power better than shear stress. After extensive flume experiments, Simons and Richardson were able to define the formation and properties of channel bedforms (ripples, dunes, antidunes, and flat beds) in alluvial sediments as a function of the particle's fall diameter and stream power, demonstrating how stream power transports sediment and alters bed resistance in sand (Vanoni, 1975).

William Bull (1991) described general stream power as that available to transport sediment and that channel degradation will occur when stream power is sufficient to overcome resistance and transport bed material. At peak stream flows, the flow width will equal the valley floor width in degrading reaches. Bedload transport will diminish when stream power declines, leading to aggradation (Bull, 1991). The conceptual stream power theory is increasingly being used as a metric for initiation of motion, channel stability, and floodplain classification. It can be used as a substitute for or verification of the more common threshold velocity or shear stress analytical methods at a large scale.

Among the channel processes and forms influenced by stream power are the planform pattern, profile type, sediment transport, channel equilibrium, and response to floods. The initial stream power in headwater reaches is low because of low flow rates, and downstream reaches may also have low stream power due to modest slopes. The highest total stream power levels are often found in the middle reaches, also known as the sediment transport zone. But there are many exceptions as channel gradients seldom decline at a uniform rate.

Stream Power for Sediment Transport

A suspended sediment transport equation was developed by Ted Yang (1972) based upon stream power, building upon the work of Bagnold. Yang first investigated and classified previous transport equations and concluded they were not universal in their application. Yang differed from Bagnold in that he addressed the unit stream power per pound of water and assumed that the suspended concentration was a function of the effective stream power, depth of water, and particle size. Yang defined his unit stream power as the product of the mean velocity and slope. Furthermore, the coefficients for depth and size had a narrow variation, and he successfully tested and verified his equation, which is still in use. Yang then developed a similar equation for the bedload transport of gravel (1984) and tested it with flume data. Yang later became chief of the Sedimentation Engineering Unit at the U.S. Bureau of Reclamation. Gomez and Church

(1989) tested sediment transport equations and found that those based upon stream power had the best results. Yang's transport equation is one of the options in SAM and Hydrologic Engineering Center's River Analysis System (HEC-RAS).

Stream Power Computations

A river's total stream power (TSP) can be easily computed from its gross characteristics of slope and discharge, so no hydraulic details are needed (Petit, 2005). Stream power is easily computed for open channels based upon the discharge and slope of uniform channels. The slope term is for the energy grade line, but when there is no hydraulic analysis available, the water profile or bed slope is used (Barker, 2008). Bed slopes may be determined from topography maps or digital elevation models (DEMs) and Light Detection and Ranging (LIDAR) remote sensing (Barker, 2008; Bizzi 2013). GIS applications are practical for large-scale analysis of entire watersheds, using the GIS to determine watershed areas and slope, then to compute hydrology from regional regression equations. Stream power is also computed by open channel software such as HEC-RAS and can be added to the output tables.

The specific stream power (SSP) is the gross or total value divided by mean flow width. The bankfull channel width may be used, from regional hydraulic geometry relations (Bizzi, 2013). Narrow confined channels will thus have higher SSP than wider channels of the same slope and discharge. For large flood events, the SSP is the peak flow rate divided by the floodplain width.

4.5.2 Critical Specific Stream Power for Particles

It is easy to compute stream power, but to be useful for river planning and design, one must be able to relate it to the critical threshold at which particle and general riverbed and perimeter movement begins.

SSP can be used to define a critical power threshold of movement for sediment transport, and a general boundary threshold for channel stability. Several researches use maximum or minimum stream power as part of external hypothesis theories to solve channel geometry dimensions. Costa and O'Conner (1995) indicate that shear stress and stream power are indicators of the geomorphic work done by floods. But the effect of stream power is also influenced by the flood duration and the resistance of the landscape (Bull, 1979; Costa and O'Conner, 1995). High energy floods that have short duration such as thunderstorms have limited time to disrupt vegetated floodplains and scour underlying materials. So in order to apply the concept of stream power to actual predictions, one must understand both its driving force and resistance to the thresholds.

Important information on depositional critical stream power levels comes from a series of paleo-hydrology studies of Pleistocene cataclysmic floods by glacial meltwaters. Costa (1983) provided a detailed paper on critical specific stream power while researching paleo-hydraulic floods in nine Colorado watersheds. The size of 75 alluvial sediment deposits moved by floods in confined channels, including boulders, was measured and compared to flood flow rates and

corresponding unit stream powers. This led to a simple regression equation for critical stream power in the following table, with both the best fit and envelop lines. This format has since been used by other researchers. Rathburn (1993) studied ancient floods at Big Lost River in central Idaho and used HEC-2 to predict SSP for erosion and deposition. Boulder deposits were found at under 600 W/M², loess hill streamlining at 600–1,000, and loess erosion at 100–600 W/M². The larger boulders (1.3- to 2.4-meter diameter) were deposited at 940–2,500 W/M².

4.5.3 Empirical Critical Specific Stream Power Equations

The large-scale critical specific (unit) stream power in gravel bed rivers in central Europe was studied by Petit et al. (2005) and compared to the literature. They found that the critical value increased with the size of the river, which is attributed to increased bed form roughness in larger channels. Petit et al. (2005) conducted field experiments along gravel bed rivers, with slopes from 5 percent on headwaters to 0.2 percent and watersheds of 0.3 to 2,660 km². Hundreds of painted rocks were placed on the bed and their movement observed after floods. Particle sizes ranged up to 230 mm.

The ratio between the critical shear stress to the total shear stress was 0.3 in small headwaters and up to 0.5 for intermediate rivers. The Petit data suggests that smaller and steeper streams have higher critical thresholds due to increased form resistance that uses up stream power. For intermediate rivers with watersheds of 40 to 500 km², the specific unit critical stream power was found to be:

$$SP_c = 0.13D^{1.438} \quad W/M^2$$

D = mm

The basic form of the critical power equation for particle movement is:

$$SP_c = AD_{50}^B \quad \begin{array}{l} \text{Critical unit power} \\ \text{W per m}^2, D_{50} = \text{mm} \end{array}$$

<u>Data source</u> <u>mm</u>	<u>Coefficient A</u>	<u>Coefficient B</u>	<u>D₅₀ Size Range,</u>
Costa, 1983	0.009-0.03	1.69	50-1000
Williams, 1983	0.079 (no movement) 2.9 (general movement)	1.30 1.30	10-1500
O'Conner, 1993	0.1 (centimeters)	1.71	30-600 CM
Jacob, 2003	0.025	1.647	700-2300
Gob, 2005	0.0253	1.62	900-2,000
Petit, 2005	0.13	1.438	20-150
Ferguson, 2005	0.0104 S ^{-0.17}	0.67	
Mao, 2008	31.5 (small steep streams)	0.488	15-357

Costa, Williams, and Jacobs all studied very coarse substrates and had similar results. In comparing threshold results, Petit (2005), Ferguson (2005), and Mao (2008) all felt that steep, small streams with bedform resistance had higher stream power thresholds than the larger, smoother river beds, suggesting two classes of response (Petit, 2005). This condition was attributed to the particle hiding factor for mixed substrate sizes and the bed armor. The Williams (1983) field-measured stream data from Europe brackets the initial beginning of particle movement and the power at which general movement was found, recognizing that at the threshold only a few particles move. The range was attributed to variations in grain shape and weight, particle size distribution, packing density, and orientation. Similarly, Costa plotted one line that was the lower envelop threshold and then a best fit line on his figure 6.

The SSP relations by Jacob (2003) and related work by Gobb (2005) are based upon lichenometric studies in France. They were able to date the age of boulder movement using the regional growth rate of certain lichens and then relate that to gauged flood flows. The assumption is that major floods remove lichens from mobile rocks, and the lichen age correlates to mobility dates. They were able to compute the SSP for large boulders up to 2 meters in diameter, with corresponding regression equations. The latter are consistent with Costa (1983) while extending the size range.

4.5.4 Critical Specific Stream Power and Channel Adjustments

Stream power is a convenient metric to use for river assessments because it is easy to predict from the reaches' slope and discharge. However, the critical value at which particle and general

bed movement is initiated has not been fully defined. The absolute values of specific unit stream power that lead to geomorphic adjustments are believed to be a function of particle size, cohesion, cross-section characteristics, confinement, and alignment. In alluvial reaches, stream power thresholds depend on sediment properties of the bed and banks (Sear et al., 2010), which is similar to critical shear stress or velocity. The role of particle sizes in determining critical SSP is discussed by Carson (1984) in regard to channel pattern thresholds because it is the excess stream power that mobilizes sediment and leads to geomorphic changes in pattern, with freely meandering rivers found at SSP above 50 WM^{-2} and active braiding above 100 WM^{-2} for 25 mm size bed material. Stream power is just beginning to be used to help define channel patterns.

Factors that affect critical stream power in rivers include particle size, cross-section expansions and width changes, river channel bends, and floodplain symmetry (Miller, 1990; Sear, 2010). Some of the highest SSPs are found during floods in narrow bedrock valleys and gorges due to their narrow widths, but geomorphic change may be minimal due to their bedrock and boulder resistance to erosion (Miller, 1990, 1995). Conversely, large rivers with high flood flows in their downstream reaches often have low gradients and broad floodplains, leading to low unit stream power. Channels with sandy bed material are most sensitive to stream power due to low thresholds of motion. River bends magnify local stream power as with shear stress.

The stream power gradient along channels and floodplains was classified by Nanson and Croke (1992) (see Section 5.0). Their energy-based system extends from high SSPs to low power for confined, semiconfined, and unconfined valleys. They consider coarse, fine granular, and cohesive materials. Floodplains that rapidly widen and have reduced SSP are prone to deposition.

For low-gradient channels, research in both Denmark and Great Britain found that unit stream powers of less than 35 watts per square meter (WM^{-2}) for small streams were stable while channels with greater values were unstable (Brookes, 1987, 1988); however, the size and strength of the boundary material was not stated. In Illinois, the low-gradient postchannelization Kishwaukee River with an unconsolidated bed of silt, clay, and sand bed was stable with very low SSPs of 3.3 to 6.8 W/M^2 while it meandered at SSPs of 10 to 20 W/M^2 .

Kochel (1988) indicates that bedload threshold conditions may only occur during great floods and discusses that influence during Hurricane Agnes in 1972. Significant erosion and floodplain scour was found in headwaters where coarse bedload was transported, but low-gradient floodplains rarely scoured. Rivers in humid climates recover rapidly after floods. Factors associated with dramatic response to floods include high gradients, coarse bedloads, and channel geometry.

Miller (1990) studied stream power in regard to historic floods with extreme discharges in the central Appalachian mountain states including Hurricanes Agnes and Camille. Unit stream power was computed for 46 gauging stations, and the sites were rated for flood damage. Widespread erosion (scour, floodplain stripping, floodplain chutes, channel widening) occurred at stream power levels from 200 to 500 WM^{-2} , with severe erosion above 300 WM^{-2} . There was

little valley floor geomorphic damage at most sites with unit stream powers below 300 WM⁻², but 11 of the 13 sites with unit stream power over 300 WM⁻² had severe damage. Erosion of valley floors led to hill slopes slides similar to Hurricane Irene in 2011. At the upper unit stream power value of 2,600, movement of boulders at and above 1.5 meters in diameter occurred. Narrow rock valleys had limited damage as did very wide valleys, but the greatest damage was in intermediate width valleys.

Magilligan (1992) studied critical stream power in a Wisconsin stream and compiled data from numerous sources. The plot of critical stream power ranged from less than 100 WM⁻² to over 1,000, with wide scatter but was not indexed to substrate type. The curve of minimum SSP versus watershed size decreased as the watershed size increased. The minimum envelop line for most points was 300 WM⁻², similar to earlier work by Miller (1990), suggesting a threshold for major channel adjustments in humid climates. He then correlated stream power to flood frequency. However, the resistance and grain size of the eroded material was not defined. This potential threshold at 300 W/SM becomes less viable as channel slopes exceed 0.01 ft/ft (Reinfelds, 2014) where high slopes contribute to high stream powers.

Compilation of Empirical Channel Specific Stream Power Trends

(Compiled From Downes, 2004; Brookes, 1990; Bizzi, 2013; Nanson, 1992; and Sear, 2010)

<u>Application</u>	<u>Original Metric Units WM-2</u>	<u>Approximate English Units Lbs./Sec.-ft.</u>
Stable low-gradient channel	1 – 35	0 – 2.4
Stable realigned channel	5 – 30	0.3 – 2.1
Eroding alluvial channels or active meandering	>35 – 100	2.4 – 6.8
Braiding or widening	>100	6.8
Sediment deposition	<15	1.0
Floodplains (Nanson, see chapter 4)		
a) high energy, vertical accretion	>300	>20
b) medium energy, lateral point bars	10 – 300	1 – 20
c) low energy, stable cohesive	<10	<0.7
Instream habitat structure failures (Brookes)		
a) by erosion	>50	>3.4
b) by sedimentation	<15	<1.0
Braided channels		
a) by sediment size	$S > 900 D_{15}^{0.42}$	
b) sand bed rivers	$S > 2.15 Q_b^{0.5}$	
c) gravel bed rivers	$S > 3.35 Q_b^{0.5}$	
Bed Form Types Bedrock reach (Jain, 2008)		
a) Pool riffle	290 – 490	
b) Plane bed	540 – 880	
c) Step pool	880 – 1,760	
d) Cascade	2,150 – 2,750	

Canadian researchers Phillips and Desloges (2014) evaluated stream power for 146 reaches of 22 rivers in glaciated southern Ontario. The selected reaches are located along graded (equilibrium) rivers as defined by Mackin (1948), with balanced sediment supply and transport. The stream power was computed based upon slopes from GIS studies and stream gauge data for the 2-year flood plus measured bankfull channel widths that were utilized in a simple regression equation. The average value was 34 W M^{-2} . The sites were then stratified by geologic conditions as tabulated below. Additional data was used to identify channel patterns and substrate size. Bed material sizes were closely associated with slope and discharge.

Specific Stream Power for: Ontario Equilibrium Rivers (Phillips and Desloges, 2014)

Glacial Kame Moraine	30 – 100
Glacial Till Moraine	20 – 50
Meltwater Outwash Plains	20 – 60
Glacialacustrine Clay Plains	2 – 10
Meandering Floodplain Channels	10 – 60
Well Developed Braided Channels	150 – 250
Entrenched River Channels	60 – 150

The equilibrium-SSP at bankfull conditions was determined for 70 gauging stations in Belgium by Petit and Hallot (2005). They identified a clear relation between SSP and channel character beginning with very stable streams at only 15 W/sm and ranging up to braided channels at 100 W/sm. Their data is summarized below:

Long-term stability	< 15 W/sm
Stable meandering channels	15-30 W/sm
Active meanders, some migration	30-40 W/sm
Active meanders, adjusting	50-70 W/sm
Active, low sinuosity, step pools	>100 W/sm

The role of unit stream power in shaping river character and in initiating motion of bed material was also described in a broad qualitative manner by Annandale (2006). Typical values are noted below:

<u>River Character</u>	<u>Approximate Unit Stream Power, w/m²</u>	<u>Lbs./sec.-ft.</u>
Mild rivers	1	0
Mid gradient	10 – 50	0.7 – 3.4
Mountain rivers	10 – 200	0.7 – 13.7
Rapids	1,000 – 2,000	68 – 137

The River Styles channel classification system is one of the first to refer to stream power. The channel classification (typology) system being adopted by the European Union also includes relationships between channel types, floodplains, and SSP (Gurnell, 2014). They provide a new approach to classification and assessment.

4.5.5 Stream Power Applications

The stream power computations developed in Chapter 7.0 for the culvert vulnerability analysis requires predicted peak-flow rates at hundreds of locations. These hydrology predictions were performed by coding the Jacobs regression equation (described in Section 3.3) into a GIS model. Watershed areas were obtained from the database of the HUC system. The mean annual precipitation data was obtained in a digital form from an Arctno product prepared by the Parameter-elevation Regressions on Independent Slopes Model – Natural Resources Conservation Service (PRISM – NRCS) program. This equation is intended for steep ungauged watersheds and is suitable for GIS applications.

The data for channel reach slopes used in the stream power computations was obtained from the GIS layer containing LIDAR topography. The slopes represent channel reaches that are generally several thousand feet long rather than local slopes just at culverts. The total stream power for bankfull conditions was obtained by dividing the total stream power of the 2-year peak discharge (Jacobs equation) by the bankfull width (Soar and Thorne equation).

The analysis covers 1,960 stream reaches in Massachusetts, broken down by order and tabulated below:

<u>Stream Order</u>	<u>Number of Reaches</u>
1	1,125
2	414
3	183
4	107
5	40
6	91

River reaches were then classified by SSP classes and color coded on the map and overlaid with culvert locations, problem sites, and predicted vulnerability. The SSP classes are as follows:

<u>Color</u>	<u>SSP, wm^2</u>
Green	0 – 30
Light Green	31 – 60
Pale Green	61 – 200
Yellow	201 – 300
Orange	301 – 600
Red	>600

The specific stream power for all reaches of selected rivers is tabulated below:

Reach	Minimum Specific Power	Average Specific Power	Maximum Specific Power
Deerfield River: Fife dam to River Road bridge	155	167	179
Chickley River	148	220	269
West Branch North River	126	260	584
South River	76	177	274
East Branch North River	156	256	348
Cold River	251	375	590

4.6 Geomorphic Changes

Major floods such as Hurricane Irene have sufficient stream power to cause major channel erosion in the horizontal (widening) or vertical (incision) directions plus cause channel filling from sediment deposition (aggradation). High energy and confined floodplains are prone to scour while broad, low energy floodplains are subject to deposition.

Geomorphic changes during floods are often magnified by human activity such as fill material, bridges, and dams that alter river valleys. Specific examples in the Deerfield watershed are where highway embankments in narrow valleys confined the channel, leading to road washouts such as at Route 100 along the West Branch near Readsboro and at Zoar Gap just upstream of the Florida bridge. The high-powered Cold River, contracted by the Route 2 road embankment, suffered tremendous damage.

Many tributaries to the Deerfield River have steep slopes that correspond to high stream power and erosion potential that decline from the upland down into the main valley. Some tributary valleys are still quite narrow and confined, not having widened yet to their mature width. Tremendous channel widening occurred after Hurricane Irene along Chickley River, Cold River, and Mill River. Steep tributaries also transported coarse sediment to the Deerfield River, which with its mild gradients could not convey it, leading to a series of deltas at the tributary confluences. Similar deposits at the same locations were discussed in a USGS report on the 1936 and 1938 floods (Jahns, 1947).

We agree with Jahns' (1947) observation that the middle reach of the Deerfield River in Charlemont and Shelburne Falls accumulates gravel and cobble at the mouth of the steep tributaries because their transport competence is greater than the lower gradient Deerfield channel. Downstream of all dams and most tributaries, the Deerfield transports primarily silty sand that is coated over the great Deerfield Meadows floodplain.

Valley widening from lateral erosion, mass bank failures, and landslides are visible in several tributary areas. Some slides are triggered by saturated soils on steep slopes and others by channel bank erosion (particularly at bends), which undermines the valley wall.

TABLE 4-5
Summary of Selected Geomorphic Activity
as a Result of Hurricane Irene, August 2011

Location	Activity
River Road at Zoar Gap	Two major road embankment washouts
Pelham Brook	Landslide, large confluence gravel delta
Cold River	Four landslides plus large bank failures
Cold River	Route 2 washed out and closed for months
Chickley River	Four miles of severe channel erosion, widening
Chickley River	Large confluence delta, bridge blockage
Chickley River	Railroad bridge abutment scour
Deerfield River, upstream Route 8A	Large debris along banks and island
Charlemont STP, school	Property flooding, sediment deposits
Deerfield River, Route 8A bridge	Debris jam at abutment
Mill Brook	Delta deposit
Avery Brook	Delta deposit
Wilder Brook	Delta deposit
Hartwell Brook	Bridge damage, replaced
Deerfield Meadows	Deep sandy floodplain deposits, inundated
Deerfield/Route 91 bridge	Scour
Shelburne Falls Village	Flooded, significant damage to buildings
East Branch North River, Route 112, state line	Several major slope failures
North River, Route 112 corridor	Floodplain deposits, flooding
North River, Colrain	Flooded, bank erosion
North River, Colrain	Dam breach, sediment scoured
South River, Conway	Numerous minor channel scour
Black Brook and Road	Scour
West River, Readsboro	Channel scour, bank failure
West River, Readsboro	Route 100 washed out
South River, Conway	Route 116 embankment damage
North River bridge	Flowing almost full
Stillwater bridge	Closed, flowing almost full
Bridge of flowers	Flowing just full, very turbulent, road flooding
Charlemont	Road flooded at cross tributaries
West Branch North River	Floodplain inundation, sediment

4.7 Geomorphic Assessment Conclusion

The fluvial assessment of slope, pattern, and bankfull dimensions is quite informative. The overall slope of the larger Deerfield alluvial segments (11, 12, and 13) is near equilibrium at slopes of 0.002 – 0.003, but the individual segments vary due to fining sediment size in the downstream direction. The lower gradient, less confined segments (12 and 17) should be prone to gradual deposition and, indeed, each has large point or medial bars.

The unconfined channel pattern in segment 17 was assessed using both empirical data and theoretical approaches. The estimated channel-forming discharge of 16,032 cfs and typical mean slope of 0.1 percent creates conditions commonly associated with a stable meandering channel type with little likelihood of avulsions. Stream power assessments confirm this.

The regional regression equations for bankfull discharges and bankfull channel width both underestimate field measurements and local gauge data. This is likely due to the above average precipitation and runoff in the mountainous Berkshire region. However, the Jacobs regression equation is a good substitute for peak flows, and the Soar and Thorne regime equations predict bankfull width well for gravel bed threshold channels in the Berkshire region. The Deerfield River is remarkably stable compared to other mountain channels.

The right column in Table 4-4 shows that the hybrid combination of the Jacobs (2010) Q_2 and Soar and Thorne's (2001) regime equation provides the best estimate of bankfull channel widths.

5.0 FLOODPLAINS

5.1 Introduction

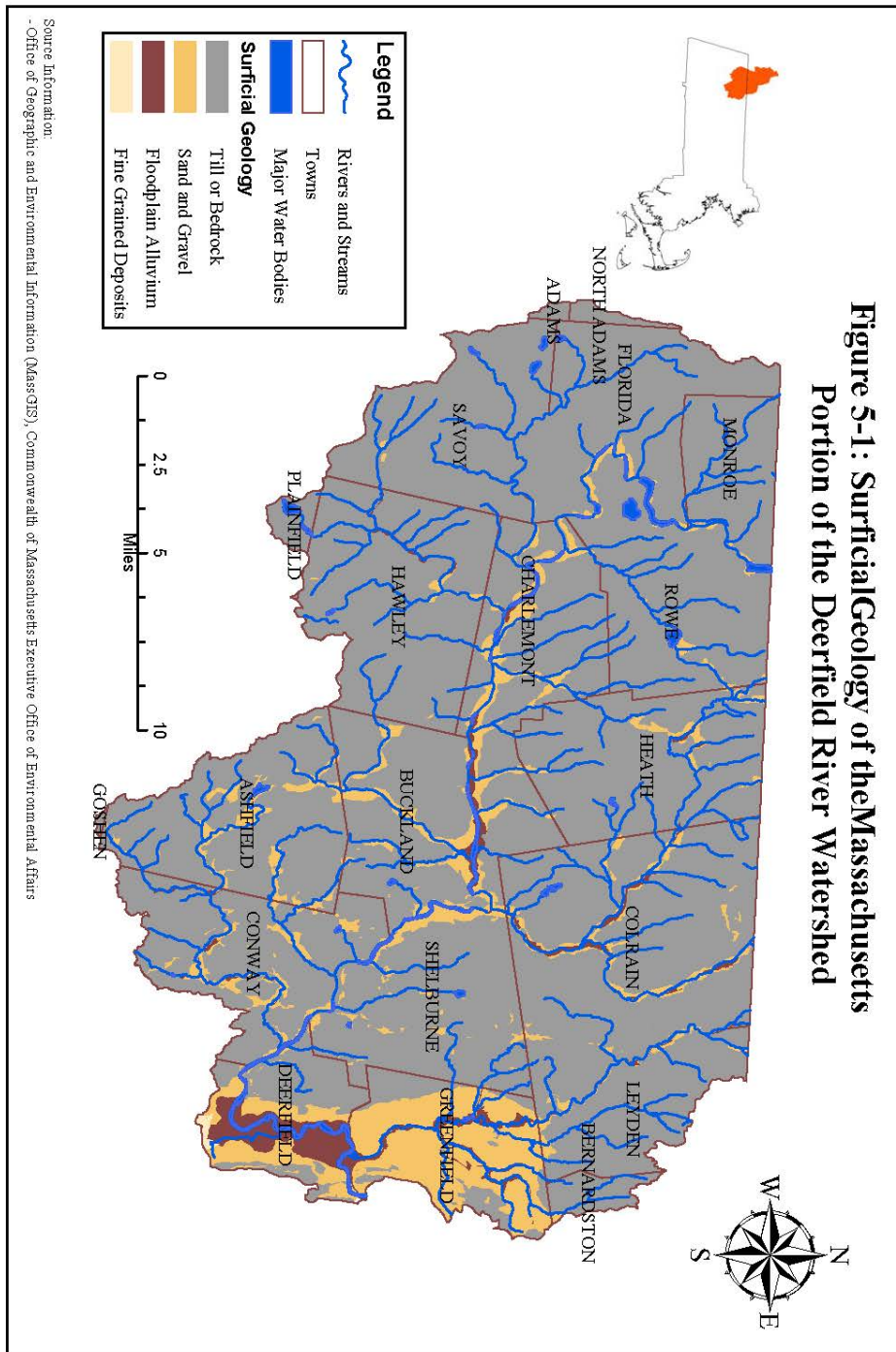
Floodplains are a key element of the fluvial system and provide a blend of ecological and cultural functions. However, active floodplains are subject to periodic inundation, and both active and former floodplains (terraces) can be subject to erosion or deposition. They begin to form along rivers that have, or had, significant sediment loads and consist of excess sediment that is temporarily stored along and over the valley bottom in segments where the sediment supply exceeds the rate of sediment transport. Floodplains seldom form along headwater streams with steep valley slopes (greater than 0.02 feet per foot [ft/ft]), nor are they common in narrow gorges that concentrate flood flows and stream power. Discontinuous floodplain "pockets" may be formed along valley bottoms with variable width on one or both sides, becoming continuous in low gradient and wide valleys. Valley slopes less than 0.001 ft/ft result in sandy flat floodplains (Jain, Fryirs, and Brierley, 2008).

Professionals have several approaches to defining and delineating floodplains. Geologists define floodplains as sedimentary deposits placed by rivers along the valley bottoms and subject to periodic inundations and reworking. Surficial geology maps that delineate glacial outwash, stratified drift, and alluvium are a watershed-wide clue to historic floodplain locations (see Figure 5-1). The famous American geologist, William Morris Davis, studied and wrote about landscape evolution long before current knowledge of tectonic uplift and plate movement. His geographical essays published in 1909 include a detailed chapter on the formation of postglacial New England floodplains and terraces long before modern hydraulic analysis of floodplains. He recognized that floodplain terraces are "river carved remnants of stratified clays, sands, or gravels that once occupied in larger volume than today the rock floored valleys of still earlier origin" (Davis, 1909, pp 516).

The USDA-NRCS County Soil Surveys provide further details on poorly drained, very poorly drained, and alluvial soils (see Franklin County Soil Survey) that are associated with flooding. The steep, narrow valleys in Vermont have few geologic floodplains while narrow geologic floodplains in Massachusetts extend from the Cold River confluence to Shelburne Falls and in the Connecticut River Valley in Deerfield, Massachusetts.

Hydrologists and hydraulic engineers define floodplains as flat and nearly flat plains subject to inundation by floods with a specific frequency of recurrence. The FEMA NFIP, FIS, refer to Flood Hazard Zones (FHZ) as a regulatory base flood that has a one percent chance of occurring each year, with a long-term statistical occurrence of once in 100 years. The FEMA FHZ is an area where hydraulic computations indicate a risk of flooding and are not limited to specific geologic formations. For example, the lower part of hillsides in a gorge may be floodprone and subject to periodic inundation but still lack a geologic floodplain or stratified drift or poorly drained soils due to scour.

**Figure 5-1: Surficial Geology of the Massachusetts
Portion of the Deerfield River Watershed**



The hydraulic-based floodplain delineations assume channels have rigid boundaries and that they are not subject to avulsions or migration. In contrast, geologic maps of floodplains track historic evidence of past scour, fill, and migration. The geologic and FEMA methods of floodplain delineation do not account for future climate change and potential future floodplain expansion or channel realignment.

Even early geologists such as Davis recognized that floodplains and terraces were dynamic features that responded to hydrologic and climate conditions. By the 1930s, it was also evident that human activities were influencing floodplains as well. The U.S. Soil Conservation Service was founded in 1935 as part of the Department of Agriculture, during the dust bowl. Its mission included control of soil erosion and selected watershed flood control. One of its first products was a detailed research project on stream and valley sedimentation including floodplains (Happ, 1940). The floodplain descriptions penned by Happ et al. are still in use today to classify floodplain deposits. The six original genetic types of deposits are listed below:

Floodplain Deposits

- Colluvium deposits
- Vertical accretion deposits
- Lateral accretion deposits
- Floodplain splay deposits
- Channel fill deposits
- Channel lag deposits

Ecological Value

Natural floodplains that are periodically inundated and subject to channel migration and avulsions are renewed by fresh sediment and grade adjustments. These dynamic processes contribute to the river corridor's habitat diversity, plants, and animals. The Deerfield River floodplains have a modified flood pulse and sediment load due to upstream dams, and the floodplains have largely been cleared. Consequently, their ecological role is also modified. The lower floodplains are frequently inundated and are often riparian wetlands. They may also have shallow groundwater, which further contributes to water-tolerant vegetation.

5.2 Flood Inundation Mapping

In 2015 following Hurricane Irene and after the first draft of this report, the USGS issued flood inundation maps for two key reaches of the Deerfield River. These excellent quality digital maps are discussed in USGS *Scientific Investigation Report 2015-5104* (Lombard and Bent, 2015) and are available on the web. The report describes the flood, and the maps depict the areas subject to inundation.

The maps are prepared using conventional hydrologic methods. New stream cross sections were surveyed. Water profiles were computed with HEC-RAS and calibrated to high water marks.

The flood limits were then plotted on LIDAR topographic maps and digitized. The resulting maps are very informative and nonregulatory. But, at the same time, they focus on areas that largely already have FEMA FIS, and they do not include any specific recommendations for flood hazard reductions.

Floodplain Services

Along the Deerfield River, from the confluence with Cold Brook in West Charlemont at mile 29 to Shelburne Falls at mile 17, there are broad floodplains and terraces used by roadways, small villages, and for agriculture. Other significant floodplains are located along the North River and its East and West Branches and where the Deerfield River crosses into the Connecticut River Valley in the town of Deerfield downstream of I-91.

Floodplains provide many essential hydrologic, ecologic, and cultural services and are a key component of our landscape. Floodplains are used extensively due to low gradients and nutrient-rich soils. Native Americans and early European colonists both used floodplains for agriculture. Today, many Deerfield River floodplains are used for corn production and cattle pastures. Many roads and railroads also use floodplains and terraces for transportation facilities.

Selected Floodplain Services and Functions

Hydrologic	Ecological	Cultural
Store sediment	Diverse habitat	Agriculture
Reduce peak flows	Rare species	Communities
Recharge groundwater	Nesting sites	Transportation routes
Convey floodwaters	Riparian wetlands	Historic sites

The Deerfield Meadows between Lower Road bridge and Route 5 are an active alluvial floodplain with rich alluvial soils, an important agricultural resource for Native Americans, early European colonists, and modern farmers. The Deerfield Meadows were discussed by Edward Hitchcock in his 1841 book *Final Report on Geology of Massachusetts*, which described alluvium up to 20 feet thick. There are four contributing geomorphic factors to this unusually large floodplain. First is the river's position lying over the earlier remnants of glacial Lake Hitchcock; second is the reduced gradient and sediment deposition as the river emerges from the deep gorge between Shelburne Falls and the former Lake Hitchcock; third is the hydraulic narrows around the north side of the trap rock Pocumtuck Mountain, which traps overbank flow on the floodplain; and forth is the reverse backwater from the Connecticut River.

5.3 High Water Marks and Historic Floods

The oldest method of delineating floodprone areas and community planning is undoubtedly the observation of actual floods and their high water marks. For example, Old Deerfield Village is carefully situated on a terrace above the elevation of most floods.

Floodplains may be identified by historic limits of inundation during great floods as recorded by news reports, photographs, elevation markers, and living memory. The high water marks, due to scour, debris, and sediment, may be plotted on topographic maps and connected along contours to determine water elevations. Flood limits are then interpreted between the high water marks to draw a flood inundation map. For example, high water marks from Hurricane Irene are still visible in the field, and many flood limits and sediment deposits are shown on Google aerial photographs taken shortly after the flood. During our fieldwork, several residents volunteered information on flood levels in Charlemont Center, Shelburne Falls, and Deerfield Meadows. Some floodplains are identified by the presence of hydrophytic vegetation, which tolerates saturated soils such as in modern soil surveys used for wetland delineation.

5.4 National Flood Insurance Program Floodplain Maps

The NFIP was established by Congress in 1968 to mitigate future flood losses. The program was advocated by geographer Dr. Gilbert White from the University of Chicago who chaired a task force on federal Flood Control Policy. It is administered by FEMA and is the nation's primary source of floodplain mapping data. A major advance in floodplain management was Executive Order 11988 in 1977, requiring federal agencies to minimize direct and indirect support of floodplain development. As part of the flood insurance program, FEMA publishes flood hazard boundary maps (FHBMs) that delineate areas subject to flooding by the 100-year frequency of recurrence base flood, which has a one percent chance each year. The maps are based on engineering studies with surveyed cross sections of the rivers, hydrology studies of peak flows (usually based upon gauging stations), and hydraulic analysis to compute floodwater profiles using one of a series of approved computer models such as HEC-2 or HEC-RAS. The computed water elevations are then plotted on topographic maps to delineate the floodplains, which become the basis of the FIRMs.

The technical "standard step" procedures for computing floodwater profiles was developed in the 1930s, and the full protocol for delineating computed floodplain boundaries was issued 30 years later (Wiitala et al., 1961).

Some early FEMA floodplain maps, plus maps in rural areas, have floodprone areas designated as "Zone A" based on approximate mapping, without detailed engineering computations. Zone A designations are based on flood history, topography, and other indirect data.

The FEMA floodplain maps have numerous limitations as summarized below:

1. They are often based upon older hydrology data prior to their publication date and, in an era of land use and climate changes, they become outdated.
2. There are no normal provisions for addressing future hydrology conditions and floodplain expansion.
3. Development is still allowed within the floodplain fringe as long as certain buildings are elevated. This encourages filling floodplains and reducing floodwater storage.
4. The NFIP does not address the ecological value of floodplains and wetlands.
5. The NFIP assumes channels and floodplains have rigid boundaries and that river dimensions are constant over time without migration or avulsion.
6. The FEMA NFIP studies identify and map flood hazards and provide recommended building and zoning criteria; they do not provide specific recommendations on reducing floodwater elevations or hazards.

In addition to mapping floodplains and predicting base floodwater elevations, FEMA studies tabulate floodway widths and the predicted flood flow velocities.

5.5 Surficial Geology Maps

Surficial geology maps that delineate broad soil groups are available for many areas of the nation and depict the generic original of earth materials. Many have been prepared by USGS and its contracts and overlie the conventional quadrangle topographic maps. The maps typically identify surface bedrock exposures, glacial till, stratified (sand and gravel) deposits, and postglacial deposits of swamps, alluvium, beaches, and artificial fill. Many earlier maps have been digitized and matched together to create large area maps (see Figure 5-1).

The stratified drift deposits are a useful guide to areas that were subject to glacial meltwater and, as such, they are more extensive than modern floodplains. The mapped alluvial soils cover a smaller area and are a subset of stratified drift, representing modern deposits that have been used to approximate current floodplains.

The mapped alluvial soil deposits in the Deerfield River basin correspond well with the FEMA mapped floodplains.

The identification of alluvium and stratified drift deposits on surficial geology maps can also be used as part of hydro-geomorphic classification systems to map both floodplains and ecological zones and their processes. Floodplain sites are mapped based upon Landform Sediment Assemblages (LSA) and related hydrology and vegetation to understand floodplain processes (Theiling et al.).

Principal sediment deposits and landforms include the following:

- Modern aquatic classes
- Active floodplain – poorly drained
- Active floodplain – well drained
- Paleo floodplain – poorly drained
- Paleo floodplain – well drained
- Natural levees
- Alluvial/colluvium aprons
- Sandy terraces

The Natural Conservancy (TNC) Active River Area (Smith, 2008) uses some elements of the LSA approach together with GIS data on saturated soils and soils to map floodplains.

5.5.1 Local Floodplain Mapping

The FEMA NFIP flood hazard maps for the various towns in the Deerfield River basin have been digitized by MMI and overlain on the GIS-based surficial geology maps in order to compare potential floodprone areas. The FEMA studies are variable; there are no studies for Monroe, Rowe, Florida, Savoy, Heath, Hawley, and Ashfield. However, all of these towns have mapped sand and gravel deposits that confirm postglacial flows and floods.

In Monroe and Rowe, there is an obviously narrow band of floodprone land along the Deerfield River, but the narrow confined valley limits the formation and width of floodplains, and there are no FEMA maps. Significant sand and gravel deposits are mapped and observed in the field along the west bank in Florida near and downstream of the tunnel, but once again, there are no FEMA flood hazard maps. In Hawley, the floodprone Chickley River is not mapped by FEMA but does have geologic mapping of both alluvium and sand and gravel. The Chickley River had high velocity erosive flood flows during Hurricane Irene with road damage.

The detailed floodplains mapped by FEMA in Deerfield, Buckland, and Charlemont agree closely with the geologic maps of alluvium while being much smaller than the mapped limits of sand and gravel. In Shelburne, no alluvium is mapped and only narrow bands of sand and gravel, which is consistent with field observations.

In Colrain, there are FEMA mapped floodplains along the North River and its West Branch, fairly similar to geologic maps of alluvium. These floodplains are used extensively for agriculture and transportation corridors and were inundated by Hurricane Irene.

Much of the town of Greenfield is mapped as having sand and gravel deposits from past glacier deposition. However, the FEMA mapped floodplain is limited, and the FEMA mapped floodplains more or less match the mapped modern alluvium. The exceptions are several small urban streams mapped by FEMA without the presence of alluvium.

The total area of the digitized FEMA 100-year frequency floodplain in the Deerfield basin is 5,906 acres while the alluvial soil area is 5,886 acres. The values are closer than the visual appearance would suggest as they are not equally distributed.

5.6 Soil Survey Data for Floodplain Mapping

An alternate method of delineating floodprone areas that have not yet been mapped by the FEMA NFIP is to use the Natural Resources Conservation Service (NRCS) soil survey maps prepared by the USDA. The original maps were assembled in county soil surveys under the National Cooperative Soil Survey programs such as the Franklin County Soil Survey. This soil information has been recompiled into a modern digital system called the "Soil Survey Geographic" (SSURGO), accessed via the Web Soil Survey (WSS) interactive maps.

Soil survey maps identify soil types overlaid on aerial photographs plus tabulate soil characteristics including their gradation, internal drainage conditions, and flood frequency conditions. Standard soil descriptions such as in the county soil surveys describe soil drainage using several descriptors including poorly drained, very poorly drained, alluvial, and peat/muck. Some areas, such as Connecticut, use soil survey maps to delineate regulated wetlands. The soil classes do not define the depth of flooding, unlike FEMA NFIP. Coulton (2014) and NRCS (Hoover and Waltman, 2013) have estimated the frequency of flooding for various soil classes as noted below:

Flooding Frequency Class	Approximate Frequency, Years	Definition
None	500	No reasonable possibility of flooding; one chance out of 500 of flooding in any year or less than 1 time in 500 years
Very rare	100 – 500	Flooding is very unlikely but is possible under extremely unusual weather conditions; less than 1 percent chance of flooding in any year or less than 1 time in 100 years but more than 1 time in 500 years
Rare	20 – 100	Flooding is unlikely but is possible under unusual weather conditions; 1 to 5 percent chance of flooding in any year or nearly 1 to 5 times in 100 years
Occasional	2 – 20	Flooding is expected infrequently under usual weather conditions; 5 to 50 percent chance of flooding in any year or 5 to 50 times in 100 years
Frequent	2	Flooding is likely to occur often under usual weather conditions; more than a 50 percent chance of flooding in any year (i.e., 50 times in 100 years) but less than a 50 percent chance of flooding in all months in any year
Very frequent	<1	Flooding is likely to occur very often under usual weather conditions; more than a 50 percent chance of flooding in all months of any year

The evidence of flooding includes a combination of surficial evidence of inundation, subsoil conditions, and remote sensing. Hoover and Waltman (2013) from the USDA National Soil Survey Center list the following characteristics:

- Actual extent of flooded area
- Flood debris and high water marks
- Aerial photographs
- Channels, oxbows, point bars, alluvial fans, meander scrolls, sloughs, natural levees, and sand plains
- Vegetation
- Soil stratigraphy
- Organic matter
- Abrupt soil layers
- Laboratory sieve tests and organic carbon

Comparisons between the FEMA NFIP flood rate maps of floodplains and the soils-based SSURGO maps have been made by the USGS (Noe, 2013) in the Chesapeake Bay region and in Indiana at Purdue University (Merwade, 2014). The USGS study concluded that the SSURGO flood frequency method can map floodplains that are not already covered by FEMA. The Purdue study prepared statewide floodplain maps and compared them to FEMA maps, where available, and was found to be a reasonable match. They offer an economical mapping process for use where FEMA maps are not available.

There are a few limitations. For glaciated areas, some floodprone areas are well drained terrace soils that do not match the SSURGO criteria for poorly drained and alluvial soils. In addition, soils-based floodplain maps do not depict the elevation of floodwater or their velocity.

Selected Floodplain Soils

The Franklin County Soil Survey (USDA, 1967) includes maps and descriptions of all soils in the county and continues to be a valuable resource. Soil maps of the Deerfield River corridor delineate glacial outwash and alluvial soils that generally correspond to floodprone lands.

In the central part of the watershed, soils along the Deerfield River are generally mapped as the Merrimac-Ondawa Association. Merrimac soils are well-drained sandy loams formed on glacial outwash terraces and plains while Ondawa soils are described as well-drained alluvial soils, typically flooded once every 1 to 5 years. Suncook and Agawam well-drained loamy sand soils are also found on bottom lands, particularly in Charlemont and Buckland, and in some places are flooded annually.

The lower watershed includes the vast Deerfield Meadows floodplain, consisting largely of the very sandy loam Hadley soils. They are deep, well-drained deposits formed of recent alluvial sediments. Local farmers mentioned that Hurricane Irene plowed new sediments, ranging from a

few inches to a few feet thick while other deposits were excavated. Poorly drained Limerick soils are mapped along riverbanks and bars.

5.7 River Corridor Floodplain Mapping

Geomorphic floodplains include land forms that have been created and shaped by fluvial processes during modern climate conditions including the active channel, floodplain, and lower terraces. The geomorphic floodplain incorporates the alluvial river meander zone across which channels have migrated and may again migrate over in the future. The location of the active river may change over time due to meander migration and avulsions, leaving floodplain features such as bars, chutes, oxbows, ridges, side channels, meander scars, backwater swamps, natural levees, and other scour or fill features.

The outer limit of the land over which the river has migrated is called the meander belt. It is assumed that over long periods of time the river may reoccupy any part of the meander belt. The meander belt widths are a function of channel characteristics (bankfull width, radius of meander curvature, meander length, etc.) plus local soils, topography, and vegetation.

Several states and nations have developed specific techniques for delineating migration zones as described below. The greatest limitation is that they are based upon the past hydrology, not the future.

Vermont Floodprone River Corridors Mapping

Several regions of the United States and Europe have adopted the delineation of floodprone river corridors to supplement traditional hydraulic-based floodplain mapping. The primary goal is to predict an active river corridor that defines potential river migration zones along unconfined channels to depict where meandering rivers may adjust their alignment. Vermont defines river corridors as an area around the present channel where fluvial erosion, channel evolution, and down valley meander migration are most likely to occur. The resulting river corridor is generally wider than conventional FEMA-designated floodplains, which are assumed to be stationary and do not allow for channel migration.

The best regional example is the *Vermont Fluvial Erosion Hazard Mapping* program (FHM). It is based upon the State of Vermont's Phase 1 and Phase 2 geomorphic assessments that use Rosgen channel classifications. The channel's bankfull width is determined, and the river is classified by type and condition. For alluvial meandering rivers, a virtual centerline is drawn through the crossover point between meander bends. Channel sensitivity ratings are then assigned by river type and condition and are used to select corresponding potential meander belt widths. The latter typically range from one to six times the equilibrium reference channel width and are drawn on a topographic map considering floodplain features. This procedure maps the probable floodprone corridor but does not provide floodwater elevations or flood risks. As with other approximate methods, it is not based upon hydrologic data and has no provisions for

climate change. It is most useful along previously channelized and straightened rivers that might return to a meandering alignment and where rivers are prone to avulsions.

For rivers that have not had formal Phase 1 or 2 assessments, Vermont uses remote sensing to delineate a meander belt width of four to six times the bankfull width, depending on slope.

5.8 Floodplain Vegetation Mapping

Ecologists map floodplains by identifying water-tolerant vegetation that is associated with periodic inundation or sustained saturated soils. The higher ends of floodplains, however, are rarely flooded and usually extend beyond the limits of hydrophytic vegetation. The USGS has issued a publication *General Classification Handbook for Floodplain Vegetation* (Dieck and Robinson, 2004) that guides the use of vegetation to delineate floodplains. Remote sensing with aerial photographs and/or ground surveys is used to identify up to 31 general vegetation classes related to the earlier Cowardin wetland classification system. The USACE protocol for mapping wetlands includes both vegetation and soil saturation among its criteria.

5.9 Floodplain Stream Power Classification

Floodplain classification and assessment is an essential step in understanding their processes and relative stability. However, none of the stream classification methods commonly used in the Northeast (Rosgen, M&B, and VTANR Assessment) includes modern quantitative procedures for floodplain evaluations and potential future conditions. Consequently, a process-based assessment is performed hereafter based upon stream power as the driving parameter. This stream power-based, process-oriented channel and floodplain analysis can be used in conjunction with geomorphic form-based systems such as that developed in Vermont to evaluate the overall stability of the meander belt.

Floodplains are divided into three broad classes representing high and medium energy (noncohesive) conditions plus low energy cohesive floodplains. High energy floodplains are generally in steeper, confined upland valleys, and their sediments are frequently subject to scour and redeposition. High energy floodplains have coarse sediments and are prone to avulsions due to new deposits.

Channel and Floodplain Energy Classification (Modified From Nansen and Croke, 1992)			
	A. High Energy	B. Medium Energy	C. Low Energy
Stream power (wm^{-2})	>300	50 – 300	<10
Accretion type	Coarse vertical	Lateral point bar or braided	Vertical fine strata
Sediment size	Coarse sand to cobbles	Sand and gravel	Cohesive, clay to sand
Dynamics	Extreme	Gradual	Slow
Flood frequency	Rare floods	1 – 5 years	1 – 5 years

Three examples of high-energy floodplains are discussed by Howard (1996). They include narrow chute-like canyons confined by bedrock walls, leaving room for only small pockets of

sediment along sheltered sections of the walls. They are bedrock systems with alluvial beds. A second type includes tributary alluvial fan canyons that discharge sediment into the main stem rivers. Vertical accretion floodplains occur in wider but moderately steep valleys; they have episodic floods that strip the floodplain surface followed by long deposition periods. They are nonequilibrium floodplains characterized by lower coarse strata overlain by finer deposits. Floodplain scour occurs in contractions and where flows leave or enter the channel. Braided streams are common.

Medium energy floodplains form primarily due to lateral accretion of point bars along sinuous channels with sand and gravel sediments. The erodible sandy sediments allow for rapid channel adjustments. Lateral channel adjustments may form and erode terraces formed of alluvial or glacial era sediments and also form low ridge and swale topography related to meander scrolls with irregular microtopography (Sear et al., 2003).

Low-energy floodplains are formed primarily by deposition of sediments during overbank flows, creating fine vertical strata of sand, silt, and clay. They may be frequently inundated, but their low stream power results in slow adjustments. Many have cohesive soils and vegetated banks that resist erosion, so channel migration rates are low. Their natural state is usually forested due to nutrient-rich sediments and high moisture content, but many were converted to agriculture or developed. Some low-energy floodplains are now isolated by levees.

The three broad floodplain energy classes noted above are further divided into sub units by geomorphic processes plus the degree of valley confinement, creating a total of 15 sub types (Nanson and Croke, 1992).

Floodplain Type	Unit Stream Power, (w/m²)	Comments
A1	>1,000	Confined coarse floodplain, steep, straight
A2	300-1,000	Confined vertical accretion, uplands
A3	300-600	Unconfined vertical accretion, sandy, flat
A4	±300	Cut and fill sandy floodplains, flat, straight
B1	50-300	Coarse braided rivers, high sediment loads
B2	30-200	Wandering gravel or sand bed rivers, high loads
B3	10-60	Lateral migrating meandering rivers, cut banks
B3a	10-60	Lateral migrating meanders, with scrolls
B3b	10-60	Lateral migrating sandy meanders with scrolls
B3c	10-60	Lateral migratory sandy rivers, back swamps
B3d	10-60	Lateral migratory, silty sand, point bars
C1	<10	Low gradient, silty, laterally stable
C2	<10	Anastomosing, sand and gravel, flat and wide
C2a	<10	Anastomosing, sand and gravel and organics, humid
C2b	<10	Anastomosing, sand and gravel, semi-arid

River Styles (Brierley and Fryirs, 2005) use a similar system to ongoing floodplain types in confined, semiconfined, and unconfined valleys with correlating stream power.

Other metrics used to classify and describe floodplains can be divided into three groups that define hydraulic, geomorphic, and biological characteristics.

Floodplain Classification Metrics		
Hydraulic	Geomorphic	Biologic
Bankfull frequency	Channel pattern	Hydrophytic species
Inundation frequency	Slope	Soil saturation
Stream power	Confinement	Communities
Flood conveyance	Sediment type	Diversity
Floodwater storage	Deposition type	Maturity
Aquifer recharge	Backwater swamps/meander belts	Seed disposal and germination Fish spawning/nutrient exchange

5.9.1 Charlemont Floodplain

Channel segment 11 from Cold River to the Route 8A bridge has continuous floodplain, first on the right bank at a campground and past the Route 2 bridge. The floodplain then continues along the left side of the valley where Route 2 is located.

The specific bankfull stream power in the upstream segment 11 is 165 w/m². Moderate instability can be expected. This higher value is consistent with field evidence of floodplain side channels and coarse riffle substrates and the large island below the Chickley River. The heavy sediment load is due to Cold River and Chickley River, both of which are degrading, exporting sediment, and have large confluence bars. Increasing flows will increase instability.

5.9.2 Charlemont Channel and Floodplain Stability, Segment 12

The long channel segment from the Route 8 bridge in Charlemont to the Dam #4 reservoir is a critical resource due to the community infrastructure, school, wastewater treatment plant, and the parallel Route 2. The left riverbank has a long but discontinuous series of pocket floodplains used by the community. Several farms are located along the left bank terraces. This segment was inspected both by foot and a canoe trip and was found to have virtually no bank erosion combined with deposition on the floodplains and new confluence bars at the tributaries. This floodplain is mapped by FEMA and is also delineated as sand and gravel soils on surficial geology maps.

Measured bankfull channel widths ranged from 195 feet to 260 feet, narrowing prior to the island deposit near the Crab Apple rest area. The regional hydraulic geometry database used for the regression equation does not cover this size watershed but, by assuming it is still valid, leads to a predicted width of 169 feet. The channel bankfull channel width was also predicted with a Lacey-type regime equation, yielding a bankfull width of 212 feet. This comparison suggests the

channel has excessive width, which is consistent with the minimal erosion during Hurricane Irene. The overbank floodplain is up to 500 feet wide.

A sediment transport-based optimization model was also used to predict channel characteristics based on discharge rates and sediment sizes as measured with a pebble count. The "Sediment Analysis Model" predicted the channel slope well, with an optimum bankfull width of 143 feet and a possibility of aggradation.

The specific stream power for the Charlemont segment (12) has been computed using the 2-year frequency flood as determined from the MMI analysis of USGS gauge data. This hydrology value of 10,943 cfs is much higher than the regional regression data for bankfull discharges. The resulting specific stream power is 79 w/m². This is a modest level that River Styles, literature searches, and MMI projects indicate as corresponding to moderately active meandering rivers. The segment 12 floodplain is a Nanson and Croke type B2.

In conclusion, this important channel segment is forecast to be stable despite rare inundation. The channel is overly large, and the floodplain is subject to mild deposition.

5.9.3 Deerfield Meadows Channel and Floodplain Stability, Segment 17

The Deerfield River has an unconfined alluvial gravel bed channel and broad depositional floodplain from the Lower Road bridge (near I-91) to the Route 5 bridge. This 6-mile-long segment has a Rosgen type C4 gravel bed meandering channel, steep banks, and an adjacent flat floodplain that is used for extensive agriculture. The floodplain was inundated during Hurricane Irene and covered with a layer of fresh, light-colored silty sand sediment ranging from a few inches to several feet thick. Fortunately, there have been no observed avulsions or significant meander migration due to this flood.

The current floodplain surface is built primarily by vertical accretion, though several old oxbows and meander scrolls attest to previous lateral channel adjustments and previous channels that must have filled in.

The measured bankfull channel widths vary from 170 feet to 250 feet with a typical bankfull depth of 12.5 feet. In comparison, the bankfull width computed with the USGS regional regression equations is 207 feet, and the predicted regime width is 257 feet using the Lacey-type equation. This consistency suggests the channel is in a well-balanced equilibrium.

The computed SSP in Deerfield River segment 17 is 65 watts per square meter for the 2-year frequency flood and bankfull width. This is within the range for stable meandering sand and gravel bed rivers with modest erosive forces. For the 100-year frequency flood, the cross-sectional average SSP is just 47 due to its great width, which is consistent with the silty sand deposition. The risk of avulsion is minimal. Based upon the Nanson and Croke classification, this is a stable type B3 floodplain.

Historic Note

The 1841 Agricultural Report of Franklin County (Coleman, 1841) describes the Deerfield Meadows as consisting of 3,000 acres, with "soils composed of fine sand and much vegetable (organic) matter, being the washings of nearby hills and deposits from the occasional overflowing of the banks which gives its strong consistency." "The meadows are overflowed, in some cases, more than once a year." "The outlet being small in proportion to the amount of water collected on the meadows to be discharge, a sort of lake is formed at times... and the enriching matter held in suspension by the waters are gradually made and to a large amount."

Coleman (1841) then describes the Green River Valley as being "alluvial, but only small portions of it are now overflowed by the stream, and there is every reason to believe that this valley and the Deerfield Valley were at one time the sites of lakes, and their richness is owing to the deposits brought from neighboring hills and mountains by various streams." The Deerfield Meadows were described as producing outstanding crops of hay and corn, which is still true.

5.9.4 Delta

Unlike the nearby Westfield River, the Deerfield River does not have a distinct fluvial delta where it enters into the Connecticut River. Presumably, this is because the large Deerfield Meadows upstream of the confluence serve as a low gradient, low power sediment deposition area, and the Connecticut River must have enough power to convey whatever sediment that gets past the meadows.

5.10 Floodplain Adjustments

None of the empirical floodplain mapping and management methods mentioned above address the likelihood of channel or floodplain adjustments occurring. Channel adjustments may be as basic as channel widening or degradation along the present alignment or as complex as meander migration and avulsions across floodplains. Channel adjustments are normally studied with detailed geomorphic assessments of historic conditions and trends and engineering hydraulics. For this project, we use a large-scale screening process to predict potential channel adjustments using the River Styles concept (Brierley and Fryirs, 2005) and stream power.

The primary floodplain adjustment observed along the Deerfield River consists of overbank sediment deposition in segments 12, 13, and 17. The regulated flood flows reduce the chance of channel migration and avulsions.

5.11 Floodplain Summary

The Vermont segment of the Deerfield River does not have any significant geologic floodplains although some areas of the East Branch are floodprone. The Massachusetts segment has three significant floodplain segments, and all are stable.

The primary American floodplain mapping and regulatory approach is the FEMA NFIP. However, many rivers in the Deerfield watershed are not mapped by FEMA, presumably due to their rural nature and the high cost of engineered FEMA studies. Unmapped floodplains that lack basic land use planning are a disaster waiting to happen. Consequently, there is reason to consider alternate low budget approaches to identification of floodprone areas. Alternate floodplain mapping would be helpful in the absence of FEMA studies. They provide low cost planning, anticipate climate change, and consider ecological conditions.

Specific methods that have been mentioned include use of high water marks, existing maps of stratified drift deposits, NRCS soil maps, vegetation, and geomorphic delineation of active areas.

Summary of Floodplain Assessment Methods

Feature	High Water Marks	Computed Water Profile	Geologic Maps	SSURGO	VT Geomorphic	Stream Power
Floodplain delineation	Yes	Yes	Yes	Yes	No	No
National database	No	No	Yes	Yes	No	No
Science basis	Historic Data	Hydraulic Computations	Geologic Deposits	Soil Formation	Historic data	Yes
Need hydrology	Helpful	Yes	No	No	No	Yes
Climate change adaptable	No	Yes	No	No	No	Yes
Floodwater elevations	Yes	Yes	No	No	No	No
Bridges and culverts	Yes	Yes	No	No	No	No
Flow velocity	No	Yes	No	No	No	No
Scour analysis	No	Yes	No	No	No	Yes
Mapping cost	Moderate	High	Low	Low	Low	Medium
Meander belt	Helps	No	Yes	No	Yes	No

Deerfield Floodplain Classification

The Deerfield River floodplains have been classified based on their quantified stream power energy levels and subjectively rated for their sensitivity to floods.

Floodplain Segment	Energy Classification	Flood Sensitivity
11	B2 medium	Moderate
12	B3B medium	Moderate
17	B3D medium	Low

Based upon the stream power analysis and field inspections, the three significant alluvial floodplains are relatively stable. This is verified by their performance during the recent Hurricane Irene flood event when all three floodplains were overtopped and were prone to overbank deposition.

However, significant geomorphic activity did occur at several confined tributary segments including Deerfield River at Zoar Gap, Cold River, Chickley River, the West Branch of North River, and short sections of South River.

6.0 MANAGEMENT ISSUES

6.1 Introduction

The Deerfield River has a complex watershed that raises the classic question of what is a natural river. Many people consider it to be a great natural resource and appreciate using it for recreation, including whitewater boating and fishing, plus riverside activities such as camping, hiking, and scenic drives. The river also is known for providing numerous services including hydroelectric power, formerly hydromechanical power, water supply, and flood attenuation.

But some river attributes are far from natural. The store, retain, and release operational mode of the hydroelectric facilities drastically alters the river hydrology on both a seasonal and daily basis. The off-site generating stations are up to several miles downstream of the corresponding dams, leading to long "bypass" segments with little flow, and none of the dams have fish passage facilities.

Summary of Hydrologic Findings

1. The Deerfield River is generally confined by bedrock valleys in Vermont and portions of its Massachusetts segments and is semiconfined with small or discontinuous floodplains from the Cold River confluence to Shelburne Falls.
2. The only significant unconfined alluvial floodplains along the main Deerfield River are the North and South Meadows in the town of Deerfield from Lower Road bridge to the Route 5 bridge.
3. The FEMA FIS cover only portions of the main Deerfield River channel including the town of Deerfield and from Cold River to Shelburne Falls and portions of some tributaries. The hydrology data used for the FEMA regulatory base flood is outdated and lower than our analysis of USGS gauges data and should not be used for design of infrastructure. The FEMA FIS should be updated.
4. The channel-forming discharges (1.1- to 2.0-year floods) as determined at the USGS gauges are much higher than the statewide regression equation bankfull discharges. In the steep Deerfield watershed, the Jacobs (2010) regression equation for peak flows performs better than the Bent (2013) equation.
5. The generic "geologic floodplains" along the Deerfield River are limited, generally agreeing with the location of FEMA FHAs.
6. The measured bankfull channel widths are greater than the Massachusetts regional regression equation bankfull widths. Regime equations provide improved predictions.

7. An analytical stream power review of the Deerfield River floodplains in the Shelburne and Deerfield Meadows segments indicates they are stable and not very prone to avulsion. During Hurricane Irene, there were deposition zones. However, several confined channel sections at Zoar Gap and along tributaries have high stream power and had severe erosion during Hurricane Irene in August 2011.
8. Floodplains should be mapped in all developed areas along the river. Where FEMA FIS cannot be prepared in the near future, approximate methods could be used in the interim.

6.2 Regulated Flows

The Deerfield River flow rates are regulated by a series of hydroelectric dams and generating facilities. There is a flow release agreement. The low-flow release of 125 cfs is insufficient for whitewater boating. Its ecological impact is unknown.

6.3 Bypass Segments

Several dams along the Deerfield River have generating powerhouses that are located well downstream of the dam in order to maximize the applied head at the turbine. The total head available to spin the turbine and generate power is the sum of the dam's height plus the river gradient from the dam to the powerhouse. This is an effective system for use on steep channels.

Dams are connected to the off-site powerhouses by either diverting water from the river to a penstock pipe (as at Searsburg Dam) or an open channel (as at Monroe #5 Dam). The flow diversion reduces or virtually eliminates flow in the river channel, called the bypass segment, between the dam and powerhouse. The flow rates in bypass segments are highly variable depending upon flow agreements, the time of day, and whether the reservoir is full and spilling water.

Bypass segments usually have poor habitat and recreational value due to dry channels or shallow flow with periodic pulses of water when release is made. It has become common practice for the FERC to negotiate and stipulate bypass segment flows as part of the overall flow management at hydroelectric dams. It is our understanding that the present release conditions were negotiated with New England Power, the former owner of most dams, and includes recreational considerations.

6.4 Fish Passage

Under natural conditions, the Deerfield River and its tributaries have coarse gravel beds, ample flow, and moderate to steep gradients that are ideal for cold-water fisheries. The Deerfield River is also tributary to the Connecticut River, which supports several species of anadromous fish that spend their adult years in the ocean but migrate to fresh water to spawn. The natural bedrock falls at Shelburne Falls would prevent migration beyond that point at river mile 17.0.

Dams and some culverts are obstacles to both fresh water and anadromous fish passage in the upstream direction and increase fish mortality in the downstream direction. While modern dams are often equipped with fish ladders or fish bypass channels, neither were common practice at the era when the lower Deerfield dams were built in the early 20th Century, and none are able to provide upstream passage to Shelburne Falls. It is noted that there is only 3.8 miles of the Deerfield River and no major tributaries between the block at Dam #2 and the natural block at Shelburne Falls.

The federal government has withdrawn its support of the salmon restoration program, but limited state efforts continue. Wild salmon spawning attempts were recently observed in the Farmington River. Facilities to aid downstream passage includes fishways, sluice gates, modified trash racks and booms, bar racks, and monitoring. Monitoring efforts have included radio tags and computational fluid dynamics (CFD) modeling.

The dams between Shelburne Falls and the Connecticut River are reportedly equipped to aid the downstream passage of stocked salmon smolts. Salmon presence below the most downstream dam is monitored to determine if they are attempting to use the Deerfield River. There is no known monitoring of other migratory species including American shad, herring, or eels.

6.5 Recreation

The middle section of the Deerfield River is a popular whitewater boating area that is also scenic and has great fishing. Water recreation is enhanced by a 1994 agreement with the hydropower industry to have scheduled water releases that enable optimum conditions. Water release schedules are on the web and available from local outfitters. The primary kayak runs are summarized below:

From	To	Length, Miles	Average Slope, FPM	Class
1. Monroe Bridge Dam #5	Dunbar Picnic Area/Fife Reservoir	2.65	78	III-IV
2. Fife Brook Dam	Zoar Gap/River Road	5	25	II-III
3. Zoar Gap	Shunpike Rest Area, Route 2	2.5		I-II
4. Shunpike Rest Area	Buckland Boat Ramp	7		I-II

Several websites provide further information on recreational opportunities (Deerfield River Whitewater Association, American Whitewater, local outfitters).

Some of the hydropower impoundments have lakeside picnic areas, hiking trails, and boat launches. They provide popular public access points, which were well maintained during site visits. Numerous out-of-state license plates were observed, confirming tourist use.

The Green Mountain State Forest in Vermont and the Mohawk Trail, Savoy Mountain, and Monroe State Forests in Massachusetts provide hiking trails. Campgrounds and picnic areas along the Cold River were noted as receiving extensive usage.

6.6 Floodplain Mapping

The FEMA FIS and FIRMs in the Deerfield River and tributaries date from the early 1980s and only cover developed areas. They do not provide current land use and flood risk guidance. The peak flood flow rates used in the FIS are generally lower than predicted by current USGS gauging station data and will underestimate floodplain boundaries. Geologic maps of alluvial soil deposits appear to correlate well with the FEMA maps and could be used to predict flood hazards in areas not yet studied by FEMA.

6.7 Conclusion

The Deerfield River is in good condition despite extensive hydromodifications and recent floods and supports a variety of users.

It is our understanding that the dams are being operated in accordance with their FERC licenses and state permits. It also appears, from informal conversations along the river, that many river users have adjusted to the operational conditions and take advantage of the scheduled flow releases, relieving potential tension between the parties. Many people have been observed using the provided (but still limited) recreational facilities for boating, fishing, and picnicking. In conclusion, an uneasy balance appears to have been made between naturalness and ecosystem services.

The hydroelectric dams help to dampen peak-flow rates, and the damages during Hurricane Irene were an unusual exception. Narrow, steep-sided valleys extend from the Vermont headwaters to the confluence of Cold River in Florida, limiting floodplain development and consequential damages. There are flood hazards associated with transportation facilities (highways and bridges) and selected villages such as Colrain Center on North River, Charlemont, and Shelburne Falls. The lower, broad floodplains in Charlemont and Deerfield have extensive agricultural uses, which are appropriate for floodplains. Floodplain land use regulations and FEMA standards must be enforced.

7.0 CULVERT AND BRIDGE VULNERABILITY ANALYSIS

7.1 Introduction

This protocol to screen bridges and culverts for vulnerability of failure moves beyond the conventional visual inspection and channel classification to include a geomorphic engineering analysis to predict channel and structure stability. The screen considers geophysical valley setting by inclusion of specific stream power and bed resistance. This work builds on past geomorphic compatibility screens (e.g., Schiff et al., 2008).

This project was a collaboration between the University of Massachusetts (UMass), Massachusetts Department of Transportation (MassDOT), Trout Unlimited (TU), and Milone & MacBroom, Inc. (MMI) (Table 7-1).

**TABLE 7-1
Vulnerability Analysis Project Team**

Project Team Member	Project Role
University of Massachusetts (UMass)	Project lead, task review, data collection, data analysis review, relate geomorphic vulnerability to other aspects of culvert screening
Massachusetts Department of Transportation (MassDOT)	Manage bridges and culverts on state highway system, data collection, original screen to build upon
Trout Unlimited (TU)	Data collection
Milone & MacBroom, Inc. MMI)	Method development, data collection, data analysis, reporting

7.2 Methods

7.2.1 Data Collection Form Development

MMI developed a field data collection form to access relevant data previously collected by TU that would be useful to have in the field and to provide a location for recording field observations. Existing data spreadsheets provided by the project team were retained in their original format, and a new spreadsheet was made that accessed existing data using CAPS ID as the unique identifier. Existing data placed on the field data form included identification information such as CAPS ID, XYcode, Culvert ID, stream name, road name, descriptive location, and latitude and longitude. Information about the structure such as number of culvert cells, culvert shape, width, height, and length; culvert slope relative to channel slope; culvert width as percent of bankfull channel width; culvert alignment with channel; selection criteria for field assessment; and past observations and damage were also included. Stream data such as drainage area, channel bankfull width, upstream channel slope, estimated bankfull flow, SSP, D₅₀, and upstream and downstream channel substrate were also placed on the form. The reverse side of the form included blank fields for data to be collected during each assessment.

7.2.2 Data Collection

MMI selected 200 bridges and culverts for field assessment in the Deerfield River watershed, yet only ultimately 197 structures were assessed due to missing existing information. Structures were selected for field assessment if they were reported or observed to be damaged in previous assessments by MassDOT, TU, or MMI. Structures with past damages were assigned a code by the towns to indicate the type of the problem (Table 7-2). Other structures were included that could potentially be damaged based on SSP derived from GIS analysis in conjunction with stream bed dominant particle size.

**TABLE 7-2
Structure Damage Codes**

O	Overtopping
E	Embankment Failed
B	Blocked by Debris
S	Structural Failure
W	Washed Out
F	Roadway Flooding
L	Fluvial Erosion
*	Repeated Failures

Structures selected for assessment were located in the field using field maps developed by MMI and the existing location data. Once located, existing data were used to confirm the identity of the structure to be assessed. During each assessment, MMI measured the structure inlet width and height, structure length and slope, channel bankfull width, and local channel slope upstream and downstream of the structure. Local channel slope, structure slope, and measurements too large to make with a folding survey rod were made using a laser rangefinder (Laser Technology, Inc.; Truepulse 360 Model; Centennial, CO; Accuracy: Inclination ± 0.25 degrees = $\pm 0.4\%$ = ± 0.004 ft/ft; Distance ± 1 foot for a reflective target, and ± 3 feet for a poorly reflecting target). Pebble counts (Wolman, 1954) were performed at any structure lacking existing median grain size (D_{50}) data using the size bins previously established by TU and UMass. Qualitative observations were made in the vicinity of the structure on dominant particle size, channel bedforms, hydraulic features, stream channel geomorphic type, and channel stability.

7.2.3 Data Analysis

Field data collected by MMI were compared to previously collected field data, regression data, and GIS-derived data to investigate relationships.

The 51 bridges and culverts identified as damaged either during MMI's field assessments or in prior assessments were analyzed in order to identify patterns in structure vulnerability.

Comparable data from different sources (e.g., field-measured bankfull channel width and regime equation-derived bankfull channel width) were plotted to determine how similar the data were.

To develop the vulnerability screen, plots comparing damaged and nondamaged structures were assembled. Data were plotted as a function of ranges of SSP to see how this variable was linked to damages. Data points were often labeled with a third variable (e.g., percent bankfull channel width, dominant particle size, slope) to explore the relationship between several variables and damages.

7.2.4 Vulnerability Screen

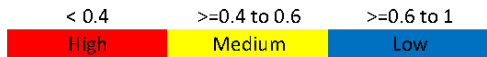
A vulnerability screen was developed to predict the potential for structure damage for the Deerfield River watershed. The final screen used the field data to refine the screen presented in our project proposal that was based on past screening work in the region, our geomorphic understanding of the Deerfield River watershed, and literature (e.g., Nanson and Croke, 1992; Knighton, 1999). An improvement from our previous screens that used SSP as a vulnerability indicator was to incorporate a variable for bed resistance to represent both sides of the balance between water and sediment (Lane, 1955) in the screen.

Variables were selected for inclusion in the vulnerability screen that tracked structure damage (Figure 7-1). Variables included in the screen were the following:

1. Specific stream power versus bed resistance: using dominant bed particle size as a proxy for bed resistance
2. Structure width = structure width/channel bankfull width (%)
3. Structure slope = local channel slope - structure slope (foot/foot)
4. Sediment continuity: based on upstream and downstream bed sediment observations
5. Structure alignment: based on structure alignment to flow in the channel

Variables with quantitative data were scored from 0 to 4 for each variable, with 0 being the most vulnerable and 4 being the least vulnerable. Variables with qualitative observational data were scored over the range of 1 to 3 due to a lower level of detail and consistency in this information. Variable scores were summed (total possible score of 18) and then normalized onto a 0 (most vulnerable) to 1 (least vulnerable) scale to match other components of the overall Deerfield River watershed project. Structures were assigned a vulnerability category of red (high vulnerability), yellow (medium vulnerability), or blue (least vulnerability).

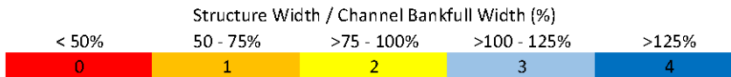
Vulnerability Score



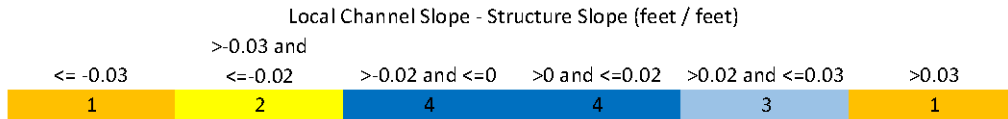
Specific Stream Power versus Bed Resistance

Specific Stream Power (W/m ²)	Dominant Particle Size (Bed Resistance)					
	Silt	Sand	Gravel	Cobble	Boulder	Bedrock
0-60	3	3	2	3	4	4
60-100	3	3	0	1	3	3
100-300	3	2	0	0	2	2
300+	2	1	0	0	1	2

Structure Width



Change in Slope



Sediment Continuity

Upstream Bed		Downstream Bed		
		Erosion	None	Aggradation
Upstream Bed	Aggradation	1	2	3
	None	2	3	3
	Erosion	3	3	3

Structure Alignment



Legend



Figure 7-1: Vulnerability Screen Variable Scoring

7.3 Results

7.3.1 The Vulnerability Screen

Results from the vulnerability screen showed an increase in the damaged structures as the vulnerability level increased as indicated by the percent of documented damages of the 197 assessed culverts in each vulnerability category (Figure 7-2). For example, 41% of the structures found to have high vulnerability were known to be damaged.

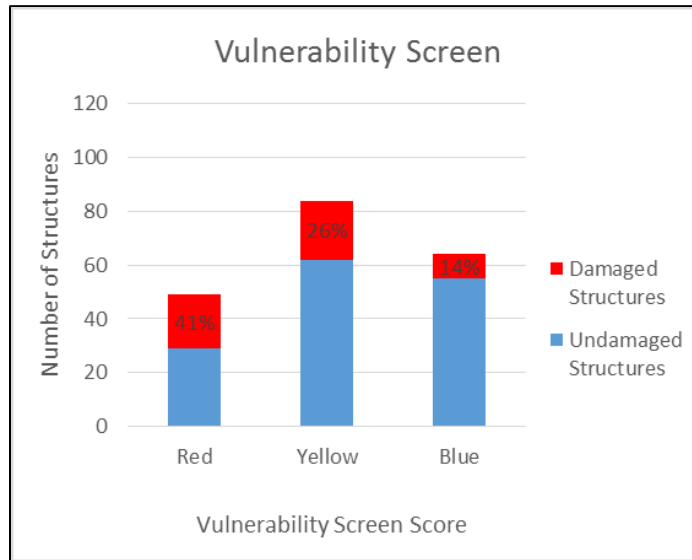


Figure 7-2: Overall Vulnerability Screen Results

The vulnerability score for each of the assessed culverts is illustrated on a large-format map showing SSP, roads, and structure damage (Attachment 1). The map shows some concentrations of vulnerability in areas where structure damages have taken place (e.g., tributaries of the Green River in Leyden and Colrain) and some areas where vulnerability is low and damages have not occurred (e.g., tributaries of the Deerfield River in Deerfield).

By design, the individual variables used in the screen tend to show a higher percentage of damages at assessed structures that received a high vulnerability (Figures 7-3 to 7-7). These variables and the overall vulnerability screen were developed based on the results of the data analysis that follow.

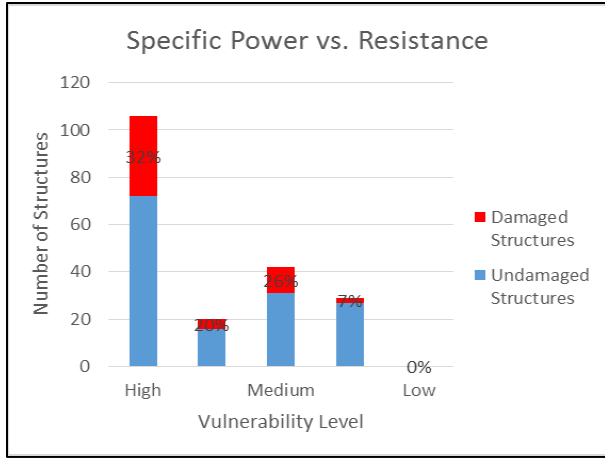


Figure 7-3: Specific Stream Power vs. Resistance Results

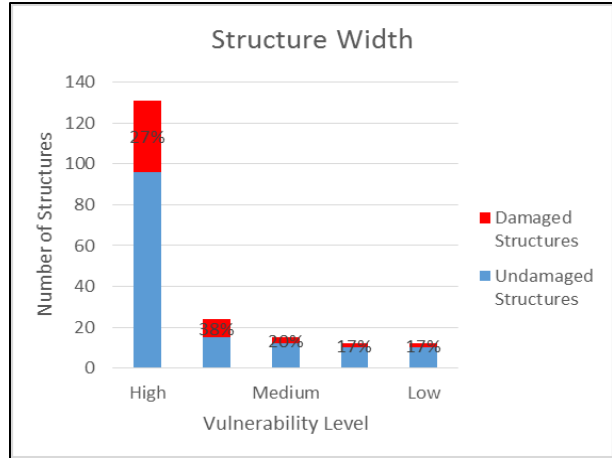


Figure 7-4: Structure Width Results

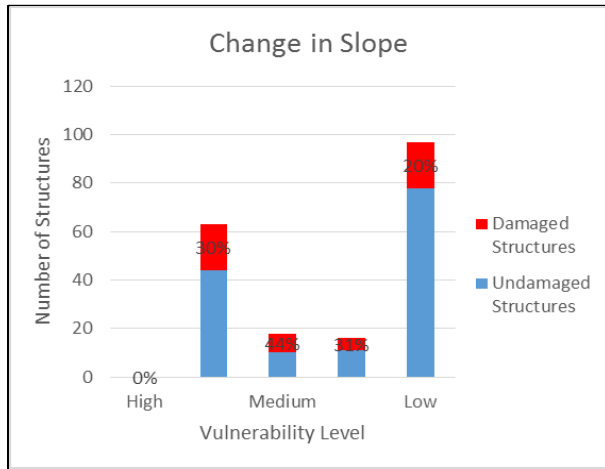


Figure 7-5: Change in Slope Results

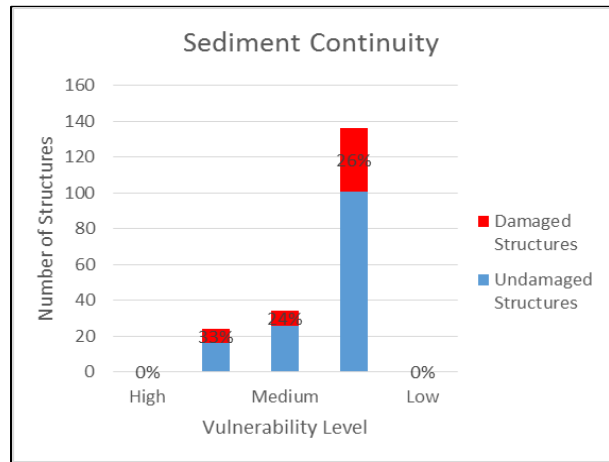


Figure 7-6: Sediment Continuity Results

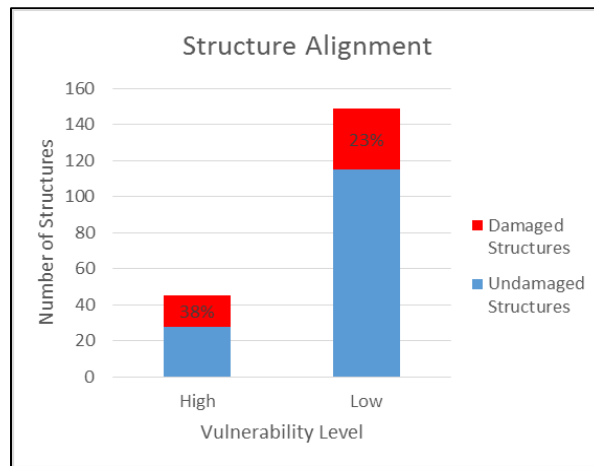


Figure 7-7: Structure Alignment Results

7.3.2 Specific Stream Power

GIS-derived SSP was compared to SSP calculated from using bankfull channel width and slope measured in the field. The data show that on average the two measurements track each other, yet the relationship is marked by variability (Figure 7-8).

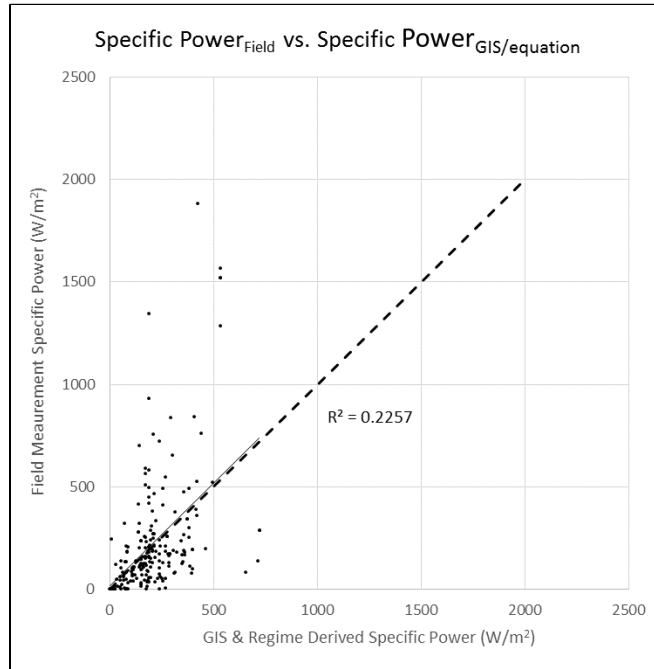


Figure 7-8: Specific Stream Power Comparison

SSP derived from GIS and regime equations was used in the data analysis due to the original findings indicating the reach slope was more appropriate for power calculations and that the regime hydrology equations accurately reflected field measurements (see Sections 7.3.8 and 7.3.9).

Bridges and culverts with observed damages tended to have SSP between 60 and 300 W/m^2 , with a moderate amount of damaged structures with specific power greater than 300 W/m^2 but less than 600 W/m^2 . Only three structures with specific power less than 60 W/m^2 were identified as damaged. Only one structure with specific power greater than 600 W/m^2 was identified as damaged (Figure 7-9).

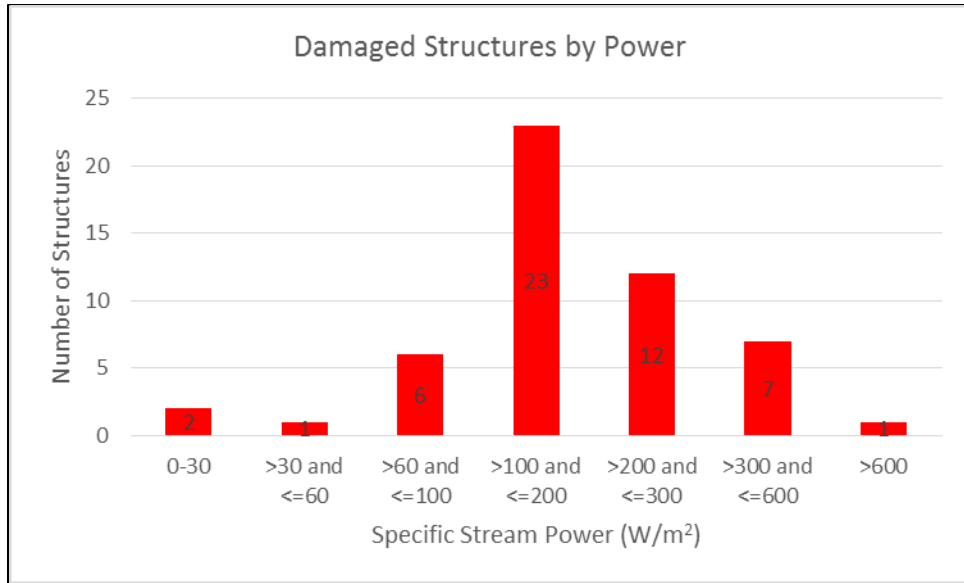


Figure 7-9: Number of Damaged Structures by Specific Stream Power

Field assessed structures were not divided evenly between SSP classes. The distribution of the percentage of structures damaged matches the distribution of the number of damaged structures that are centered on the 60 to 300 W/m² range. On low order streams, the observed concentration of damages over the SSP range of 60 to 300 W/m² is even more evident (Figure 7-10).

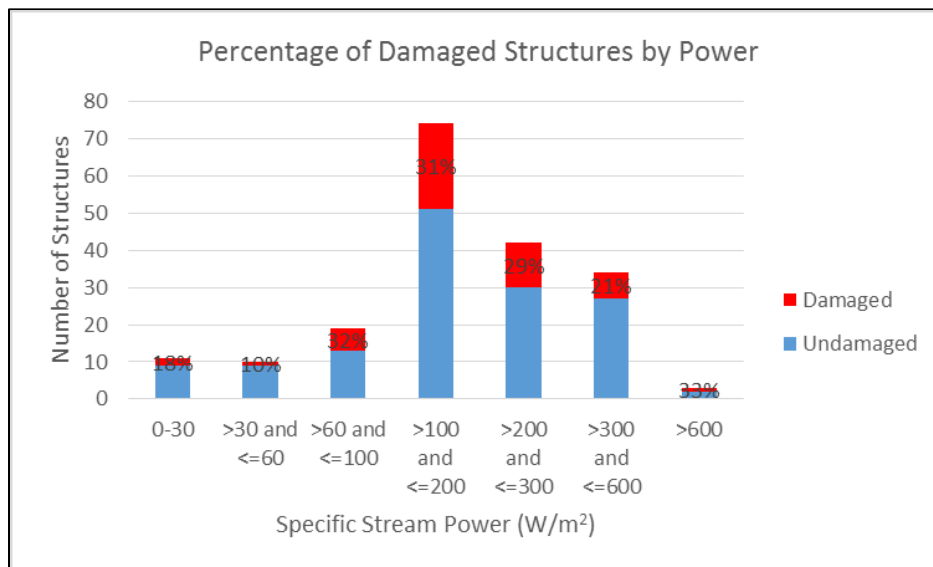


Figure 7-10: Percentage of Damaged Structures by Specific Stream Power

7.3.3 Dominant Bed Particle Size (Indicative of Resistance to Erosion)

The highest number of damaged structures and the highest percentage of assessed damaged structures are located in streams with local bed sediment sizes dominated by gravel and cobble (Figure 7-11).

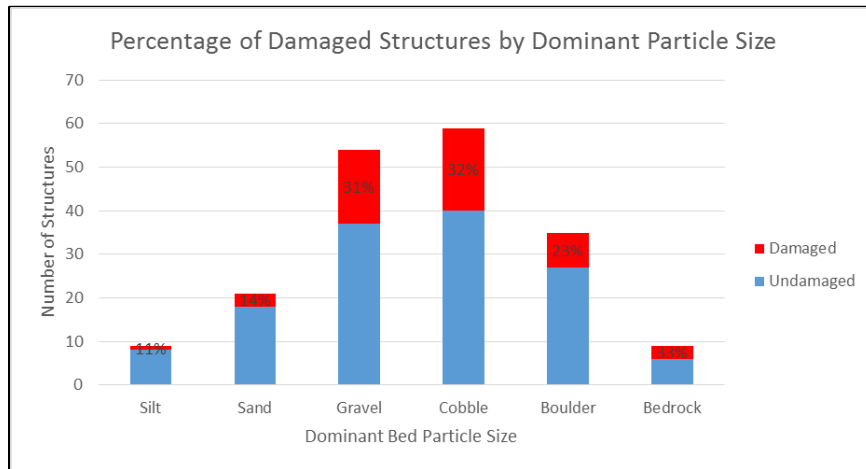


Figure 7-11: Percent of Damaged Structures by Dominant Bed Particle Size

7.3.4 Power and Resistance

SSP tended to increase with dominant bed particle size (indicative of resistance to erosion). Structures in cobble and boulder tended to have the highest power while gravel and cobble bed channels tended to have a wider range of specific power (Figure 7-12).

It is assumed that silt and sand is less commonly found in higher powered streams because it is eroded and not sustainable.

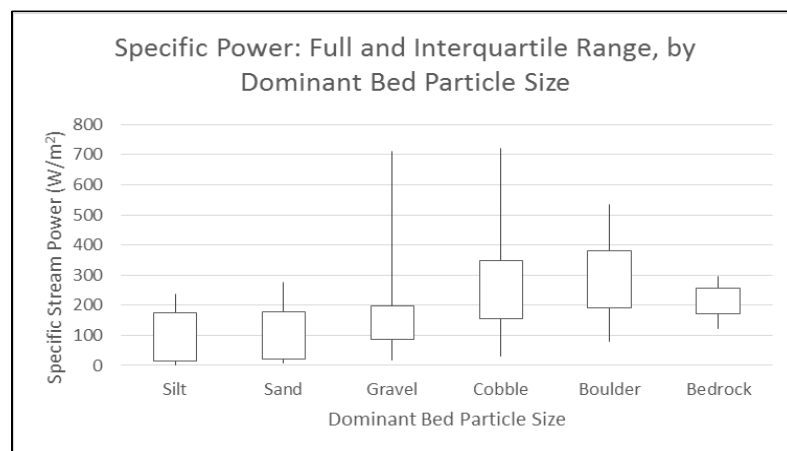


Figure 7-12: Specific Stream Power Full and Interquartile Range by Dominant Bed Particle Size

In gravel, cobble, and bedrock channels, damaged structures tended to fall in the 60 to 300 W/m² range (Figures 7-13 and 7-14).

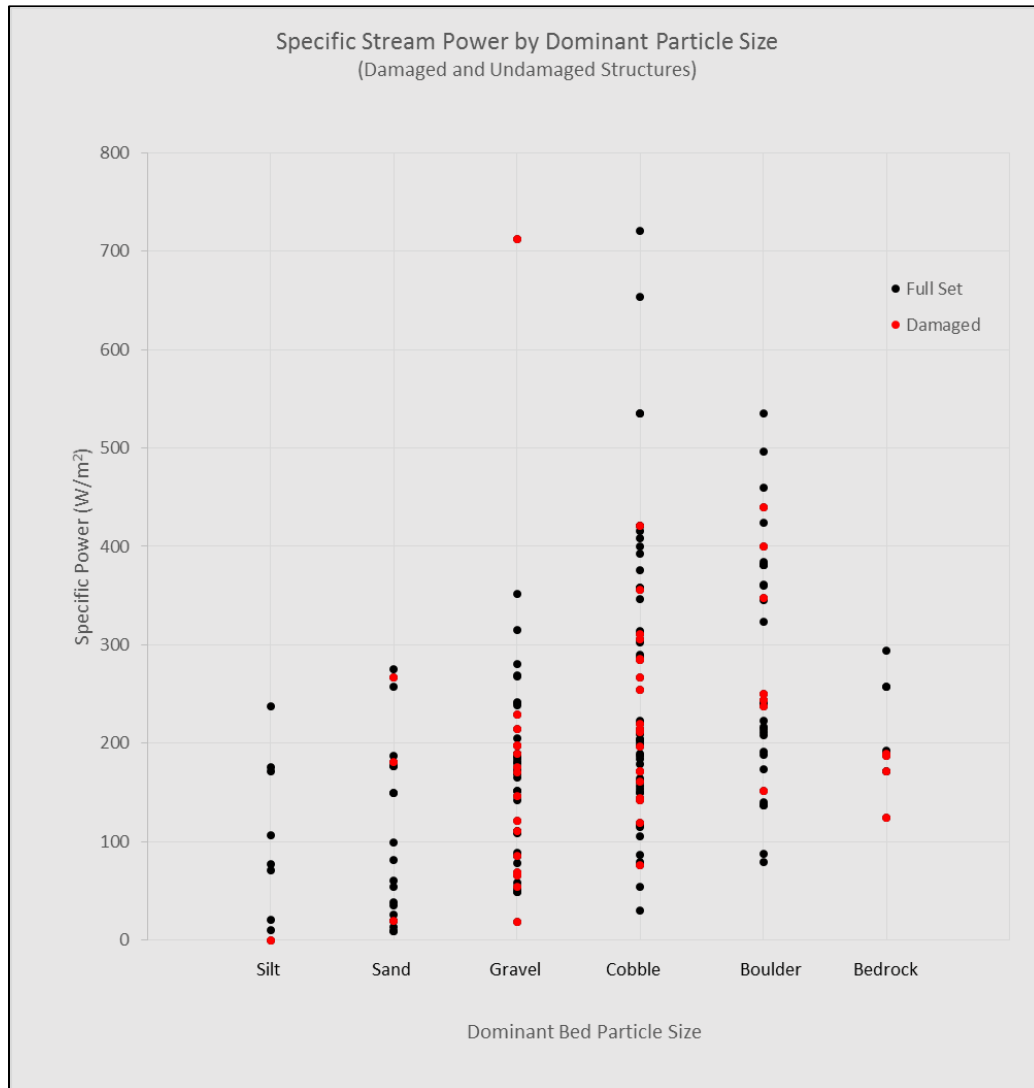


Figure 7-13: Specific Stream Power vs. Dominant Bed Particle Size, Data Colored by Damage

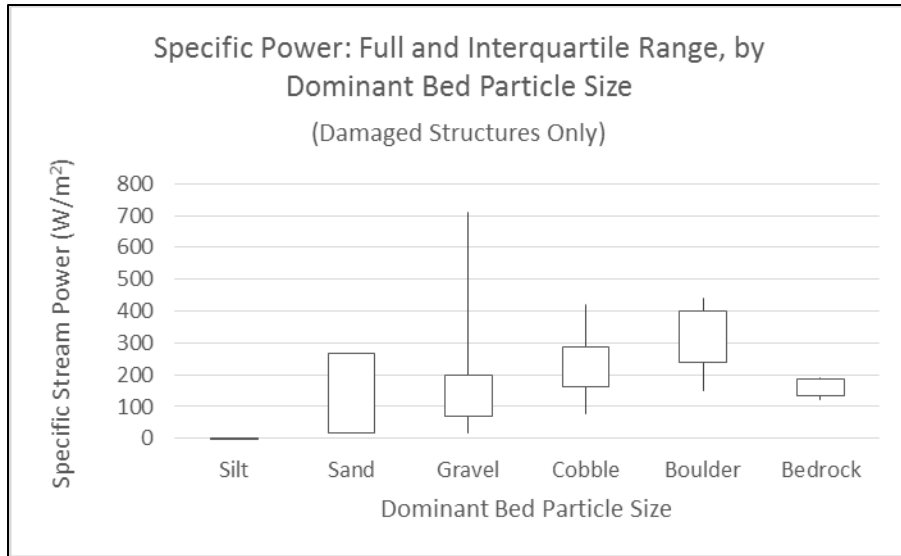


Figure 7-14: Specific Stream Power Full and Interquartile Range by Dominant Bed Particle Size, Damaged Structures Only

7.3.5 Structure Width

The distribution of percent bankfull width (structure span/channel bankfull width) for the field data set closely matched the distribution in the full data set of 1,041 structures (Figure 7-15).

The most common culvert width ratio is between 25% and 50% of the stream's bankfull width based upon 1,041 structures. This group also had one of the highest failure rates (Figure 7-17).

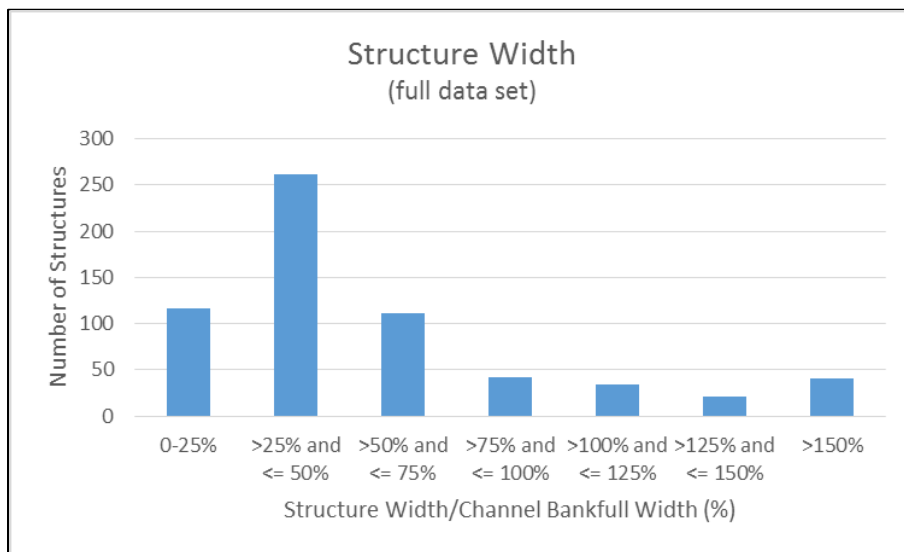


Figure 7-15: Number of Structures by Structure Width/Channel Bankfull Width (full Deerfield data set)

A higher percentage of structures had damages when the structure span was less than 75% of bankfull channel width. These data confirmed that damages tended to be more common on undersized structures (Figure 7-16).

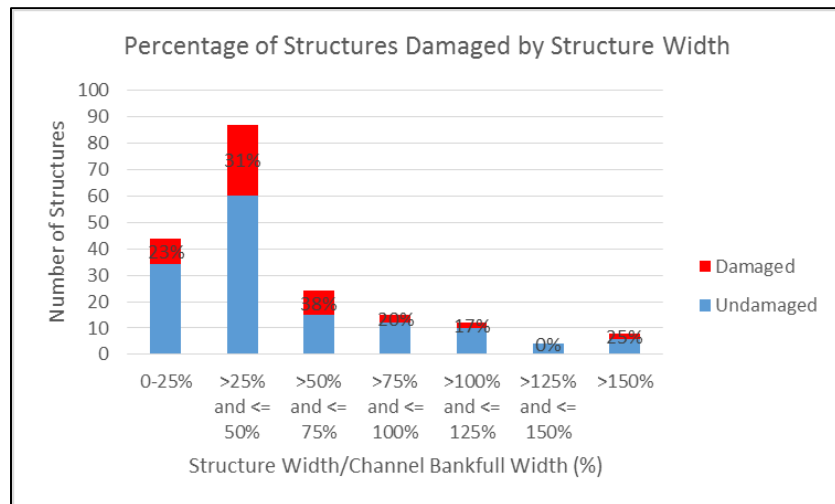


Figure 7-16: Percentage of Damaged Structures by Structure Width/Channel Bankfull Width

Structures that had overtopping, embankment failure, or had been blocked by debris tended to be undersized (less than 50% bankfull width) while structures that had structural damage and fluvial erosion tended to have a larger range of percent bankfull widths (Figure 7-17).

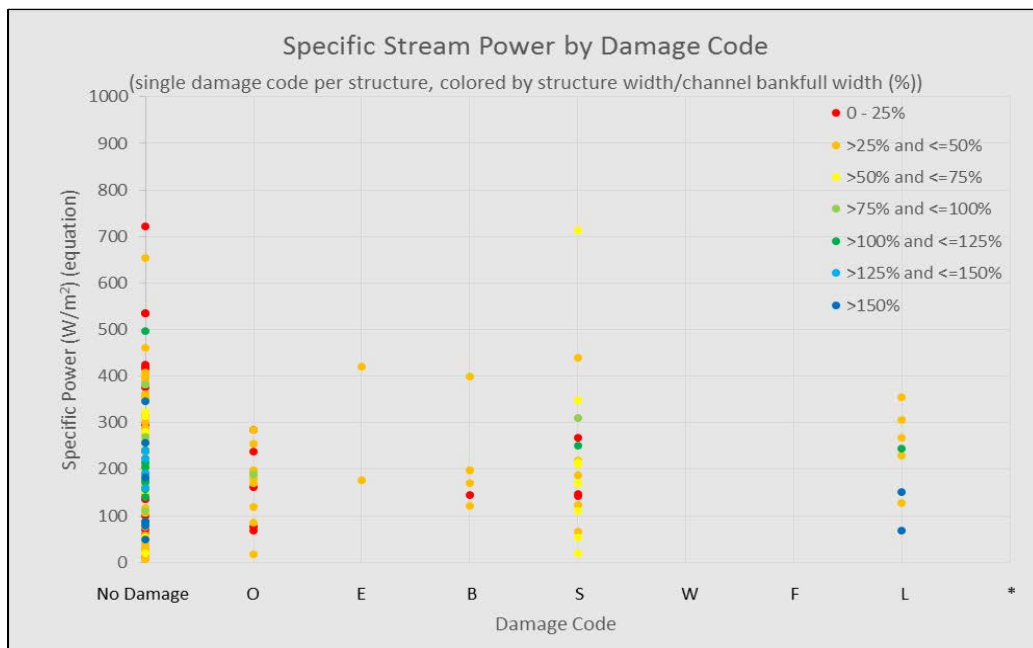


Figure 7-17: Specific Stream Power vs. Damage Code, Data Colored by Structure Width/Channel Bankfull Width (%)

7.3.6 Structure Slope

A higher percentage of structures were damaged when their slopes were either flatter or steeper than the local channel slope (Figure 7-18).

This data suggests that it is beneficial to have culvert slopes similar to the stream bed slope.

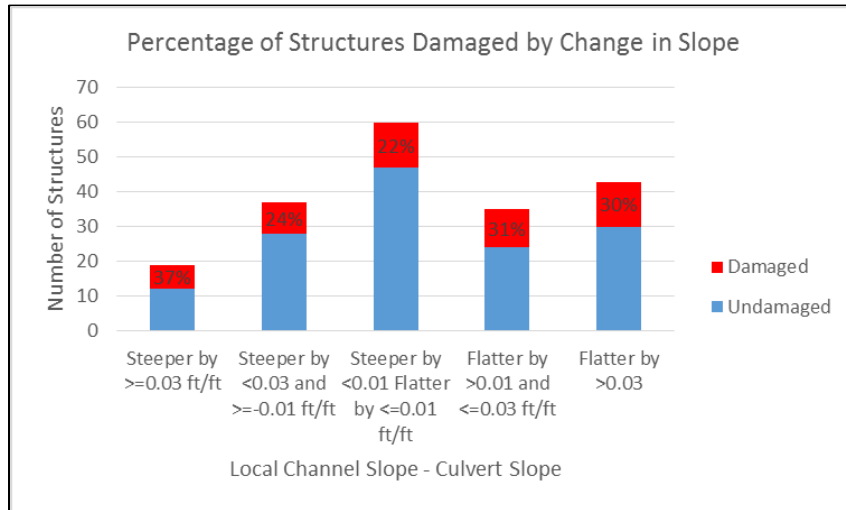


Figure 7-18: Percent of Damaged Structures by Difference Between Local Channel Slope and Structure Slope

In particular, structures that were overtopped or blocked by debris tend to be flatter compared to the local slope (Figure 7-19).

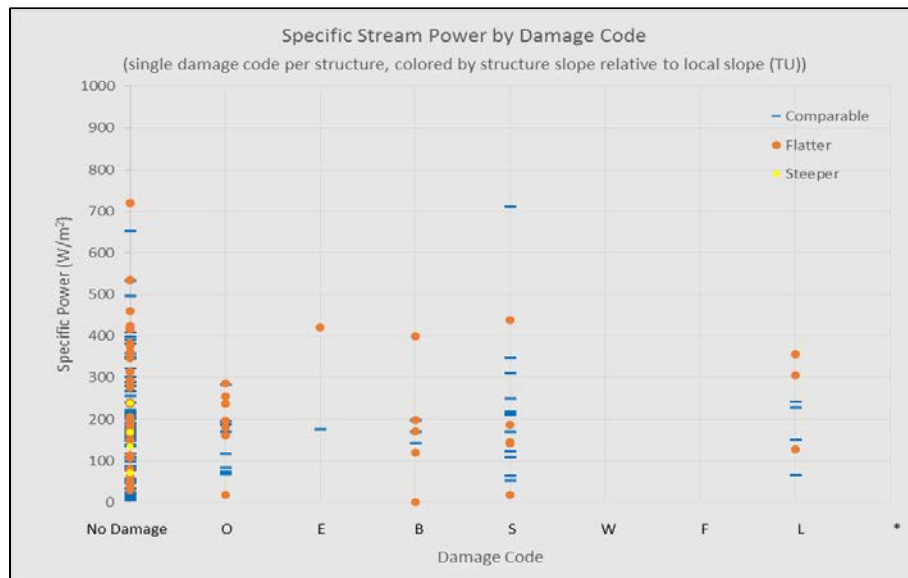


Figure 7-19: Specific Stream Power vs. Damage Code, Data Colored by Structure Width/Channel Bankfull Width

7.3.7 Structure Alignment

A much higher percentage of structures are damaged when the structure is not aligned with the channel (Figure 7-20).

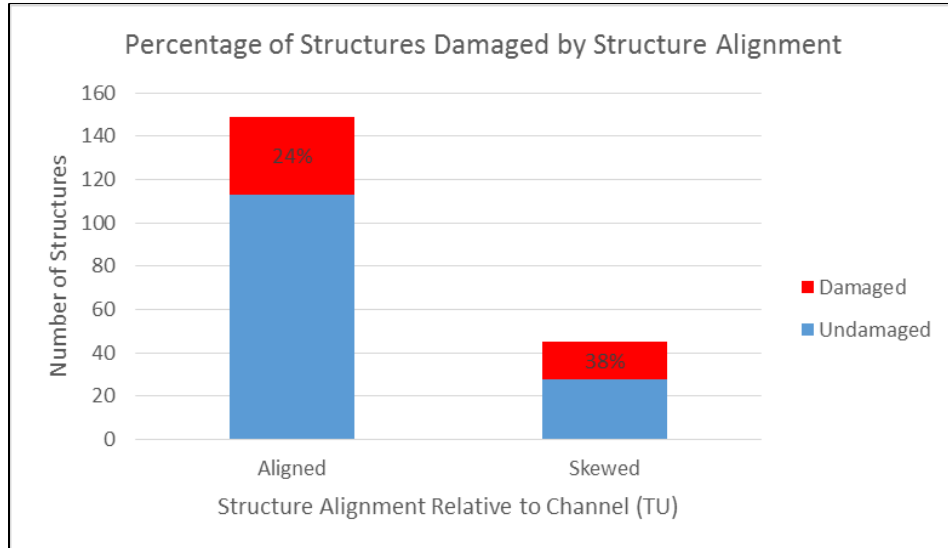


Figure 7-20: Percent of Damage Structures by Structure Alignment Relative to Channel

In particular, structures that are overtopped tend to be skewed (Figure 7-21).

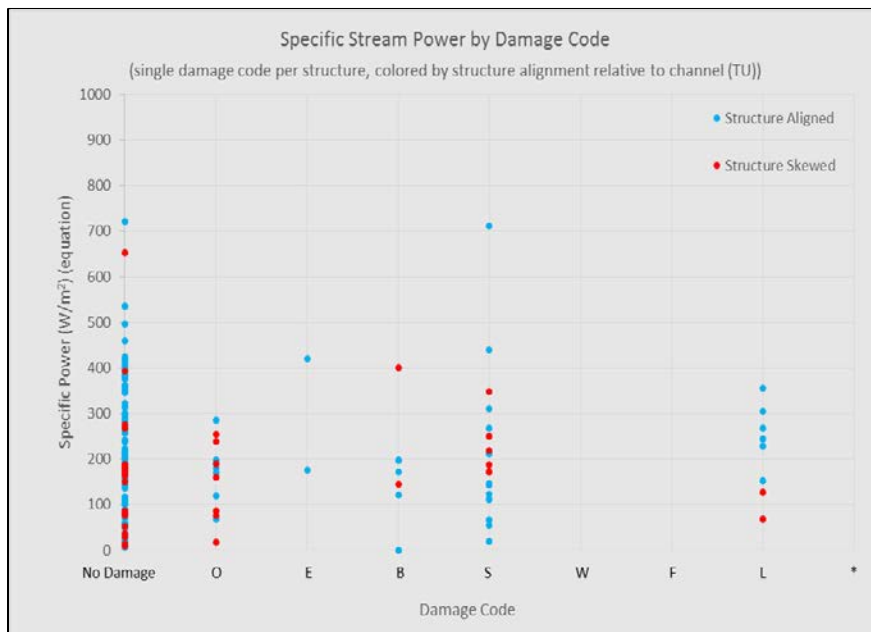


Figure 7-21: Specific Stream Power vs. Damage Code, Data Colored by Structure Alignment Relative to Channel

7.3.8 Bankfull Channel Width

Bankfull width field measurements from TU/MassDOT and MMI were averaged and compared with Soar and Thorne regime-equation-derived bankfull widths (Figure 7-22). There was a strong correlation between the calculated and measured bankfull widths. The regime equation was thus a good representation of field-measured bankfull width.

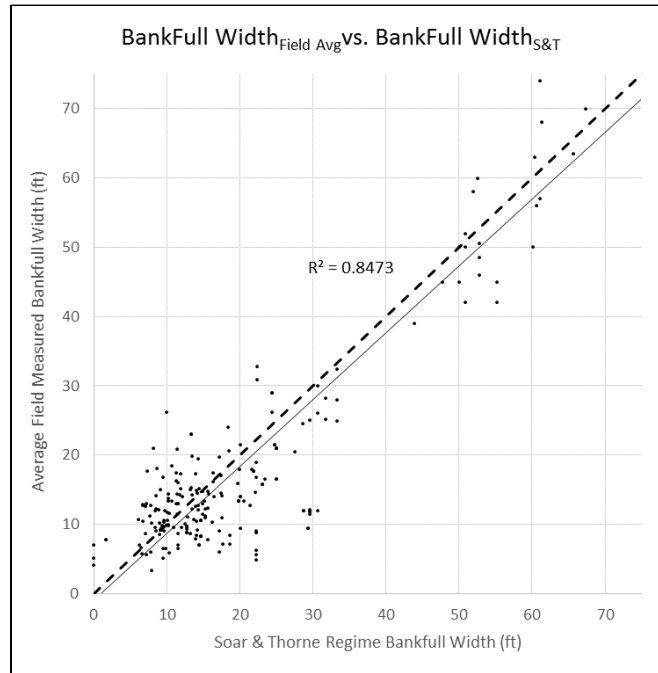


Figure 7-22: Bankfull Width Comparison

7.3.9 Channel Slope

Local channel slope was measured upstream and downstream of each structure and averaged based on the length of the measurement. Field-measured channel slope was compared with GIS-derived slope and showed a varying relationship (Figure 7-23). The variability was driven by the local scale of field measurements (~100 feet) versus the reach scale of the GIS measurement (2,000 to 5,000 feet). The two variables were thus fundamentally different. As expected, local slope variation decreased with increasing stream order (Figure 7-24).

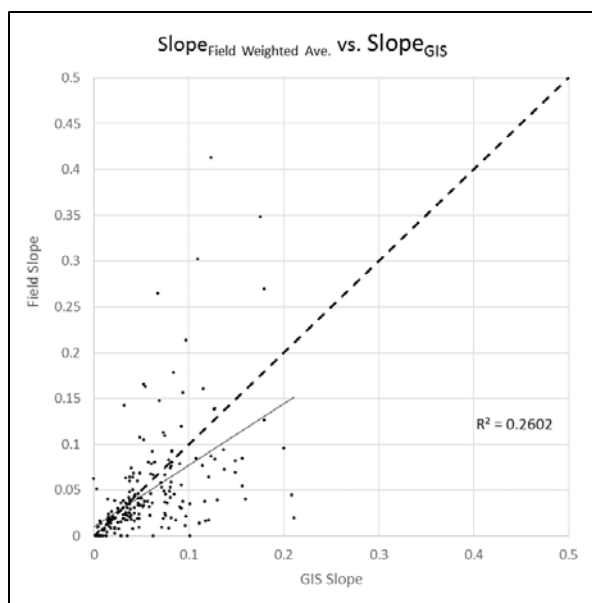


Figure 7-23: Slope Comparison

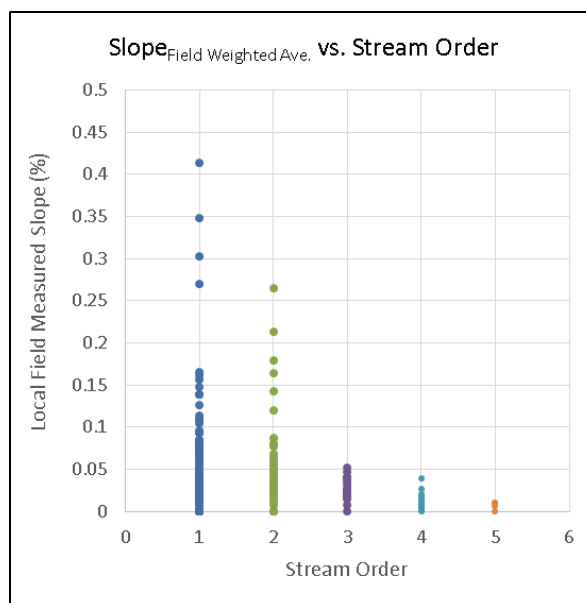


Figure 7-24: Slope and Stream Order Comparison

It is possible for the local stream slope over short distances to be flat with zero slope, in which case the computed local stream power would be zero. However, on a reach scale, stream power is always positive.

SSP is a reach-level parameter, so the GIS-derived reach slope was used for SSP calculations.

7.4 Discussion

7.4.1 Specific Stream Power and Damages

Based on literature and prior work, structures were initially divided into SSP ranges of 0 to 30 W/m², 30 to 60 W/m², 60 to 200 W/m², 200 to 300 W/m², 300 to 600 W/m², and greater than 600 W/m². It was assumed that damaged structures would tend to fall on the extreme ends of this scale where deposition or erosion could be excessive. Structures were selected for field assessment, in part, based on this assumption to explore areas of high potential vulnerability. Results showed damages to be more common in mid-range power (i.e., 100 to 300 W/m²) (see Figures 7-9 and 7-10). This trend has been seen in past screening of Vermont's stream network (Schiff et al., 2015) and in studies of changes in stream power moving down a stream network (Knighton, 1999). The increased potential for damages where specific stream power is 100 to 300 W/m² and alluvial gravel and cobble exist is a key finding of this study. Higher stream power correlates with boulder and bedrock streams that are less prone to damage.

7.4.2 Comparing Power Calculated Using GIS and Equations versus Field Measurements

An assumption going into this project was that for a given flow SSP calculated using regime-derived bankfull width and reach slope in GIS and SSP calculated from bankfull width and local channel slope field measurements would produce similar results. Data show that these two methods of calculating power differed due to differences in local channel slope measured in the field and reach-based average slope measured using GIS. We opted to use the GIS reach slope in the data analysis since power is more of a reach-based variable. Reach and local channel slope are not the same, and this difference must be considered when comparing power measurements using equations and GIS versus field measurements.

7.4.3 The Vulnerability Screen

Variables were selected for inclusion in the vulnerability screen based on data analysis indicating a relationship between a given variable and known damages, the availability of quantitative data, and variables used in previous vulnerability screens. Vulnerability scores for each variable was developed based on trends in the data analysis and known patterns of damages from existing structure screenings (see Figure 7-1).

The "specific stream power versus bed resistance" variable was scored based on field data showing a majority of damaged structures in gravel and cobble-dominated channels with specific stream power between 100 and 300 W/m². Also, the scoring follows the expected pattern of a general increase in vulnerability as SSP increased and bed resistance decreased. An estimate of the dominant channel particle size was used as a proxy for bed resistance, with resistance increasing with particle size.

The "structure width" variable shows that vulnerability increases as the percent of bankfull width covered by the structure's width decreased. Results showed that the majority of structures had widths between 25% and 50% of bankfull channel width, a pattern commonly seen in past bridge and culvert assessments in the region.

The "change in slope" variable indicates that less vulnerability exists when the structure and channel slope are the same. Vulnerability increases as the structure becomes flatter or steeper than the local channel slope. Data suggest that a higher percentage of steeper structures were damaged than flatter structures, and thus the scoring of this variable reflects that trend.

The "sediment continuity" variable considers channel bed process (e.g., aggradation or degradation) upstream and downstream of the structure with the assumption that vulnerability increases if channel processes are disrupted by the structure. For example, structures with aggradation upstream and degradation downstream are likely to be inhibiting sediment transport and can lead to a high level of vulnerability relative to other conditions. Due to the qualitative nature of these field data and the fact that repeat observations seemed to vary widely, the variable was scored on a scale of 1 to 3 to reduce the maximum value, and this gives the variable a lower weighting.

Structures identified as "skewed" were considered more vulnerable than those identified as "aligned" for the "structure alignment" variable. The further the structure alignment deviates from being parallel to the direction of flow the more vulnerable the structure is. Due to the qualitative nature of the field observations, the variable was scored on a scale of 1 to 3 to reduce the maximum value, and this gives the variable a lower weighting.

The results of this study show the highest percentage of structures with known damages exists when the vulnerability screen result is "high," and damages tend to decrease for medium and low screen scores. However, it is important to note that some damaged structures do get a vulnerability score of "low," which illustrates the inexact nature of a screening tool. The vulnerability screen is not an exact predictor of damages yet is most appropriately used to flag sites where the potential vulnerability for damages is high or medium. All findings using the vulnerability must be field verified as part of project development.

7.4.4 Data Comparison – Quality Control Check

Twenty structures were inspected by MMI using the TU Culvert and Bridge Assessment ("TU+Elev" spreadsheet), MassDOT Culvert Condition Assessment ("Condition" spreadsheet), and UMass Road-Stream Crossing Inventory ("Stream Continuity" spreadsheet) field data forms. The MMI assessment data for each structure were then compared to the prior assessments performed by TU, MassDOT, and UMass for quality assurance purposes. In general, good agreement existed for quantitative variables (e.g., bankfull width and structure dimensions). Most data discrepancies between the assessments occurred for qualitative data (e.g., UMass "Crossing Condition" and TU "Substrate Particle Size"). Some of the differences may be explained by changing field conditions since data were collected a year apart. The MMI assessment reported "None" more frequently for the "Streambed: Erosion/Aggradation/None" and "Deposit Type" fields.

Some large differences in collected data did exist. For example, width measurement for larger bridges varied between the TU and MMI data. TU appeared to be measuring the road span of the bridge while MMI measured the width of the hydraulic opening between the abutments. Larger differences also existed for the "Floodplain filled by roadway" variable. TU consistently indicated more floodplain fill than MMI. MMI observed the amount of floodplain actually covered by the road embankment. Perhaps TU noted the amount of floodplain disconnected from the channel by a road embankment.

7.4.5 Particle Size Data

Pebble counts were conducted to identify the substrate characteristics (e.g., median grain size D_{50}) that could represent bed resistance to erosion. Out of the 197 structures assessed by MMI, UMass provided pebble counts for 34, with particle sizes placed into 11 size bins (<2 mm, 2-8 mm, 9-16 mm, 17-64 mm, 65-90 mm, 91-128 mm, 129-256 mm, 257-512 mm, 513-1,024 mm, >1,024 mm, and bedrock). MMI used this bin system for pebble counts performed on the

remaining 166 structures. When D_{50} was calculated from the pebble count data it became evident that these bins were too wide, so most of the D_{50} calculations landed in the same size grouping. The concentration of the data may be obscuring the relationships between D_{50} and channel characteristics like slope, bankfull width, SSP, and damages.

A qualitative observation of dominant bed particle size was substituted for D_{50} when developing the "specific stream power and bed resistance" vulnerability screen variable because it seemed to do a better job indicating bed particle size and resolving damages. It is recommended that standard gravelometer-sized bins be used in future work in order to obtain quantitative data on bed resistance.

7.4.6 Structure Damages

Structures with reported damage were assigned a damage code to differentiate between various types of damages and failures (see Figure 7-18). Many damaged structures had more than one associated code, and damage codes appeared to have overlapping definitions (e.g., What differentiates an "overtopped" structure from a structure with "roadway flooding"?). Standardizing and simplifying the damage codes would help with such future analyses.

7.4.7 Data Substitution in Vulnerability Screen

The vulnerability screen uses data obtained during MMI field assessments whenever possible. Qualitative data from prior fieldwork conducted by project team members is available for the dominant particle size and structure slope relative to local channel slope. These qualitative data may be substituted for missing field data if necessary but will likely result in a loss of detail in the vulnerability screen. An initial trial was conducted to replace the variable indicating the difference in the slope of the local channel and structure with a qualitative observation of a "steeper" or "flatter" culvert. The loss of detail limited the use of the slope variable to help identify when structure damages are more likely. It may be best to eliminate a variable with missing data rather than substitute qualitative information. More work is needed to determine the best data substitution method.

7.4.8 Future Implementation Work

The vulnerability screen can be applied to the full 1,041 structure database for the Deerfield River watershed. It is recommended that local channel slope and structure slope be measured for each structure, but already available qualitative data may be substituted. Based on the results of the vulnerability screen, field investigations of high vulnerability structures can be conducted to verify predictions and develop projects where needed. These data can also be provided to local municipalities to help guide resource allocation for repairs and preventative maintenance for high vulnerability structures.

APPENDIX A

GEOMORPHIC SEGMENTATION AND DESCRIPTIONS

In order to describe and assess the Deerfield River in an orderly process, MMI has identified a series of river segments numbered from 1 to 18, with segment 1 at the upstream headwaters and segment 18 at the confluence of the Connecticut River, plus a series of key tributary segments. Remote sensing data was then reviewed for each segment, which were then inspected in the field during 2014. Initial segment boundaries were then adjusted. Each segment is described from upstream to downstream including its geomorphic characteristics and its physical condition. The former includes the length and slope, its planform pattern and profile features, sinuosity, watershed area, channel size, bed material, and a corridor description including infrastructure and floodplains.

The break points between individual segments are based on multiple factors including the level of detail needed (effects segment lengths), confluences of major tributaries, valley confinement, changes in stream patterns, hydraulic control points, confinement, dams, and highway crossings. The objective is for each stream segment to have consistent similar hydrology and stream processes.

The segment summary is a compilation of various sources including remote sensing (aerial photographs, topography), existing literature, field inspections, channel classification, and interpretations.

RIVER SEGMENT NO. 1

FROM: Main Branch headwaters

TO: RM 61

RIVER MILES

LENGTH: 12.1 miles

SLOPE: 48.6 feet per mile

CHANNEL TYPE: B

DRAINAGE AREA, SM: 50.9

TYPICAL BANKFULL WIDTH: Up to 75 feet

RIVER CHARACTER: Wild

CORRIDOR CHARACTER: National forest

GENERAL DESCRIPTION

The main branch of the Deerfield River originates in rough road less terrain in the Green Mountain National Forest west of National Forest Route (NFR) 71 and south of the rural Stratton-Arlington Road. It flows in a southerly direction parallel to NFR71 to the confluence with the East Branch at RM 61, at the head of Searsburg Reservoir about 2 miles north of the well-known Route 9.

The watershed area just before the confluence is a substantial 50.9 square miles. The channel has a steep mean gradient of 48.6 feet (drop) per mile, equal to 0.9 percent. At this gradient, channels generally have many pools and riffles and a coarse substrate. According to the USGS *StreamStats* hydrology software, the predicted 2-year frequency flood is 1,710 cfs.

A new aluminum truss footbridge crosses the main branch near RM 61, leading to the East Branch trail. The straight channel is 75 feet wide at this point with shallow, rapid flow on a cobble bed. The channel is slightly incised and lacks any floodplain. The Rosgen classification is type B3, without any unusual sediment erosion or deposition.

**RIVER SEGMENT NO. VT East
Branch**

FROM: East Branch headwaters
TO: Searsburg Reservoir, RM 61
RIVER MILES to 61
LENGTH: 15.7 miles
SLOPE: 52 feet per mile
CHANNEL TYPE:

DRAINAGE AREA, SM: 30.9
TYPICAL BANKFULL WIDTH:
RIVER CHARACTER:

CORRIDOR CHARACTER: Rural national forest

GENERAL DESCRIPTION

The headwaters of the Deerfield River originate in the Green Mountains of southern Vermont, immediately west of Stratton Mountain and Mt. Snow resorts. Most of this area is remote, in the Green Mountain National Forest, with few roads. The headwaters area is crossed by the famous Long Trail hiking path. The headwaters include the North Branch, which is east of the East Branch, the main stem, which is west of the East Branch, and the shorter West Branch.

The longest of the four headwaters is the East Branch, which begins near the back west side of Stratton Mountain and then was dammed in 1912 to form the giant 1,514-acre Somerset Reservoir that is used for seasonal-scale storage at RM 66. This large reservoir is surrounded by protected wild lands and is popular for nonpower boating. The East Branch then continues on a southerly course to its confluence with the main stem at RM 61 just above Searsburg Dam. It is located in the long, wild valley on the west side of the mountain ridge that includes Mt. Snow and Haystack ski resorts.

RIVER SEGMENT NO. 2

FROM: Searsburg Reservoir
TO: Harriman Delta
RIVER MILES 61 to 56
LENGTH: 5 miles
SLOPE: 65.6 feet per mile
CHANNEL TYPE:

DRAINAGE AREA, SM: 99.3
TYPICAL BANKFULL WIDTH: 80 feet
RIVER CHARACTER: Rapids, cobble bed
CORRIDOR CHARACTER: Rural forest

GENERAL DESCRIPTION

This short river segment extends from the confluence of the East and Main Branches of the Deerfield River at the head of Searsburg Reservoir to the delta at the head of the giant Harriman Reservoir. Flows in this segment are regulated by the Somerset Reservoir upstream along the East Branch plus by flow diversions at Searsburg Reservoir to its off-site pump station.

The watershed area along the main branch at the Harriman Reservoir delta is 99.3 square miles with a predicted 2-year flood of 2,260 cfs.

From the small 30-acre Searsburg Reservoir, the river flows downstream a short distance to Route 9, then parallels the highway southeasterly to the delta at Harriman Reservoir. There are three significant bridges over the river in just one-half mile as the river and highway share a narrow valley bottom. Route 9 is a major east-west connector across the Green Mountains from I-91 to Route 7.

The channel segment from Searsburg Reservoir to Route 9 is in a sinuous, incised bedrock canyon with a measured bankfull width of 80 feet. The channel bed is armored with a static bed of boulders and cobbles with a rapids-type profile. Large boulders are present in some areas. It is a bypass segment with a wood stove pipe, 8-foot-diameter penstock, which runs parallel to the river from the dam to its powerhouse along Route 9. The channel is generally laterally and vertically stable except for local bank erosion such as at the bend by Route 9 at RM 59.

The second channel segment that extends parallel to Route 9 to Harriman Reservoir has a wider bankfull width of 110 feet and a flat cross section bed with many cobbles and boulders. The channel is confined by a steep hillslope on one side and highway embankment on the other. It is a Rosgen type B channel.

RIVER SEGMENT NO. 3

FROM: Harriman Reservoir RM 56
TO: RM 48.5
RIVER MILES
LENGTH: 7.5
SLOPE: N/A
CHANNEL TYPE: Reservoir

DRAINAGE AREA, SM: 184
TYPICAL BANKFULL WIDTH: N/A
RIVER CHARACTER: Reservoir
CORRIDOR CHARACTER: Mountain valley

GENERAL DESCRIPTION

The 7.5-mile-long Harriman Reservoir is a large storage impoundment used to regulate seasonal flows for the downstream hydropower dams. It is the largest body of water totally within the state of Vermont and was built in 1923 by the New England Power Company, now owned by TransCanada, with a watershed area of 184 square miles. It represents over 10 percent of the Deerfield River's overall length and therefore warrants its own segment designation. The reservoir is formed by a 215-foot-high earth dam with a "morning glory" spillway and has a surface area of 2,039 acres. Most of its perimeter consists of steep forest covered slopes with limited road access. The maximum water depth is reportedly 180 feet with a useable drawdown of 86 feet (TransCanada Northeast, LIHC application). The associated powerhouse, built in 1925, is 2.5 miles downstream and connected by a tunnel.

The main Deerfield River enters the northwest end of the reservoir and has formed a 1,500-foot-long sand and gravel delta, up to 500 feet wide. The East Branch Deerfield River discharges into the northeast end of the reservoir. The large impoundment volume and long duration drawdown enable the reservoir to trap and settle most inflow sediments, removing them from channel conveyance. The reservoir is known for fishing, boating, and ice fishing. There are several small boat launches at the north end along Route 9 and along the east side. There are no roads to the west shore.

RIVER SEGMENT NO. 4

FROM: RM 48.5, Harriman Dam
TO: RM 44.6, West Branch
RIVER MILES
LENGTH: 3.9
SLOPE: 37.5

DRAINAGE AREA, SM: 191
TYPICAL BANKFULL WIDTH: 100
RIVER CHARACTER: Confined rapids, bypass segment
CORRIDOR CHARACTER: Steep hillside forests

CHANNEL TYPE:

GENERAL DESCRIPTION

This short river segment extends from the giant Harriman Dam to the confluence with the West Branch Deerfield River at Readsboro, Vermont. This 3.9-mile segment is highly confined on both sides of the river, and its flow is regulated by the dam. It is also a "bypass" segment because the dam diverts water via a long penstock to the off-site Harriman red brick powerhouse downstream of Readsboro, leaving minimal flow in this segment.

The channel follows a narrow, sinuous valley with little floodplain due to confinement. It has a gravel and cobble bed and a typical width of 100 feet and shallow depth. The banks are heavily vegetated with road access limited to a section of Route 100 near the village.

A 10-foot-high bedrock rapids capped with a low, decayed timber dam is located in the village of Readsboro just before the confluence with the West Branch. Site inspections reveal most of its small pool is filled with debris. Route 100 crosses the river on a high bridge just below the rapids.

The total watershed area on the Deerfield River just upstream of the confluence with the West Branch is 191 square miles. The mean segment slope is a moderate 37 feet per mile.

RIVER SEGMENT NO. West Branch to Readsboro

FROM: Headwater

TO: Readsboro

RIVER MILES

LENGTH: 11

SLOPE: 100

CHANNEL TYPE:

DRAINAGE AREA, SM: 31.8

TYPICAL BANKFULL WIDTH: 50 feet

RIVER CHARACTER: Steep

CORRIDOR CHARACTER: Rural and confined

GENERAL DESCRIPTION

The West Branch of the Deerfield River originates in the town of Woodford and flows southeast to join the main channel in Readsboro. The West Branch has a total watershed area of 31.8 square miles and is very steep with a mean channel slope of 100 feet per mile. For 5 miles from Heartwellville to Readsboro, it flows in a fully confined narrow valley parallel to Route 100. Several sections of the highway were destroyed by erosion during Hurricane Irene and had to be rebuilt and the riverbanks reinforced with stone riprap. Each of the highway repairs corresponds to sections where the channel is extra narrow and confined by bedrock or bank boulders. *StreamStats* predicts the 2-year flood frequency peak flow to be 1,100 cfs and the 100-year to be 4,250 cfs. High failures along the left bank also occurred right in the village behind School Street, 400 feet upstream of Tunnel Road.

The Vermont Basin 12 water quality assessment rates the macroinvertebrate community as excellent, and the river supports wild brook and brown trout with great habitat. The West Branch is also a challenging kayak run during high water in the spring.

The narrow valley and highway encroachments mean there is no floodplain, and the segment is subject to concentrated stream power and future erosion. Bedrock is visible in some areas. The Branch Hill Road and Tunnel Road bridges cross the West Branch River just before its confluence with the Deerfield River.

RIVER SEGMENT NO. 5

FROM: RM 44.6 West Branch Confluence

TO: RM 42.1, Sherman Dam

RIVER MILES

LENGTH: 2.5 miles

SLOPE: 47 feet per mile

CHANNEL TYPE: Incised plain bed

DRAINAGE AREA, SM: 224

TYPICAL BANKFULL WIDTH: 120

RIVER CHARACTER: Rapids and run

CORRIDOR CHARACTER: Steep narrow valley

GENERAL DESCRIPTION

The Readsboro to Sherman Dam segment has a length of 2.5 miles with a mixture of a confined and semiconfined channel to the Sherman Dam impoundment. Beginning at the small village of Readsboro, there is a large confluence bar at the mouth of the sediment-laden West Branch, and the channel is incised with a high terrace on the left and a lower terrace on the right. Both terraces are developed with roads parallel to the river. The channel top width averages 150 feet as it sweeps into a double bend. A prominent point bar is located along the left bank along a gentle bend followed by a rocky rapids 1 mile downstream of the confluence. At this point, the right terrace has faded out, and Tunnel Road is located close to and overlooking the right bank.

The left bank continues to have a ± 20 -foot-high terrace and narrow vegetated buffer zone, then a ball field, a wastewater treatment lagoon, and then the Harriman Power Plant, at which point the bypass segment ends and the river is back to full discharge. Several mid-channel gravel bars, the beginning of a delta, are present just before the power plant's short tailrace as the river is influenced by the backwater from the Sherman pool.

The channel profile for this segment has a mean gradient of 47 feet per mile and is slightly concave, declining near the reservoir. The bed is covered with cobbles and boulders.

The bypassed segment has an incised channel measured at up to 187 feet wide at its top of bank and 120 feet at the estimated bankfull elevation. However, the actual wetted width during inspection was only 70 feet with shallow flow. The channel bed edges were grass covered, reflecting the reduced flow rates.

RIVER SEGMENT NO. 6

FROM: Sherman Delta
TO: Sherman Dam
RIVER MILES RM 42.0
LENGTH: 2.0
SLOPE: N/A
CHANNEL TYPE:

DRAINAGE AREA, SM: 236
TYPICAL BANKFULL WIDTH:
RIVER CHARACTER: Reservoir

CORRIDOR CHARACTER: Very steep valley,
forested

GENERAL DESCRIPTION

The Sherman Dam Reservoir is located across the Vermont-Massachusetts border, just upstream of the Village of Monroe Bridge. It is the last large impoundment on the Deerfield River in the downstream direction. The 2-mile-long pool has a surface area of 218 acres and was built for hydropower, weekly pool and release storage. The pool has steep forested hillsides and no floodplains. The 100-foot-high dam is an earth fill structure built in 1927. The former Yankee Rowe Nuclear Power Plant was once located on the banks of the pool, which was used for cooling water, but has been decommissioned and demolished after its 1992 shutdown.

The South Branch of the Deerfield River, which originates on the east side of the Hoosic Mountain Range, flows east directly into the Sherman Reservoir. This is a small, steep, rural tributary stream.

The dam has a large side channel spillway into a bedrock channel. The backwater from the Monroe Bridge Dam (No. 5) extends a flat water pool 3,500 feet upstream almost to the base of the Sherman Dam.

There is a small parking area and boat launch along Tunnel Road providing public access to Sherman Reservoir.

RIVER SEGMENT NO. 7

FROM: Sherman Dam
TO: Fife Brook Dam
RIVER MILES RM 42 to RM 37
LENGTH: 5 miles
SLOPE: 50 feet per mile (dryway)
CHANNEL TYPE: Regulated and modified

DRAINAGE AREA, SM: 253
TYPICAL BANKFULL WIDTH: 100-150
RIVER CHARACTER: Confined, dry bypass
CORRIDOR CHARACTER: Confined valley

GENERAL DESCRIPTION

The Deerfield River flows through a spectacular steep-sided narrow gorge for 5 miles from the base of the Sherman Dam to the Fife Brook Dam. Within the gorge, the crowded valley bottom has three distinct segments, one after the other, plus River Road along the right bank and a railroad track on the left bank.

The Deerfield No. 5 hydropower development in this segment is a complex system built in 1974 and owned by TransCanada. It has a modest height (35 feet) concrete dam at RM 41.2 that backs up a small linear pool to the Sherman Dam and diverts most flow into a 2.7-mile-long headrace canal along and above the right bank to a powerhouse at RM 38.5, which is also at the upstream end of the Fife Brook Dam Reservoir. The 2.7-mile-long bypassed segment of the river is known locally as the "dryway;" it has a narrow, steep channel but little flow except releases timed for special whitewater sports events. Boater access to the dryway in Monroe Bridge is very poor with limited parking near an abandoned factory and few signs. The reported minimum flow is 73 cfs while short-duration sports event releases are up to 1,000 cfs. The dryway is further discussed in various whitewater sports-related web pages.

The dryway channel segment has a series of rocky rapids rated whitewater classes II through a challenging IV. Release rates and diversions have been reportedly discussed and negotiated for many years with the owner, TransCanada, and FERC. The FERC license #2323 runs until 2037. The water quality is good; it meets Massachusetts class B standards.

The dryway terminates in the Fife Brook reservoir where a parking lot and boat ramp are located. Water levels and flow rates may rapidly change in this segment.

RIVER SEGMENT NO. 8

FROM: Fife Dam, RM 37
TO: River Road bridge
RIVER MILES RM 31.5
LENGTH: 5.5
SLOPE: 25 feet per mile
CHANNEL TYPE:

DRAINAGE AREA, SM: 263 sm
TYPICAL BANKFULL WIDTH: 170 ft.
RIVER CHARACTER: Semiconfined rapids
CORRIDOR CHARACTER: Entrenched sinuous valley

GENERAL DESCRIPTION

The river segment from the Fife Brook dam downstream to River Road bridge near Zoar Gap is a popular whitewater class II-III run for intermediate skill levels. The flow is totally regulated by the upstream dams.

The channel itself is confined to semiconfined by steep valley walls leaving limited space for the disconnected terraces. The wide, shallow channel has a cobble and boulder bed, creating fast runs and some rapids. Alternate and point bars are visible upstream of the railroad bridge during low flow. The bankfull width was measured at 176 feet with a bankfull depth of only 4 feet.

Outwash terraces are located on the left bank opposite and downstream of the Hoosic railroad tunnel and used to support a railroad station and village. A larger terrace is located on the right bank beginning near Whitcomb Road and extending downstream for 1 mile. It reportedly was the site of tunnel worker housing in the 1800s.

Tunnel Road follows the right bank to the bridge at Zoar Gap, then changes name to Zoar Road. The railroad follows the left bank with the channel conferred between the railroad (left) and highway (right). Hurricane Irene caused 300 linear feet of embankment failures a short distance upstream of the Zoar Gap bridge, in a narrow contraction. An 800-foot-long, high, steep road embankment failure occurred where the narrow 60-foot-wide channel and in-channel boulders contributed to very high velocities at the sharp bend 1 mile upstream of Pelham Brook. The steep, high banks are repaired at both sites with rock riprap but remain vulnerable due to channel geometry. A second embankment failure 400 feet long occurred at RM 34 along a sharp, narrow river bend to the left; it also was repaired with riprap.

The railroad follows the left bank, crosses the river near RM 35.5, and goes through the famous Hoosic Tunnel to North Adams.

RIVER SEGMENT NO. 9

FROM: Florida Bridge, 31.5

TO: Cold River, 29

RIVER MILES

LENGTH: 2.5

SLOPE:

CHANNEL TYPE: Confined

DRAINAGE AREA, SM: 279

TYPICAL BANKFULL WIDTH: 175 feet

RIVER CHARACTER: Runs and rapids

CORRIDOR CHARACTER: Confined rural

GENERAL DESCRIPTION

Zoar Road and the railroad share the river's left bank from the Florida bridge crossing, past Pelham Brook, to the major confluence with Cold River. This segment of the Deerfield River has a series of fast runs, riffles, and pools with a coarse cobble bed and many boulders. It is a popular recreation area for fishing, tubing, and kayaking. The channel has a single stem with an average width of 175 feet with high firm banks.

The forested right bank is fully confined by the steep, forested flanks of Todd Mountain with its pointed crest and narrow ridgeline.

The left bank downstream of the bridge has a large public picnic area and canoe launch along the riverbank on a terrace provided by the TransCanada Power Company. The terrace then narrows in the downstream direction crowding the railroad and highway, requiring a riverbank retaining wall to the mouth of Pelham Brook.

Pelham Brook enters on the left at RM 30.5. It is a steep, clear-water tributary with step pools and rapids. A locally significant hillside failure occurred recently a few hundred yards upstream of the confluence. Pelham Brook sediments create bed changes in the Deerfield River, including lateral bars and a large riffle. Most noticeably, a large bar present prior to 2010 is largely gone after Hurricane Irene in 2011.

RIVER SEGMENT NO. 10 – Zoar Gap Rapids

FROM: RM 32

TO:

RIVER MILES

LENGTH: 200 feet

SLOPE: 6 percent

CHANNEL TYPE: A1

DRAINAGE AREA, SM: 279

TYPICAL BANKFULL WIDTH: 75

RIVER CHARACTER: Confined, contraction

CORRIDOR CHARACTER: Rock gorge

GENERAL DESCRIPTION

After passing Beaver Island at a sharp right bend, the river channel spreads out to a bankfull width of almost 300 feet. The railroad is on the left bank along the base of Negus Mountain, and River Road is on the right side high above the shallow river. The channel then steadily narrows as it approaches the River Road bridge in Florida. The well-known Zoar Gap Rapids, a popular kayak class IV run, precedes the bridge and has an access point on the right bank prior to the two sets of rapids.

The channel width at the primary rapids decreases from over 250 feet to just 75 feet. The rapids begin at a pair of medium boulders in the left central part of the channel, which create whitewater, followed by a series of three giant boulders projecting into the left side of the channel, opposite a line of medium boulders parallel to the right bank, creating a mid-channel chute only 30 feet wide. The head of the chute has at least two submerged boulders that create standing waves and reverse eddies. The chute ends in a deep pool. Easier boat passage and upstream fish passage is along the right bank.

A secondary rapids is located a few hundred feet downstream with three main clusters of boulders in the 75-foot-wide trapezoidal channel. They obstruct about 25 percent of the channel's base width. The first cluster has three large protruding boulders in the center and left side of the channel, followed by about four submerged boulders, then a second cluster with two pairs of boulders on each side of the channel with an open slot down the middle. The third cluster of boulders forms an open triangle in the mid channel with enough of a gap to go in the middle slot or on either side, depending on water levels.

The rapids have a measured 6-foot drop in a length of 200 feet. The takeout point is on the left bank after the Florida River Road bridge.

RIVER SEGMENT NO. Chickley
River

FROM: West Hawley

TO: Deerfield River

RIVER MILES

LENGTH: 10

SLOPE:

CHANNEL TYPE: Modified

DRAINAGE AREA, SM: 27.4

TYPICAL BANKFULL WIDTH: Modified

RIVER CHARACTER: Channelized

CORRIDOR CHARACTER: Rural, forest

GENERAL DESCRIPTION

The Chickley River headwaters are on the high plateau in the towns of Savoy and Plainfield, and much of the land is watershed land state forest. The channel length is 10 miles with a drop of 1,500 feet, leading to a very steep gradient of 150 feet per mile. Its ungauged watershed size is similar to that at the South River gauge, so its runoff rates should be similar to that gauge.

The Chickley River drains a rural watershed of 27.4 square miles and flows into the Deerfield River at RM 27.0. The lower main branch is 5 miles long and runs northerly parallel to Route 8A. It was known as a moderate-sized cold-water trout stream that was stocked as part of the salmon restoration program even though downstream dams on the Deerfield River prevent anadromous upstream migration. It had a gravel and cobble bed with excellent forest cover and was listed as a class III whitewater stream.

Hurricane Irene caused extensive Chickley River channel erosion, washed out sections of Route 8A, and damaged the Hawley Public Works Department garage. In response, the town engaged a contractor who dredged and channelized approximately 5 miles of river, removing all pools, riffles, and fish habitat, and shaping the banks and new levees with former bed material; all channel boulders and woody material were removed. MassDEP concluded that the contractor significantly deepened and straightened the river in violation of state regulations, isolating it from the floodplain. Emergency road repairs were necessary to reopen Route 8A to traffic.

A minimalist river restoration project has been installed based upon a downstream reference segment. The project raised the bed, removed stone linings from the upper banks, and placed some boulders and logs along the bed. However, the channel has not recovered its earlier pool structure and is overly wide and devegetated, and the outlet bridges are partially blocked by coarse sediment. Bank plantings are in progress during 2015. Natural recovery will eventually help revegetate and repair the flood damage to the river corridor.

The Town of Hawley does not have a FEMA FIS and, therefore, does not have regulated floodplains or floodways.

The middle segment of the Chickley River that was severely damaged by Hurricane Irene has a mean slope of 3.8 percent, a typical flood width of 100 feet, and an estimated bankfull (2 year)

discharge of 1,906 cfs based on the South River gauge. The resulting bankfull SSP is a high 307 watts per square meter and a crushing 1,383 watts per square meter for Hurricane Irene. It is not surprising that there was severe erosion to the channel and Route 8A.

RIVER SEGMENT NO. 11 – Deerfield River

FROM: Cold River Confluence
TO: Charlemont Center, Route 8
bridge

RIVER MILES

LENGTH:

SLOPE: 0.0032

CHANNEL TYPE: C

DRAINAGE AREA, SM: 340

TYPICAL BANKFULL WIDTH: 175-220

RIVER CHARACTER: Unconfined alluvial

CORRIDOR CHARACTER: Village and pastoral

GENERAL DESCRIPTION

The Deerfield River character and condition change immediately after the confluence with Cold River. The latter adds 31.7 square miles of watershed plus a significant sediment load, followed 2 miles downstream by the input from the Chickley River with another 27.4 square miles. The total watershed area at the Route 8A bridge in the center of Charlemont is 340 square miles.

After the Cold River delta of fresh coarse sediment, the river flows easterly past a floodprone campground on the right floodplain and under the large Route 2 bridge, then past a picnic area and canoe launch (locally known as "Shunpike") located on the low left terrace, past continuing low terrace geologic formations on both overbanks, to the Route 8A bridge over the river and the center of Charlemont. The channel has several large cobble bars on alternate banks from the Cold River confluence to the Route 2 bridge, representing the input of sediment from the Cold River mass bank failures. The terraces on both banks along Route 2 on the left and along Route 8A on the right are both mapped by FEMA as floodplains. The left floodplain near Legate Road at Route 2 was covered by fresh sediment after Hurricane Irene and has log jams along the banks. Similarly, the riverfront portion of the left bank linear field near Zoar Outdoor was also covered with sand. Aerial photographs show that the right floodplain along West Hawleyville Road flooded. Farther downstream, the school grounds and firehouse flooded, and the wastewater treatment plant's sand filters were out of service for over a year; all of these public infrastructure facilities are in the mapped floodplain.

The measured bankfull channel width at the picnic area/boat launch near the Route 2 bridge is 220 feet with high, with well-defined banks and a deep pool with a cobble bed. Limited bedrock was visible at the left bank. Farther downstream at the Zoar Outdoor parking lot and canoe launch, the channel is only 175 feet wide with lower banks, which helps explain why the river overtopped this section. There are several long, shallow riffles in this segment composed of surprisingly large cobble with an estimated D_{50} of 6 inches.

In terms of bed features, there is a large gravel confluence bar at the mouth of the Chickley River that contributes to a riffle at the next bend. The large floodplain on the left bank opposite the Chickley River has a side channel, possibly a remnant channel, on its north side, and there is a half-mile-long mid-channel island on the right half of the channel ending at Zoar Outdoor. The vegetated island has several cross chutes that convey water only during high flow. These fluvial

sediment features reflect deposition zones for the additional sediment influx from the Chickley River, so this is an active alluvial zone, encouraged by the channel narrowing past the wastewater treatment plant where higher banks create a semiconfined valley.

The twin span railroad bridge and road bridges across the mouth of the Chickley River are both about 50 percent obstructed by gravel and cobble deposits, reflecting the river's high load of coarse bedload sediment. This material should be removed. The asymmetric flow contributes to a scour hole under the railroad bridge.

The Route 8A bridge over the Deerfield River at Charlemont is a large, high structure with four spans of steel beams and three concrete piers. The left abutment and left pier are on bedrock. The center pier has a 6-foot scour hole, and the top of the footing is exposed, but the depth of footing or piers is unknown. This 1944 bridge replaced a historic long timber bridge damaged in the great 1938 hurricane.

RIVER SEGMENT NO. 12 – Deerfield River

FROM: Charlemont, RM 26
TO: Dam #4, RM
RIVER MILES
LENGTH: 5.6
SLOPE: 0.0017
CHANNEL TYPE:

DRAINAGE AREA, SM: 361
TYPICAL BANKFULL WIDTH: 220'
RIVER CHARACTER: Semiconfined
CORRIDOR CHARACTER: Rural, farms

GENERAL DESCRIPTION

As the Deerfield River flows east out of Charlemont center, the left floodplain narrows beyond the wastewater treatment plant and the confluence bar at Mine Brook. The right floodplain also narrows, forcing the railroad and road close together as they pass the side of Thunder Mountain. Most of this segment is partially confined on the right bank, with limited alluvial unconfined floodplains on portions of the left bank. The right bank is generally steep, forested, stable, and nonalluvial. The river is remarkably uniform with a straight alignment and cobble bed. The channel has a series of long pools and riffles, the latter with shallow summer flow with many cobbles and boulders. The pools are typically 3 to 4 feet deep with gravel substrate.

The left bank has a discontinuous terrace supporting Route 2, with occasional lower narrow floodplain patches. The terraces support the Academy at Charlemont, the Mile Long Farm, and Hall Tavern Farm. A local schist bedrock control extends along 500 feet of the left bank, east of the Academy, creating a mild rapids with a low flow width of only 90 feet. Elsewhere, the bankfull width is typically up to 260 feet with a cobble and gravel bed. The bankfull depth is only 4 to 6 feet in riffle cross sections. Remnants of a potential former oxbow are present on the low left floodplain near East Oxbow Road.

There are significant cobble confluence bars several feet high at most of the tributary confluences. They represent bedload sediments that have moved through the tributaries and are a major source of the Deerfield River substrate material. A large mid-channel island and gravel bars are located at the head of the pool of Dam #4, representing a delta where the Deerfield River bedload sediments settle as they enter the backwater from the dam.

The river character begins to change at Wildler Brook (left bank) and Purinton Road (right bank). The valley bottom is unconfined; the bed material composition has more sand and gravel; and the banks have fine-grain cohesive soil.

The USGS operates a long-term stream gauge in East Charlemont with a watershed area of 361 square miles. FEMA has published an FIS for Charlemont that includes a map of this segment showing a narrow floodway and floodplain that generally corresponds to geologic map deposits of alluvial outwash material.

The FEMA FIS indicates that this long, straight run from its station 27.2 to 21.6 (5.6 miles) has a mean gradient of 0.00172 feet per foot, or 0.17 percent. Based on gauging station flows in this segment, the SSP is a modest 79 watts per square meter, which is barely enough to carry sand, so the channel has little erosion potential. Even during a 100-year flood such as Irene, the SSP in typical 500-foot-wide floodplains is 173 watts, which enables some deposition and no avulsions. This explains why the Hurricane Irene confluence bars are still in place and largely intact, and there is little bank or floodplain surface erosion. In fact, the floodplains were generally deposition areas.

RIVER SEGMENT NO. Mill Brook

FROM: Charlemont
TO:
RIVER MILES
LENGTH: 6 miles
SLOPE: 3.1 percent
CHANNEL TYPE:

DRAINAGE AREA, SM: 11.9
TYPICAL BANKFULL WIDTH: 30 feet
RIVER CHARACTER: Mountain stream

CORRIDOR CHARACTER: Rural, forested

GENERAL DESCRIPTION

Mill Brook is a steep, rocky mountain stream that discharges in the Deerfield River next to the Charlemont Wastewater Treatment Plant where its confluence bar of sediment could attenuate. It is named after the 18th and 19th Century mills that once lined its banks.

The headwaters originate in the mixed forest uplands just south of the Vermont border. The Rosgen type B cobble bed channel flows south parallel to Route 8A through segments with numerous mass bank failures and recent channelization to the Mountain Road bridge. Overbank flooding and extensive deposition occurred during Hurricane Irene down to the former Mill Brook Reservoir and the remnants of its dam and the beautiful restored Bissell wood covered bridge at Route 8A. The downstream channel is in a narrow, rocky gorge to Route 2, then is channelized to the Deerfield River.

This clear cold-water mountain stream has excellent trout habitat, dropping 1,000 feet in just 6 miles for a mean gradient of 3.1 percent.

RIVER SEGMENT NO. North River

FROM: Wilmington, VT

TO: Deerfield River

RIVER MILES

LENGTH: 20 miles

SLOPE:

CHANNEL TYPE: Semiconfined,
types B, C, F

DRAINAGE AREA, SM: 92.9

TYPICAL BANKFULL WIDTH: 80-100 feet

RIVER CHARACTER: Broad, flat gravel and
cobble bottom

CORRIDOR CHARACTER: Rural, small farms
on floodplains

GENERAL DESCRIPTION

The North River is the largest single tributary to the Deerfield River with a total watershed area of 92.9 square miles. Its East Branch originates on the south side of Wilmington, Vermont, and flows south, parallel to Route 112, to the town of Colrain where it joins the smaller West Branch of the North River. The combined waters then flow south 3.3 miles to the Deerfield River at Shelburne. The North River and its East Branch both have flat erosion-prone bottom lands composed of stratified drift outwash deposits, visible along the channel banks and terrace scarps. The bottom lands are used for corn and grazing. The North River is listed as having class B cold-water fisheries and is a stocked stream.

The USGS stream gauge on the North River at Shattuckville has discharge records since 1939 including Hurricane Irene. The latter event is the flood of record, almost three times larger than the second ranked flood, with an average return frequency of just over 500 years. Evidence of the flood is still visible in the valley in the form of road and bridge repairs, bank erosion, and sediment-covered fields.

Beginning in Jacksonville, Vermont, the headwaters were measured at only 12 feet wide with a cobble bed and riffles, a Rosgen type B4 classified channel. Farther downstream approaching the Halifax to Colrain town line, there are massive bank failures along the right side at the confined Halifax Gorge, up to 25 feet high by 300 feet long. This section of Route 112 is prone to erosion damage to the embankment due to the narrow confined valley. Channel dredging appears to have occurred near the intersection of Route 112 and Fowler Road.

Downstream of the Route 112 bridge near Thompson Road, there has been almost continuous floodplain aggradation over agricultural fields parallel to the river. The typical channel bankfull width is 80 to 90 feet while the deposition zone visible on aerial photography is an average of 400 feet wide (Google Earth). The channel is gradually enlarging, and the floodplain aggrading.

In the center of Colrain, there has been flood damage to roads and buildings including the Highway Department garage. The high left bank is eroding at the bend about a half mile downstream of Colrain center.

An 8-foot-high dam segment was observed at Griswoldville at the confluence of the East and West Branches. The timber crib spillway failed at its left end, drying out a mill headrace at the BBA Nonwovens Mill. The low right bank near the dam allowed the Irene event to inundate the unconfined floodplain to a width of over 500 feet. This facility has a NPDES permit and wastewater treatment plant that also receives municipal waste.

The North River becomes fully confined (type F4 channel) with less floodplain as it approaches the Deerfield River with a coarser cobble bed. It has a bankfull width of 105 feet and bankfull depth of 4 feet, then passes under a 120-foot-wide green steel truss bridge with concrete abutments and into the Deerfield River at a popular swimming and fishing hole known as Sunburn Beach.

A USDA Soil Conservation Service report (1990) also discusses the same channel erosion trends, specifically after the 1987 flood.

The West Branch of the North River is a significant tributary and was subject to erosion, floodplain overbank flows, and deposition. The confluence area appears to have been dredged to remove excess sediment. The presence of stratified drift and more recent alluvium along the valley bottom enabled common bank erosion and avulsions during Hurricane Irene between Adamsville and Route 112.

RIVER SEGMENT NO. 13, Dam #4
to Dam #3, Shelburne Falls

FROM: 19

TO: 17

RIVER MILES

LENGTH: 2.6

SLOPE:

CHANNEL TYPE: A1, B3

DRAINAGE AREA, SM: 498

TYPICAL BANKFULL WIDTH:

RIVER CHARACTER: Confined

CORRIDOR CHARACTER: Confined

GENERAL DESCRIPTION

This segment extends from Dam #4 in Shelburne near the high Route 2 bridge to Shelburne Falls at Dam #3. This short segment has three distinct segments beginning at the 35-foot-high dam. The river flows clockwise around a half loop through an inaccessible narrow, steep, rocky ravine parallel to North River Road to the confluence with the North River at Main Street (Route 112). The combined waters then flow south through riffles to the dam's off-site powerhouse, which receives water from a penstock that cleverly cuts across the "loop." After one more riffle 500 feet downstream of the powerhouse, waters pass under Route 2 and enter the one-mile backwater pool to Shelburne Falls. There are several lateral bars and a riffle, probably reflecting bedload from the sediment-rich North River. The bars have grown during and since the 2011 hurricane.

A large, flat terrace is present along the left bank downstream of the North River, with a farm and businesses, and then the terrace is on the right bank below the powerhouse with a lumber mill and DOT maintenance garage. The river remains entrenched to Shelburne Falls without an active floodplain. Water levels rise and fall about 8 feet due to powerhouse needs.

RIVER SEGMENT NO. 14, Dam #3

FROM: Shelburne Falls

TO: RM 17.0

RIVER MILES: N/A

LENGTH: N/A

SLOPE: N/A

CHANNEL TYPE: Bedrock Falls

DRAINAGE AREA, SM: 498.4

TYPICAL BANKFULL WIDTH: 310 (dam pool)

RIVER CHARACTER: Modified, dam

CORRIDOR CHARACTER: Urban village

GENERAL DESCRIPTION

Salmon Falls in the village of Shelburne Falls is a natural waterfall composed of metamorphic gneiss bedrock and is the "headcut" at the upstream end of the 9-mile-long ravine that extends to Upper Road in Deerfield. It has an irregular jagged cascade with a total drop of about 34 feet over a length of 400 feet; the base bedrock has dozens of scoured "potholes." The crest of the falls has a concrete ogee crest spillway dam up to 13 feet high, which is topped by 6-foot-high wood flashboards that provide a total grade change of about 50 feet. Hydroelectric plant #3 is located downstream of the right abutment with a 1,800-foot-long bypass segment. The falls are the first known natural migratory fish barrier upstream from the Connecticut River, but downstream dams are the effective barrier.

The village of Shelburne Falls extends along both banks of the river in the towns of Shelburne and Buckland. State Highway 112 crosses the river upstream of the combined falls and dam using a three-span steel truss bridge, and an adjacent five-span concrete arch trolley bridge was converted to pedestrian use and is decorated with flowers. The village supports a moderate tourist trade with several bookstores, art galleries, and restaurants. Several mills have used water power at the falls.

During Hurricane Irene, the Bridge of Flowers was flowing full, and water spilled over the right bank along State Street in Buckland, damaging commercial property. State Street is on a narrow, low terrace about 5 feet lower than the left upper bank terrace that supports Water Street and Main Street in Shelburne. State Street is mapped in a FEMA 500-year frequency flood hazard area.

The Shelburne and Buckland FEMA studies define the 100-year frequency regulatory base flood at 62,650 cfs. In comparison, the measured flow at the upstream USGS gauge in Charlemont was 54,000 cfs, and the downstream gauge in West Deerfield measured 103,000 cfs. It is likely that Hurricane Irene's peak flows in Shelburne Falls exceeded the 100-year frequency event. Dam #3 obviously raises floodwater levels higher than natural conditions, even when the flashboards break away.

The FEMA FIS for Buckland predicts that the 100-year frequency flood would pass under the Bridge of Flowers while the 500-year event would be well over the bridge. This is a reasonable representation of what actually happened during Hurricane Irene.

RIVER SEGMENT NO. 15 – Deerfield River

FROM: RM 17, Shelburne Falls

TO: RM 13.2 Dam #2

RIVER MILES

LENGTH: 3.8

SLOPE: Impounded

CHANNEL TYPE: Impounded

DRAINAGE AREA, SM: 507

TYPICAL BANKFULL WIDTH: N/A

RIVER CHARACTER: Impounded

CORRIDOR CHARACTER: Rural, forested

GENERAL DESCRIPTION

The Deerfield River downstream of Shelburne Falls consists of several flow-regulated bypass segments and impoundments for the next 3.8 miles. The river and its impoundments are fully confined on both sides by steep, high valley walls without floodplains. Immediately below the falls is a 2,000-foot-long shallow, wide bypass segment leading to the Shelburne Falls Dam #3 powerhouse. The powerhouse is located on the right bank at the end of Cricket Field Road, below a large head pool. At this point, all flow is returned to the natural channel and goes immediately into the backwater pool of the Gardner Falls Dam, an older 30-foot-high hydroelectric dam built in 1904 at RM 15.8.

The Gardner Falls Dam has a 1,200-foot-long headrace and bypass segment to its powerhouse, also on the right bank. The powerhouse discharges into a short, rocky transition channel leading to the 1.5-mile-long (and narrow) backwater pool for the TransCanada Dam #2, a 70-foot-high structure built in 1913.

The railroad is located along the right bank for this entire industrial river segment with its three hydroelectric facilities and essentially no public access. A portion of the modern Mahican-Mohawk Trail extends above the steep left bank, with access near the State Police headquarters on Route 2, but the trail is closed. There are no upstream fish passage facilities, so all fish are blocked by Dam #2.

RIVER SEGMENT NO. 16 – Deerfield River

FROM: RM 13.2, Dam #2
TO: RM 7.5, Lower Road
RIVER MILES
LENGTH: 5.7
SLOPE: 0.0027 feet per foot
CHANNEL TYPE: B, F

DRAINAGE AREA, SM: 562 SM
TYPICAL BANKFULL WIDTH: 250
RIVER CHARACTER: Confined runs
CORRIDOR CHARACTER: Rural gorge

GENERAL DESCRIPTION

This long channel segment is located in a slightly sinuous entrenched valley that is confined by steep forested hill slopes that rise hundreds of feet. The average channel bed slope is a moderate 15 feet per mile (0.0027 feet per foot) with a cobble and bedrock stream bed. The bankfull channel width was measured at two cross sections and tabulated below:

<u>Site</u>	<u>Watershed Area, SM</u>	<u>Bankfull Width, Ft</u>
Bardwells Ferry bridge	528	175 (bedrock influence)
Lower Road bridge	562	252 (alluvial)

The South River State Forest extends along the right bank for much of the length between Dam #2 and Upper Road. The river has intermittent rapids from Dam #2 to Bardwells Ferry bridge and is fully confined without floodplains. The railroad is on the right bank well above the river, then crosses to the left bank prior to the Bardwells Ferry bridge. The Mahican-Mohawk Trail is on the left bank to the bridge. There are no local roads to the river. Two tributaries, Bear River and Hawkes Brook, are deeply incised to meet the grade of Deerfield River.

The Bardwells Ferry bridge over the Deerfield River from Conway to Shelburne is a historic steel truss structure built in 1882 and is on the National Register of Historic Places. It has a one-lane timber deck with a span of 200 feet, supported by stone masonry abutments. The deck is 40 feet above the bedrock channel.

The river remains in a deep, steep-sided valley for the next 3 miles to the Stillwater bridge at Upper Road in Deerfield. The wide, shallow single-stem channel has a mild gradient with gravel and cobbles, plus a few boulders. The parallel banks are 200 to 250 feet apart, except at the bridge, with occasional bedrock exposures. The railroad is halfway up the left bank; the foot trail is halfway up the right bank. There are no floodplains in this entrenched, confined valley until the Upper Road bridge. This river reach is popular with recreational tubers.

RIVER SEGMENT NO. South River

FROM: Ashfield

TO: Deerfield River

RIVER MILES

LENGTH:

SLOPE: Mean 1.3 percent

CHANNEL TYPE: B, F

DRAINAGE AREA, SM: 26.3

TYPICAL BANKFULL WIDTH: 50 feet

RIVER CHARACTER: Incised alluvial

CORRIDOR CHARACTER: Agricultural

GENERAL DESCRIPTION

The South River is a significant tributary to the Deerfield River, with a watershed area of 26.3 square miles. The river originates in the Berkshire uplands of Ashfield west of Ashfield Lake, then flowing east parallel to Route 116 into Conway where it has narrow floodplains at and beyond the village center. South River then flows north in a narrow valley, entering a steeper confined gorge as it downcuts to meet the incised Deerfield River. The confluence is downstream of all Deerfield River dams.

The long-term South River gauge in Conway has annual flood data since 1966 with a 2-year frequency flood flow of 1,906 cfs and a 100-year recurrent peak flow of 12,531 cfs. In contrast, Hurricane Irene was originally reported at 13,000 cfs, then revised to 9,300 cfs, resulting in moderate channel erosion and some infrastructure damage. It is noted that the three highest flows over the almost 50 years of record have been in the past 10 years, so channel erosion is to be expected due to increasing frequency of peak flows. Some riverbanks along Route 116 and in the town center have been reinforced.

Conway does have a FEMA FIS dated December 1979. Portions of South River received a detailed study, other areas an approximate study. It was noted that there was little floodplain development. At that time, there was only 10 years of gauge data, and the three modern floods had not yet occurred. The FEMA FIS is out of date and underestimates peak flows and the floodplain size. It is our understanding that a Vermont-style Fluvial Erosion Hazard Assessment with delineation was scheduled for 2014-2015. However, this type of empirical assessment does not define flood risk elevations.

Bank erosion has occurred and has been repaired in several areas along Route 116 and at the Main Street bridge. High stream power is predicted in the reach approaching Main Street. Stratified drift deposits and legacy deposits at old mill dams and former dams are prone to local erosion.

From the center of town at Route 116 and Pumpkin Hollow Brook northwards to Newell Crossing, South River is semiconfined to unconfined with a moderate slope, sinuous alignment, and floodplain used for agriculture. The segment has a 70-foot drop over a length of 2 miles with a mild mean slope of just 0.006 feet per foot. The river then enters a deepening gorge, extending past Graves Road and the Conway Electric Reservoir and dam, to Deerfield River.

This steep, nearly inaccessible segment has a valley length of 2.2 miles and mean slope of 0.025 feet per foot. The entrenched channel has rapids and cascades with slides and bedrock control. The end of the segment has a confluence sediment bar at Deerfield River.

The Conway Electric Reservoir was reportedly built in 1899 and currently is filled to the dam crest with sandy sediment, storing no water.

RIVER SEGMENT NO. 17, Deerfield Meadows

FROM: RM 8.0

TO: RM 1.5

RIVER MILES

LENGTH: 6.0

SLOPE: 0.001

CHANNEL TYPE: C

DRAINAGE AREA, SM: 662

TYPICAL BANKFULL WIDTH: 170-250 feet

RIVER CHARACTER: Alluvial, unconfined,
meandering

CORRIDOR CHARACTER: Farmland on
floodplains

GENERAL DESCRIPTION

The Deerfield River emerges from its gorge at the Upper Road bridge next to Stillwater Road. The four-span bridge is high above the water, and the 1980 FEMA FIS shows little head loss. The floodplain begins to flare out on both the left and right banks. A small parking lot used by fishermen is located on the right terrace near the south end of the bridge. The gravel bed alluvial channel has a mild bend at the bridge, leading to a sandy point bar under the right span of the bridge. The alluvial Type C channel has a variable width, typically up to 250 feet.

Continuing downstream, the river passes under the multispans, high I-91 bridges with concrete beams and steel beams currently being repaired. A town water supply well is on the right floodplain adjacent to the bridge. A large, lightly vegetated bar with a side channel extends under the bridge along the left bank, probably due to the reduced gradient after the gorge.

From I-91 to the Route 5 bridge 6.5 miles downstream, the Deerfield River flows across a unique active floodplain that has been farmed since the mid 1600s. The meandering channel is generally on the left side of the valley with point bars and several cutoff chutes at the bends. The type of meander bends, with point bars and chutes, are a Brice Type D. The sand and gravel channel after I-91 has a typical bankfull width of 170 to 250 feet and depth of 12 feet, as tabulated below. A major floodplain is on the right bank.

<u>Station</u>	<u>Bankfull Width (ft.)</u>	<u>Bankfull Depth (ft.)</u>
RM 7.6	225	9
RM 7.5	250	?
RM 5.5	198	13
RM 5.0	170	12+
<u>RM 3.5</u>	<u>245</u>	<u>16</u>
Mean	218	12.5

Mill Village Road and a low stone riprap levee run parallel to the right bank near RM 7 at the farm. The river then bends away from the road and meanders past cornfields. The Deerfield Wastewater Treatment Plant is on the right bank near RM 5, and a large bedrock outcrop is visible along the left bank at RM 4.

There are numerous connected and unconnected oxbow lakes and dry meander scrolls on the right floodplain. The 10- to 15-foot-high banks are steep and lightly vegetated, with some bend

erosion. But the large hardwood trees in the buffer zone along most of the segment length indicate there is little meander migration.

Historic Old Deerfield Village is located on a low terrace at the right (east) side of the valley bottom. Several buildings had wet basements and land damage from Hurricane Irene, but it was the lower fields that had deep (8 foot) inundations and were covered with sediment.

The river bends to the right at RM 3 where high bank erosion occurs on the left side opposite a point bar. The Green River then enters on the left near the golf course as one comes to the Route 5 bridge. The natural constriction at and downstream of the Route 5 bridge serves as a throttle, contributing to upstream floodplain inundation and deposition.

The surface of the Deerfield Meadows has a slight gradient from south to north, ranging from elevation 145 along Mill Village Road at Stillwater Road to elevation 125 along Pogues Hole Road in the North Meadows. In contrast, Old Main Street in Old Deerfield Village is on a terrace at elevation 154. The FEMA predicted flood elevations are at 134, 140, 143, and 149 for the 10-, 50-, 100-, and 500-year frequency events, largely due to the Connecticut River backwater.

RIVER SEGMENT NO. Green River

FROM: Headwaters

TO: Deerfield River

RIVER MILES

LENGTH: 30

SLOPE:

CHANNEL TYPE: Confined to
meandering

DRAINAGE AREA, SM: 88

TYPICAL BANKFULL WIDTH: 50

RIVER CHARACTER: Alluvial, gravel bed

CORRIDOR CHARACTER: Rural to urban

GENERAL DESCRIPTION

The Green River headwaters are in Marlboro, Vermont, from where it extends over 30 miles to the Deerfield River in Greenfield, Massachusetts. Their confluence is just 2.5 miles upstream of the Connecticut River, so the Green River has little influence upon the Deerfield River. The Green River has a significant watershed area of 89 square miles. The Vermont section of the river had significant damage during Hurricane Irene, washing out gravel roads and a small dam in the narrow, steep valley.

The river has an important USGS long-term stream flow gauging station near its midpoint. The Massachusetts segment has a FEMA FIS.

The middle segment of the river in Massachusetts begins at a small water supply intake and then enters a wider, flat valley with extensive stratified drift deposits of sand and gravel. A small dam and covered bridge washed out at Eunice Williams Drive, and severe bend erosion occurred downstream, leaving large bars and woody debris. A few barbs have since been installed. There is evidence of a cutoff-type avulsion near Auclair Vincent Drive and abandoned meander loops. A town swimming hole near Nash's Mill Road is partially filled with sediment upstream of the I-91 bridge.

The downstream reach is impounded by dams at River Road and Meridian Street that block fish passage, followed by rapids in a confined urban area. The wastewater treatment plant is near the river's confluence with Deerfield River.

RIVER SEGMENT NO. 18 Outlet

FROM: RM 1.5

TO: RM -, CT River

RIVER MILES

LENGTH: 1.5

SLOPE: 0

CHANNEL TYPE: F

DRAINAGE AREA, SM: 665

TYPICAL BANKFULL WIDTH: 300 feet

RIVER CHARACTER: Backwater

CORRIDOR CHARACTER: Confined

GENERAL DESCRIPTION

The last downstream segment of the Deerfield River extends from the Route 5 bridge in Greenfield to the Connecticut River. This is a confined segment, constricted by high ground on both sides, without floodplain. The right side is the north end of the basalt Pocumtuck Range and a rock quarry. The river is subject to backwater from the Connecticut River and effectively has no gradient. The channel bankfull width is typically 300 feet.

REFERENCES

- Bailey, Robert G., 1995. "Descriptions of the Ecoregions of United States," U.S. Department of Agriculture Forestry Service, Publication 1391, Washington, DC.
- Bent, G.C. and Andrew M. Waite, 2013. "Equations for Estimating Bankfull Channel Geometry and Discharge for Streams in Massachusetts," U.S. Geological Survey Scientific Investigations Report 2013–SISS, Reston, Virginia.
- Bent, Gardner C., 2006. "Equations for Estimating Bankfull Channel Geometry and Discharge for Streams in the Northeastern United States," abstract, Proceedings Eight Interagency Sedimentations Conference, Reno, Nevada.
- Caleb, Slater, January 28, 2010. Letter to Fred Ayer from Massachusetts Division of Fisheries and Wildlife.
- Coleman, Henry, 1841. Report on the Agriculture of Massachusetts, Counties of Franklin and Middlesex, Boston.
- Collins, Matt, 2011. "Flood Frequency Estimate for New England River Restoration Projects," NOAA Fishery Services FS-2011-01.
- Coulton, Kevin, 2014. "Using Soil Data to Map National Floodplains," Water Resources Impact Vol. 16, No. 2.
- Davis, William Morris, 1909. "Geographical Essays," Ginn and Co., Boston.
- Dieck, Jennifer and Larry R. Robinson, 2004. "General Classification Handbook for Floodplain Vegetation in Large River Systems," Chapter 1 of Collection of Environmental Data, U.S. Geological Survey.
- EOEA, 2004. "Deerfield River 5-Year Action Plan," Commonwealth of Massachusetts, Boston, Mass.
- EOEA, 2004. "Deerfield River Assessment Report," Commonwealth of Massachusetts, Boston, Mass.
- Friesz, P.J., 1996. "Geohydrology of Stratified Drift and Streamflow in the Deerfield River Basin, Northwestern Massachusetts," WRIR96-4115, U.S. Geological Survey.
- Happ, Stafford and G.C. Dobson, 1940. "Some Principles of Accelerated Stream and Valley Sedimentation," Tech Bulletin 695, U.S. Dept. of Agriculture.

- Hoover, David and Sharon Waltman, 2013. "Soil Survey Information for Floodplain Mapping," USDA-NRCS, National Soil Survey Center.
- Howard, A.D., 1996. "Modeling Channel Evolution and Floodplain Morphology," in *Floodplain Processes*, Edited by Malcolm G. Anderson et al., John Wiley & Sons.
- Jacobs, Jennifer, 2010. "Estimating the Magnitude of Peak Flows for Steep Gradient Streams in New England," prepared for The New England Transportation Consortium NETCR81, Project No. NETC-04-3.
- Jain, Vikrant, Kirstin Fryirs, and Gary Brierly, 2008. "Where Do Floodplains Begin? The Role of Total Streampower and Longitudinal Profile Form on Floodplain Initiation Processes," *GSA Bulletin* V. 120. N. ½, P. 127-141.
- Knighton, A. D., 1999. Downstream Variation in Stream Power. *Geomorphology* 29(3-4):293-306.
- Lane, E. W., 1955. The Importance of Fluvial Morphology in Hydraulic Engineering. *In Proceedings of: American Society of Civil Engineering, Journal of the Hydraulics Division*. 81(paper 745):1-17.
- Lombard, Pamela J. and Gardner C. Bent, 2015. "Flood Inundation Maps for the Deerfield River," Scientific Investigation Report 2015-5104, U.S. Geological Survey.
- MacBroom, James, G., 2014. "Applied Fluvial Geomorphology, 2nd edition, Class Notes for FES 729", Yale University, New Haven.
- Merwade, Venkatesk, 2014. "Flood Inundation Mapping Using SSURGO Soil Data," American Water Resources Association, 2014 Spring Specialty Conference, Salt Lake City.
- Montgomery, David and John Buffington, 1993. "Channel Classification, Prediction of Channel Response, and Assessment of Channel Condition," Washington Timber, Fish, and Wildlife, TFW-SH 10-93-002, Seattle.
- Nanson, G.C. and J.C. Croke, 1992. "A Genetic Classification of Floodplains," *Geomorphology*, 4, 459-486, Elsevier Science Publishers.
- NCHRP, 2004. "Handbook for Predicting Stream Meander Migration," Transportation Research Board of the National Academies, Report 533, Washington, DC.
- Noe, Greg, 2013. "Mapping Floodplains in the Chesapeake Bay Watershed," USGS National Research Program, Reston, Virginia.

- Olsen, Scott, 2003. "Flow Frequency Characteristics of Vermont Streams," USGS WRIR 02-4238, U.S. Department of Interior.
- River Management Program, 2006. "Vermont Regional Hydraulic Geometry Curves," Vermont Department of Environmental Conservation.
- Schiff, R., J. S. Clark, and S. Jaquith, 2008. The Vermont Culvert Geomorphic Compatibility Screening Tool. Prepared by Milone & MacBroom, Inc. with the VT DEC River Management Program, Waterbury, VT.
- Schiff, R., J. C. Louisos, E. Fitzgerald, J. Bartlett, and L. Thompson, 2015. The Vermont River Sensitivity Coarse Screen. Prepared by Milone & MacBroom for the Vermont Land Trust and its conservation partners, Waterbury, VT.
- Smith, Mark, Roy Schiff, Arlene Olivero, and James MacBroom, 2008. "The Active River Area," The Nature Conservancy, Boston, Mass.
- Soar, Phillip and Colin Thorne, 2001. "Channel Restoration Design for Meandering Channels" ERDC CR-01-1, US Army Corps of Engineers, Vicksburg, Mississippi.
- Theiling, Charles et al., 2012. "Hydro-Geomorphic Classification and Potential Vegetation Mapping for Upper Mississippi River Bottomland Restoration," ISBN978-953-51-0361-5, U.S. Army Corps of Engineers.
- USDA, 1967. "Soil Survey, Franklin County, Massachusetts," Soil Conservation Service.
- USDA, 1990. "North River Flood Plain Management Study," Soil Conservation Service, Amherst, Massachusetts.
- Walter, Meghan and Richard Vogel, 2010. "Increasing Trends in Peak Flows in the Northeastern United States and Their Impact on Design," 2nd Joint Federal Interagency Conference, Las Vegas, NV.
- Wandle, S. William, 1984. "Gazetteer of Hydrologic Characteristics of Streams in Massachusetts – Connecticut River Basin," WRIR-84-4282, U.S. Geological Survey.
- Wiitala, Sulo, Karl Jetter, and Allan Sommerville, 1961. "Hydraulic and Hydrologic Aspects of Floodplain Planning," Water Supply Paper 1526, U.S. Geological Survey.
- Wolman, M. G., 1954. A Method of Sampling Coarse River-Bed Material. Transactions of American Geophysical Union 35:951-956.

Yellen, B., J. D. Woodruff, L.N. Kratz, S.B. Mabee, and A.M. Martini, 2014 (in press). "Source, Conveyance, and Fate of Suspended Sediments Following Hurricane Irene, New England USA." *Geomorphology*.

4297-03-mr2917-rpt.docx

Appendix F JACOBS OVERVIEW

In 2010, a study was led by Dr. Jennifer Jacobs to develop a set of regression relationships to predict peak flows with recurrence intervals of 2, 5, 10, 25, 50, 100, and 500 years in ungaged, unregulated, steep streams in New England. The resulting methods are most appropriate for streams where slopes exceed 50 ft/mi. The project was a collaboration between the New England Transportation Consortium (NETC), the University of New Hampshire (UNH), and Tufts University. The study was commissioned to address apparent deficiencies of the regression relationships published for all of the New England states by the United States Geological Survey (USGS) for predicting peak flows in steep watersheds (Jacobs, 2010; Hodgkins, 1999).

F.1 Considered Basins and Characteristics

184 watersheds across New England, excluding Rhode Island, were selected for inclusion in the study. The main channel slope for the 184 watersheds ranged from 50 – 625 ft/mile. Peak flows for each watershed were estimated utilizing the PeakFQ software developed by the USGS. Based on previous studies, a set of potential explanatory variables were identified and calculated for each watershed. The following basin characteristics were considered as possible explanatory variables:

- Drainage Area (mi²),
- Basin Length (mi),
- Basin Perimeter (mi),
- Basin Slope (ft/mi),
- Relief (ft),
- Width (mi),
- Channel Length (mi),
- Main Channel Slope (ft/mi),
- Mean Annual Precipitation (in),
- Percent of Basin Area of Lakes or Ponds,
- Soil Index,
- Storage,
- Percent Forest,
- Mean Basin Snowfall, and
- 24-hr 2-year Rainfall Intensity.

F.2 Regression Equations

Development of the regression equations is described in Jacobs (2010) and not repeated here. The final peak-flow regression equations are as follows:

$$Q_2 = 0.01601 A^{0.889} P^{2.12}$$

$$Q_5 = 0.01965 A^{0.889} P^{2.19}$$

$$Q_{10} = 0.02430 A^{0.891} P^{2.21}$$

$$Q_{25} = 0.03387 A^{0.893} P^{2.20}$$

$$Q_{50} = 0.04372 A^{0.895} P^{2.18}$$

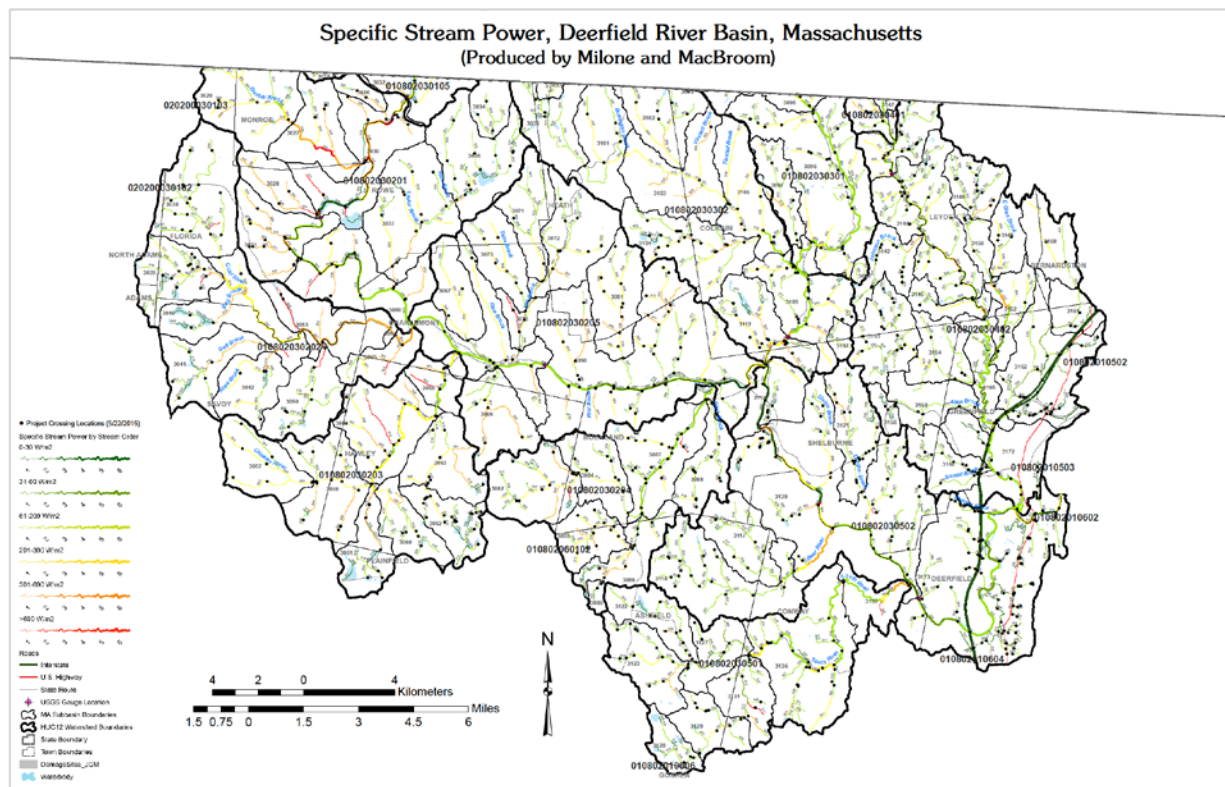
$$Q_{100} = 0.05765 A^{0.897} P^{2.15}$$

where Q is peak flow in cubic feet per second, A is drainage area in square miles, and P is mean annual precipitation in inches based on the PRISM 1961 – 1990 maps (Daly et al. 1994, Daly et al. 1997). Details on error estimates and appropriate equation application methods and techniques are also provided by Jacobs (2010).

F.3 References

- Daly, C., R.P. Neilson, and D.L. Phillips. 1994. A statistical-topographic model for mapping climatological precipitation over mountainous terrain. *Journal of Applied Meteorology* 33: 140-158.
- Daly, C., G.H. Taylor, and W.P. Gibson. 1997. *The PRISM approach to mapping precipitation and temperature*. In reprints: 10th Conf. on Applied Climatology, Reno, NV, American Meteorological Society, 10-12.
- Hodgkins, G. 1999. *Estimating the Magnitude of Peak Flows for Streams in Maine for selected recurrence intervals*. U.S. Geological Survey Water –Resources Investigations Report 99-4008.
- Jacobs, J. 2010. *Estimating the Magnitude of Peak Flows for Steep Gradient Streams in New England. Prepared for The New England Transportation Consortium. (NETCR81), Project No. NETC 04-3. Available on-line: http://www.ct.gov/dot/LIB/dot/documents/dresearch/NETCR81_04-3.pdf.*

Appendix G SPECIFIC STREAM POWER MAP



Appendix H CULVERT FLOW CAPACITY

H.1 Method Theoretical Details

H.1.1 Bentley's CulvertMaster

To calculate the flow through a culvert, CulvertMaster assesses the culvert through an inlet control assumption and an outlet control assumption to compare resulting headwater depths. The inlet control assumption computes the upstream headwater depth that results from the constricting culvert entrance while neglecting barrel friction and other minor losses. On the other hand, the outlet control assumption considers losses such as friction and entrance in computing the upstream headwater elevation. The greatest calculated headwater from each assumption becomes the controlling headwater depth from which flow is computed. These assumptions use methods from *Hydraulic Design Series No. 5: Hydraulic Design of Highway Culverts (1985)*.

For inlet control, the hydraulic control section is the culvert entrance, therefore losses by the entrance constriction supersede other minor losses such as barrel friction. In general, barrel flows are supercritical, leaving the outlet velocity to be determined using frontwater gradually varied flow profiles. CulvertMaster computes the inlet control headwater depth using equations from the design nomographs published in HDS-5. This project requires only conditions involving the inlet being submerged, therefore only the submerged inlet control working equation is listed below:

$$\frac{HW_i}{D} = c \left[\frac{Q}{AD^{0.5}} \right]^2 + y - 0.5S^2$$

where HW_i is the headwater depth above the inlet invert (ft), S is the culvert barrel slope (ft/ft), D is the interior height of the culvert barrel, Q is the discharge (ft³/s), A is the cross-sectional area of the culvert, and y and c are constants dependent on the shape, material, and inlet edge of the barrel. For mitered inlets, the slope correction factor should be changed from $-0.5S$ to $+0.7S$. This equation can be applied only to submerged inlets with $\frac{Q}{AD^{0.5}} \geq 4.0$.

The outlet control assumption computes headwater depth by summing all head losses (entrance, friction, exit) using the following equation:

$$HW_o + \frac{V_u^2}{2g} = TW_o + \frac{V_d^2}{2g} + H_L$$

where HW_o is the headwater depth above the outlet invert, V_u is the approaching upstream velocity, TW_o is the tailwater depth above the outlet invert, V_d is the exit velocity, and H_L is the sum of all losses (entrance, friction, and outlet). Rather than using the simplified procedures and nomographs suggested by HDS-5, which result in degenerative solutions in low-flow conditions that require performance curve analysis, CulvertMaster has instead employed a set of gradually varied flow algorithms that more accurately analyze partial flow, pressure flow, composite pressure and free surface flows, composite flow regime profiles, and adverse and horizontal culverts.

There are two methods involved in analyzing gradually varied flow; the direct step method, and the standard step method. The direct-step method iterates over a range of depth changes that results from backwater. In doing so, it solves for the distance interval that results in the correct amount of

head loss in the energy balance; these distance intervals total to be the distance of the flow profile. The following equation provides an expression for a basic energy balance for the culvert:

$$H_1 = H_2 + h_f + h_e$$

where H_1 is the total head at section 1, H_2 is the total head at section 2, h_f is the friction head loss, and h_e is the eddy head loss. Total head at each section can be computed using:

$$H = Z + \frac{V^2}{2g}$$

where H is the total head, Z is the water surface elevation above the datum, and V is the velocity at the end of the section. For most channels, the eddy loss is negligible and is therefore assumed to be zero by CulvertMaster. This leaves the friction loss (h_f) to be computed using the following equation:

$$h_f = S_f \Delta x = \frac{1}{2} (S_1 + S_2) \Delta x$$

where S_f is the friction slope, S_1 and S_2 are the friction slopes at the start and end of the section, and Δx is the change in horizontal distance in the section. The standard-step method uses the same three equations, however the calculations are performed for a number of sub-reaches from one section to the next. The depth is iterated to the correct value that produces a balanced energy equation. This process continues until the slope friction relationship yields an average friction slope (S_f); balancing the energy between the sub-reaches.

To account for the losses resulting from the culvert material's roughness, CulvertMaster uses Chezy's equation and Manning's equation:

$$\text{Chezy: } Q = CA\sqrt{RS}$$

$$\text{Manning: } C = K \frac{R^{1/6}}{n}$$

where R is the hydraulic radius, S is the friction slope, A is the cross-sectional flow area, C is the Chezy roughness, n is Manning's roughness, and K is a constant (1.0 m, or 1.49 ft).

In comparison to HY-8, the results will generally be very similar. However, there are several instances where CulvertMaster's estimates are more accurate than those in HY-8. To calculate the inlet control headwater, CulvertMaster uses inlet control equations from HDS-5, while HY-8 uses polynomial curve fits. For M2 backwater flow profiles, HY-8 simplifies the calculation for tailwater when the outlet is submerged and has a discharge in excess of full-flow. This is due to HY-8 assuming a pressurized flow throughout the full length of the culvert, while CulvertMaster computes the M2 profile backwater curve and will transition to pressurized flow where the flow profile reaches the top of the culvert.

H.1.2 Manning's Equation

Manning's Equation is one of the most commonly used equations for estimating open channel flow. Manning's Equation is only applicable under uniform flow conditions, when slope of the channel bottom is equivalent to the slope of the energy grade line and water surface. This is a reasonable assumption for non-pressurized flow through a uniform cross-section. Manning's equation is as follows:

$$Q = VA = \left(\frac{1.49}{n}\right) A R^{2/3} \sqrt{S}$$

where Q is the flow rate (ft³/s), V is velocity (ft/s), A is the flow area (ft²), R is the hydraulic radius (ft), S is channel slope (ft/ft), and n is the Manning's roughness coefficient, identified through tables, "type" photographs published in the literature, and/or visual estimates based on field conditions using experience.

H.2 Culvert Master Interface

To solve for discharge using CulvertMaster, there are several types of inputs required in the "Quick Culvert Calculator" including maximum allowable headwater, tailwater elevation, and properties of the section, inlet, and inverts. The "Culvert Calculator" outputs headwater elevations based on inlet and outlet control, and exit results such as discharge, velocity, and depth.

In general, culverts are designed using an initial discharge that is based on precipitation intensity and upstream watershed area; this is the discharge that the design needs to accommodate. The initial discharge is used to select a culvert from a variety of dimensions and styles by iterating for an optimal discharge that accommodates the initial discharge, meets headwater and tailwater design restrictions, and fits in the allotted budget. The iteration for the headwater and tailwater elevations are based on calculating and comparing the inlet controlled headwater/tailwater depth, and the outlet controlled headwater/tailwater depth given the selected culvert's design discharge (based on its dimensions, not the initial discharge). The larger of the two becomes the design headwater and tailwater depth which the inlet and outlet dimensions must accommodate. Both the design discharge (dependent on culvert dimensions) and headwater/tailwater elevations are adjusted until all requirements and restrictions are satisfactory.

Similarly, the "Quick Culvert Calculator" uses the specified culvert properties along with the maximum allowable headwater and tailwater elevation to calculate the corresponding discharge. Using the user-specified "Maximum Allowable HW" as the headwater elevation, it solves for discharge under an inlet control and outlet control condition; the lesser of the two calculated discharges is the value outputted by the "Calculator." Using this lesser value as the critical discharge, it calculates the headwater elevation of the non-controlling inlet/outlet, and outputs it to the "Headwater Elevations" section of the calculator listed as "Inlet Control" and "Outlet Control."

H.3 Culvert Master Performance Curve

As an example, here are inputs and outputs from the "Quick Culvert Calculator" along with its corresponding performance curve for a culvert (ID: 9485, xy4251696672754228) in the South River sub-watershed. From the "Culvert Calculator," the user-specified "Maximum Allowable HW" is 100ft; this means that when solving for discharge in an inlet or outlet controlled culvert, the headwater is set to 100 ft (Figure H-1). From the performance curve, there are two discharges; one solved from inlet control and the other from outlet control (Figure H-1). Because the outlet controlled discharge (blue curve, Figure H-2) is less than the inlet controlled discharge calculated for the "Maximum Allowable HW", the critical discharge is 100.82 cfs which is outlet controlled (Figure H-2). The "Inlet Control" and "Outlet Control" output boxes correspond to the headwater elevation at which that type of control gives the same value as the critical discharge (Figure H-1). In this case, the outlet controlled headwater is 100ft (remember: this gave the lesser of the two calculated discharges from outlet/inlet control from

setting both headwater elevations to 100ft), and the inlet controlled headwater is 99.67ft. This can be seen on the graph when looking for the corresponding headwater elevation at discharge equal to 100.82 cfs on the inlet curve (red curve, Figure H-2).

Figure H-1: Inputs (black) and Outputs (grey) of "Culvert Calculator" for CulVID: 9485, xy4251696672754228

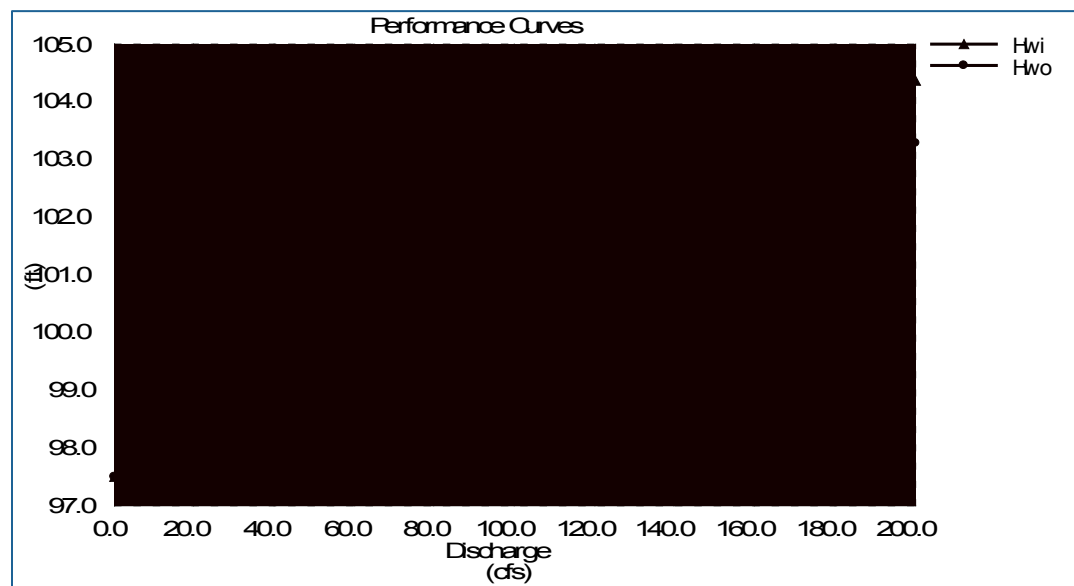


Figure H-2: CulvertMaster performance curve from Figure H-1 inputs. The blue and red lines on the graph show the discharge predicted for a given HW elevation for outlet and inlet control, respectively. Based on a maximum allowable HW of 100 ft, looking horizontally across the culvert is outlet controlled (e.g., outlet control results in a smaller discharge that can be accommodated), with a maximum discharge that can be accommodate of 100.82 cfs (Figure H-1 provides exact value).

H.4 Estimating Entrance Coefficients and Manning's Roughness

The "Culvert Calculator" requires that the user specifies the shape, material, and inlet entrance type to calculate discharge. The shape and material correspond to Manning's roughness number (n), while the entrance coefficient (K_e) is dependent on the inlet entrance type.

Assigning Manning's roughness values to each culvert is generally straightforward², however, there is uncertainty when it comes to culverts made of corrugated metal pipes due to unknown corrugation types and sizes; leaving the range of n quite large for this type of culvert.

The listed inlet entrance type for each culvert can be inaccurate when it comes to assigning a K_e value due to various levels of degradation of the structure and/or blockages. Consequently, each culvert's inlet must be assigned a K_e value from visual inspection through pictures.

H.5 Effects of Tailwater Elevation Variation on Critical Discharge

The goal of this evaluation is to identify the most appropriate tailwater condition under which the critical discharge is determined in CulvertMaster, given the three headwater conditions. Culvert 9485 is used in this example, Figure H-3. The conditions examined are:

$$HW_1 = 1.0D$$

$$HW_2 = 1.2D$$

$$HW_3 = \text{Road elevation less 1ft}$$

$$TW_1 = 0.75D \text{ for culvert slope } > 2\%$$

$$TW_2 = 1.0D \text{ for culvert slope } < 2\%$$

$$TW_3 = D + 1 \text{ ft}$$

To evaluate the effect of a change in tailwater elevation on the critical discharge output by the "Quick Culvert Calculator," tailwater elevation was plotted against the critical discharge for two culverts (culVID: 9485, 9926). Alongside the plots are the matrices used for the various headwater and tailwater elevation combinations with their corresponding critical discharge, Figure H-4. The discharges computed by the "Culvert Calculator" that are based on inlet control are highlighted in green, while the outlet controlled discharges are the remaining. Broadly speaking, the critical discharge decreases as tailwater increases (Figure H-4). This first example is a round concrete culvert (ID: 9485), with a 4.5ft inlet and 5ft outlet. The slope of the culvert is 3.3%, which suggests the use of TW1. This is true for the "HW3" curve; however, the "HW1" curve shows that the TW2 condition provides the greatest discharge, while the "HW2" curve has the greatest discharge at an elevation between TW2 and TW3.

² Tabulated values for this project were based on those published in the Michigan DOT's Drainage Manual: https://www.michigan.gov/documents/MDOT_MS4_App_91727_7.05_B_Drainage_Manual.pdf



Figure H-3: Culvert 9485 inlet and outlet. The inlet (left) has a diameter of 4.5 ft. The outlet (right) has a diameter of 5 ft.

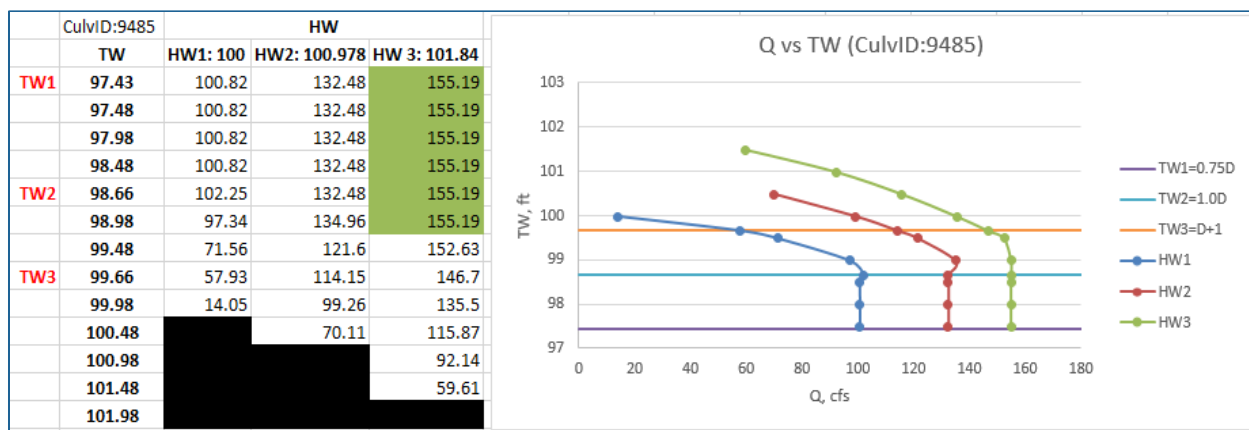


Figure H-4: Headwater conditions with varying tailwater matrix (left), Discharge vs. Tailwater plot (right) for CulvID: 9485, xy4251696672754228. Note: CulvertMaster was run using a diameter of 4.5ft (inlet dimension).

The second example is a round culvert made of a corrugated metal pipe with a diameter of 10ft at both the inlet and the outlet (ID: 9926, Figure H-5). The slope of the culvert is 1.8%, suggesting the TW2 condition; however, the TW1 condition provides a larger discharge than TW2 with the greatest discharge for all three curves between the TW1 and TW2 (Figure H-6).

In summary, these two example culverts suggest that the steeper sloping culverts (>2%) experience the greatest discharge when the outlet is submerged within 1ft above the top of the outlet, while milder sloping culverts (<2%) have the greatest discharge when the tailwater elevation is between 75-100% of the outlet height. The discharges are most sensitive to tailwater elevation when the pressure gradient between the upstream and downstream ends of the culvert becomes small, or in other words, when the both the inlet and outlet are submerged (portion of curves above TW2). This explains the minimal changes in discharge when the tailwater elevation is less than the height of the outlet; with

only one end submerged (inlet), the pressure gradient increases as the discharge sensitivity to tailwater decreases.



Figure H-5: Culvert 9926 inlet (top) and outlet (bottom) with a diameter of 10 ft on both sides.

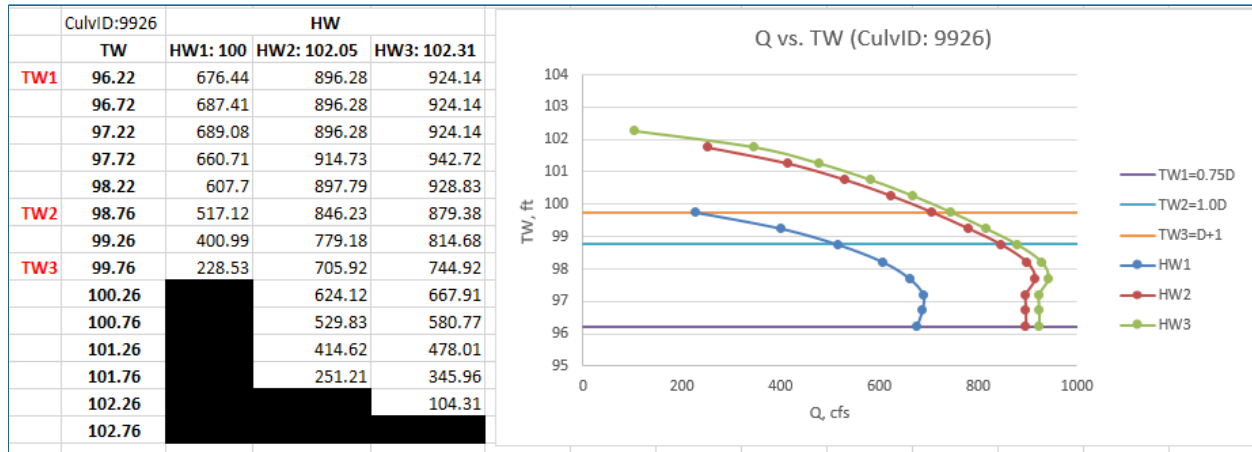


Figure H-6: Headwater conditions with varying tailwater matrix (left), Discharge vs. Tailwater plot (right) for CulvID: 9926, xy4248241272760207

H.6 Flow Sensitivity to Manning's Roughness Coefficient

Manning's roughness coefficient is used in flow calculations to describe a material's surface roughness of open channel flows. To calculate volumetric flow, the equation is as follows:

$$Q = \frac{A \cdot K_n}{n R^{2/3} S^{1/2}} \quad \text{Eq. 1}$$

where A is the cross-sectional area of flow, K_n is 1.0 for SI units or 1.486 for English units, n is Manning's roughness coefficient, R is the hydraulic radius, and S is the slope of the channel/pipe. Given the definition of the hydraulic radius being

$$R = \frac{A}{P} \quad \text{Eq. 2}$$

where P is the wetted perimeter of the channel, and A is the cross-sectional area of flow. By substituting eq. 2 into eq. 1, the equation for flow becomes:

$$Q = \frac{A^{1/3} P^{2/3} K_n}{n S^{1/2}} \quad \text{Eq. 3}$$

For our purposes, the slope (S) and K_n remain constant; leaving the cross-sectional area of flow (A), wetted perimeter (P) and Manning's roughness (n) as variables in this analysis. From the equation, Manning's roughness is inversely related to flow, which is represented in Figure H-7 as a negative correlation. Despite CulvertMaster requiring headwater and tailwater elevation inputs, the cross-sectional area and wetted perimeter do not remain constant as Manning's varies. This is due to the changing roughness depths implied by a changing Manning's coefficient, causing the cross-sectional area and wetted perimeter to decrease and increase, respectively (Table H-1). These two variables—cross-sectional area and wetted perimeter—have opposite effects on flow; however, the wetted perimeter has a larger exponent (2/3) than cross-sectional area (1/3) and therefore drives the increase in flow. On the other hand, the wetted perimeter term has a smaller increasing effect than Manning's

roughness' decreasing affect due to its exponent being less than that of Manning's. This explains the shape of the curve shown on Figure H-7 and in Table H-1.

Table H-1: CAPS ID 9926 using the HW₃ and TW₃ conditions with a fixed Ke of 0.7 in CulvertMaster. The variation of n affects Q by also changing A and P.

CAPS ID 9926: HW ₃ & TW ₃ Condition @ Ke=0.7				
Input	CM Outputs		Calculated	
n	Q, cfs	V, ft/s	A, ft ²	P, ft
0.011	756.62	9.63	78.56906	0.072596502
0.012	753.87	9.6	78.52813	0.082288596
0.013	750.91	9.56	78.54707	0.092229015
0.014	747.75	9.52	78.54517	0.102424218
0.015	744.4	9.48	78.52321	0.11284521
0.016	740.87	9.43	78.56522	0.123399539
0.017	737.17	9.39	78.50586	0.13418672
0.018	733.31	9.34	78.51285	0.145045918
0.019	729.28	9.29	78.50161	0.156015687
0.02	725.12	9.23	78.56121	0.166990373
0.021	720.81	9.18	78.51961	0.178117583
0.022	716.38	9.12	78.55044	0.189195412
0.023	711.82	9.06	78.56733	0.200291143
0.024	707.16	9	78.57333	0.211393442
0.025	702.39	8.94	78.56711	0.222480934
0.026	697.53	8.88	78.55068	0.233542058
0.027	692.58	8.82	78.52381	0.244560093
0.028	687.56	8.75	78.57829	0.255380294
0.029	682.47	8.69	78.5351	0.266272403
0.03	677.32	8.62	78.57541	0.276926886
0.031	672.11	8.56	78.51752	0.287644111
0.032	666.86	8.49	78.54653	0.298091222
0.033	661.56	8.42	78.57007	0.30841245

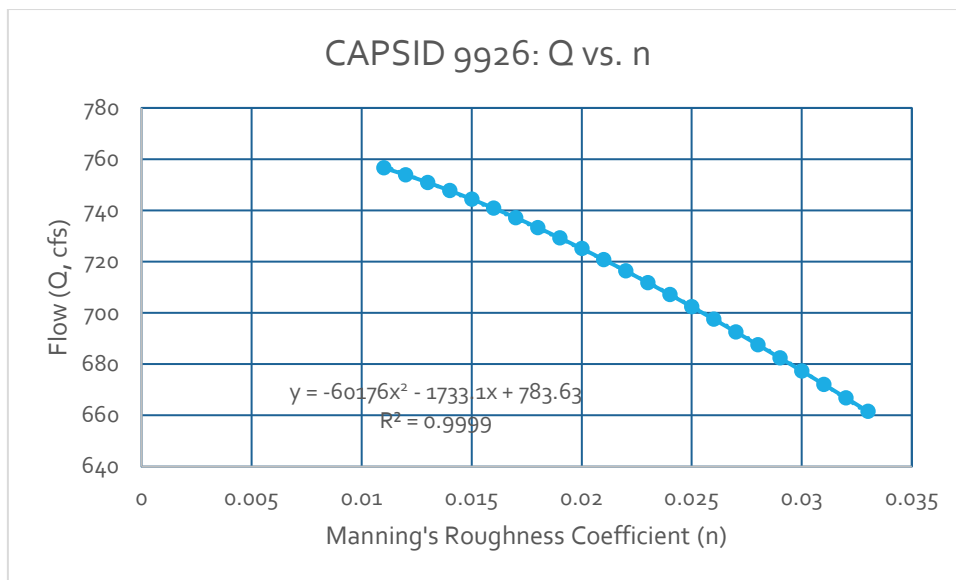


Figure H-7: Plot of CAPS ID 9926 (xy4248241272760207) volumetric flow with a varying Manning's roughness coefficient fixed at HW₃ and TW₃ elevations.

H.7 Flow Sensitivity to Varying Entrance Coefficients

Minor loss coefficients, also known as the entrance loss coefficient in this case (K_e), is used to represent the efficiency of the inlet in bringing upstream flow into the culvert; ultimately it is used to calculate head loss using this equation

$$H_L = K_e \frac{V^2}{2g} \quad \text{Eq. 4}$$

where H_L is head loss, K_e is the entrance loss coefficient, V is velocity, and g is the gravitational constant. Given the definition of volumetric flow (Q) is

$$Q = VA \quad \text{Eq. 5}$$

where V is velocity, and A is the cross-sectional area of flow. The combination of the two equations (Eq. 4 and 5) gives the equation below:

$$Q = A * \sqrt{\frac{H_L}{K_e}} * \sqrt{2g} \quad \text{Eq. 6}$$

In this equation, the cross-sectional area (A), gravity ($\sqrt{2g}$), and head loss (H_L) terms are constant, leaving K_e to be the driving effect on flow. Despite eq. 4 indicating that head loss is dependent on K_e , CulvertMaster requires headwater and tailwater elevations where the difference between the two is a fixed head loss while varying K_e . As K_e increases, flow (Q) decreases through an inverse power relationship as shown in Figure H-8.

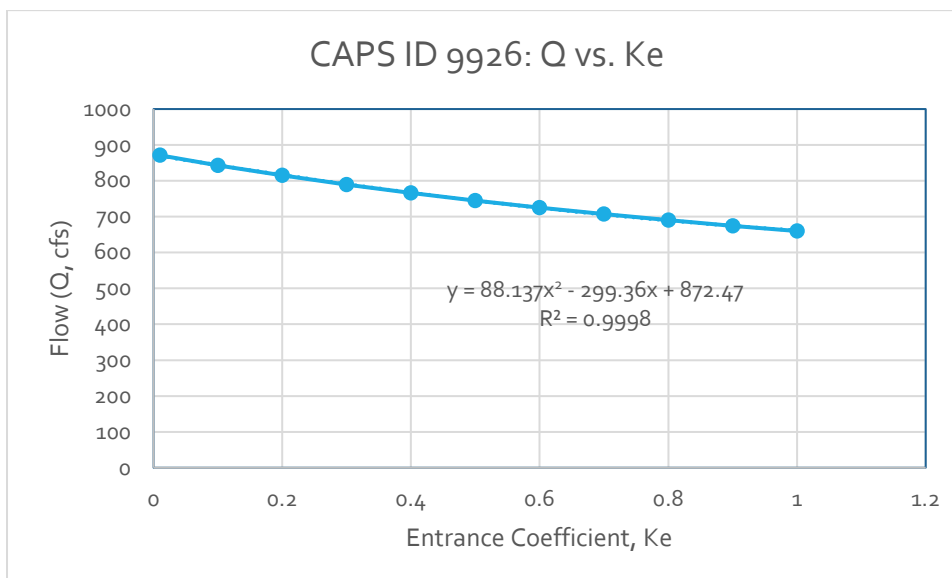


Figure H-8: Plot of CAPS ID 9926 (xy4248241272760207) volumetric flow with a varying entrance coefficient fixed at HW₃ & TW₃ elevations and a Manning's of 0.024.

Appendix I USGS RPF E OVERVIEW

I.1 Overview of Methodology

One of the most widely used methods for estimating flood discharges at select annual exceedance probabilities (AEPs) is through the development of Regional Peak Flow Equations (RPF Es). The U.S. Geological Survey (USGS) has developed RPF Es specific to each state based on data collected by their network of stream gauges.

RPF E equations are developed utilizing multiple-regression techniques to identify basin characteristics (independent variables) that best estimate flood discharges. Generalized least-squares regression techniques are preferred over ordinary least-squares regression, as they compensate for differences in record length and facilitate cross-correlation of concurrent records among stream gauges. A variety of basin characteristics are typically considered for inclusion, and both transformed and untransformed values are included. Transformations are useful for obtaining the most linear relations, and the most effective translation technique varies by characteristic. Common transformations include logarithms, square roots, squares, and raising the values to the -0.125 power. Statistical software packages enable the use of correlation data and stepwise linear regression to identify the most significant explanatory variables.

The USGS-developed RPF Es for MA, NH, and VT are provided below. For details, please refer to the USGS Scientific Investigation Reports published for the respective states.

I.2 MA RPF Es

It should be noted that the equations were updated in 2017 by Zarriello. Unfortunately the updated equations were not available in time for utilization in this project. Instead, the Massachusetts RPF Es developed by Wandle (1983) were utilized in this project. Wandle (1983) developed three unique RPF Es based on region. Those developed for the western Massachusetts region were utilized in this project.

$$Q_2 = 0.933 A^{0.970} SI^{0.158} E^{0.429}$$

$$Q_5 = 1.05 A^{0.969} SI^{0.178} E^{0.469}$$

$$Q_{10} = 1.23 A^{0.969} SI^{0.187} E^{0.480}$$

$$Q_{25} = 1.31 A^{0.969} SI^{0.205} E^{0.505}$$

$$Q_{50} = 1.41 A^{0.970} SI^{0.215} E^{0.520}$$

$$Q_{100} = 1.51 A^{0.971} SI^{0.225} E^{0.533}$$

Where

- Q_T is the estimated flood discharge, in cubic feet per second, at a T-year recurrence interval;
- A is the drainage area of the basin, in square miles;

- SI is the slope of the main channel, in feet per mile, determined between points 10- and 85-percent up the main channel from the selected stream site extended to the drainage divide; and
- E is the mean basin elevation, in feet.

1.3 NH RPFES

The New Hampshire RPFES were last updated in 2008 (Olson, 2009). The log-Pearson Type III probability distribution was utilized for estimating flood-discharge magnitude and frequency from the annual maxima series data for 117 stream gauges across the state. Record extension was utilized to improve estimates of flood discharges at locations with records of only 10 to 15 years. A total of 110 basin characteristics were considered in the generalized least-squares regression. Logarithmic base-10 transformations were utilized on all final variables except for the percentage of the basin covered by wetlands. The final regression equations for estimating flood discharges on ungaged, unregulated streams in rural drainage basins in New Hampshire are as follows:

$$Q_2 = 2.60 A^{0.958} P^{1.5} 10^{-0.0245(W)} S^{0.205}$$

$$Q_5 = 3.23 A^{0.929} P^{1.73} 10^{-0.0245(W)} S^{0.211}$$

$$Q_{10} = 3.88 A^{0.912} P^{1.83} 10^{-0.0247(W)} S^{0.211}$$

$$Q_{25} = 4.99 A^{0.892} P^{1.90} 10^{-0.0250(W)} S^{0.207}$$

$$Q_{50} = 5.96 A^{0.879} P^{1.94} 10^{-0.0252(W)} S^{0.203}$$

$$Q_{100} = 7.13 A^{0.867} P^{1.98} 10^{-0.0254(W)} S^{0.198}$$

Where

- Q_T is the estimated flood discharge, in cubic feet per second, at a T-year recurrence interval;
- A is the drainage area of the basin, in square miles;
- P is the basinwide mean of the average April precipitation, in inches, determined with the PRISM 1971 – 2000 April precipitation dataset (PRISM Group, Oregon State University, 2006c) resampled with bilinear interpolation to a 180-ft-cell resolution;
- W is the percentage of the basin with land cover categorized as wetlands or open water, plus 1.0, from the National Land Cover Data (Multi-Resolution Land characteristics Consortium, 2003) using a GIS. Waterbody areas from the National Hydrography Dataset (U.S. Geological Survey, 2007b), which include lakes, ponds, and swamps were used in areas north of the New Hampshire-Quebec border where the NLCD does not extend; and
- S is the slope of the main channel, in feet per mile, determined between points 10- and 85-percent up the main channel from the selected stream site extended to the drainage divide using the ArcHydro Software (Environmental Systems Research Institute, Inc., 2008) and elevation datasets derived from the National Elevation Dataset (U.S. Geological Survey, 2007a).

The equations are valued for the range of explanatory values used in development of the equations, listed in Table I-1. Accuracy of the equations and methods for calculating 90-percent confidence intervals are provided by Olson (2009) but were not utilized in this project. Alternative, drainage area based only equations are also provided for basins with characteristics outside those listed in Table I-1.

Table I-1: Range of explanatory variables valid for NH RPFES

Explanatory variable	Minimum	Maximum	Mean
Drainage area, in square miles	0.70	1,290	83.6
% of basin covered by wetlands	0	21.8	4.86
Basin-wide mean of the average April precipitation, in inches	2.79	6.23	3.94
Main channel slope, in feet per mile	5.43	543	114

1.4 VT RPFES

Olson updated the RPFES for Vermont in 2014. Logarithmic base-10 transformations were made on all final variables in the equations. A total of 117 basin characteristics were originally included. The regression equations for estimating flood discharges on ungaged, unregulated streams in rural drainage basins in Vermont are as follows:

$$Q_{50-AEP} \text{ (or 2 year RI)} = 0.145 A^{0.900} W^{-.274} P^{1.569}$$

$$Q_{20-AEP} \text{ (or 5 year RI)} = 0.179 A^{0.884} W^{-.277} P^{1.642}$$

$$Q_{10-AEP} \text{ (or 10 year RI)} = 0.199 A^{0.875} W^{-.280} P^{1.685}$$

$$Q_{4-AEP} \text{ (or 25 year RI)} = 0.219 A^{0.866} W^{-.286} P^{1.740}$$

$$Q_{2-AEP} \text{ (or 50 year RI)} = 0.237 A^{0.860} W^{-.291} P^{1.774}$$

$$Q_{1-AEP} \text{ (or 100 year RI)} = 0.251 A^{0.854} W^{-.297} P^{1.809}$$

Where,

- Q_P is the estimated flood discharge, in cubic feet per second, at the P-percent annual exceedance probability;
- A is the drainage area of the basin, in square miles;
- W is the percentage of the basin with land cover categorized as wetlands or open water, plus 1.0, from the National Land Cover Data (Fry et al, 2011) using a GIS; and
- P is the basin-wide mean of the average annual precipitation, in inches, determined with the PRISM 1981 – 2010 annual precipitation dataset (PRISM Group, Oregon State University, 2012a) resampled to an 800-meter-cell resolution by using bilinear interpolation.

Note that the RI, utilized throughout the rest of this report, is equivalent to the inverse of the AEP, thus here $Q_{50} = 2$ year RI flood, $Q_{20} = 5$ year RI flood, $Q_{10} = 10$ year RI flood, $Q_4 = 25$ year RI flood, $Q_2 = 50$ year RI flood, and $Q_1 =$ the 100 year RI flood. The equations are valued for the range of explanatory

values used in development of the equations, listed in Table I-2. Formulas for estimating the 90 percent upper and lower CIs are provided in Olson (2014) but were not utilized for this project.

Table I-2: Range of explanatory variables valid for VT RPFES

Explanatory variable	Minimum	Maximum	Mean
Drainage area, in square miles	0.18	689	84.2
% of basin covered by wetlands	0	18.5	3.42
Basin-wide mean of the average annual precipitation, in inches	33.5	70.4	47.6

1.5 References

Environmental Systems Research Institute, Inc., GIS for water resources, accessed April 1, 2008, at http://www.esri.com/industries/water_resources/index.html/

Fry, J.A., Xian, George, Jin, Suming, J.A. Dewitz, C.G. Homer, Yang, Limin, C.A. Barnes, N.D. Herold, and J.D. Wickham. 2011. *Completion of the 2006 national land cover database for the conterminous United States*. PE&RS, v. 77, no. 9, p. 858–864.

Multi-Resolution Land Characteristics Consortium. 2003. 2001 National Land Cover Data: U.S. Geological Survey, accessed March 31, 2008, at <http://www.mrlc.gov/>

Olson, S.A. 2009. *Estimation of flood discharges at selected recurrence intervals for streams in New Hampshire*. U.S. Geological Survey Scientific Investigations Report 2008-5206, 57 p.

Olson, S.A. 2014. *Estimation of flood discharges at selected annual exceedance probabilities for unregulated, rural streams in Vermont, with a section on Vermont regional skew regression, by Veilleux, A.G.*: U.S. Geological Survey Scientific Investigations Report 2014-5078, 27 p. <http://dx.doi.org/10.3133/sir20145078>

PRISM Group, Oregon State University. 2006. *United States average monthly or annual precipitation, 1971–2000, 30 arc-second normal*. Corvallis, OR, Oregon State University, accessed October 2, 2007, at <http://www.ocs.oregonstate.edu/>

PRISM Group, Oregon State University. 2012. *United States average monthly or annual precipitation, 1981–2010, 30 arc-second normal*. Oregon State University, PRISM Climate Group, accessed September 16, 2013, at <http://www.prism.oregonstate.edu/>

U.S. Geological Survey. 2007. National elevation dataset, 1/3 arc second, accessed March 31, 2008, at <http://ned.usgs.gov/>

U.S. Geological Survey. 2007. National hydrography dataset, high resolution, accessed March 31, 2008, at <http://nhd.usgs.gov/>

Wandle, S.J. 1983. *Estimating Peak Discharges of Small, Rural Streams in Massachusetts*: U.S. Geological Survey Water-Supply Paper 2214, 31 p.

Zarriello, P.J. 2017. *Magnitude of flood flows at selected annual exceedance probabilities for streams in Massachusetts*. U.S. Geological Survey Scientific Investigations Report 2016–5156, 54 p.
<https://doi.org/10.3133/sir20165156>

Appendix J TU MODEL PROTOCOL

A summary of the methods utilized by the TU Model is provided below, taken directly from documentation prepared and provided by Joel Ballesterero.

J.1 Introduction

For the Excel modeling part of the project, there are two main components, the hydrology and the hydraulics. The hydrology is a summary and analysis of runoff upstream of the culvert, and calculates the peak flow at five defined return periods for each culvert. The hydrologic analysis is based off data from the GIS component of the project (watershed area, flow path, etc.). The hydraulics analysis describes how the crossing passes the calculated flows, and is accomplished with user input about the crossing. The model on the whole is meant to be a guide to help determine the overtopping susceptibility of analyzed culverts for specific flood flows, and is not meant to be exact in its analysis. Both hydrologic and hydraulic components use some estimates and simplifying assumptions in order to generate results, and this leads to certain limitations in their respective methods (discussed further on).

J.2 Hydrology

The hydrology component calculates the peak flood flow coming to each culvert at five return intervals; 2-, 10-, 25-, 50-, and 100-yrs. There are many ways to calculate peak flows from a watershed, and a full watershed model should be performed for culverts that demonstrate overtopping susceptibility. Full watershed models are very involved, require increased input data, and are time-consuming. For the purpose of obtaining flood flows with limited information requirements, two quick and easy methods were employed for this model: the SCS Method (TR-55) and the Regional Regression Equations for New Hampshire (Olson, 2002). These methods require much less data to run than full watershed models, yet both are considered to be acceptable methods of analysis in lieu of discharge data at a site.

J.2.1 SCS Method

The SCS Method is a very common method used to compute peak flows, and is in many cases the industry standard. The method assumes an even depth of rainfall over the entire watershed at a set intensity; estimates the amount of the total volume that will influence the peak flow; and accounts for the hydrograph dampening that occurs due to travel time and land cover in the watershed. A full description of the entire method, components, and equations can be found at <http://www.cpsc.org/reference/tr55.pdf>. This method is good for estimating flows from watersheds that are relatively homogenous, in rural areas with few impoundments and storage. In general, this method should be used for watersheds larger than 2 square miles which have a time of concentration not exceeding 10 hours. This method is generally considered to result in very conservative (high) peak flows.

The data required to use this method for each crossing are determined from the GIS portion of the project. The data may also be entered in manually, if desired. The direct data that is input from GIS includes: the Drainage Area, the upstream watershed runoff Curve Number, the 24-hour Precipitation Depth for the 2-, 10-, 25-, 50-, and 100-yr storms, the Watershed Slope, the Area of Wetlands and Ponds in the Watershed, and the Watershed Length. The Drainage Area is simply the total upstream

area of the watershed that contributes flow to the culvert undergoing analysis, and it should be given in square feet (the actual equation in this method uses the area in square miles, but this conversion occurs internally in the Excel model). The Curve Number is basically a coefficient used in the model's equations that estimates precipitation losses due to infiltration capacities, watershed land cover, and antecedent soil moisture condition, among other things. A curve number value is assigned to each sub-area in the watershed, and a weighted value is developed for the entire watershed. The Curve Number is unitless. The 24-hour Precipitation depths for the five return periods are determined in GIS using new, updated rainfall amounts published by the Northeast Regional Climate Center located in the Department of Earth and Atmospheric Sciences at Cornell University. These updated rainfall amounts account for climate change, and reflect the rising trend in rainfall amounts in the northeast. Each amount represents the expected rainfall depth to occur over a 24-hour period for specific average return periods. Model input rainfalls are in inches. The Watershed Slope is the USGS 10-85 method, which for runoff hydrology is the most representative watershed slope, rather than the overall watershed slope which may be slightly steeper (and not as well correlated to flood flows). Oftentimes on a river system there is a steep slope at the beginning and/or the end of the runoff travel path. Hills may exist upstream, and often in the northeast, dams are seen towards the downstream, or the coast. Thus the 10-85 method of determining the slope takes the stream elevations at 10% and 85% of the runoff travel path upstream of the culvert, and divides their elevation difference by the travel length between them. This slope is dimensionless (ft/ft), though in this method's calculations, it is used in the equations in percent. The TU model converts the slope input as ft/ft to percent internally for use in the SCS equation. The Area of Ponds and Wetlands is determined in GIS from the ponds and wetlands, in the same manner as the watershed areas are determined. This area should be given in square feet. Finally, the Watershed Length is determined for the path that would take a drop of water the longest time to reach the outlet. This is difficult to automate, and can be estimated using the longest flow path, given in feet. The model then uses all these watershed properties to calculate the expected peak flow for each crossing for each of the five return periods.

J.2.2 Regional Regression Equations for New Hampshire

The Regional Regression Equations for New Hampshire were developed by the USGS in cooperation with the NH Department of Transportation. These equations were determined using many watershed properties as variables and comparing the predicted flows to observed flows at 117 gaged locations. A full description of how the equations were developed, the methods, procedures, and equations can be found at <http://pubs.usgs.gov/sir/2008/5206/pdf/sir2008-5206.pdf>. The regressions are unique to New Hampshire, based on gaged stream floods, and an equation is given for each of the five return periods. This method is most suited for estimating peak flows on rural, ungaged streams in New Hampshire. These equations are most likely only accurate within the ranges of properties of the watersheds used in the study; within a Drainage Area of 0.70 and 1,290 square miles, a Mean April Precipitation between 2.79 and 6.23 inches, a Percentage of Wetlands between 0 and 21.8%, and a Watershed Slope between 5.43 and 543 feet per mile (or 0.1 to 10%).

The equations given in this method are empirical relationships based on four watershed properties: the Drainage Area, the Mean April Precipitation, the Percent of Wetlands and Ponds in the watershed, and the Watershed Slope. The Drainage Area, the Wetlands and Ponds and the Watershed Slope are all the same as described in the SCS Method section. The Mean April Precipitation is a value given in inches determined from average monthly rainfall amounts over the last 30 years, as published by the PRISM Climate Group from Oregon State University. Each return period has its own equation, and

though the four watershed properties remain constant, each equation has unique coefficients and exponents.

J.2.3 Discussion

While both hydrologic methods employed in this model are published government methods, neither is a substitute for a full watershed analysis. Both methods are first-cut estimates of the flood peak flows expected at the crossing. Both methods suggest using watersheds that are relatively rural and somewhat homogenous. This is because the more urban the watershed, the more complex the runoff characteristics, and the more hydrograph routing required, all of which add variability to the flood peak estimates. Neither of the employed methods performs hydrograph routing. As the watershed becomes more urban, peak flow becomes more unpredictable on a large scale. On one hand, the peak flow can increase due to factors such as the straightening/channelization of streams, or the larger amount of impervious surfaces. However, more urbanized environments typically have more hydraulic controls such as road crossings, stormwater ponds, and dams, which act to attenuate and lag peak flows. The two employed methods, however, are the best two methods available for the purpose of this model. They were selected in part for their wide acceptance, the ease of understanding and use by the end-user, and for the level of complexity of the model.

The two models calculate flows at each crossing, but only one of the models is selected by the program, based on the previously mentioned limits of use for each model in each culvert analysis. In the development of this program, several watersheds were analyzed and the two methods were compared. It was determined that for all watersheds under 1 square mile with a time of concentration not exceeding 10 hours, the program uses the SCS Method. For all other watersheds, the Regression Equations are used.

J.3 Hydraulics

The hydraulic component of the project involves analyzing how a selected culvert performs in passing the calculated flows: that is, the depth of water upstream of the culvert for each flood flow: the Headwater Depth. The calculation method is based on the US Department of Transportation Federal Highway Administration's Hydraulic Design Series number 5 (HDS-5), Hydraulic Design of Highway Culverts. This method involves user-collected information about a crossing, and empirical formulas. As a simplifying assumption for this program, inlet control was assumed to occur at each culvert, which means that for the floods, the culvert inlet hydraulically acts as an orifice. The program computes headwater depths based on field-collected crossing information. For re-sizing culverts, the program uses a geomorphic approach such that the culvert acts under outlet control whereby flow in the culvert is more like the open channel flow in a stream.

J.3.1 Existing Culvert Hydraulics

The existing stream crossing hydraulics are analyzed for the peak flows determined from the hydrology. Additional input is user-determined culvert properties. HDS-5 describes equations developed for various possible culvert hydraulic conditions; inlet control, outlet control, submerged and unsubmerged. The equations for unsubmerged culverts generally apply to a Headwater to Interior Rise (culvert height) Ratio of 1, while the equations for submerged culverts apply from about a ratio of 1.5 and higher. Between ratios of 1 and 1.5, the Headwater depth can be approximated using a linear interpolation between the submerged and unsubmerged equations. This results in an iterative process

that would be complex to code in the Excel model. Therefore, the same methodology used in the FHWA free computer program HY-8, which is based on the HDS-5 report, was employed in this program. This method uses a 5th order polyline fit to the empirical culvert hydraulic relationships for inlet control. For variable, the equation relates Headwater Depth divided by culvert Rise (height) to Flow divided by Area times the square root of the Rise. This polyline is a very close fit for all ratios of Headwater Depth to Rise from 0.5 to 3. Above a ratio of 3, the standard orifice equation for a submerged culvert under Inlet Control can be used. Below a value of 0.5, the Headwater is not calculated, as the culvert is considered successful in passing the flow (outlet control). Each culvert type is described by the shape of the culvert, the material it is made of, the inlet edge configuration, and the inlet end type. Varying one of these four descriptors varies the culvert type, and results in different coefficients and variables used in the equation to compute Headwater Depth. The required user input for the hydraulic section is the Culvert Type Reference Number (based off the four variables described previously for the Culvert Type), the Culvert Length, the Inlet Elevation, the Outlet Elevation, the Road Elevation, the Number of Barrels, the Interior Rise, the Interior Span, the Culvert Wall Rise (only applicable to Arch pipes), and Embedded Depth (only applicable to Embedded culverts). The three Elevation values, the Number of Culvert Barrels, and the Culvert Length are all as they seem. The Interior Rise is the rise in the culvert from the invert of the culvert, or from the bottom of the thalweg of the sediment in an embedded culvert or open-bottom culvert. The Interior Span is the width of the culvert. The Culvert Wall Rise applies only to Arch pipes, and refers to the height of the side wall of the arch. Finally the Embedded Depth refers to the depth of sediment above the invert of the culvert. The Interior Rise and the Embedded Depth should add up to the total culvert Rise. All of the above required user input has information, examples, and images in the model to help the user understand and correctly collect and enter the required information into the model. The Excel model uses the user input to determine the Headwater Depth for each flow to the culvert. The culvert is then rated based on the ratio of the Headwater Depth to the Interior Rise ratio of the culvert. The culvert is considered Passing if the ratio is under 0.85, the culvert is considered Failing if the ratio is over 1.15, and the culvert is considered Transitional if the ratio is between 0.85 and 1.15.

These hydraulics methods used in the Excel model were chosen for two main reasons. The first was because the required input is easy to understand and collect. The model is meant for non-engineers, and the hydraulics do a good job approximating the results. They also require much less effort in calculations internal to the model, while still providing results that may be used for rating each culvert. As stated in the opening paragraph of the hydraulics section, there are equations for submerged and unsubmerged culverts hydraulics, both used in the model, and for Inlet and Outlet Control. For simplicity, the Excel model assumes culverts under Inlet Control. The Outlet Control Headwater depths are not calculated due to their complexity in integrating them within the model, and the potential error in the collection of the data by the users. Despite not calculating the Outlet Control Headwater depths, the model should still give an accurate enough representation of the culvert ratings for the purpose of this model. When the model computes a Headwater Depth to the Interior Rise ratio less than 1.15, users should consider the potential for outlet control, especially if the culvert is under the influence of downstream backwater (ponding) effects.

J.3.2 Proposed Culvert Hydraulics

Proposed crossings are offered for two types of culvert installations; Rectangular culvert(s) and 20% Embedded Circular culverts. There are of course other possibilities; however, for simplicity of coding this model gives two options for the user to consider. The approximate stream bankfull width is

calculated using the Regional Hydraulic Geometry Curves and Regression Equations (NHST, 2005 or Schiff, MacBroom, and Armstrong Bonin, 2007), and the recommended minimum natural-channel stream crossing span is determined using the guidelines in the NH Stream Crossing Guidelines (NHDES, 2009). Determining the proposed number of barrels and the sizes for both culvert types is accomplished by setting the desired Headwater Depth to Rise ratio to 1 in the Unsubmerged Inlet Control equation, then solving for the Area times the square root of the Internal Rise parameter. When this value is determined, the model finds a similar value from a table of culverts by size and quantity. This method of calculating proposed culvert sizes is different than what is suggested in the HDS-5 report. It uses very approximate equations and very general assumptions. The proposed culvert sizes are not intended to be used as an exact design; rather, they should be used as a guide to estimating the size of required openings, and develop options from there.

J.4 Instructions for Using the Excel Model

The Excel model is designed to be as user-friendly as possible. The hope is that the model can provide a user with a rough idea of how selected culverts will perform during storm events without the user having to know the engineering and mathematics that is required to calculate such things. The results should be used as a preliminary analysis of the culvert performances, and in no way are the results to be used as a final design.

The model has four tabs visible to the user: Instructions, GIS Input, User Input, and Results. These four tabs contain all the information and data entry locations that are required to run the analysis. There are additional hidden tabs where the calculations and lookup tables are located. The four visible tabs, and instructions on how to use them, are described below.

In order for the model to run, it needs input data. Separate from the Excel part of the model, data will need to be obtained from GIS (refer to the GIS portion of the project), and from field-collected data. Obtain these two sets of data first, before attempting to run the model.

J.4.1 Instructions

The first tab, labeled Instructions, is where all the information is contained as to how to run the model. The tab also has information such as a legal disclaimer, an overview of the project, the limitations of the model and methods, and some quick navigation buttons. All of this information should be read and thoroughly understood before entering in any data or running the model. The information contained on this sheet has implications as to the effectiveness of the model. When all of this information has been read, proceed to the GIS Input tab.

J.4.2 GIS Input

The data entered into the GIS Input tab is all the data that will be obtained from GIS, and is all the data necessary to calculate the hydrologic portion of the analysis. This data can be entered in two different ways. The first way is to import the data from a file, created from GIS. This file, if the GIS instructions are followed, will contain all the information in the correct format to import into this sheet. Before importing the data, however, the file must be named appropriately, and in the correct location. As detailed on the sheet, the text string "gis output" (letters may be of any case but must be separated by a space, for example "Town of Madbury GIS Output" or "gis output may 2014") must be somewhere in the file name. Second, the file must be in the same folder as the Excel model file. Finally, be sure that

the folder containing the GIS data has no other files with the string "gis output" in it. This will allow the program to find the correct file to import. If there are multiple scenarios to be analyzed, it may be easiest to have separate folders for each scenario, with each folder containing its own model file and GIS Output file. After these guidelines are met, click the button Import Data from File. The data should show up, and the table should be formatted to fit it all. This data may then be edited, if the user decides it is necessary, by clicking the Edit Imported Data button. If the user would like to insert the data manually, just click the Insert Data Manually button. If there are values that are inserted into the table for the Mean April Precipitation, the Watershed Slope, or the Area of Wetlands and Ponds that are outside of the recommended ranges of values for the calculations, these values show up colored orange and in italics. If this happens, all the calculations will still be performed in the model, but it should be noted that the calculated results for these crossings may be poor results. Information from the GIS Input tab is utilized to set the data input needs for the subsequent data tables.

J.4.3 User Input

The User Input tab is where all the field-collected data will be entered into the model. This information is all required to perform the hydraulic part of the analysis. The table should already be pre-formatted, if the GIS Input tab has been completed. All the data in this tab should be inserted by the user from the collected data. The data to be entered should be fairly straight-forward, with the exception of the first value, the Culvert Type Reference Number. This number is a value that the program uses to assign the correct coefficients to the equations used in the calculations. These coefficients are given based off the culvert type, shape, material, inlet condition, and edge condition. To select the correct Culvert Type Reference Number, follow the instructions at the left side of the sheet. The shape of the culvert should be selected first, followed by the material. In the next column, the user should select the value for both the inlet and edge type that best describe the culvert inlet condition. Following this, in the final column, will be the value for the reference number that should be inserted into the table. As a check, the user can look below each column and find the culvert shape, material, and end and edge type, as defined by the culvert type reference number entered.

There are two rows of data at the bottom of the table that are optional. These will be gray if they are unnecessary or appear as the other input cells do if needed.

J.4.4 Results

When the two input tabs have been completed, the results may be viewed under the Results tab. The results are shown for the currently-selected return period. This may be changed by the user at the top-left corner of the sheet, using the drop-down selection box. In the results table, the values will update when the return period is changed. The first eight rows of results all show existing crossing properties that were either entered by the user or calculated for each crossing. The culvert rating will show Pass, Transitional, or Fail for the result, and both the Culvert ID and the rating will show as green, yellow, or red, respectively. The next three rows show proposed geomorphic properties calculated for the crossing based off the flows. These were calculated using equations from the Regional Regression Equations. The following eight rows show results for proposed rectangular and 25% embedded circular culverts that might be required to pass the flows. Both of the proposed culvert results are programmed calculations, and should not be used for design, but rather to give the user an idea of what might be required at the site.

Below the table of results, some statistics are included that show the total number of culverts that are passing, transitional, or failing, as well as the overall percentage of each. To the right of this, a pie chart can be found representing these statistics.

J.5 References

- NHDES, New Hampshire Stream Crossing Guidelines, Concord, NH. 2009. Available at:
http://www.streamcontinuity.org/pdf_files/nh_stream_crossing_guidelines_unh_web_rev_2.pdf
- NHST, New Hampshire 2005 Regional Hydraulic Geometry Curves (Provisional). 2005. The New Hampshire Stream Team, Concord, NH.
- Olson, S.A. 2002. *Flow-frequency characteristics of Vermont Streams*: U.S. Geological Survey Water-Resources Investigations Report 02-4238, 47 p.
- Schiff, R., J.G. MacBroom, and J. Armstrong Bonin. 2007. *Guidelines for Naturalized River Channel Design and Bank Stabilization*. NHDES-R-WD-06-37. Prepared by Milone & MacBroom, Inc. for the New Hampshire Department of Environmental Services and the New Hampshire Department of Transportation, Concord, N.H.

Appendix K HBV AND HSPF OVERVIEW

K.1 Model Overviews

K.1.1 Hydrologiska Byråns Vattenbalansavdelning (HBV) Model

The Hydrologiska Byråns Vattenbalansavdelning (HBV) model is a process-based, continuous streamflow simulation watershed model that has been characterized as a semi-distributed conceptual model (Lindstrom et al., 2005; Parajka et al., 2007). It is often applied in a lumped-conceptual structure (e.g., Merz and Blöschl, 2004; Yu and Yang, 2000; Sing and Woolhiser, 2003; Berstrom 1976). The model was designed by the Swedish Meteorological and Hydrologic Institute (Berstrom, 1992; Berstrom and Lindstrom, 2015) for application in cold, mountainous European climates. It has been utilized in more than 50 countries around the world, including extensively in Finland, Norway, and Sweden. It has not been used extensively in the northeastern U.S. but holds promise due to similarities between the northeastern U.S. and the mountainous European climates for which it was developed.

There are three main routines for the model, Figure K-1 including snow accumulation and melt, soil moisture accounting, and a response and channel routing routine. Input for the HBV model includes daily precipitation, air temperature, and potential evapotranspiration estimates. The snow routine consists of a simple degree-day and threshold approach. The soil moisture accounting routine computes an index of the wetness of the entire watershed, and it accounts for interception as part of the soil moisture storage (Bergstrom, 1992). The runoff response transforms the excess water from the soil moisture routine into river flow. This routine consists of two tanks (reservoirs) that represent different time dependent contribution to the river flow. A triangular distribution is used to attenuate the flood pulse at the watershed outlet. Further information on the model and its application in ungaged watersheds is available from Bergstrom (2006).

K.1.2 Hydrologic Simulation Program Fortran (HSPF) Model

The Hydrologic Simulation Program Fortran (HSPF) is a process-based, semi-distributed, continuous simulation watershed model for quantifying runoff and addressing water quality impairments associated with both point and non-point sources (Bicknell et al., 1996; Johnson et al., 2003). The HSPF model was developed in the early 1970s by the U.S. Environmental Protection Agency (EPA), and was derived from the Stanford Watershed Model (SWM). The HSPF model is maintained by the EPA and exists as a core watershed model tool in EPA's software application BASINS (Better Assessment Science Integrating Point and Non-point Sources) in version 4.0 (2013).

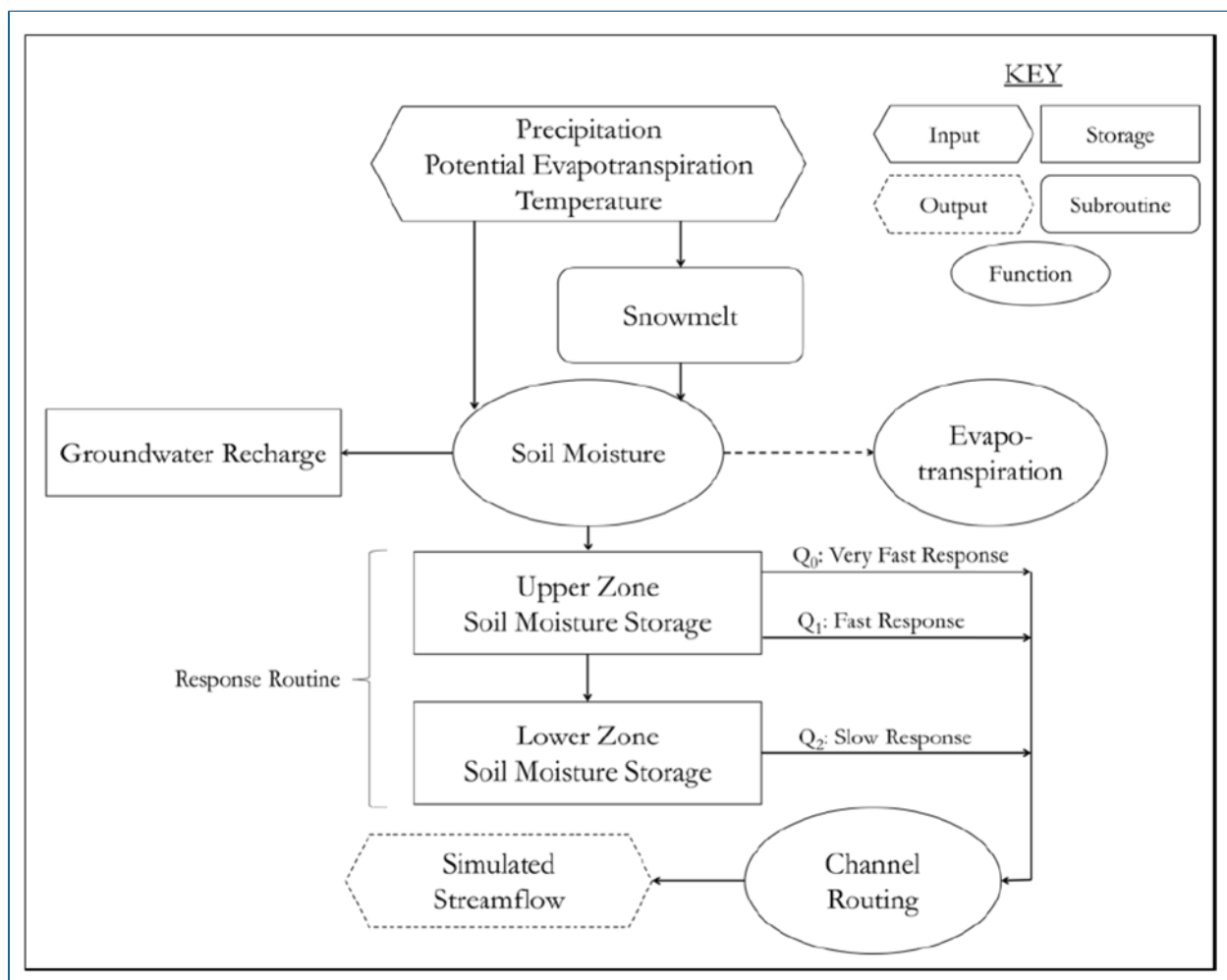


Figure K-1: Conceptual flow diagram for the HBV model (Source: Clark, 2016)

In HSPF water mass and energy balances are simulated through the use of hydraulic response units (HRUs). The model is typically used at a spatial resolution that ranges in extremes from 10 to 100 km². HRUs provide a distributed calculation of surface runoff, interflow, and groundwater flow to streams by processes that determine the fate of water through losses and storage. Flows from the HRUs are typically directed to streams and routed by the kinematic-wave method to simulate streamflow. HSPF can simulate any period from a few minutes to hundreds of years using a time step ranging from sub-hourly to daily. Usually the model is executed for a time span ranging from 5 to 20 years or more using an hourly time step (Duda et al., 2012).

Input data include both topographical controls and meteorological drivers. Meteorological drivers can include various climate data such as hourly precipitation, estimates of potential evapotranspiration, and air temperature. Topographical controls include vegetation, digital elevation model (DEM) data, hydrography, and land-use type layers.

Major elements of the HSPF model are reproduced from Crawford and Linsey (1966) in Figure K-2. The calculations represented in this conceptual model diagram can be carried out by any number of reaches (HRUs) from any number of meteorological input stations. Upper and lower zone storages control overland flow, infiltration, interflow, and inflow to the groundwater while these two zone

storages also combine together with groundwater storage to represent soil moisture profiles and groundwater conditions (Crawford and Linsey, 1966). Surface runoff is simulated as essentially an infiltration-excess process. The output from each HRU represents the average amount of precipitation that is routed to a stream channel (Johnson et al., 2003). Flow is routed downstream from reach to reach by a kinematic wave method. A degree-day snow simulation was also applied for the HSPF model that uses a simple approach for estimating snow in the watersheds using minimum and maximum daily temperature data.

For this project, BASINS was used to develop the HSPF model files as well as assemble the climate data needed for the model. The WinHSPF v3.0 interface within BASINS was used to automatically estimate the F-Tables for all the reaches in the model for the channel routing sub-routine. Reaches within each subbasin were defined using automatic watershed delineation methods in BASINS using a minimum drainage-area threshold of 2.5 km².

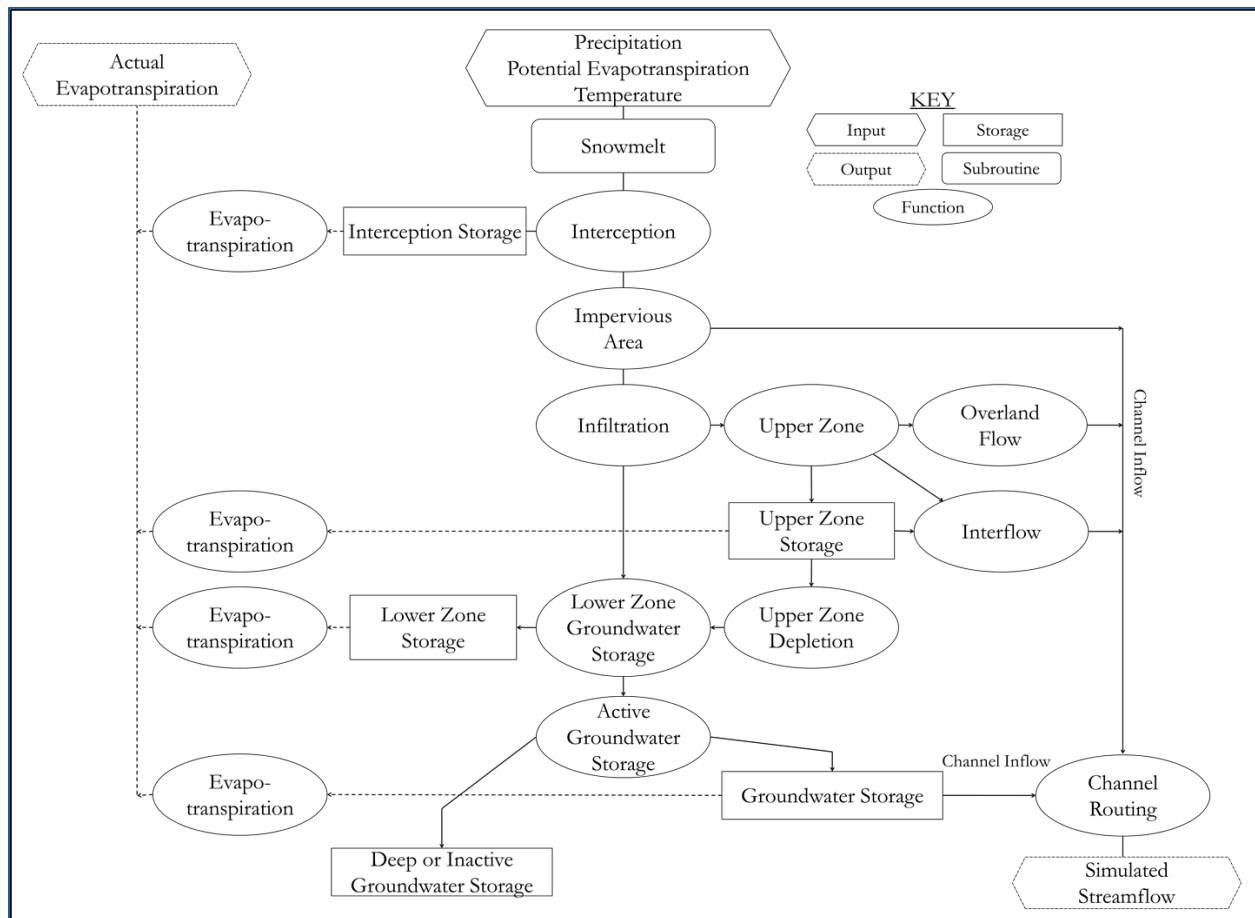


Figure K-2: Conceptual flow diagram for the HSPF model based on a similar figure for the SWM published by Linsey and Crawford (1966) (Source: Clark, 2016)

K.2 Regionalization

One of the primary challenges of applying process-based, rainfall-runoff modeling methods at ungauged locations is the lack of local runoff data that could be used for model selection and calibration (Blöschl, 2013). This is also called the regionalization problem in hydrological modeling.

Regionalization can be defined as the process of transferring hydrological information (e.g., process-based model parameters) from one catchment to another (Blöschl and Sivaplan, 1995).

Regionalization without runoff data can be a very difficult task and may be approached in several ways: (a) a-priori estimation of model parameters from catchment characteristics; (b) transfer of calibrated model parameters from gauged catchments, for example by assuming spatial proximity/similarity, or transferring parameters by developing regressions between calibrated model parameters and catchment characteristics; (c) constraining model parameters by regionalized runoff characteristics; and (d) constraining model parameters by dynamic proxy data. For this project, the calibrated model parameters are related to catchment characteristics in the basin to inform regression based regionalization.

The following expression was utilized to define functional relationships between model parameters and catchment characteristics:

$$\hat{\theta}_L = F(\theta_R|\Phi) + \varepsilon_R$$

where $\hat{\theta}_L$ is the estimated model parameter at the ungauged site, $F()$ is a functional relation for the parameters, Φ is the set of catchment characteristics, θ_R is a set of regional model parameters, and ε_R is an error term. An ordinary-least-squares (OLS) linear regression approach defines the functional relationship between highly correlated catchment characteristics (Φ) with the rainfall-runoff model parameters (θ_R), with the underlying assumption that the model parameters are independent. A Shapiro-Wilks test is used to determine if the set of calibrated model parameters and catchment are normally distributed and standard transformations are used on values from this test that were <0.05 . If the distribution of a catchment characteristic was not correctable using a standard transformation, they were removed from the subsequent analysis.

Pearson's r value is calculated between the regional model parameters (θ_R) and the catchment characteristics across the subbasins (Φ) and significant relationships between these two independent data are determined. A threshold of 0.514 was used to identify significant relationships (p value < 0.05). If a rainfall-runoff model parameter (dependent variable) had more than one significant relationship to a catchment characteristic (independent variable), a principal component analysis (PCA) was applied to the significant independent variables and the first component was used in the OLS regression for each parameter. Otherwise, if the dependent variable had only one significant relationship or none that were above the threshold, the most significant independent variable was selected for OLS regression. The use of the PCA in the regression development reduced both the dimensionality of the independent variables and eliminated the effects of colinearity between the catchment characteristics.

To compare the usefulness of our regression regionalization approach, two other methods are evaluated, namely spatial proximity and naïve approaches. Spatial proximity uses the parameter set from the closest donor catchment. The Euclidean distance is calculated between the ungauged catchment and the gauged catchments in the region and the catchment with the minimum distance is

selected to be the donor catchment in this approach. The naïve mean is also compared in which the mean of the model parameters across the gauged sites are used at an ungauged site.

A “jack-knife” or “leave-one-out” cross validation (LOOCV) approach was used after the regression development. This LOOCV method was applied in a closed-form approach, in which the accuracy of hydrologic model parameter estimations were evaluated without running the model, as well as an open-form approach, in which the model parameters estimated were then used to simulate the streamflow and standard goodness-of-fit (GOF) measurements were calculated. For the closed-form analysis, the ordinary residuals and the leverages are used instead of fitting fifteen separate least-squares models and omitting each observation once. The hat matrix is calculated for each of the eight model parameter regressions, which describes the influence of each response value on each fitted value. The diagonal of the hat matrix is then used to calculate the deleted-residuals for each regression. These deleted-residuals are then used to create a plot with the estimated hydrologic model parameter value that has been left out through calculation of the deleted-residual with the actual calibrated values. In addition, the residuals from the OLS regression equations are calculated for each parameter in the hydrologic models and are mapped to the subbasins to identify any potential spatial clustering.

K.3 Climate Data

Historical climate data used for modeling included precipitation, temperature, and potential evapotranspiration. Hourly precipitation and temperature data were averaged across four NWS CO-OP stations, selected based on the time-period of record and quality of data (Amherst, Readsboro, Searsburg and Ball Mountain). Two are located in the watershed and two are adjacent, as previously described. Daily potential evapotranspiration (PET) was estimated using Hamon (1963) for the HBV model based on daytime length and the saturated vapor density, calculated using the mean daily air temperature and a coefficient of 0.0065. The Hamon PET model was applied because of its simplicity of data inputs and accuracy (Lu et al., 2005; Federer et al., 1996; Vorosmarty et al., 1998; McCable et al., 2015).

The HBV model was run in a lumped mode, where the climate data inputs were averaged for each of the subbasins. For the HSPF model, climate data were distributed across the subbasins by spatial proximity.

K.4 Flow Data Utilized for Calibration

There are seven USGS streamflow gages in the Deerfield River watershed, with data available through the USGS National Water Information System (NWIS) network. Only three of these gages, the Green River (1170100), South River (01169900) and North River (01169000) gauges, are considered unimpaired, as there are several major dams in the watershed. Together these three catchments represent about 23% of the total drainage area of the Deerfield River watershed. Calibration is based on unimpacted watersheds because these are the conditions the model calibration parameters represent. These conditions are also representative of most of the road-stream crossings in the watershed. The impact of dams is not explicitly accounted for in the models due to lack of information necessary for calibrating downstream routing. As a result, the hydraulic risk for crossings located downstream of dams is likely overestimated, as dams will tend to decrease flood peaks.

Estimates of streamflow at 12 additional major subbasins within the Deerfield River watershed were developed using the Connecticut River UnImpacted Streamflow Estimation (CRUISE) tool for use as surrogate data for calibration. Vleeschouwer and Pauwels (2013) suggest that in the case when no observed discharge records are available, calibration can be carried out successfully based on a rescaled discharge time series of a “very similar” donor catchment. The CRUISE tool was deemed appropriate because the Deerfield River watershed falls within the larger Connecticut River watershed. The CRUISE tool uses a geostatistical approach to select the donor catchment, calculates the cross-correlation coefficients of runoff with unimpacted streamflow gages in the Connecticut River watershed, and then interpolates these correlation coefficients in space using kriging (Blöschl et al., 2013).

K.5 Catchment Characteristics

Catchment characteristics were calculated from publically available raster datasets consistent with the project. The USGS National Elevation Dataset (NED) was downloaded and clipped to the catchment area where it was used to delineate the subbasins used in this study and derive the elevation, slope, and aspect characteristics. The USGS National Hydrography Dataset (NHD) was used to determine the total length of stream and the stream density of the subbasins. The National Land Cover Database 2011 (NLCD, 2011) was used to determine the different types of land cover in the basins, which was reclassified to represent agricultural, forest, and developed land categories (Homer et al., 2011). The National Resources Conservation Service (NRCS) SSURGO database was used to estimate the different hydrological soil groups across the subbasins. Finally, the PRISM raster datasets were used to provide estimates of average annual climate characteristics (PRISM Climate Group, 2004). This particular dataset was chosen because it has been used extensively in evaluating annual normal for precipitation and temperature in addition to being homogeneously applied throughout the region as a single uniform dataset. Catchment characteristics were all chosen based on their hydrologic value, but also based on their accessibility and ease of computation.

For CRUISE, basin characteristics are computed using the online USGS Streamstats tool and these characteristics are then used in this procedure to identify the most suitable catchment. This method has been shown to give better runoff estimates than when choosing the nearest stream gauge as the donor (Blöschl et al., 2013; Archfield et al., 2013).

Table K-1 summarizes the catchment characteristics of these three watersheds. Forest cover is the dominant land-use.

Table K-1: Catchment characteristics of the three unimpaired streamflow gauges in the Deerfield River watershed

Catchment Property	01170100 Green River (11)	0116900 North River (12)	01169900 South River (14)
Drainage Area (km ²)	107.66	231.24	62.78
Mean Annual Precipitation (mm) ^a	1384.04	1378.52	1289.08
Mean Temperature (°C) ^a	6.61	6.61	7.28
Max Temperature (°C) ^a	12.44	12.36	13.15
Mean Elevation (m) ^b	413.51	430.79	343.22
Mean Slope (m) ^b	9.8	8.6	8.8
North Facing (%) ^b	7.9	9.3	12.3
East Facing (%) ^b	16.9	17.6	17.9
Developed (%) ^c	3.0	4.4	6.8
Forest (%) ^c	90.3	84.0	78.6
Agriculture (%) ^c	3.8	7.8	10.0
Hydrological Group B (%) ^d	20.8	22.1	16.3
Hydrological Group C (%) ^d	0.7	0.7	0.8
Hydrological Group D (%) ^d	1.3	10.1	9.5
Stream Density (km/km ²) ^e	1.67	1.40	1.31
Length of record (years)	49	73	48
Notes: ^a PRISM (2004, 2011); ^b USGS NED (2002), reclassified based on Homer et al. (2011); ^c NLCD (2011); ^d NRCS SSURGO Dataset; ^e USGS NHD High Resolution Dataset			

K.6 Model Application Details

The TUWmodel package in R was utilized to simulate the HBV model in the Deerfield River watershed. This package was developed at the Vienna University of Technology (Parajka and Viglione, 2012). As noted above, the model was run in a lumped mode, where the climate data inputs were averaged for each of the subbasins. The TUWmodel uses fifteen parameters to simulate runoff response in a watershed. For the purposes of this project, the parameter set was reduced to the eight most sensitive parameters informed through the literature (Zhang and Lindstrom, 1997; Merz and Blöschl, 2004; Parajka et al., 2007; Harlin and Kung, 1992) as well as from a Hornberger-Spear-Young generalized sensitivity analysis (HSY - GSA) method approach similar to Harlin and Kung (1992) (Hornberger and Spear, 1981; Young, 1983; Beck, 1987).

The HSPF model was executed using WinHSPFLt called through the Windows 7 command line interface using RStudio and R (ver 3.2.1). Post-processing of the model output was performed using R coupled with the Python (ver 3.4.3) 'wdmtoolbox' package (ver 0.9.0) that allowed the extraction of the model output data from the HSPF binary WDM files. HSPF utilizes more than 100 parameters to

model streamflow. Utilizing all the model parameters is almost impossible, and typically only the most sensitive are included in calibration to reduce correlation and interdependence between parameters. For this project, HSPF calibration parameters were selected based on peer-reviewed literature (Seong et al. 2015; Kim et al, 2007; Iskra and Droste, 2007; Gao et al, 2014; Doherty et al, 2003; Bicknell, 2000; Duda et al., 2002, US EPA, 1999) and the personal modeling experience of the project team.

For this project, the models were applied to fifteen subbasins in the Deerfield River watershed, calibrated as described below.

K.7 Calibration and Validation

The models were calibrated utilizing both direct and indirect methods, based on the observed data from the three unimpaired sites combined with the derived data for the 12 additional subbasins. A more accurate representation of the physical hydrological processes and landscape heterogeneity is expected as a result of increasing the number of subbasins available for calibration of the HBV and HSPF rainfall runoff models by combining the indirect streamflow estimates derived by CRUISE with the observed data from the three unimpaired USGS gauges.

Model calibration was performed in R with the “hydromad” library (ver. 0.9) that contained code for the shuffled complex evolution method developed at the University of Arizona (SCA-UA). SCE-UA was utilized to perform split sample calibration and validation based on the Kling-Gupta Efficiency (KGE) criterion as the objective function. The calibration period took place from January 1, 1980 to December 31, 1990 with a one-year warm-up period. Model validation was performed over January 1, 1991 to December 31, 1995.

The objective function for the calibration period was to minimize the (-) KGE criterion at a daily-timestep. The KGE has been used in hydrologic modeling as an objective function that serves to mitigate some of the shortcomings of the Nash Sutcliffe efficiency (NSE) value. In particular, this metric has advantages over the NSE because it removes interactions between error components and reduces negative variability bias in simulation results (Steinschneider et al., 2014). This criterion is composed of three independent components including mean bias, variability bias, and the correlation between simulated and observed flows. It can be expressed by the following equations:

$$KGE = 1 - ED$$

$$ED = \sqrt{(r - 1)^2 + (a - 1)^2 + (b - 1)^2}$$

$$a = \frac{S_y}{S_x}, \quad b = \frac{\bar{x}}{\bar{y}}$$

where r is the correlation coefficient, \bar{x} is the arithmetic mean of observed daily streamflow, \bar{y} is the arithmetic mean of modeled streamflow data; and S_x and S_y represent the standard deviations for the observed and predicted data, respectively. The a term is a measure of relative variability of the predicted and observed values and b is the bias defined as the ratio of the mean and predicted flows to the mean of the observed flows. ED represents the Euclidean distance from the ideal point in the

scaled place. The KGE value ranges from minus infinity to 1. Model accuracy is maximized as the KGE approaches unity.

As already noted, the parameter set was reduced to the eight most sensitive parameters informed through literature. A Monte Carlo approach was used to randomly generate parameter combinations from a uniform distribution based on the parameter constraints defined by Parajka and Viglione (2012) for 50,000 simulations. Model output is categorized as either behavioral or non-behavioral based on a threshold KGE value of 0.3. Behavioral simulations have a KGE value greater than 0.3 while non-behavioral simulations have a KGE value of less than 0.3, defined approximately by the average KGE value across all the Monte-Carlo simulation runs.

After calibration, model performance was evaluated using a suite of performance criteria to achieve a more holistic interpretation of the model's performance (Table K-2).

Table K-2: Model goodness-of-fit criteria

	Name	Abrv.	Equation	Range
(1)	Kling Gupta Efficiency Value	KGE	$KGE = 1 - ED$ $ED = \sqrt{(r - 1)^2 + (a - 1)^2 + (b - 1)^2}$ $a = \frac{S_y}{S_x}; b = \frac{\bar{x}}{\bar{y}}$	-inf to 1
(2)	Coefficient of Determination	R ²	$R^2 = \left[\frac{\frac{1}{N} \sum_{i=1}^N (x_i - \bar{x})(y_i - \bar{y})}{S_x S_y} \right]^2$	0 to 1
(3)	Nash-Sutcliffe Efficiency Value	NSE	$NSE = 1 - \frac{\sum_{i=1}^N (x_i - y_i)^2}{\sum_{i=1}^N (x_i - \bar{x})^2} = 1 - \frac{MSE}{S_x^2}$	-inf to 1
(4)	Normalized Root Mean Square Error	NRMSE	$NRMSE = \frac{\sqrt{\frac{1}{N} \sum_{i=1}^N (y_i - x_i)^2}}{S_x}$	0 to inf
(5)	Percent Bias	PBIAS	$PBIAS = 100 \frac{\sum_{i=1}^N (y_i - x_i)}{\sum_{i=1}^N x_i}$	0 to inf
(6)	Volumetric Efficiency	VE	$VE = 1 - \frac{\sum_{i=1}^N y_i - x_i }{\sum_{i=1}^N x_i}$	0 to 1

Notes: x_i is a set of observations; y_i is a set of predictions; \bar{x} is the arithmetic mean of observed data, \bar{y} is the arithmetic mean of the predicted data; S_x and S_y represent the standard deviations for the observed and predicted data, respectively; MSE represents the mean-square-error; ED represents the Euclidean distance from the ideal point in the scaled space; r is the correlation coefficient; a is a measure of relative variability of the predicted and observed values; and b is the bias defined as the ratio of the mean and predicted flows to the mean of the observed flows.

The coefficient of determination (R^2) describes the amount of variance explained by a model. It is the ratio of explained variation to the total variation represented as the square of the correlation coefficient. Values range from 0 to 1, with unity representing a model of perfect fit. The Nash-Sutcliffe Efficiency (NSE) goodness-of-fit value (GOF) is a modification of the mean-square-error (MSE) value and describes comparative ability compared to a baseline model. The NSE value ranges from negative infinity to 1. If the NSE value is 0, then the model is no better than using the observed mean as a predictor. If the MSE is zero, then an NSE value of unity indicates the model is a perfect fit. While the NSE value has been commonly utilized to describe GOF in hydrologic modeling applications, it does have some limitations, including an inability to fully capture model performance, lack of a lower bound, sensitivity to outliers, and inability to infer a sampling distribution (McCuen et al., 2006; Jain and Sudheer, 2008). The KGE criterion decomposes the NSE and MSE value. It ranges in value between negative infinity and 1, with values closer to one indicating increasing accuracy.

K.8 Results

For the HSPF model a total of eight parameters were adjusted to achieve an acceptable fit between the modeled and observed streamflow data. The final parameter values are listed in Table K-3. These parameters were constrained using values suggested by Bicknell (2000) and initial parameter values were established using the HSPF Parameter Database (HSPFParm) (US EPA, 1999). Similar to Seong et al. (2015) the 'infiltr' parameter was changed by a multiplier that retains difference between infiltration values across the different land use types. Unlike other studies (e.g., Seong et al, 2015; Kim et al, 2007), the nominal upper zone soil moisture term 'uzsn' was not allowed to vary monthly in order to reduce effects of colinearity between model parameters, increase numerical stability, and decrease non-uniqueness (equifinality) of calibrated parameter sets.

The analysis of the TUWmodel (HBV) model using the HSY-GSA method indicates that there is a range of sensitivities of parameters in the model. The cumulative distributios of each parameter in the behavioral and non-behavioral sets are compared using the non-parametric Kolmogorov-Smirnov d statistic, which is used as an index of relative difference with higher d-values representing parameters that are more sensitive. A visualization of the behavioral and non-behavioral cumulative distribution curves provides a graphical representation of these results, with more sensitive parameters showing the most divergence between these two curves and the less sensitive parameters showing little to no change between these two groups, Figure K-3. The Kolmogorov-Smirnov (K-S) statistic provides a quantitative accounting of this sensitivity analysis approach and shows agreement with the behavioral cumulative distribution curves. Both analyses suggest that the 'cperc' and 'lsuz' parameters are the most sensitive parameters for the Deerfield River watershed, followed by two flow recession parameters 'k1' and 'ko' and then several snow melt parameters including 'SCF' (snow correction factor), 'DDF' (degree day factor), 'Tm' (threshold melt temperature, followed by another soil moisture parameter 'fc' (field capacity, i.e., max soil moisture storage). These results correlate closely to other sensitivity analyses performed in the literature using this model (Harlin and Kung, 1992; Abebe et al., 2010) providing support to this sensitivity analysis approach utilized.

Note that the HSY-GSA analysis and the K-S statistic was only applied to the TUWmodel (HBV) model to identify sensitive parameters while the literature was used to support the most sensitive parameters for the HSPF model.

Table K-3: Selected sensitive parameters for each hydrological model, lower and upper bounds, and final calibrated range between all of the subbasins

	Param	Description	Units	Lower	Range	Upper
HSPF	agwrc	Groundwater recession rate	1/day	0.85	0.8503 – 0.9403	0.999
	deepfr	Fraction of infiltrating water lost to deep aquifers with the remaining fraction assigned to active groundwater storage	-	0	0.00011 – 0.38796	0.5
	infiltr	Index to mean soil infiltration rate	in/hr	0.001	0.06745 – 0.49976	0.5
	intfw	Coefficient for the amount of water which enters ground from surface detention storage and becomes interflow	-	1	1.8 – 9.998	10
	irc	Interflow recession coefficient	1/day	0.001	0.031	0.85
	kmelt	Constant degree-day factor for the temp index snowmelt method	in/degF	0	0.03416 – 0.13815	none
	lzn	Lower zone nominal moisture storage	in	2	2 – 10	15
	uzsn	Upper zone nominal moisture storage	in	0.05	0.01 – 1.4	2
HBV	Scf	Snow correction factor	-	0.9	0.9 – 1.5	1.5
	Ddf	Degree day factor	mm/degC/day	0	1.11 – 2.78	5
	tm	Threshold temperature above which melt starts	deg C	-2	-2 to 2	2
	Fc	Field capacity, i.e. max soil moisture storage	mm	0	5.6 – 600	600
	Ko	Storage coefficient for very fast response	day	0	0.555-2	2
	K1	Storage coefficient for fast response	day	2	2.02 – 29.24	30
	Lsuz	Threshold storage state, i.e. the very fast response start if exceeded	mm	1	15.46 – 71.70	100
	cperc	Constant percolation rate	mm/day	0	0 – 1.355	8

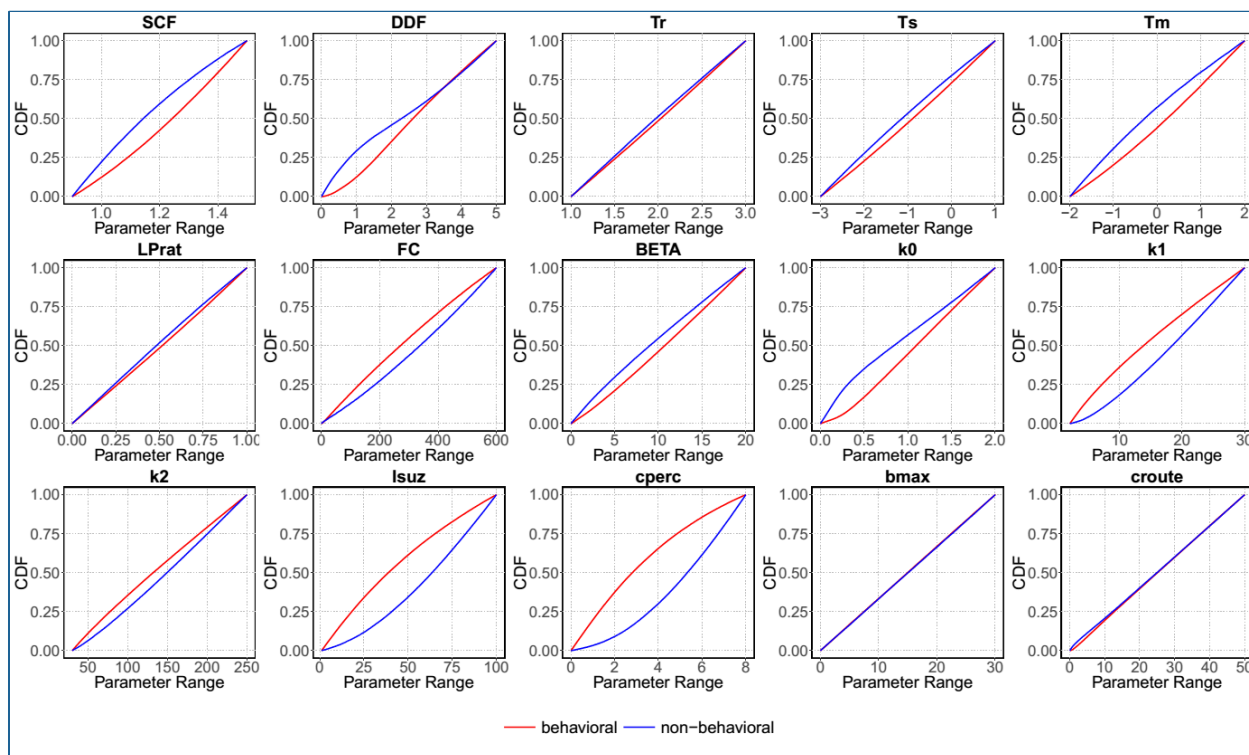


Figure K-3: Results of the HSY-GSA for the 15 parameters of the TUW model (HBV) (Source: Clark, 2016)

Model performance on a daily time step was calculated with a split sample calibration and validation approach for both the HBV model and the HSPF model across the fifteen subbasins in the Deerfield River watershed using the period from 1981 to 1990 for calibration and from 1991 to 1995 for model validation, Table K-4. The calibration performance over the ten-year period differed between the two models. HSPF tended to outperform the HBV across the subbasins and generally had higher KGE, R₂ and NSE values. The model bias (PBIAS) was slightly lower across the subbasins for the HSPF model, although there was a slightly greater range as well for this model compared to the HBV model. The results from the model performance over the validation period showed slightly lower performance, as expected. However, the values are similar to the calibrated values indicating the models are not over-parameterized (parsimonious) and appropriate.

Table K-4: Goodness-of-fit summary for HSPF and HBV calibration/validation

	Calibration		Validation	
	HBV	HSPF	HBV	HSPF
KGE	0.67 (0.58 – 0.73)	0.78 (0.71 – 0.86)	0.66 (0.41 – 0.74)	0.73 (0.67 – 0.86)
R ²	0.46 (0.34 – 0.54)	0.63 (0.52 – 0.74)	0.49 (0.27 – 0.59)	0.66 (0.58 – 0.77)
NSE	0.35 (0.15 – 0.46)	0.59 (0.45 – 0.72)	0.30 (-0.21 – 0.46)	0.53 (0.37 – 0.74)
NRMSE	0.80 (0.73 – 0.92)	0.64 (0.52 – 0.74)	0.83 (0.73 – 1.10)	0.68 (0.51 – 0.80)
PBIAS	-4.34 (-12.1 – 4.1)	-3.08 (-16.9 – 8.4)	1.04 (-7.7 – 7.9)	3.29 (-23.9 – 11.7)

Note: Values in parentheses represent the minimum and maximum range of values across the subbasins. Calibration was performed from Jan 1, 1980 to Dec 31, 1990 (one-year ramp up period). Validation was performed from Jan 1, 1991 to Dec 31, 1995.

A Shapiro-Wilks test was performed on the parameters for the two models as well as the catchment characteristics to assess the normality of these assumed to be independent variables. Standard log and square-root transformation were applied to variables that had a p-value < 0.05. If the transformation increased the p-value from the Shapiro-Wilks test, it was used for the remainder of the analysis. However, there were several variables in which the transformations either reduced the normality of the variable or were ineffective for other reasons (e.g., domain included negative values). Parameters that could not be corrected by a standard transformation or for which the transformation reduced the normality (as indicated by the Shapiro-Wilks test) were noted. Only two of HSPF parameters were so impacted – 'lzsln-log' and 'deepfr_log'. These were parameters that tended to bump into their upper/lower limits during calibration.

Details on the Shapiro-Wilks test for normality results for the model parameters, spatial and climate variables, as well as the correlation coefficients between the calibrated model parameters and model catchments, are available from Gordon (2016). In general, HSPF had a greater number of significant catchment characteristics as well as higher correlation values associated with the calibration parameters. When multiple catchment characteristics were significant, the first principal component of the most significant catchment characteristics was selected using a PCA approach for use in regression equations to select the appropriate parameter values for each model/subcatchment. The PCA approach was only needed for two of the HBV model parameters compared to five of the eight HSPF parameters. The percentage of variance explained for the parameters in which the PCA approach was utilized was at least 70%. The percentage of the catchment facing east and the minimum topographic index value in the catchment were most often related to HBV model parameters, while the mean elevation and both annual average precipitation and temperature were most often correlated with HSPF parameters. Residuals from the regressions for each parameter are mapped to their spatial location within the basin in Figure K-4: Spatial mapping of model residuals from the regionalization regressions by subbasin (Source: Clark, 2016). There is no obvious clustering pattern occurring across the parameters.

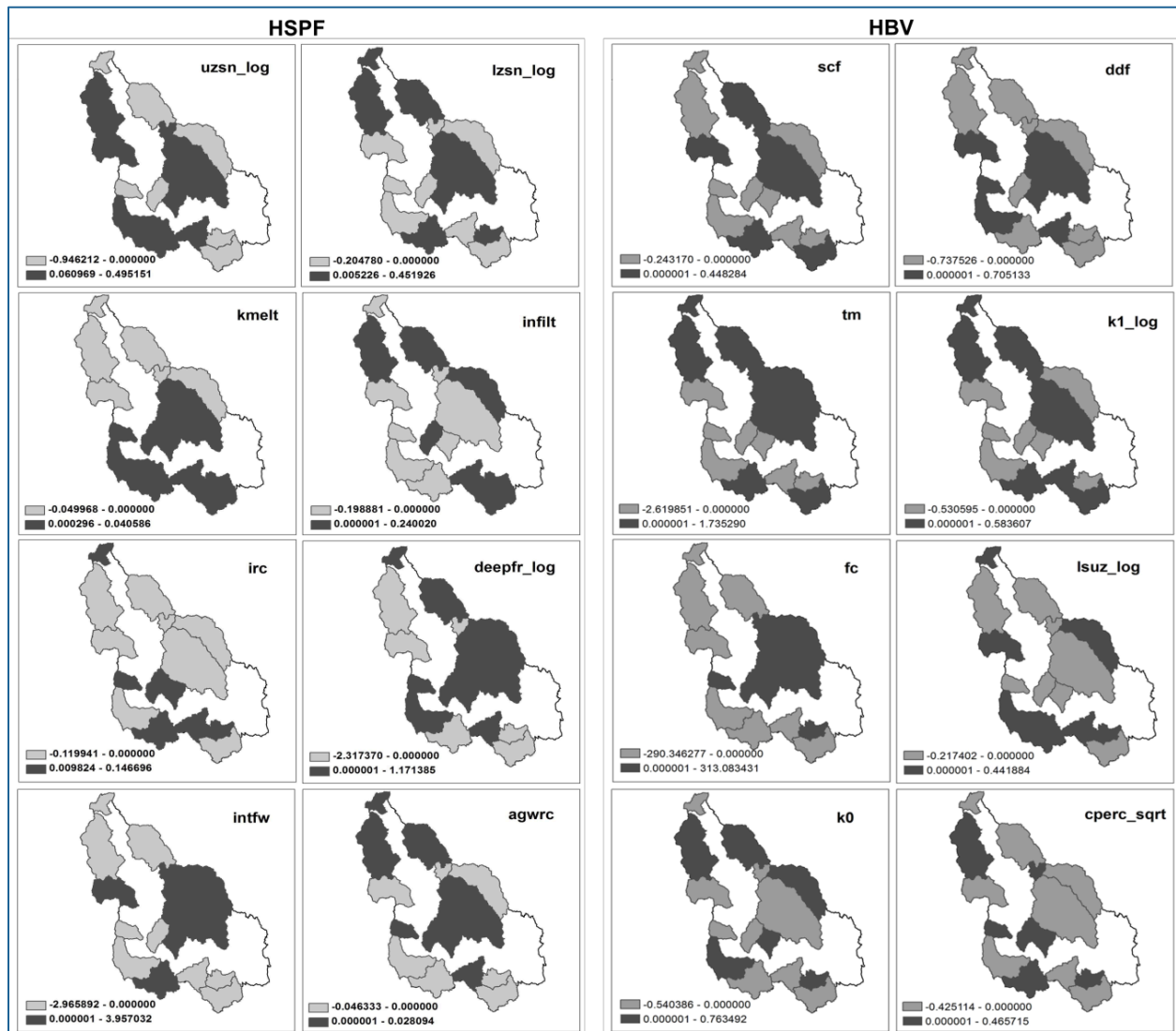


Figure K-4: Spatial mapping of model residuals from the regionalization regressions by subbasin (Source: Clark, 2016)

Model performance based on parameters estimated from the regression, proximity, and naïve mean regionalization methods were compared utilizing both closed-form and open-form validation techniques (Gordon, 2016). Closed-form validation compares predicted and calibrated parameters, while open-form validation compares model output generated based on the estimated and calibrated parameter sets. Both validation methods indicate that the HBV model generally performed less well across all performance criteria compared to the HSPF model. Further details are available in Gordon (2016).

Overall, the HSPF model tended to perform better than the HBV model in the Deerfield River watershed over the calibration period with median KGE values of about 0.78 and 0.68, respectively. The HSPF model also had higher median R² and NSE values over the calibration period of about 0.65 and 0.61, respectively, with the HBV model having significantly lower median values of 0.58 and 0.33. The NRSME error is lower for the HSPF model and the percent-bias (PBIAS) measure was closer to 0 on average for the HSPF model compared to HBV. In addition, volumetric efficiency (VE) was greater across the calibration and regionalization methods for the HSPF model compared to the HBV model.

The semi-distributed HSPF model seemed to perform better compared to the lumped-conceptual structure overall, suggesting this discretization difference might serve to better represent landscape heterogeneity as well as distribute the climate data more accurately. The semi-distributed nature of the HSPF model may lead to more accurate representations of the physical processes that drive surface runoff in the Deerfield River watershed. However, uncertainties associated with the modeling process for both HSPF and HBV, in addition to the lack of available data in the Deerfield River watershed, make it difficult to fully assess the ability of either model to represent the physical processes at the basin scale accurately. As such, hydraulic risk estimates based on both the HSPF and HBV models were developed.

Model parameters estimated based on the regression regionalized method performed best compared to calibrated parameters. When streamflow observations are not available to calibrate rainfall runoff models such as HSPF and HBV, regression-based regionalization to estimate parameter values provides the best accuracy of the methods evaluated in this project.

It is necessary to evaluate the accuracy of different models and methods for making predictions of runoff at ungaged locations because many of our rivers across the globe are not gaged. This study provides a framework for assessing the accuracy of estimating the parameters of process-based rainfall-runoff models in the region and also provides an assessment of model performance as applied within small forested northeastern U.S. catchments.

K.9 Acknowledgements

The descriptions of HBV, HSPF and their implementation for this project application were adapted from the M.S. thesis "Hydrologic Modeling at Ungauged Locations in Support of the Development of a Vulnerability Ranking Protocol System for Road-Stream Crossing Infrastructure" completed by Gordon Clark as part of this project.

K.10 References

- Archfield, S. A., P.A. Steeves, J.D. Guthrie, and K.G. Ries III. 2013. Towards a publicly available, map-based regional software tool to estimate unregulated daily streamflow at ungauged rivers. *Geoscientific Model Development*, 6(1), 101-115.
- Beck, M. B. 1987. *Water quality modeling: a review of the analysis of uncertainty*. Water Resources Research, 23(8), 1393-1442.
- Bergström, S. 1976. *Development and application of a conceptual runoff model for Scandinavian catchments*.
- Bergström, S. 2006. *Experience from applications of the HBV hydrological model from the perspective of prediction in ungauged basins*. IAHS publication, 307, 97.
- Bergström, S., J. Harlin, and G. Lindström. 1992. Spillway design floods in Sweden. I. New guidelines. *Hydrol. Sci. J.* 37(5), 10/1992, 505-519.
- Bergström, S., and G. Lindström. 2015. Interpretation of runoff processes in hydrological modelling—

- experience from the HBV approach. *Hydrological Processes*, 29(16), 3535-3545.
- Bicknell, B. R., J.C. Imhoff, J.L. Kittle Jr, A.S. Donigan Jr, and R.C. Johanson. 1996. *Hydrological simulation program-FORTRAN*. User's manual for release 11. US EPA.
- Blöschl, G. (Ed.). 2013. *Runoff prediction in ungauged basins: synthesis across processes, places and scales*. Cambridge University Press.
- Blöschl, G., M. Sivapalan, and T. Wagener. 2013. *Runoff prediction in ungauged basins: synthesis across processes, places and scales*. Cambridge University Press.
- Blöschl, G. and M. Sivapalan. 1995. Scale issues in hydrological modeling: a review. *Hydrological processes*, 9(3-4), 251-290.
- Crawford, N. H. and R.K. Linsley. 1966. *Digital Simulation in Hydrology*. Stanford Watershed Model 4.
- Doherty, J., and J.M. Johnston. 2003. *Methodologies for calibration and predictive analysis of a watershed model*.
- Duda, P. B., P.R. Hummel, A.S. Donigan Jr, and J.C. Imhoff. 2012. *BASINS/HSPF: Model use, calibration, and validation*. Transactions of the ASABE, 55(4), 1523-1547.
- Federer, C. A., C. Vörösmarty, and B. Fekete. 1996. *Intercomparison of methods for calculating potential evaporation in regional and global water balance models*. Water Resources Research, 32(7), 2315-2321.
- Gao, W., H.C. Guo, and Y. Liu. 2014. Impact of Calibration Objective on Hydrological Model Performance in Ungauged Watersheds. *Journal of Hydrologic Engineering*, 20(8), 04014086.
- Hamon, W. R. 1963. *Computation of direct runoff amounts from storm rainfall*. publisher not identified.
- Harlin, J. and C.S. Kung. 1992. Parameter uncertainty and simulation of design floods in Sweden. *Journal of Hydrology*, 137(1), 209-230.
- Homer, C.G., J.A. Dewitz, L. Yang, S. Jin, P. Danielson, G. Xian, J. Coulston, N.D. Herold, J.D. Wickham, and K. Megown. 2015. Completion of the 2011 National Land Cover Database for the conterminous United States-Representing a decade of land cover change information. *Photogrammetric Engineering and Remote Sensing*, v. 81, no. 5.
- Hornberger, G. M. and R.C. Spear. 1981. Approach to the preliminary analysis of environmental systems. *J. Environ. Manage.* (United States), 12(1).
- Iskra, I. and R. Droste. 2007. *Application of non-linear automatic optimization techniques for calibration of HSPF*. Water environment research, 647-659.
- Jain, S.K. and K.P. Sudheer. 2008. Fitting of hydrologic models: a closer look at the Nash-Sutcliffe index. *Journal of Hydrologic Engineering*, 13 (10).

- Johnson, M. S., W.F. Coon, V.K. Mehta, T.S. Steenhuis, E.S. Brooks, and J. Boll. 2003. Application of two hydrologic models with different runoff mechanisms to a hillslope dominated watershed in the northeastern US: a comparison of HSPF and SMR. *Journal of Hydrology*, 284(1), 57-76.
- Kim, S. M., B.L. Benham, K.M. Brannan, R.W. Zeckoski, and J. Doherty. 2007. *Comparison of hydrologic calibration of HSPF using automatic and manual methods*. Water resources research, 43(1).
- Lindstr.m, G., J. Rosberg, and B. Arheimer. 2005. *Parameter precision in the HBV-NP model and impacts on nitrogen scenario simulations in the R.nne. River, southern Sweden*. *Ambio* 34(7), 533–537.
- Lu, J., G. Sun, S.G. McNulty, and D.M. Amatya. 2005. *A comparison of six potential evapotranspiration methods for regional use in the southeastern United States*.
- McCabe, G. J., L.E. Hay, A. Bock, S.L. Markstrom, and R.D. Atkinson. 2015. Inter-annual and spatial variability of Hamon potential evapotranspiration model coefficients. *Journal of Hydrology*, 521, 389-394.
- McCuen, R.H., Z. Knight, and A. G. Cutter. 2006. Evaluation of the Nash-Sutcliffe efficiency index, *Journal of Hydrologic Engineering*, 11(6).
- Merz, R. and G. Blöschl. 2004. Regionalisation of catchment model parameters. *Journal of Hydrology*, 287(1), 95-123.
- NLCD (2011) – See Homer et al. 2015, preferred citation.
- Natural Resources Conservation Service (NRCS), United States Department of Agriculture. Soil Survey Geographic (SSURGO) Database. Available online at <https://sdmdataaccess.sc.egov.usda.gov>
- Parajka, J., G. Blöschl, and R. Merz. 2007. *Regional calibration of catchment models: Potential for ungauged catchments*. Water Resources Research, 43(6).
- Parajka, J., R. Merz, and G. Blöschl. 2005. A comparison of regionalisation methods for catchment model parameters. *Hydrology and earth system sciences discussions*, 9(3), 157-171.
- Parajka, J. and A. Viglione. 2012. TUWmodel: Lumped hydrological model developed at the Vienna University of Technology for education purposes, R package version 0.1-2.
- PRISM Climate Group. 2004. Oregon State University, <http://prism.oregonstate.edu>, created 4 Feb 2004.
- PRISM Climate Group. 2011. Oregon State University, <http://prism.oregonstate.edu>, created 4 Feb 2004.
- Seong, C., Y. Her, and B.L. Benham. 2015. Automatic calibration tool for Hydrologic Simulation Program-FORTRAN using a shuffled complex evolution algorithm. *Water*, 7(2), 503-527.
- Singh, V. P. and D.A. Woolhiser. 2002. Mathematical modeling of watershed hydrology. *Journal of hydrologic engineering*, 7(4), 270-292.

- Steinschneider, S., Y.C.E. Yang, and C. Brown. 2015. Combining regression and spatial proximity or catchment model regionalization: a comparative study. *Hydrological Sciences Journal*, 60(6), 1026-1043.
- US EPA. 1999. HSPFParm: An Interactive Database of HSPF Model Parameters, Version 1.0. EPA-823-R-99-004. U.S. Environmental Protection Agency, Office of Water, Washington, DC. Available from the BASINS website, <http://www.epa.gov/ost/basins/support.htm>
- USGS. 2017. National Hydrography Dataset Plus High Resolution (NHDPlus HR) – USGS National Map Downloadable Data Collection. Available on-line: <https://catalog.data.gov/dataset/national-hydrography-dataset-plus-high-resolution-nhdplus-hr-usgs-national-map-downloadable-da>
- Vleeschouwer, N. D. and V.R. Pauwels. 2013. Assessment of the indirect calibration of a rainfall runoff model for ungauged catchments in Flanders. *Hydrology and Earth System Sciences*, 17(5), 2001-2016.
- Vorosmarty, C. J., C.A. Federer, and A.L. Schloss. 1998. Potential evaporation functions compared on US watersheds: Possible implications for global-scale water balance and terrestrial ecosystem modeling. *Journal of Hydrology*, 207(3), 147-169.
- Young, P. 1983. The validity and credibility of models for badly defined systems. In *Uncertainty and forecasting of water quality*, pp. 69-98. Springer Berlin Heidelberg.
- Yu, P. S. and T.C. Yang. 2000. Fuzzy multi-objective function for rainfall-runoff model calibration. *Journal of hydrology*, 238(1), 1-14.
- Zhang, X. and G. Lindstr.m. 1997. Development of an automatic calibration scheme for the HBV hydrological model. *Hydrological Processes*, 11(12), 1671-1682.

Appendix L WRFH OVERVIEW

L.1 Model Summary

The National Center for Atmospheric Research (NCAR) Weather Research and Forecasting model (WRF) hydrologic extension package, referred to subsequently as WRFH, is an open source, community-based modeling framework for coupling multiple atmospheric and terrestrial hydrologic process representations. It can be run either in a coupled architecture, linking atmospheric and hydrologic models directly, or as a stand-alone hydrological modeling suite. The WRFH architecture allows it to be configured to represent a wide range of landscapes and hydrologic conditions, accounting for region specific land-atmosphere interactions, land surface processes, subsurface storage and flow, overland and channel flow, and water management. Multi-scale functionality allows modeling at different spatial grid scales. Figure L-1 provides an overview of the modeling framework, showing both the coupled and stand-alone hydrologic modeling capability. Figure L-2 provides further details on elements and linkage capabilities for representing terrestrial hydrologic processes.

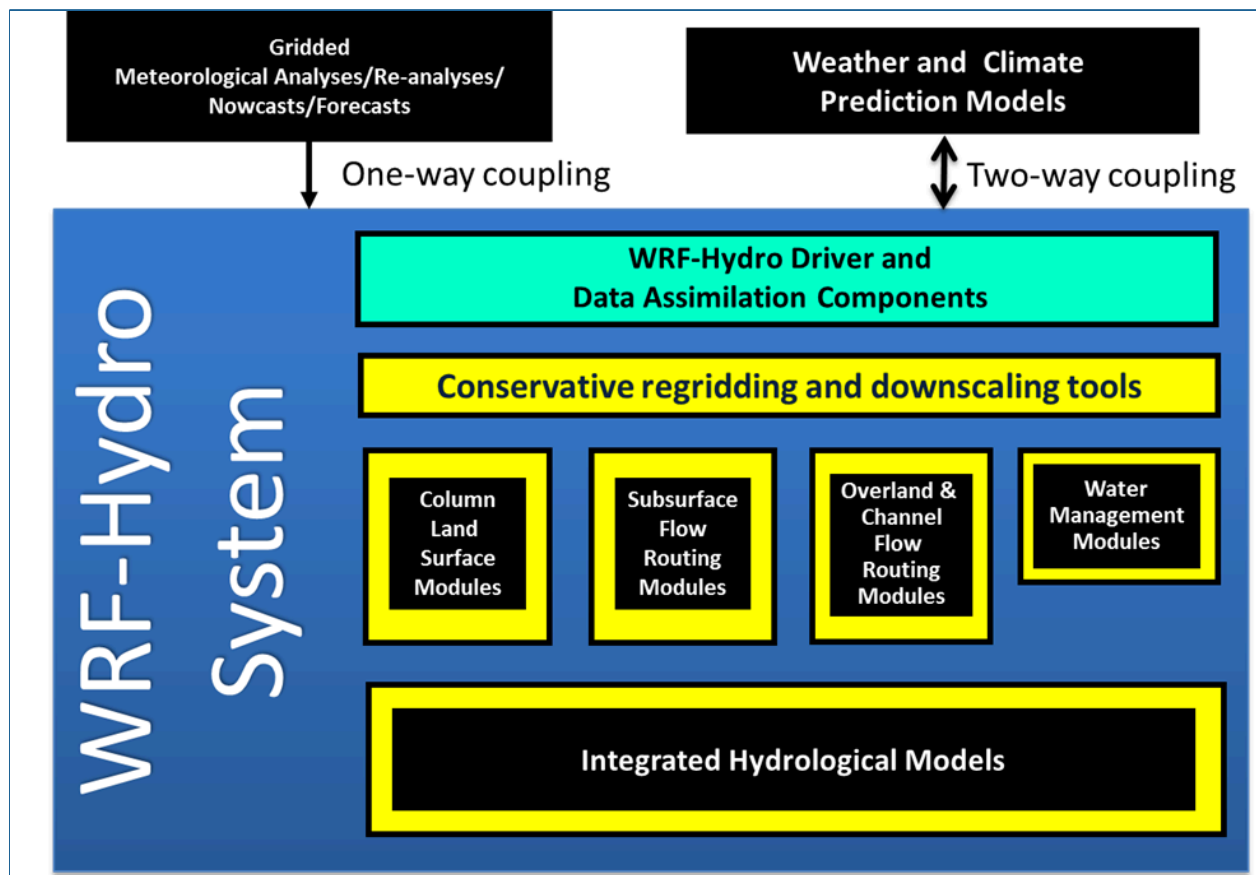


Figure L-1: Schematic of the modularized multiscale, multi-physics WRFH modeling framework, from Gochis et al. (2015)

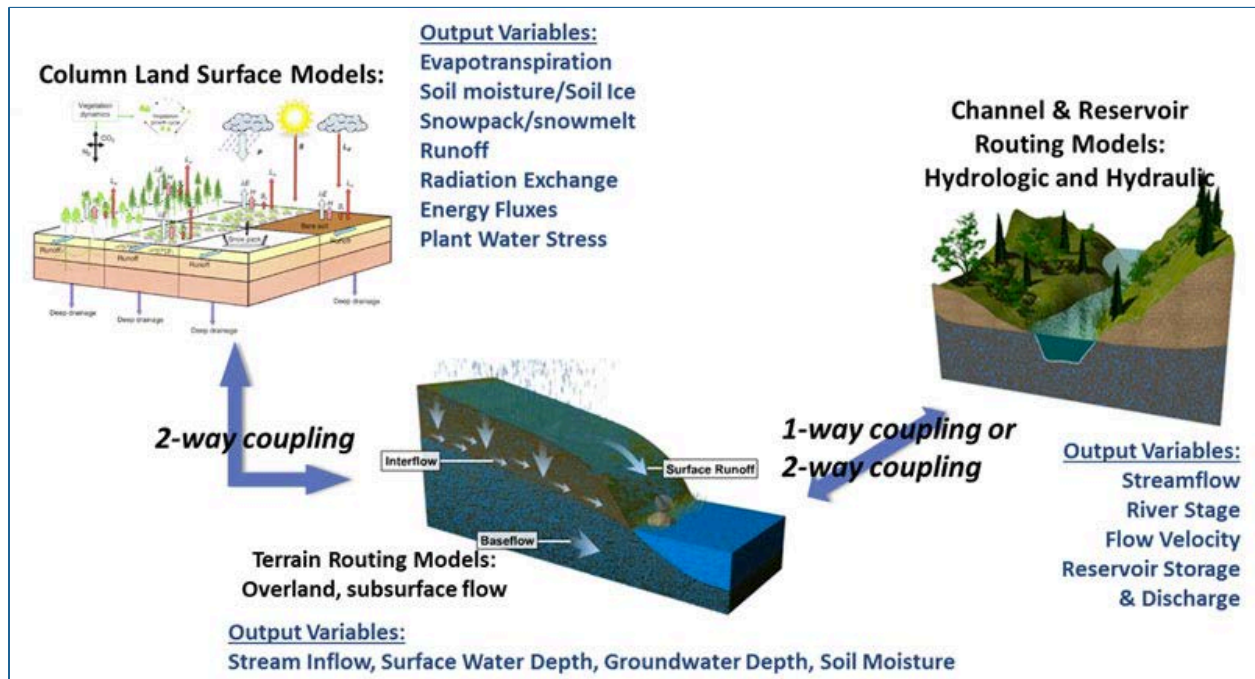


Figure L-2: Conceptual diagram of terrestrial hydrologic processes and linkages, from Gochis et al. (2015)

The WRFH system has been utilized across a wide range of settings for both research and operational applications. It is the core model for the National Water Model, which provides streamflow forecasts for river reaches across the U.S.

L.2 Implementation for Deerfield River Watershed

The WRFH uncoupled configuration (WRFH uncoupled/standalone) model was applied to generate projected streamflows. This model allows for generating ensemble results by changing the physics used in the modeling framework or, as done for this project, the climate forcing. For the Land Surface Model (LSM), the Noah LSM with multi-parameterization (MP) option was utilized (Yang et al., 2011a, 2011b). Noah LSM is widely used in operational systems by the National Centers for Environmental Prediction (NCEP) as part of the North American Land Data Assimilation System project (Xia et al., 2012a, 2012b), by the Weather Research Forecast (WRF) model community, and by the Air Force Weather Agency (Niu et al., 2011).

WRFH, compared to other hydrology models, is computationally expensive; therefore, the number of runs utilized to calibrate the model was limited. The number of physical parameters that must be defined make a manual procedure impractical (Givati, Gochis, Rummeler, & Kunstmann, 2016; Yucel, Onen, Yilmaz, & Gochis, 2015). For this reason calibration was done utilizing Monte Carlo Markov Chain data parameter estimation as part of the SPOTting Model. The SPOTting Model is a ready-made python package (SPOTPY) (Houska, Kraft, Chamorro-Chavez, & Breuer, 2015), similar to PETS that was used by Senatore et al. (2015) to calibrate WRFH. The procedure followed is similar to previous work by (Givati et al., 2016; Senatore et al., 2015; Yucel et al., 2015); however, measures of Kling-Cupta Efficiency (KGE) were used instead of a Nash-Sutcliffe Efficiency (NSE) to minimize bias (Gupta et al., 2009). The variables used in this calibration are infiltration factor (REFTKD 0.5-5) (Niu, 2011); SLOPE, which is a coefficient between 0.1-1.0 that modifies the drainage out of the bottom of

the last soil layer (a larger surface slope implies larger drainage, Mitchell et al., 2005); saturated soil hydraulic conductivity (DKSAT) (Mitchell et al., 2005); an exponential coefficient within the bucket model of WRFHNoahMP; and a geometry and infiltration parameter in the groundwater bucket model. For the routing modules of WRF-hydro, the OVROUGH scaling factors that change the rugosity of the terrain routing and the RETDEPRT scaling factor that modifies the depth that water needs to allow water movement from one cell to the next following the gradient (Gochis, Yu, & Yates, 2013; Senatore et al., 2015) were included in the calibration. Additionally, the channel roughness and channel geometry was calibrated (for more details see Gochis, Yu, & Yates, 2015).

A prominent factor in determining an adequate and robust engineering design is the magnitude of peak flows; particularly when addressing flood risk. The estimation of peak flows involves the estimation of travel time and attenuation of the flood waves; this is otherwise known as flood routing. For most applications, flows are considered unsteady in open-channels, and can be solved for using the Saint Venant Equations developed by Barre de Sainte-Venant in 1848, which accounts for continuity and momentum for one-dimensional flow (Heatherman, 2008). The momentum equation accounts for gravity, pressure variation, and friction due to the channel walls. A full solution that employs all terms of the Saint Venant equations is considered to be a 'hydraulic' solution, whereas simplifications are called 'hydrologic' solutions, in which one or more terms in the momentum equations are omitted. Because a hydraulic solution is very computationally intensive, most approaches are simplifications of the Saint Venant equations in which solutions are empirical approximations (Heatherman, 2008). The most commonly used method to approximate the Saint Venant equations is the Muskingum method, originally developed for use by the Army Corps of Engineers. The Muskingum method relies on two coefficients, K and X, that are used to represent the travel time and attenuation of flood waves, respectively. This routing approximation maintains constant calibration parameters that do not vary with flow, and was utilized for this project through a code written in Python. The river routing method utilizes the National Hydrography Dataset Plus (NHDPlus) dataset to provide the network of flowlines within each selected watershed. In order to visualize the data, the NHDPlus network was utilized to geo-locate the stream-lines for which projections of streamflow data were needed.

The justification for using physical models such as WRFH is that they can provide information on streamflow in ungaged watersheds. The model was calibrated to a short period, from July to October 2011, in order to set the characteristic parameterization for the Deerfield River watershed. This period was selected to evaluate how well the model could replicate impacts of Hurricane Sandy, which occurred in August 2011. A period of 30 plus years was utilized for the validation period to evaluate the performance of the model in a long-term run. WRFH for the Deerfield River watershed was calibrated against two reference streamflow gauge stations maintained by USGS, the Green River near Colrain and the North River at Shattuckville station. For the calibration period, the Nash Sutcliffe Efficiency is 0.79 and 0.8; percentage bias is 16.36% and 23.8%; and correlation of 0.9 and 0.92 for the Green River and North River Stations respectively (Figure L-3 and Figure L-4). For the validation period, the Nash Sutcliffe Efficiency is 0.6 and 0.55; percentage bias is 12.88% and -5.51%; and correlation of 0.81 and 0.77 for the Green River and North River Stations respectively.

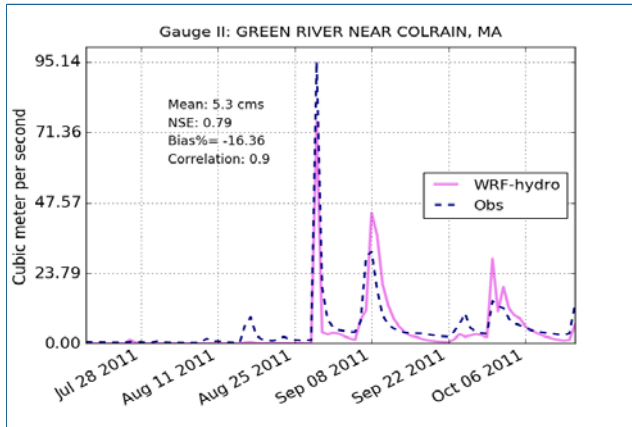


Figure L-3: Green River Near Colrain, MA. hydrograph for calibration period.

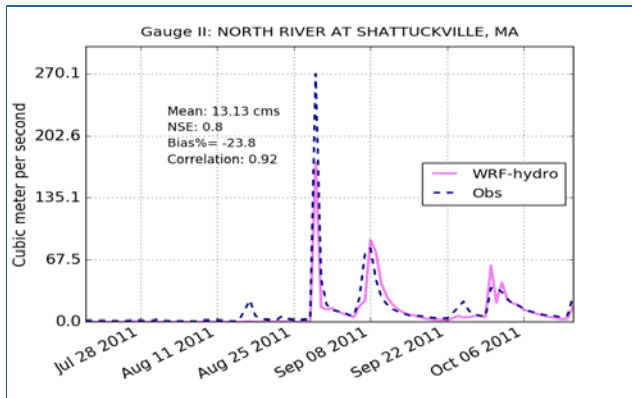


Figure L-4: North River at Shattuckville, MA. hydrograph for calibration period.

L.3 Application

WRFH was run for a number of subwatersheds across the Deerfield, Figure L-5, ranging in size from 0.024 – 1,720 km². Flood flows estimates were derived from the modeled daily streamflow estimates as described in Chapter 5.3.2.3. Model results were then downscaled from the subbasin to crossing location as described in Chapter 5.3.2.4 utilizing the DA index method and coefficient “b” values derived as part of this study.

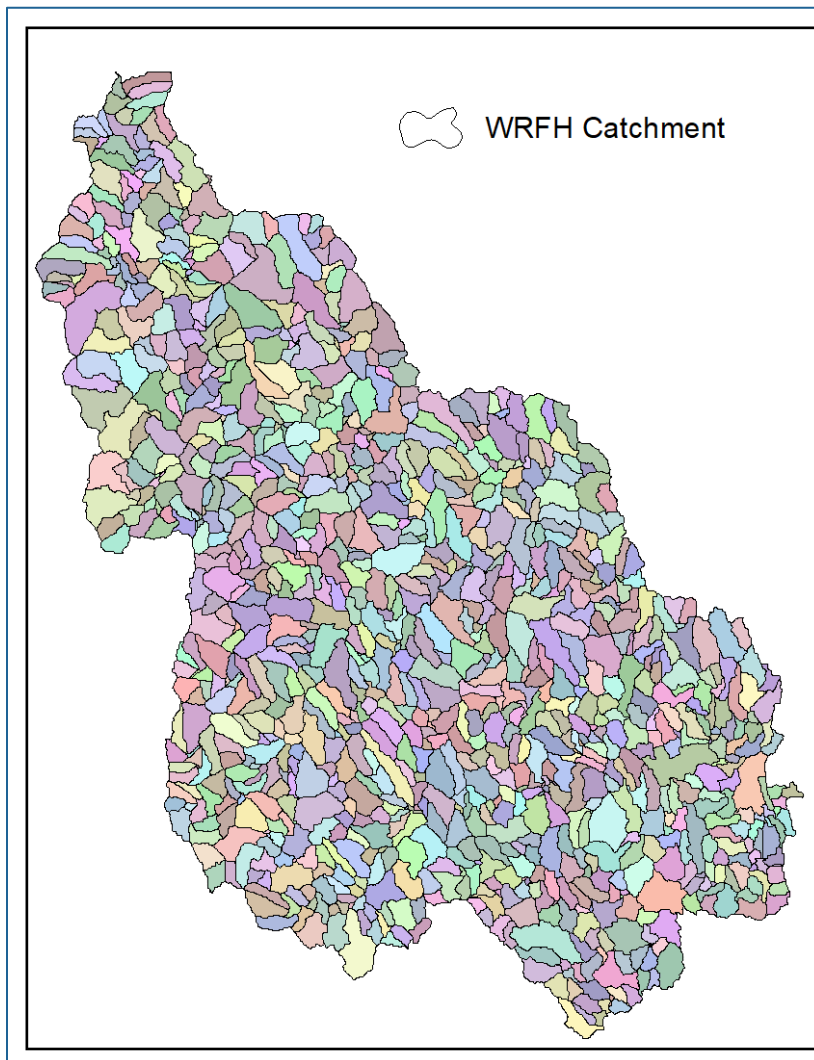


Figure L-5: The subbasins in the Deerfield River watershed that are the basis of the WRFH model

L.4 References

- Givati, A., D. Gochis, T. Rummeler, and H. Kunstmann. 2016. Comparing One-Way and Two-Way Coupled Hydrometeorological Forecasting Systems for Flood Forecasting in the Mediterranean Region. *Hydrology*, 3(2), 19. <https://doi.org/10.3390/hydrology3020019>
- Gochis, D., W. Yu, and D. Yates. 2013. WRF-Hydro Technical Description and User's Guide.
- Gochis, D., W. Yu, and D. Yates. 2015. *WRF-Hydro Technical Description and User's Guide Version 3*.
- Gupta, H. V., H. Kling, K. K. Yilmaz, and G. F. Martinez. 2009. Decomposition of the mean squared error and NSE performance criteria: Implications for improving hydrological modelling, *J. Hydrol.* 377(1–2), 80–91, doi:10.1016/j.jhydrol.2009.08.003.
- Heatherman, W.J. 2008. *Flood Routing On Small Streams: A review Of Muskingum Cunge, cascading Reservoirs, and Full Dynamic Solutions*. PhD Dissertation, University of Kansas: Lawrence, KS. Available from KU ScholarWorks: <http://hdl.handle.net/1808/4349>

- Houska, T., P. Kraft, A. Chamorro-Chavez, and L. Breuer. 2015. SPOTting model parameters using a ready-made python package. *PLoS ONE*, 10(12), 1–22.
<https://doi.org/10.1371/journal.pone.0145180>
- Mitchell, K., M. Ek, V. Wong, D. Lohmann, V. Koren, J. Schaake ... P. Ruscher. 2005. *Noah Land Surface Model (LSM) User's Guide*. NCAR Research Application Laboratory (RAL).
- Niu, G.-Y. 2011. *The community Noah land surface model (LSM) with Multi-physics options. User Guide. Heritage*.
- Senatore, A., G. Mendicino, D.J. Gochis, W. Yu, D.N. Yates, and H. Kunstmann. 2015. Fully coupled atmosphere-hydrology simulations for the central Mediterranean: Impact of enhanced hydrological parameterization for short and long time scales. *Journal of Advances in Modeling Earth Systems*, n/a-n/a. <https://doi.org/10.1002/2015MS000510>
- Xia, Y. et al. 2012a. Continental-scale water and energy flux analysis and validation for North American Land Data Assimilation System project phase 2 (NLDAS-2): 2. Validation of model-simulated streamflow, *J. Geophys. Res.*, 117, D03110, doi:10.1029/2011JD016051.
- Xia, Y. et al. 2012b. Continental-scale water and energy flux analysis and validation for the North American Land Data Assimilation System project phase 2 (NLDAS-2): 1. Intercomparison and application of model products, *J. Geophys. Res. Atmos.*, 117(D3), n/a-n/a, doi:10.1029/2011JD016048.
- Yang, Z., X. Cai, G. Zhang, A. a Tavakoly, Q. Jin, L. H. Meyer, and X. Guan. 2011a. The Community Noah Land Surface Model with Multi-Parameterization Options Technical Description, *Cent. Integr. Earth Syst. Sci. Dep. Geol. Sci. Univ. Texas Austin, Austin, TX, USA*.
- Yang, Z.-L. et al. The community Noah land surface model with multiparameterization options (Noah-MP): 2. Evaluation over global river basins, *J. Geophys. Res.*, 116(D12), D12110, doi:10.1029/2010JD015140
- Yucel, I., A. Onen, K.K. Yilmaz, and D.J. Gochis. 2015. Calibration and evaluation of a flood forecasting system: Utility of numerical weather prediction model, data assimilation and satellite-based rainfall. *Journal of Hydrology*, 523(November), 49–66.
<https://doi.org/10.1016/j.jhydrol.2015.01.042>

L.5 Acknowledgments

WRFH modeling was completed by Dr. Marcelo Somos Valenzuela as part of his post-doctoral research.

Appendix M Cornell's Culvert Capacity Calculations

Cornell University's *Determining Peak Flow Under Different Scenarios and Assessing Organism Passage Potential: Identifying and Prioritizing Undersized and Poorly Passable Culverts* project determines peak flow capacity under head conditions at the inlet up to the height of the road surface. To determine peak flow capacity, Cornell's method uses standard engineering equations for circular pipe flow based on the culvert's size, shape, inlet type, length, slope, and culvert material. It is assumed that max capacity is when the inlet is fully submerged under a water elevation equal to that of the road, but not spilling over. This leaves three flow conditions: submerged outlet control, unsubmerged outlet control, and inlet control; each with a unique equation to calculate flow. For outlet controlled flows,

$$q = \frac{A\sqrt{2gH}}{\sqrt{1+K_e+K_c l}} \quad \text{Equation 1}$$

where A = cross-sectional area, K_e = entrance loss coefficient, l = length of pipe, K_c = pipe friction loss coefficient (Eq. 2), and H = head loss (Eq. 3, 4). The pipe friction loss coefficient (K_c) is calculated with the following equation:

$$K_c = \frac{2gn^2}{R^{4/3}} \quad \text{Equation 2}$$

where R = hydraulic radius and n = manning's roughness. Head loss (H) is dependent on whether the outlet is submerged:

$$H = I s_a \text{ (Submerged)} \quad \text{Equation 3}$$

$$H = I s_a + 0.4D \text{ (Unsubmerged)} \quad \text{Equation 4}$$

where s_a = culvert slope, and D = culvert diameter. For inlet controlled orifice flow, Cornell uses an equation from *Schall et al. (2012)*:

$$q = A\sqrt{D} \sqrt{\frac{H-y-K_s s_a}{c}}$$

where H = headwater depth from invert to top of road, A = cross-sectional area, D = culvert diameter, s_a = culvert slope, K_s = slope adjustment; usually -0.5 or +0.7 for mitered inlets, and lastly, y and c are tabulated constants that are based on material and inlet type.

References

Schall, J.D., P.L. Thompson, S.M. Zerges, R.T. Kilgore, and J.L. Morris. 2012. Hydraulic Design of Highway Culverts, Third Edition. Hydraulic Design Series Number 5, FHWA-HIF-12-026. U.S. Department of Transportation, Federal Highway Administration: Washington, D.C.

Appendix N HYDRAULIC RISK METHODOLOGY COMPARISON

N.1 Overview

Recent projects in New York (NY) and New Hampshire (NH) also aim to identify culverts at risk of hydraulic failure under current and future climate conditions. The New York and New Hampshire methodologies are briefly compared against the UMass/DOT method in this appendix.

N.2 Summary of Other Project Methods

N.2.1 Cornell

Cornell University's *Determining Peak Flow Under Different Scenarios and Assessing Organism Passage Potential: Identifying and Prioritizing Undersized and Poorly Passable Culverts* project determines peak flow capacity under head conditions at the inlet up to the height of the road surface. To determine peak flow capacity, Cornell's method uses standard engineering equations for circular pipe flow based on the culvert's size, shape, inlet type, length, slope, and culvert material. It is assumed that max capacity is when the inlet is fully submerged under a water elevation equal to that of the road, but not spilling over. This leaves three flow conditions: submerged outlet control, unsubmerged outlet control, and inlet control; each with a unique equation to calculate flow. The equations utilized in the Cornell method are provided in Appendix M.

N.2.2 Trout Unlimited

For this project, Trout Unlimited (TU) was subcontracted to modify a web-based tool they had developed for other projects in order to provide the MA, VT, and NH RPF equation estimates for this project. The TU tool was specifically developed for evaluating the potential of culverts to fail under current and future climate conditions. TU's method for assessing failure differs significantly from that utilized in this project. Specifically, rather than calculating culvert capacity based on a given headwater depth (HW) elevation and comparing capacity against RI estimates (as done in the Cornell and UMass methods), TU estimates the HW elevation associated with each RI estimate. Culvert "status" is assigned based on the resulting ratio of HW to interior rise of the culvert. The culvert is considered 'passing' if the ratio is under 0.85, the culvert is considered 'failing' if the ratio is over 1.15, and the culvert is considered 'transitional' if the ratio is between 0.85 and 1.15. Output consists of a score (passing, transitional, failing) for each RI considered.

N.3 Risk Assessment Comparison Approach

In summary, the three approaches to estimating hydraulic risk of failure are as follows:

UMassDOT

- Road-stream crossing capacity is calculated and compared against RI estimates for current and future climate scenarios,
 - Capacity of culverts and small bridges that function as culverts is based on HDS-5 equations considering both inlet and outlet control, calculated with CulvertMaster® software. Capacity of structures larger than can be calculate in CulvertMaster® is estimated via Manning's equation.
 - Three HW conditions are utilized to determine capacity, selected based on the culvert material.

- Output consists of a $Q_{critical}$ value, the maximum predicted based on inlet or outlet control, for the HW permitted based on culvert material.
- A single hydraulic risk of failure score is assigned to the crossing based on an empirical equation developed specifically for the project (described below) based on capacity and the Q_{25} RI estimate.

Cornell

- Road-stream crossing capacity is calculated and compared against RI estimates for current and future climate scenarios,
 - Capacity is determined based on pipeflow equations considering inlet and outlet control. Only circular culverts are evaluated.
 - It is assumed that max capacity is when the inlet is fully submerged under a water elevation equal to that of the road, but not spilling over. No consideration of possible failure due to culvert material at lower HW elevations is made.
 - Output consists of a $Q_{critical}$ value based on the HW condition.
- A single hydraulic risk of failure is determined based on the maximum return period that can be accommodated based on the calculated capacity.

TU

- HW depth associated with a range of RI discharge estimates is calculated,
 - HW depth for a given RI discharge value based on a parabolic equation estimate of the HDS-5 equations.
 - RI discharge values are calculated based on one of the USGS RPFs except for very small basins, where the SCS method is used.
- Multiple hydraulic risk of failure estimates are identified, one for each RI,
 - The culvert is rated based on the ratio of the back-calculated HW elevation to the Interior Rise of the culvert.
 - The culvert is considered Passing if the ratio is under 0.85, the culvert is considered Failing if the ratio is over 1.15, and the culvert is considered Transitional if the ratio is between 0.85 and 1.15.
 - Output consists of a score (passing, transitional, failing) for each RI considered.

N.4 Comparison of Results

Due to the underlying differences in the three approaches it is difficult to directly compare hydraulic risk of failure estimates. However, the UMass and Cornell approaches are similar enough that $Q_{critical}$ results based on the Cornell method may be calculated and then run through the UMass empirical equation for comparison purposes. The UMass and Cornell hydraulic risk estimates may then be compared against the TU estimates qualitatively. Although beyond the scope of the project, such a comparison is of interest and was completed for a subset of road stream crossings.

A subset of 441 road stream crossings where hydraulic risk could be evaluated by all three methods was identified. $Q_{critical}$ values were then calculated based on Cornell's methods and applied in the UMass empirical equation for hydraulic risk based on the ratio of $Q_{critical}$ to Q_{25} . These estimates are compared against the TU risk estimates based on their 'pass', 'transitional', and 'fail' criteria for the 25-year RI in Figure N-1 for current climate and Figure N-2 for mid-century (TU results for mid-century are not available and thus not included). TU results based on the 25-year RI are deemed most appropriate for the comparison, as this is the RI utilized in the UMass empirical equation.

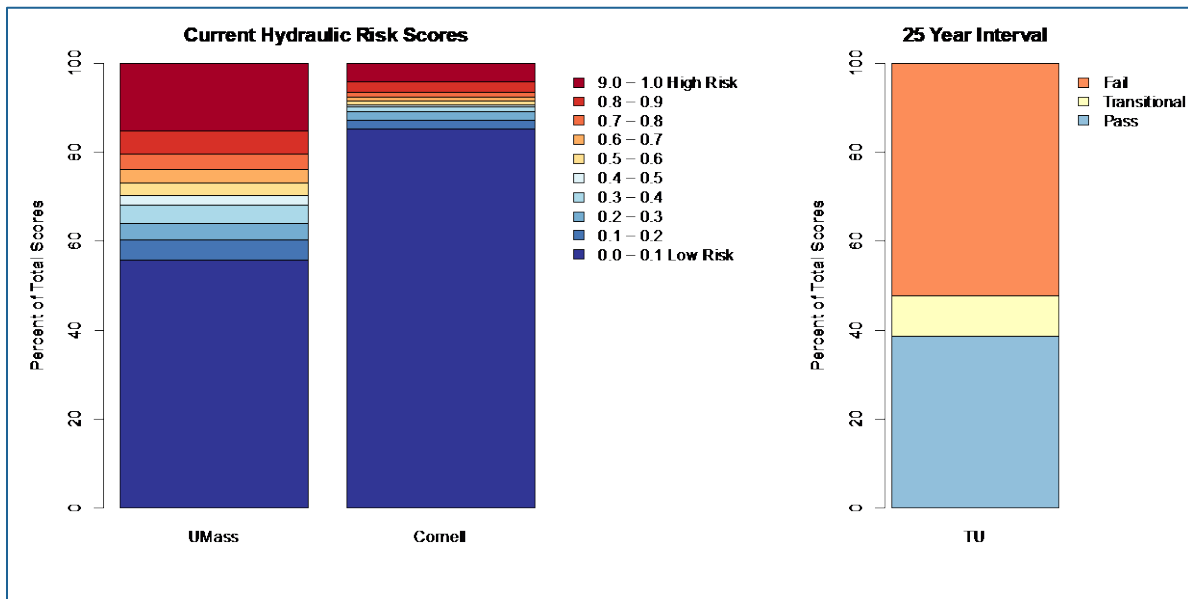


Figure N-1: Comparison of hydraulic risk across the three methods for current climate

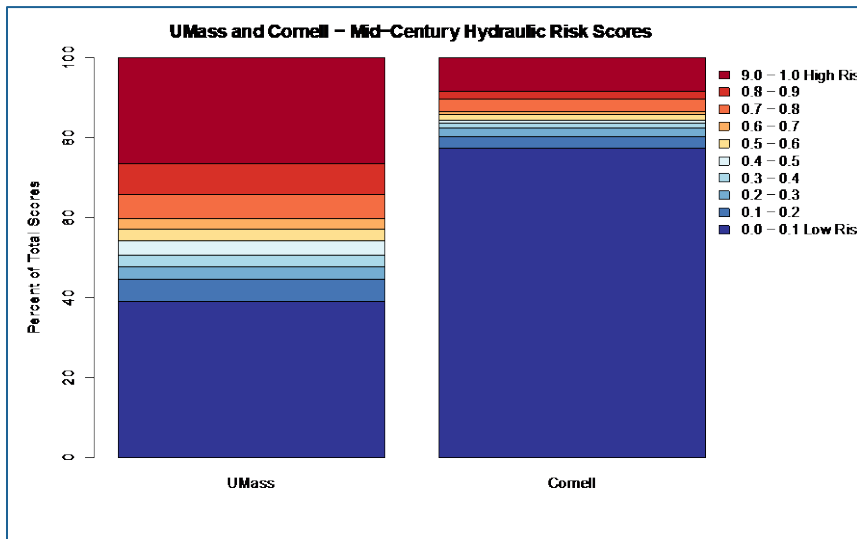


Figure N-2: Comparison of hydraulic risk across the three methods for mid-century (results for TU mid-century are not available)

Cornell’s methodology resulted in higher estimates for $Q_{critical}$, on average, compared to the UMass methodology. The higher $Q_{critical}$ values in turn translated to lower estimates of hydraulic risk (e.g., more low scores, indicated by blues in the figures). For example, at mid-century approximately 40% of culverts have a hydraulic risk score <0.1 based on the UMass method, compared to approximately 80% of culverts based on the Cornell estimates of $Q_{critical}$ applied within the UMass empirical equation for hydraulic risk. Although not directly comparable, the TU method predicts a higher level of risk, predicting that more than half of the 441 road-stream crossings will fail to pass the 25 year RI flow under current conditions.

There is no way to determine which of the three methods of hydraulic failure risk assessment is most accurate. However, this comparison is valuable for understanding the different levels of sensitivity across the three methods. The UMass methodology provides a middle ground between the NY-Cornell method (lower risk predicted) and the NH-TU method (higher risk predicted) for estimating hydraulic failure risk. It is important to recall that the hydraulic failure risk estimates that Cornell would provide directly would differ from those utilized in this comparison. "Published" Cornell hydraulic risk estimates would consist of the highest RI predicted to safely pass through the road-stream crossing.

The comparison shown here focuses on the impact of differences in the HW criteria and methods utilized for $Q_{critical}$ calculation between the two approaches. The Cornell method utilizes a higher allowable HW criterion, resulting in the lower failure risk. Theoretically, the higher allowable HW, equivalent to the top of the road surface, potentially subjects the road-subsurface to piping and failure. The UMassDOT project team considered this an unreasonable risk. The TU method uses a much lower allowable HW criterion, resulting in higher failure risk. Theoretically, the lower allowable HW does not allow water to pond upstream of the culvert. The UMassDOT project team considered this an unreasonable constraint, as culverts are typically designed to pond.

Appendix O DIGITAL REPOSITORY

The following electronic files were provided separately to MassDOT.

O.1 GIS Layers

The following GIS files are provided as part of the project database:

- 30m DEM (raster)
- Flow accumulation (raster)
- Stream power (vector)
- Snap point crossings (vector)
- NAACC crossings: basic data and scores (vector)
- Color coded damage and historic failures (vector)
- Road networks (vector)
- Hydrography (vector)

Metadata for the project was prepared for all spatial data layers, rasters and summary spreadsheets. Metadata was created using the FGDC Content Standard for Digital Geospatial Metadata (FGDC-STD-001-1998) and is provided in two formats, xml and html. Xml formatted metadata was created and error-checked in XML- Notepad and converted to html format in ArcGIS 10.4.x using the USGS metadata wizard stylesheet. Note: not all xml metadata was converted to html format. The conversion needs to be completed after MassDOT determines where the data from this project will be housed. Without knowing where the data will be housed the onlink³ field in the metadata that tells the user where to find the data cannot be filled in.

O.2 Access Database

O.2.1 Raw Data

Raw data are considered data collected specifically for the project with minimal processing. These data included information collected by TU, MMI, and UMass in the field as well as data from MassDOT bridge inspection reports. Climate projection data utilized for running the physical hydrologic models is also included. The following raw data are provided in the relational database:

- NAACC Database
- UMass Stream Continuity Project (UMass protocol data)
- Culvert condition assessment
- TU custom data (elevation, pebble counts)
- UMass Geosciences Crew field data
- MMI field data
- MassDOT bridge inspection data
- NARCCAP data after bias adjustment for Deerfield River watershed
 - NARCCAP current temperature
 - NARCCAP future temperature
 - NARCCAP current precipitation
 - NARCCAP future precipitation

³ "Onlink" is the field name in the Federal Geospatial Data Committee metadata content standard schema where the metadata creator fills in the URL or internet link where the user can find the data that the metadata describes.

O.2.2 Derived Data

Derived data are considered values that are calculated or modeled based on the raw and GIS data.

Readme files in the database provide descriptions of each data field. Specifically these data include:

- Derived Geomorphic crew data (Manning's N, slope, area)
- Geomorphic assessment and scoring
- MMI stream power data
- Structural risk scoring
- Ecological disruption data and scoring
- Criticality assessment and scoring
- The estimated Q_{critical} flows for each road stream crossing, identified by xycode, as well as the input data and method of calculation
- GIS-derived attribute data utilized in models – data for each road stream crossing, including the xycode, area, slope, precipitation, mean elevation, channel slope, and “b” values. These data were utilized as part of the HSPF, HBV, UMass MA RPFE streamflow modeling efforts.
- Modeled flows for
 - 2-, 5-, 10-, 25-, 50-, and 100-year RI estimates
 - 5 statistical models (Jacobs, UMass MA RPFE, TU MA RPFE, TU NH RPFE, TU VT RPFE)
 - 3 Physical models (HSPF, HBV, WRFH) for three CI each (5%, 50%, 95%)
 - Current, Mid-Century, and End-Century (statistical models only) estimates for:
 - Physical model results based on daily climate predictions from seven (WRFH) or nine (HBV and HSPF) dynamically downscaled projections (GCM-RCMs) available from NARCCAP, bias adjusted specifically for the Deerfield River Watershed
 - Statistical models – three climate conditions: low, most-likely or “best”, and high future rainfall estimates
- Summary of the 25-year RI estimates for the models and conversion to hydraulic risk scores
- Hydraulic condition categories for individual model outputs and climate conditions for current and mid-century climate. Note that for the physical models, condition categories are also provided for the 5%, 50% and 95% CI estimates of RI. For the statistical models at mid-century, condition data are also provided based on the low, most-likely or “best”, and high estimates of future rainfall.
- Hydraulic risk scores for individual model outputs and climate conditions, as well as combined scores for three time periods:
 - Current
 - Mid-century
 - End-century

Note that for the physical models, individual hydraulic risk scores are also provided for the 5%, 50%, and 95% CI estimates of RI. For the statistical models at mid-century, individual hydraulic risk scores are also provided based on low, most-likely or “best”, and high estimates of future rainfall.

O.3 Stream Crossing Explorer Data

The Stream Crossing Explorer can be viewed at <http://sce.ecosheds.org/>

Data layers include:

Catchments
Counties
DOT districts
Environmental Justice
HUC 12 watersheds
NHS Roads
Road Jurisdiction
Streams
Towns

O.4 Additional Data

Additional data are provided as separate zipped Excel files, including:

- Excel files for 108 crossings with Geomorphic crew data
- File that summarizes comparison of RI discharge estimates for finalizing the hydraulic risk formulation
- MMI field and analysis data
 - Field data
 - Field data analysis
 - Vulnerability screen
 - Damaged structure analysis
- TU pebble count data
- TU custom data
- MassDOT bridge inspection data
- Bias adjusted NARCCAP climate data
- DOT CMIP climate processing tool data
 - Downloaded datafiles
 - Processed individual model results